



Universiteit  
Leiden  
The Netherlands

## **Combinatorial prospects of nanoparticle mediated immunotherapy of cancer**

Silva, C.G. da

### **Citation**

Silva, C. G. da. (2021, June 24). *Combinatorial prospects of nanoparticle mediated immunotherapy of cancer*. Retrieved from <https://hdl.handle.net/1887/3191984>

Version: Publisher's Version

License: [Licence agreement concerning inclusion of doctoral thesis in the Institutional Repository of the University of Leiden](#)

Downloaded from: <https://hdl.handle.net/1887/3191984>

**Note:** To cite this publication please use the final published version (if applicable).

Cover Page



Universiteit Leiden



The handle <https://hdl.handle.net/1887/3191984> holds various files of this Leiden University dissertation.

**Author:** Silva, C.G. da

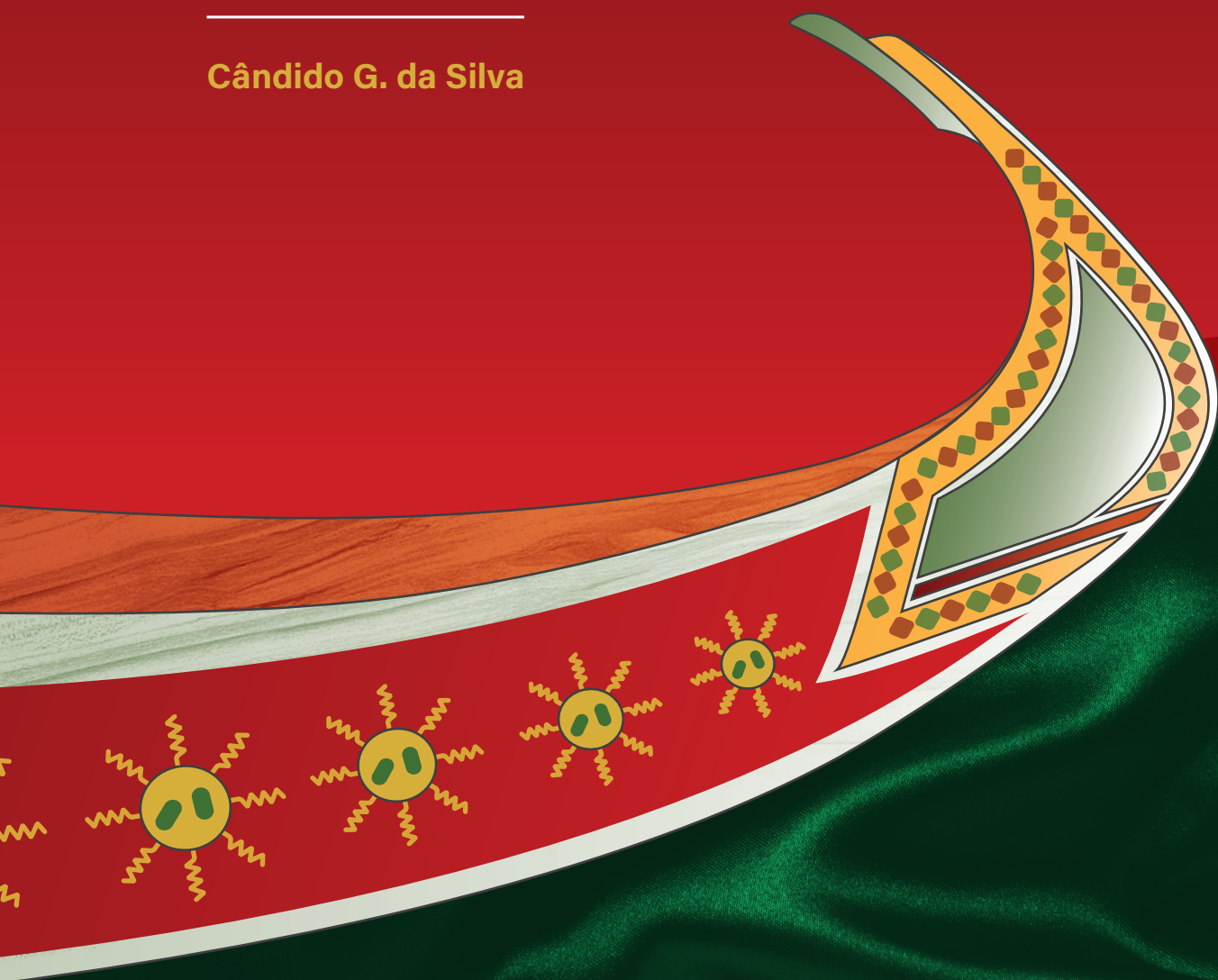
**Title:** Combinatorial prospects of nanoparticle mediated immunotherapy of cancer

**Issue Date:** 2021-06-24

# COMBINATORIAL PROSPECTS OF NANOPARTICLE MEDIATED IMMUNOTHERAPY OF CANCER

---

Cândido G. da Silva



# **COMBINATORIAL PROSPECTS OF NANOPARTICLE MEDIATED IMMUNOTHERAPY OF CANCER**

Cândido Geraldo da Silva

The research described in this thesis was performed at the departments of immunology and radiology at the Leiden University Medical Center, the Netherlands. The work described in this thesis was funded by a grant of the Netherlands Organization for Scientific Research (NWO) number 723.012.110 (Vidi).

ISBN: 978-94-6419-233-9.

Lay-out: Jeroen M.M. Heuts and ngchoyiu,seewhy

Cover design: Cândido G. da Silva and Jeroen M.M. Heuts

Thesis printing: GildePrint - The Netherlands

Copyright © 2021 by Cândido G. da Silva. All rights reserved. Nothing from this thesis may be reproduced or transmitted in any form or by any means without written and explicit permission from the author.



# **COMBINATORIAL PROSPECTS OF NANOPARTICLE MEDIATED IMMUNOTHERAPY OF CANCER**

Proefschrift

ter verkrijging van  
de graad van doctor aan de Universiteit Leiden,  
op gezag van rector magnificus prof.dr.ir. H. Bijl,  
volgens besluit van het college voor promoties  
te verdedigen op

donderdag 24 juni 2021 klokke 13:45

door

**Cândido Geraldo da Silva**  
geboren te Delft in 1981





**Promotoren:**

Prof. Dr. F.A. Ossendorp

Prof. Dr. C.W.G.M. Löwik

**Co-promotor:**

Dr. L.J. Cruz Ricondo

**Leden promotiecommissie:**

Prof. Dr. M.J. Jager

Prof. Dr. G.J. Peters (Amsterdam UMC, Nederland)

Prof. Dr. H. Zhang (University of Amsterdam, Nederland)

Dr. R. Arens

# CONTENT

<b>01</b>	GENERAL INTRODUCTION	<b>10</b>
<b>02</b>	COMBINATORIAL PROSPECTS OF NANO-TARGETED CHEMOIMMUNOTHERAPY	<b>36</b>
<b>03</b>	THE EFFECT OF INJECTION ROUTE OF PLGA NANOPARTICLES ON THE BIODISTRIBUTION AND ICG BLOOD CLEARANCE RATE IN TUMOR BEARING MICE	<b>84</b>
<b>04</b>	EFFECTIVE CHEMOIMMUNOTHERAPY BY CO-DELIVERY OF DOXORUBICIN AND IMMUNE ADJUVANTS IN BIODEGRADABLE NANOPARTICLES	<b>98</b>
<b>05</b>	CO-DELIVERY OF IMMUNOMODULATORS IN BIODEGRADABLE NANOPARTICLES IMPROVES THERAPEUTIC EFFICACY OF CANCER VACCINES	<b>142</b>
<b>06</b>	COMBINING PHOTODYNAMIC THERAPY WITH IMMUNOSTIMULATORY NANOPARTICLES ELICITS EFFECTIVE ANTI-TUMOR IMMUNE RESPONSES IN PRECLINICAL MURINE MODELS	<b>186</b>
<b>07</b>	THE POTENTIAL OF MULTI-COMPOUND NANOPARTICLES TO BYPASS DRUG RESISTANCE IN CANCER	<b>230</b>
<b>08</b>	GENERAL DISCUSSION	<b>266</b>
	<b>APPENDICES</b>	<b>280</b>
	NEDERLANDSE SAMENVATTING	
	DANKWOORD	
	CURRICULUM VITAE	
	LIST OF PUBLICATIONS	

1

# GENERAL INTRODUCTION

# Introduction

---

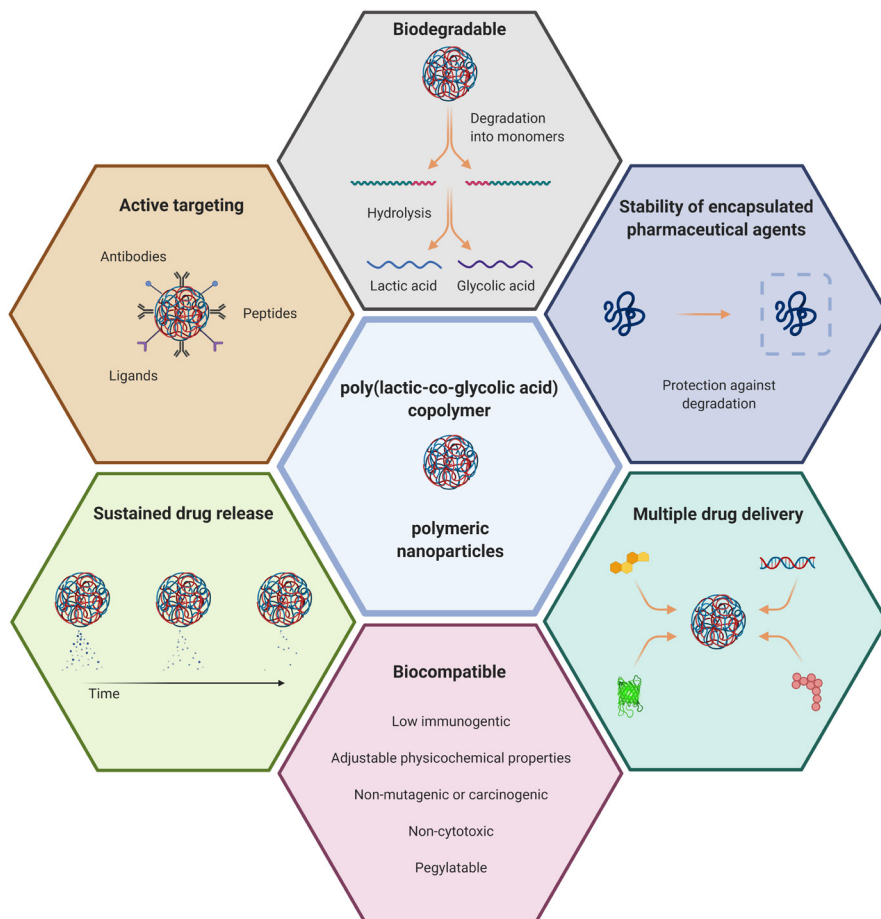
Beyond the macro- and microscale, it is there where the tangible structures that we are built of, perceive, and experience, are composed. It is matter at the nanoscale. The lecture of the American physicist Richard Feynman "There's Plenty of Room at the Bottom" [1] laid the crib in the late 1950s to what we understand nowadays as Nanotechnology; although it was the Austrian chemist Richard Zsigmondy the first to observe and perform size measurements of particles at (and coined the term) "nanometer" scale almost 100 years ago [2]. Both were formidable pioneers who laid the foundations of a new field in science and awarded righteously with the Nobel Prize in Chemistry for their accomplishments in 1925. Yet it took many years for nanotechnology to reveal its potential applications in medicine and to emerge as an ever so tiny, yet powerful, tool to join the combat against human diseases.

## THE NANOMEDICINE FIELD OF RESEARCH

Nanotechnology generally refers to the field of science and study of (synthetic) molecular structures with diameters in size smaller than a micrometer, usually between 1 to 500 nanometers (nm). While this field has a wide overlapping span to many other scientific branches, pronouncedly in chemistry and physics, it is referred to as Nanomedicine when its study is attributed to the field of Medicine. There, the manipulation of matter at the nanoscale is applied to the synthetic assembly of (preferably biocompatible) materials and structures for a wide range of applications, including the delivery of drugs, with the purpose of diagnosis and therapy of human pathophysiology. However, it is generally the application of nanotechnology for

medical purposes that defines the name rather than the operating size scale, as arguably, the fields of molecular biology and pharmacology operate at similar size scale. One of the main problems that researchers working in the field of nanomedicine try to solve is to reduce the biodistribution of drugs while maintaining effective dosage of drugs on the target site; as drugs tend to distribute in all organs, tissues and cells within the organism most particularly at higher doses [3]. The biodistribution of a drug in an organism often lies root to unwanted adverse effects due to human pharmacological intervention that is aimed to treat or ameliorate disease symptoms with drugs. After all, a drug designed to kill cancer cells should not accumulate elsewhere than in the tumor and is toxic when accumulated, for example, in the heart. To address this problem, synthetic nanoparticles were proposed as vehicles to transport, protect, and deliver drugs aimed to reduce drug biodistribution and, under certain circumstances, even enhance drug delivery to the anatomical site of interest. For this purpose, several nanoparticle types, with differing compositions and shapes, were developed during the past years that can be generally divided in two main categories: of either inorganic or organic etiology. Inorganic nanoparticles are mostly composed of colloids of silver, gold or silicon. Organic nanoparticles are mostly composed of lipids, sugars, and (biodegradable) polymers. Within the different types, one or multiple drugs can be simultaneously encapsulated, entrapped, or attached by ion bonds or covalently, in, between, or on the outside of nanoparticles. One of the most important biological aspect of the nanoparticles physicochemical properties is its size. Nanoparticles for medical application are usually assembled within the size range of 20 to 500nm, based on the balance between optimal blood circulation time to facilitate tumor accumulation versus drug loading capacity [4]. Particles smaller than 10 nm are rapidly cleared by the kidneys and bigger nanoparticles tend to be removed gradually in time from blood circulation via opsonization and clearance by the mononuclear phagocytic system and via phagocytosis in the liver [5]–[7]. Pegylation, a chemical process where polyethylene glycol groups are added to the outer layers of nanoparticles, can slow down opsonization and reduce interactions with the immune system, which increases blood circulation time [8]. The nanoparticle size range is also an important factor in a biological process known as the enhanced permeability and retention (EPR) effect. The EPR effect is hypothesized to occur within some solid tumors where the local vasculature is aberrantly formed, which includes the absence of a smooth muscle layer covering the blood vessels and the presence of wide gaps between endothelium cells [9]. Combined with ineffective lymphatic drainage in the tumor tissue, nanoparticles tend to passively accumulate more in the tumor than

in other organs [10]. When extravasated from the blood vessels to inside the tumor tissue, binding of the nanoparticles to cancer or other cell types of interest can be further enhanced by modifying the surface of nanoparticles with specific antibodies, peptides, or receptor ligands. When nanoparticles acquire higher binding capability to cells of interest, most specifically guided to receptors with endocytosis capacity, these nanoparticles are termed targeted nanoparticles [11]. Other physicochemical properties of the nanoparticles can be further adjusted for sustained, sequential, or slow drug release depending on the surrounding milieu such as temperature, specific enzymes, or pH. An overview illustration of these properties is depicted in **Figure 1** for poly(lactic-co-glycolic) (PLGA) copolymer-based nanoparticles.





- < **Figure 1. An overview of the properties and applications of polymeric poly (lactic-co-glycolic) nanoparticles.** The poly (lactic-co-glycolic) (PLGA) copolymers are FDA approved for human medical applications. PLGA nanoparticles have strong biodegradable and biocompatible traits [12]. The remnants of PLGA nanoparticles are lactic and glycolic acid which are also produced by cells during normal metabolic function [13]. Additional noteworthy traits are: **1)** enhanced drug protection capabilities. For instance, genetic products (e.g. silencing RNA, proteins, mRNA, CRISPR-Cas, etc.) are protected inside the PLGA nanoparticles from direct degradation and removal from the blood. **2)** Capacity to load multiple drug types into one nanoparticle and maintaining a sustained controlled release of the drugs [14], [15]. **3)** Surface functionalization of nanoparticles for active targeting to specific cells (e.g. with antibodies, ligands, peptides, etc.) [16].

## NANOMEDICINE IN CANCER RESEARCH AND THERAPY

Many nanoparticle-based nanomedicine modalities for cancer diagnosis and therapy are currently in late phase clinical trials [17]. Some were already approved decades ago, for instance Doxil®, a liposomal variant of the chemotherapy drug doxorubicin, received FDA approval in 1995. Doxil® solved a problem induced by doxorubicin (i.e. cardiotoxicity) by reducing doxorubicin exposure to the heart (i.e. reduced biodistribution) while maintaining anti-cancer efficacy [18]. Since then, Abraxane® and Onivyde® were also introduced as nanoparticle variants of paclitaxel and irinotecan, respectively. More recently, VYXEOS® and Hensify® were FDA approved for the treatment of cancer. VYXEOS® is a combination chemotherapy nanoparticle of cytarabine and daunorubicin for the treatment of myeloid leukemia [19]. Hensify® is a hafnium loaded nanoparticle that significantly enhances standard radiation oncological procedures [20]. Similar combined drug nanomedicine solutions to VYXEOS® and the emergence of nanoparticle-based combined/multiple drug combination therapy (such as the combination of chemotherapy with immunotherapy) is reviewed and discussed in chapter 2. The type of applications of nanoparticles in oncology is vast as still rapidly growing. Nanoparticle technology in nanomedicine is currently regarded as de facto delivery platform for chemotherapy and other standard anti-cancer drugs, but also for direct or indirect tumor microenvironment remodeling, systemic immune modulation or immune modulation of the tumor microenvironment and lymph nodes; as well as mediators of delivery or adjuvant therapy of immunotherapy, gene therapy, radiotherapy, therapeutic cancer vaccine therapy, photodynamic and photothermal therapy and other sub-types of anti-cancer therapies [21].

## THE GENESIS OF THE IMMUNE SUPPRESSED TUMOR MICROENVIRONMENT AND THE REGULATION OF IMMUNE ACTIVATION

A tumor microenvironment which is characterized as immune suppressed is thought to be acquired after selective interactions with the immune system during tumor development. During these interactions, it is likely that cancerous cell clones which have harbored highly immunogenic mutations were eliminated, while weak immunogenic cancer cells escape immune surveillance, a process named immunoediting [22]. The process of immunoediting may continue for several cycles, where the surviving cancer cells acquire more mutations and undergo epigenetic alterations thereby selecting the clones which can proliferate and escape immune attack [23], [24]. This will lead to an immune suppressed microenvironment which increasingly becomes impregnable for cancer cell killing immune cells [25]. At this point, even newly developed cancer cell clones with additional immunogenic mutations may not be eliminated anymore and the cancer becomes established. An important part of the process to acquire such a milieu is attained by tumor cells that produce specific chemokines (**Figure 2**). Chemokines are small molecules that can attract specific cell types. For instance, the chemokines CCL2, CCL5, CCL17 and CCL22 are commonly found in tumors that can recruit Myeloid derived suppressor cells (MDSCs) [26], Tumor associated macrophages (TAMs) [27], and Regulatory T cells (T-regs) [28] to the tumor area. In part, the recruitment of these cells may be the product of the evolution process of the cancer cells that acquire this ability due to selection. A putative mechanism has been put forward relating chromosome instability to both immune evasion and metastasis [24]. On the other hand, the recruitment of these cells may also be part of the immune resolution process, a negative feedback mechanism that takes place after the elimination of highly immunogenic cancer clones. Which process initiates or how significantly it contributes to the immune suppressed microenvironment in different cancer types is currently not fully understood. It is very likely that not only one process is responsible but several. However, regardless of the type of process responsible for the migration of these cells to the tumor area, the consequence is the establishment of a chronically immune suppressed environment (i.e. for cancer killing immune cells) that facilitates the continuous expansion of cancer cells, as well as the recruitment of MDSCs, TAMs and T-regs. This environment is also self-maintaining by the production of cues and cytokines such as ARG1, iNOS, TGF $\beta$ , IL10, COX2 and

IDO produced by MDSCs [29]. TAMs can produce VEGF-A, TGF $\beta$ , FGF $\beta$ , IL10, CCL17, CSF1 and TREM2 as well as the PD-L1 marker [30]–[40] while T-regs can express several markers and immune suppressive factors like CTLA-4, TIM-3, LAG-3, GITR, TGF $\beta$  and IL10 [41], see figure 2. This process will continue allowing the cancer cells to grow large in numbers and acquire a tumor mass until a point it will start to induce symptoms on patients as it invades surrounding tissue and metastasize to distal parts of the organism. The production of the cues that maintain the immune suppressive microenvironment is likely to also start to affect the systemic function of the immune system and homeostasis [42], [43]. Regarding the treatment for the patient, whether the tumor and the metastases will respond to different types of therapy is dependent of several factors and mechanisms. A therapy modality that is composed of multiple drugs is most commonly required for effective clinical responses [44].

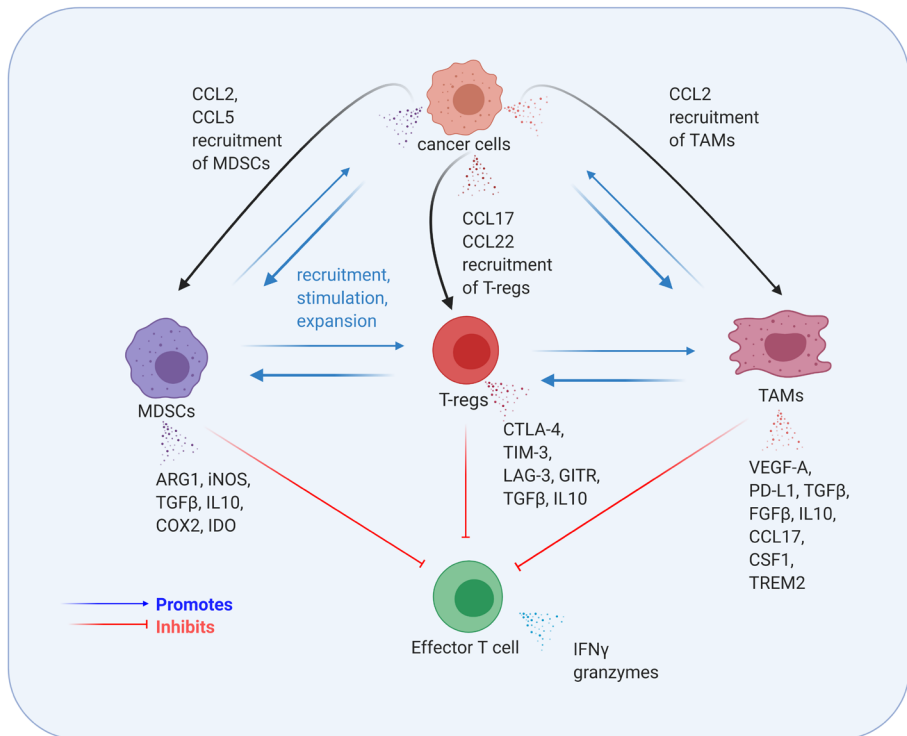


**Figure 2. The role of chemokines to establish an immune suppressed tumor microenvironment.** Cancer cells and other tumor-associated cells produce CCL2, CCL5, CCL17 and CCL22 that recruits Myeloid derived suppressor cells (MDSCs) [26], Tumor associated macrophages (TAMs) [27], and Regulatory T cells (T-regs) [28] to the tumor area. A chronic inflamed milieu that facilitates the continuous recruitment, stimulation, and expansion of cancer cells, MDSCs, TAMs and T-regs is maintained by the production of cues and cytokines such as ARG1, iNOS, TGFβ, IL10, COX2 and IDO produced by MDSCs [29]; VEGF-A, PD-L1, TGFβ, FGFβ, IL10, CCL17, CSF1 and TREM2 by TAMs [30]–[40]; and CTLA-4, TIM-3, LAG-3, GITR, TGFβ and IL10 by T-regs [41]. The recruitment of MDSCs, T-regs, and TAMs to the tumor area facilitates cancer cell survival, proliferation, angiogenesis, invasion and metastasis, immunosuppression, and drug resistance.

The process of immunoediting commonly starts with the recognition of cancer cells by specific T lymphocytes. This recognition is made possible as cancer cells acquire unique mutations in their DNA leading to the translation of 'altered' proteins which can be presented as small processed peptides in the major histocompatibility complex (MHC) molecules at the cell surface [45]. The MHC loaded with the antigenic peptide (i.e. neoepitope) can be recognized by the T cell receptor (TCR) of cognate T cells [46]. Activation and expansion of such T cells (i.e. that can recognize neoepitopes on cancer cells) will be initiated by antigen-presenting cells (APCs), such as dendritic cells (DCs) which can process and (cross)present cancer cell-derived antigenic peptides [47]. For their activation, T cells require 3 signals. The first signal is provided by the binding between the TCR and the MHC I and/or II, containing the neoepitope. The second signal is provided by co-stimulatory or co-inhibitory receptors. Naïve T cells require the co-stimulatory binding of CD28 with CD80/86 on APCs for their survival and proliferation. Negative feedback is also part of the regulatory process to control the magnitude of the immune response in the form of the expression of the CTLA-4 receptor which, at a certain point, will start to compete with CD28 for the co-inhibitory binding to CD80/86 on APCs. Also, other co-stimulatory interactions like CD27 with CD70 on APCs are important for activated T cells to develop effector functions. Since signal 2 provided by APCs is crucial to initiate an adaptive response, expression of these co-stimulatory molecules is tightly regulated to avoid autoimmunity. Immature APCs are poor (cross)presenters of antigen by default and display a non-activated phenotype (i.e. low MHC-I and II, low CD40, CD70, CD80 and CD86). However, APCs can acquire an activated phenotype when exposed to ligands of the pattern recognition receptors (PRRs) family which is broadly divided into two types, the damage-associated molecular pattern molecules (DAMPs) or pathogen-associated molecular pattern molecules (PAMPs). Due to the dysregulated expansion of cancer cells, some of these cells die and secrete DAMPs. These DAMPs are contained in the membranes of dead cancer cells or released by adjacent living cells in response to cell death and stress. When APCs engulf the dead cancer cells or debris, their PRRs can be activated by DAMPs and it can contribute to the activation of APCs. In turn, the activation of the APCs can incite the expression of MHC-I and MHC-II and of co-stimulatory receptors (e.g. CD40, CD70, CD80 and CD86).

The third signal is provided by cytokines which will influence the type of immune response that will be generated. The APC derived IL12 cytokine will induce a Th type 1 (Th1) immune response characterized by IFN $\gamma$  and IL2 production, which will optimally

stimulate cytotoxic T lymphocytes (CTLs). The Th type 2 (Th2) immune response is characterized by IL4 cytokine production, which is aimed to stimulate extracellular immunity via antibodies. A Th1 or a Th2 response is thought to be regulated by differential activation of the type of PRRs by DAMPs and PAMPs.

After optimal initiation and activation, T cells will start to proliferate and then migrate to the tumor and will be able to kill cancer cells. However, the survival, proliferation rate, killing capacity, and activation status can still be modulated, most commonly when T cells arrive in the suppressive environment in the tumor. For instance, activated T cells can be deactivated by ligands for the Programmed cell death protein 1 (PD-1) receptor, which is expressed on activated T cells [48]. When arriving at the tumor site, cancer and non-cancer cells can express the PD-L1 or PD-L2 ligands of PD-1 receptor which effectivity renders the T cells inert. Moreover, when the T cells arrive at the immune suppressed tumor microenvironment they are likely to encounter T-regs that express the co-inhibitory cytotoxic T-lymphocyte-associated protein 4 (CTLA-4) receptor and abundant IL10, TGF $\beta$ , and other suppressive cytokines that can also effectively abrogate T cells [49]. Besides the aforementioned examples, a plethora of similar immune checkpoints and other immune regulatory cues are already currently described and likely more are to be discovered in the future [50].

## TARGETS FOR CANCER IMMUNOTHERAPY

The aim of cancer immunotherapy is to initiate de novo immune responses or to augment and/or recommence existing suppressed T cell immune responses against cancer cells. Immune checkpoint inhibitors are currently the most common form of immunotherapy where co-inhibitory receptors are targeted by blocking antibodies thereby 'releasing the breaks' from existing, but inactive tumor-specific T cells. Ipilimumab and tremelimumab are antibodies against CTLA-4 that can be administered to hinder the interaction of CD80/86 with CTLA-4 thereby facilitating the interaction of CD80/86 with CD28 which enhances T cell activation. Similarly, the interaction of the T cell inhibitory receptor PD-1 with its ligands PD-L1 and PD-L2 can be inhibited with nivolumab or pembrolizumab thereby leading to T cell activation [51]. Another type of immunotherapy is guided to modulate immune responses, often targeted to innate immune cells. Immune adjuvants (also known as immune modulators or immune stimulants) commonly aim to activate specific PRRs in APCs [52]. As previously described, during cancer development many cancer cells die and

release DAMPs that principally induce Th1 type activation. However, APC activation with DAMPs can be limited by the secretion of immune suppressive cues from the tumor microenvironment or even initiate another type of immune response other than Th1 but this is dependent on the type and concentration of DAMPs. Therapy with photo dynamic therapy, immunogenic chemotherapy or with other drugs that kills cancer cells directly can also induce the release of high concentrations of DAMPs. However, a type of PRRs in DCs that mainly recognize PAMP molecules can be exploited therapeutically to force a Th1 type immune response and induction of tumor specific CTLs. The Toll-like receptor (TLR) family is a type of PRRs that can recognize PAMPs such as microbial fragments, including viral and bacterial fragments [53]. TLRs can also be activated with immune adjuvants including synthetic viral facsimile molecules, such as poly (I:C) or resiquimod. Upon binding of the immune adjuvants to the respective TLRs, the DCs upregulate the expression of CD40, CD80, and CD86 and initiate the secretion of IL12, which differentiates naïve Th to Th1 T cells as described above. Therapeutic cancer vaccines combine the administration of defined antigens with immune adjuvants to induce a strong antigen-specific Th1 immune response and CD8 CTLs [54].

## THE INTRATUMORAL ADMINISTRATION OF IMMUNE ADJUVANTS AND ABSCOPAL EFFECTS

The therapeutic potential of immune adjuvants also extends further when administered directly in the tumor [55], [56]. The direct intratumoral administration concept is certainly not new, as the American surgeon William Coley, in the beginnings of the 1890s, observed that some tumors on sarcoma patients temporarily shrank upon injection of live bacteria directly in the tumors [57]. More recently, research has provided a much better understanding of this process and developed improved and safer drugs and methods specifically tuned to harness the power of the immune system to direct it against the tumor more efficiently and with less side effects. For instance, immune adjuvants can resolve the immune suppressed phenotype of TAMs, M2-like macrophages, and MDSCs in the tumor and tumor-draining lymph nodes and abrogate T-regs from suppressive activity [58], [59]. Some immune adjuvants can reverse cytotoxic T cells in the tumor from an anergic state to an activated state and invigorate NK killing capacity [60]. Also, whether it is advantageous to activate single or multiple TLRs simultaneously has been studied [61]. For instance, it has

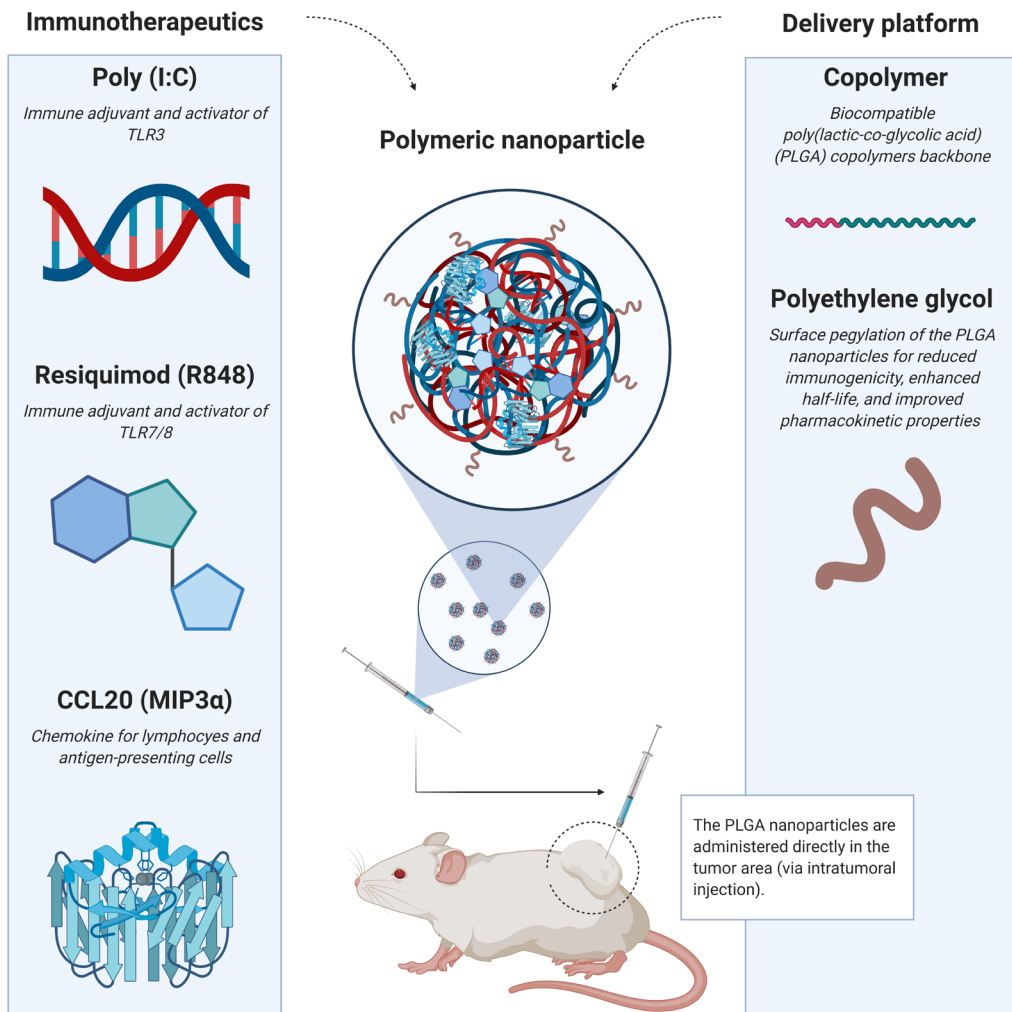


**Figure 3. Design and composition of the PLGA nanoparticles that is central to this thesis.** The immune adjuvants Poly (I:C) and Resiquimod, and the chemotactic CCL20, were simultaneously encapsulated into pegylated PLGA nanoparticles and injected intratumorally.



been reported that the combined activation of TLR3 and TLR7 synergizes in cytokine production in vitro [61]–[63]. The activation of TLR3 by Poly (I:C), a synthetic analog of double-stranded RNA, induces NK- $\kappa$ B and IRF3 activation via the TRIF-RIP1-TRAF6 axis that culminates in the production of inflammatory cytokines and type I IFNs such as IL6, IL8, TNF $\alpha$ , IFN $\alpha$  and IFN $\beta$  [64], [65]. The activation of TLR7/8 by resiquimod, an imidazoquinoline compound, induces NK- $\kappa$ B and IRF5/7 activation via the MyD88-IRAK4 route and leads to robust production of pro-inflammatory cytokines and type I IFNs including IL1 $\beta$ , IL6, IL12, TNF $\alpha$  and IFN $\alpha$  [66]. Despite that both poly (I:C) and resiquimod activate the same subfamily of PAMPs, their effects exerted on the immune system and tumor response outcomes can be quite distinct [67]. While in vitro exploratory research provided indications of potential immunological additive or synergistic effects when both immune adjuvants were combined, the therapeutic effects of this combination in cancer models in vivo remains underexplored [61]–[63]. Another interesting strategy to improve immune responses against cancer cells is to recruit more immune cells to the tumor area. This can be accomplished by chemokines, such as CCL20 [68]. More drugs are administered intratumorally nowadays, following many reports showing optimal therapeutic effect with less side-effects which have been validated in the clinic for several cancer types [69]. Most importantly, the effects of local treatment commonly induces abscopal effects, which are imperative for the control of metastases [70], [71]. In addition, the administration of drugs in the region of the tumor-draining lymph node has also been recommended for less accessible tumors with similar therapeutic outcomes [72].

## A STRIKE FROM MULTIPLE DIRECTIONS: CANCER CHEMOIMMUNOTHERAPY AND PHOTODYNAMIC THERAPY

Chemotherapy is an ablative class of cytotoxic and/or cytostatic drugs with the aim to eliminate as many cancer cells as possible. A tumor responsive to chemotherapy will initially display a mass shrinkage but the effects are usually only temporary due to other resistance mechanisms that emerge against the applied chemotherapy. Besides killing cancer cells directly, there are indications that chemotherapy can reverse the immune suppressed state in tumors (i.e. release of DAMPs) under certain specific circumstances and by eliminating suppressive immune cells directly. Furthermore, the systemic immune system appears less affected when chemotherapy is provided at lower doses. Research exploring the combination of (lower dose) chemotherapy with immunotherapy, either administered simultaneously or one before the other,

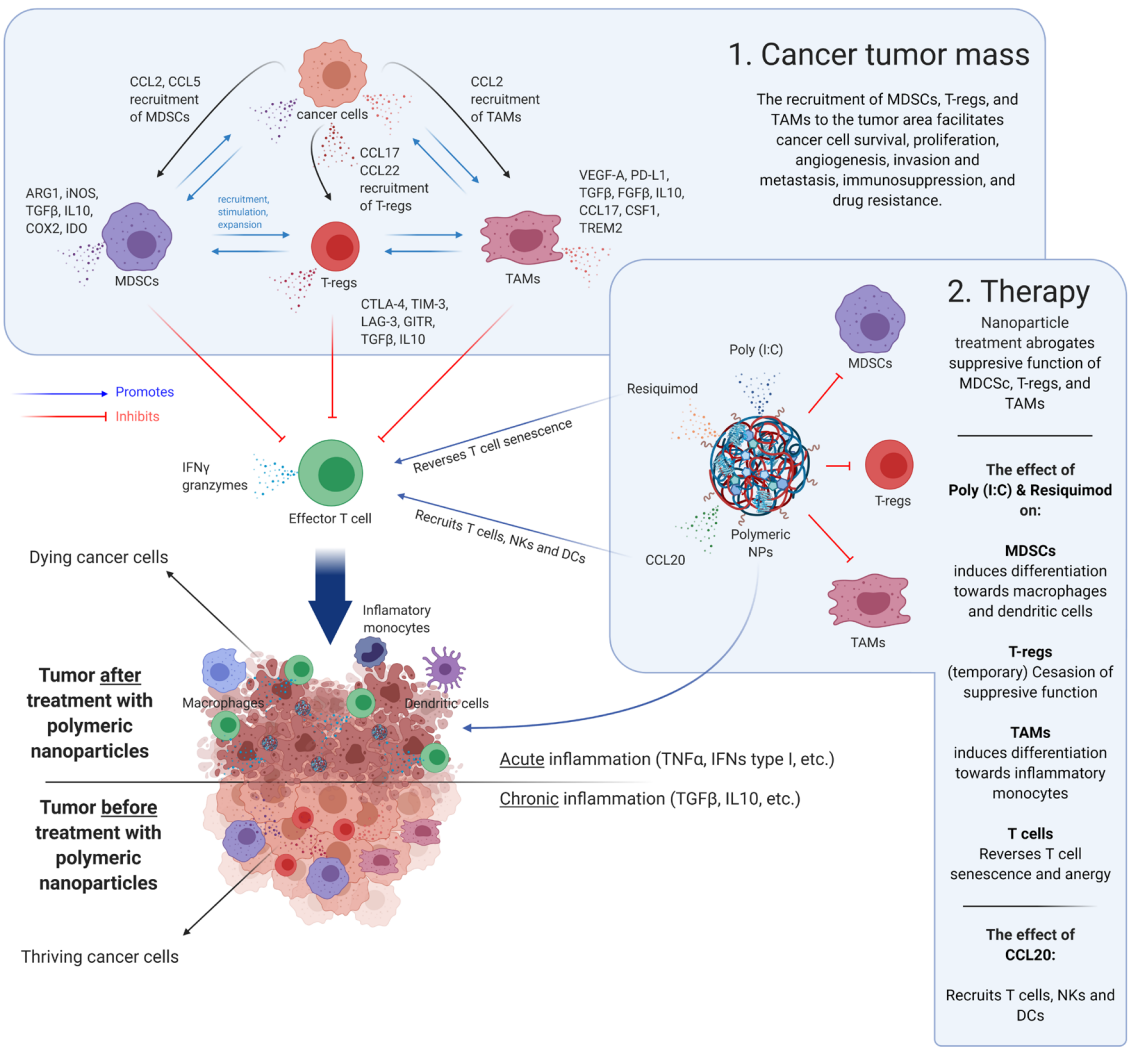
is compelling and has the potential to enhance therapeutic strategies for cancer patients in the near future. The therapeutic strategy of chemotherapy combined with a form of immunotherapy is regarded as a cancer chemoimmunotherapy.

An upcoming modality is photodynamic therapy, which ablates tumor cells by a two-step treatment. First, a photosensitizer drug is administered to the patient and allowed to accumulate in cells after which a light source (i.e. a laser) emanating light, often at a specific wavelength. Upon encountering such light, the photosensitizer will utilize the light's energy to initiate a chemical process that results in the generation of reactive oxygen species or other reactive molecules, however the type of reaction or effect can vary depending on the type of photosensitizer. In turn, the reactive oxygen species can induce severe local structural alterations to cell components and membranes, ultimately leading to cell death. It is not uncommon that a high generation of DAMPs takes place during this ablative process as well as the release of cancer antigens that can facilitate immune responses against remaining cancer cells and metastases via abscopal effects [73]. Two major advantages of photodynamic therapy are the possibility to only expose the tumor tissue to harmless visible light, and therefore induce no meaningful damage to non-exposed tissue in contrast to radiotherapy, and it is not mutagenic therapy. A disadvantage of photodynamic therapy is that it is currently limited to tumor types which are easily accessible for laser illumination.

## THE SCOPE OF THIS THESIS

The work presented in this thesis was the result of multi-disciplinary cooperation between the fields of Nanotechnology, Oncology, and Immunology. The aim was to study novel therapeutical concepts to improve insights and therapy responses for cancer patients in the near future. The concept of injecting bacteria or bacterial products directly in tumors is an established approach but we improved intratumoral delivery with modern nanotechnology and well-defined synthetic compounds. Since there is a population of patients that do respond to this type of therapy, there is a window of opportunity to improve therapy responses by utilizing the current knowledge on the mechanisms of immunotherapy and of nanotechnology. In this thesis, a novel therapeutic drug combination was tested. Instead of using live bacteria or bacterial products, two well defined synthetic immune adjuvants, namely poly (I:C) and resiquimod (also known as R848), were combined with the chemotactic CCL20 (also known as MIP3 $\alpha$ ) and incorporated into one nanoparticle treatment modality (**Figure 3**).

The hypothesis is centered on the combination of poly (I:C) with resiquimod that could effectively modulate the immune system to abrogate the local immune suppressed state when injected intratumorally. Furthermore, the combination with CCL20 could yield better therapeutic results due to the capacity of CCL20 to recruit cancer fighting immune cells to the tumor [74]–[76]. To reduce rapid drug diffusion to the blood and to contain the drugs to the tumor area, poly (I:C), resiquimod, and CCL20 were simultaneously encapsulated into pegylated PLGA nanoparticles and injected intratumorally. An overview of the putative mechanisms is depicted in **Figure 4**



- < **Figure 4. The putative effects and mechanisms of the PLGA nanoparticles loaded with poly (I:C), resiquimod, and CCL20, when injected in the tumor area.** The immune adjuvants Poly (I:C) and resiquimod can neutralize most of these immune suppressive generating processes. For instance, MDSCs can differentiate towards (mature, M1-like) macrophages and dendritic cells upon activation of TLR7 [77]; type I interferons produced by MDSCs and TAMs upon treatment with Poly (I:C) and/or resiquimod can directly inhibit T-regs [58], [59], [78], [79]; Activation of TLR3 in TAMs promotes differentiation towards a mature, M1-like, tumoricidal phenotype [80], [81]; Both activation of TLR3 and TLR7 in T cells have invigorating effects, such as reversal of T cells senescence and anergy [58], [82]. Finally, the artificial administration of CCL20 into the tumor area can directly repress the proliferation of myeloid progenitors [68] and actively attract cells expressing CCR6/CD196 such as dendritic cells, (memory) T cells, natural killer cells, and granulocytes [74]–[76], [83], [84]. The resulting inhibition of immune suppression is a milieu less friendly to cancer cells and more friendly to (cytotoxic) T cells and other (innate) tumoricidal cells.

In **chapter 2**, current published literature on the combinatorial prospects of nano-targeted chemoimmunotherapy is summarized, reviewed, and discussed to set the stage for studying the combination of the triple immune stimulation nano-sized modality with doxorubicin chemotherapy as described in chapter 4. In **chapter 3**, the biodistribution and the blood clearance rate was studied on tumor-bearing mice utilizing a surrogate nanoparticle loaded with a near-infrared dye upon intratumoral, subcutaneous, or intravenous administration of the nanoparticles.

In **chapter 4**, a study about the additive potential of nanoparticle mediated delivery of poly (I:C), resiquimod, CCL20, and doxorubicin to eradicate established tumors in two distinct *in vivo* aggressive cancer models is reported. In addition to the tumor growth inhibition and survival, in depth tumor microenvironment, circulating cancer specific T cells, and immune organ analysis is also studied. In **chapter 5**, the effect of each immune adjuvant and the chemokine encapsulated (i.e. separately but also in combination) combined with therapeutic cancer vaccines was studied and reported. The therapeutic potential of the nanoparticle-based modality was studied in combination with photodynamic therapy and the results reported in **chapter 6**. In **chapter 7**, the potential of multi-compound nanoparticles to bypass drug resistance in cancer is reviewed and discussed. A general discussion of these chapters and the potential and caveats of the nanoparticle-based modality reported here is provided in **chapter 8**.

## REFERENCES

- [1] R. P. Feynman, Miniaturization: There's plenty of room at the bottom. 1961.
- [2] T. Mappes, N. Jahr, A. Csaki, N. Vogler, J. Popp, and W. Fritzsche, "The Invention of Immersion Ultramicroscopy in 1912-The Birth of Nanotechnology?," *Angew. Chemie Int. Ed.*, vol. 51, no. 45, pp. 11208–11212, Nov. 2012.
- [3] V. P. Torchilin and A. N. Lukyanov, "Peptide and protein drug delivery to and into tumors: Challenges and solutions," *Drug Discovery Today*, vol. 8, no. 6, pp. 259–266, 15-Mar-2003.
- [4] S. A. A. Rizvi and A. M. Saleh, "Applications of nanoparticle systems in drug delivery technology," *Saudi Pharmaceutical Journal*, vol. 26, no. 1. Elsevier B.V., pp. 64–70, 01-Jan-2018.
- [5] N. Hoshyar, S. Gray, H. Han, and G. Bao, "The effect of nanoparticle size on in vivo pharmacokinetics and cellular interaction," *Nanomedicine*, vol. 11, no. 6. Future Medicine Ltd., pp. 673–692, 01-Mar-2016.
- [6] E. C. Dreaden, L. A. Austin, M. A. MacKey, and M. A. El-Sayed, "Size matters: Gold nanoparticles in targeted cancer drug delivery," *Therapeutic Delivery*, vol. 3, no. 4, pp. 457–478, Apr-2012.
- [7] D. E. Owens and N. A. Peppas, "Opsonization, biodistribution, and pharmacokinetics of polymeric nanoparticles," *International Journal of Pharmaceutics*, vol. 307, no. 1, pp. 93–102, 03-Jan-2006.
- [8] J. V. Jokerst, T. Lobovkina, R. N. Zare, and S. S. Gambhir, "Nanoparticle PEGylation for imaging and therapy," *Nanomedicine*, vol. 6, no. 4. NIH Public Access, pp. 715–728, Jun-2011.
- [9] J. W. Nichols and Y. H. Bae, "EPR: Evidence and fallacy," *Journal of Controlled Release*, vol. 190. Elsevier B.V., pp. 451–464, 28-Sep-2014.
- [10] H. Maeda, "Macromolecular therapeutics in cancer treatment: The EPR effect and beyond," *Journal of Controlled Release*, vol. 164, no. 2. Elsevier, pp. 138–144, 10-Dec-2012.
- [11] D. Rosenblum, N. Joshi, W. Tao, J. M. Karp, and D. Peer, "Progress and challenges towards targeted delivery of cancer therapeutics," *Nature Communications*, vol. 9, no. 1. Nature Publishing Group, 01-Dec-2018.
- [12] J. M. Anderson and M. S. Shive, "Biodegradation and biocompatibility of PLA and PLGA microspheres," *Advanced Drug Delivery Reviews*, vol. 28, no. 1. Elsevier Sci B.V., pp. 5–24, 13-Oct-1997.
- [13] D. Sathish Sundar, M. Gover Antoniraj, C. Senthil Kumar, S. S. Mohapatra, N. N. Houreld, and K. Ruckmani, "Recent Trends of Biocompatible and Biodegradable Nanoparticles in Drug Delivery: A Review," *Curr. Med. Chem.*, vol. 23, no. 32, pp. 3730–3751, Jun. 2016.

- [14] D. J. Hines and D. L. Kaplan, "Poly(lactic-co-glycolic) acid-controlled-release systems: Experimental and modeling insights," *Crit. Rev. Ther. Drug Carrier Syst.*, vol. 30, no. 3, pp. 257–276, 2013.
- [15] J. Ghitman, E. I. Biru, R. Stan, and H. Iovu, "Review of hybrid PLGA nanoparticles: Future of smart drug delivery and theranostics medicine," *Materials and Design*, vol. 193. Elsevier Ltd, p. 108805, 01-Aug-2020.
- [16] J. A. D. Sequeira, I. Pereira, A. J. Ribeiro, F. Veiga, and A. C. Santos, "Surface functionalization of PLGA nanoparticles for drug delivery," in *Handbook of Functionalized Nanomaterials for Industrial Applications*, Elsevier, 2020, pp. 185–203.
- [17] A. C. Anselmo and S. Mitragotri, "Nanoparticles in the clinic: An update," *Bioeng. Transl. Med.*, vol. 4, no. 3, Sep. 2019.
- [18] M. Xing, F. Yan, S. Yu, and P. Shen, "Efficacy and cardiotoxicity of liposomal doxorubicin-based chemotherapy in advanced breast cancer: A meta-analysis of ten randomized controlled trials," *PLoS One*, vol. 10, no. 7, Jul. 2015.
- [19] A. C. Krauss et al., "FDA approval summary: (daunorubicin and cytarabine) liposome for injection for the treatment of adults with high-risk acute myeloid leukemia," *Clin. Cancer Res.*, vol. 25, no. 9, pp. 2685–2690, 2019.
- [20] S. Bonvalot et al., "NBTXR3, a first-in-class radioenhancer hafnium oxide nanoparticle, plus radiotherapy versus radiotherapy alone in patients with locally advanced soft-tissue sarcoma (Act.In.Sarc): a multicentre, phase 2–3, randomised, controlled trial," *Lancet Oncol.*, vol. 20, no. 8, pp. 1148–1159, Aug. 2019.
- [21] S. Rezvantlab et al., "PLGA-based nanoparticles in cancer treatment," *Front. Pharmacol.*, vol. 9, no. NOV, Nov. 2018.
- [22] R. D. Schreiber, L. J. Old, and M. J. Smyth, "Cancer immunoediting: Integrating immunity's roles in cancer suppression and promotion," *Science*, vol. 331, no. 6024. American Association for the Advancement of Science, pp. 1565–1570, 25-Mar-2011.
- [23] D. Hanahan and R. A. Weinberg, "Hallmarks of cancer: The next generation," *Cell*, vol. 144, no. 5. pp. 646–674, 04-Mar-2011.
- [24] J. Li et al., "Metastasis and immune evasion from extracellular cGAMP hydrolysis," 2020.
- [25] F. R. Balkwill, M. Capasso, and T. Hagemann, "The tumor microenvironment at a glance," *J. Cell Sci.*, vol. 125, no. 23, pp. 5591–5596, Dec. 2012.
- [26] V. Kumar, S. Patel, E. Tcyganov, and D. I. Gabrilovich, "The Nature of Myeloid-Derived Suppressor Cells in the Tumor Microenvironment," *Trends in Immunology*, vol. 37, no. 3. Elsevier Ltd, pp. 208–220, 01-Mar-2016.

- [27] D. Argyle and T. Kitamura, "Targeting macrophage-recruiting chemokines as a novel therapeutic strategy to prevent the progression of solid tumors," *Frontiers in Immunology*, vol. 9, no. NOV. Frontiers Media S.A., p. 2629, 13-Nov-2018.
- [28] B. Chaudhary and E. Elkord, "Regulatory T cells in the tumor microenvironment and cancer progression: Role and therapeutic targeting," *Vaccines*, vol. 4, no. 3. MDPI AG, 01-Sep-2016.
- [29] D. I. Gabrilovich, "Myeloid-derived suppressor cells," *Cancer Immunol. Res.*, vol. 5, no. 1, pp. 3–8, Jan. 2017.
- [30] E. J. Yeo et al., "Myeloid wnt7b mediates the angiogenic switch and metastasis in breast cancer," *Cancer Res.*, vol. 74, no. 11, pp. 2962–2973, Jun. 2014.
- [31] P. Pathria, T. L. Louis, and J. A. Varner, "Targeting Tumor-Associated Macrophages in Cancer," *Trends in Immunology*, vol. 40, no. 4. Elsevier Ltd, pp. 310–327, 01-Apr-2019.
- [32] M. Molgora et al., "TREM2 Modulation Remodels the Tumor Myeloid Landscape Enhancing Anti-PD-1 Immunotherapy," *Cell*, vol. 0, no. 0, Aug. 2020.
- [33] S. K. Biswas et al., "A distinct and unique transcriptional program expressed by tumor-associated macrophages (defective NF- $\kappa$ B and enhanced IRF-3/STAT1 activation)," *Blood*, vol. 107, no. 5, pp. 2112–2122, Mar. 2006.
- [34] L. S. Ojalvo, W. King, D. Cox, and J. W. Pollard, "High-density gene expression analysis of tumor-associated macrophages from mouse mammary tumors," *Am. J. Pathol.*, vol. 174, no. 3, pp. 1048–1064, 2009.
- [35] D. M. Kuang et al., "Activated monocytes in peritumoral stroma of hepatocellular carcinoma foster immune privilege and disease progression through PD-L1," *J. Exp. Med.*, vol. 206, no. 6, pp. 1327–1337, Jun. 2009.
- [36] I. Kryczek et al., "B7-H4 expression identifies a novel suppressive macrophage population in human ovarian carcinoma," *J. Exp. Med.*, vol. 203, no. 4, pp. 871–881, Apr. 2006.
- [37] Anfray, Umarrino, Andón, and Allavena, "Current Strategies to Target Tumor-Associated-Macrophages to Improve Anti-Tumor Immune Responses," *Cells*, vol. 9, no. 1, p. 46, Dec. 2019.
- [38] A. R. Dwyer, E. L. Greenland, and F. J. Pixley, "Promotion of tumor invasion by tumor-associated macrophages: The role of CSF-1-activated phosphatidylinositol 3 kinase and Src family kinase motility signaling," *Cancers*, vol. 9, no. 6. MDPI AG, 18-Jun-2017.
- [39] T. Fujimura et al., "Receptor activator of nuclear factor kappa-B ligand (RANKL)/RANK signaling promotes cancer-related inflammation through M2 macrophages," *Exp. Dermatol.*, vol. 25, no. 5, pp. 397–399, May 2016.



- [40] F. Zhu, X. Li, S. Chen, Q. Zeng, Y. Zhao, and F. Luo, "Tumor-associated macrophage or chemokine ligand CCL17 positively regulates the tumorigenesis of hepatocellular carcinoma," *Med. Oncol.*, vol. 33, no. 2, pp. 1–12, Feb. 2016.
- [41] G. Plitas and A. Y. Rudensky, "Regulatory T Cells in Cancer," *Annual Review of Cancer Biology*, vol. 4. Annual Reviews Inc., pp. 459–477, 04-Mar-2020.
- [42] N. G. Zaorsky et al., "Causes of death among cancer patients,," *Ann. Oncol. Off. J. Eur. Soc. Med. Oncol.*, vol. 28, no. 2, pp. 400–407, 2017.
- [43] V. E. Baracos, L. Martin, M. Korc, D. C. Guttridge, and K. C. H. Fearon, "Cancer-associated cachexia," *Nature Reviews Disease Primers*, vol. 4, no. 1. Nature Publishing Group, pp. 1–18, 18-Jan-2018.
- [44] R. B. Mokhtari et al., "Combination therapy in combating cancer," *Oncotarget*, vol. 8, no. 23. Impact Journals LLC, pp. 38022–38043, 2017.
- [45] J. Neefjes, M. L. M. Jongsma, P. Paul, and O. Bakke, "Towards a systems understanding of MHC class I and MHC class II antigen presentation," *Nature Reviews Immunology*, vol. 11, no. 12. Nature Publishing Group, pp. 823–836, 11-Dec-2011.
- [46] J. E. Smith-Garvin, G. A. Koretzky, and M. S. Jordan, "T Cell Activation," *Annu. Rev. Immunol.*, vol. 27, no. 1, pp. 591–619, Apr. 2009.
- [47] A. Lanzavecchia and F. Sallusto, "Regulation of T cell immunity by dendritic cells," *Cell*, vol. 106, no. 3. Cell Press, pp. 263–266, 10-Aug-2001.
- [48] L. M. Francisco, P. T. Sage, and A. H. Sharpe, "The PD-1 pathway in tolerance and autoimmunity," *Immunol. Rev.*, vol. 236, no. 1, pp. 219–242, Jun. 2010.
- [49] Y. Togashi, K. Shitara, and H. Nishikawa, "Regulatory T cells in cancer immunosuppression — implications for anticancer therapy," *Nature Reviews Clinical Oncology*, vol. 16, no. 6. Nature Publishing Group, pp. 356–371, 01-Jun-2019.
- [50] D. M. Pardoll, "The blockade of immune checkpoints in cancer immunotherapy," *Nature Reviews Cancer*, vol. 12, no. 4. pp. 252–264, Apr-2012.
- [51] P. Darvin, S. M. Toor, V. Sasidharan Nair, and E. Elkord, "Immune checkpoint inhibitors: recent progress and potential biomarkers," *Experimental and Molecular Medicine*, vol. 50, no. 12. Nature Publishing Group, 01-Dec-2018.
- [52] G. E. Kaiko, J. C. Horvat, K. W. Beagley, and P. M. Hansbro, "Immunological decision-making: How does the immune system decide to mount a helper T-cell response?," *Immunology*, vol. 123, no. 3. Wiley-Blackwell, pp. 326–338, Mar-2008.
- [53] R. Medzhitov, "Toll-like receptors and innate immunity," *Nature Reviews Immunology*, vol. 1, no. 2. European Association for Cardio-Thoracic Surgery, pp. 135–145, 2001.

- [54] S. H. van der Burg, R. Arens, F. Ossendorp, T. van Hall, and C. J. M. Melief, "Vaccines for established cancer: overcoming the challenges posed by immune evasion," *Nat. Rev. Cancer*, vol. 16, no. 4, pp. 219–233, Apr. 2016.
- [55] M. R. Sheen and S. Fiering, "In situ vaccination: Harvesting low hanging fruit on the cancer immunotherapy tree," *Wiley Interdisciplinary Reviews: Nanomedicine and Nanobiotechnology*, vol. 11, no. 1. Wiley-Blackwell, 01-Jan-2019.
- [56] M. Shi, X. Chen, K. Ye, Y. Yao, and Y. Li, "Application potential of toll-like receptors in cancer immunotherapy: Systematic review.," *Medicine (Baltimore)*, vol. 95, no. 25, p. e3951, Jun. 2016.
- [57] C. WB, "The Treatment of Malignant Tumors by Repeated Inoculations of Erysipelas: With a Report of Ten Original Cases," *Am. J. Med. Sci.*, vol. 10, pp. 487–511, 1893.
- [58] Y. Yang, C.-T. Huang, X. Huang, and D. M. Pardoll, "Persistent Toll-like receptor signals are required for reversal of regulatory T cell-mediated CD8 tolerance," *Nat. Immunol.*, vol. 5, no. 5, pp. 508–515, May 2004.
- [59] Y.-S. Lin et al., "In vitro and in vivo anticancer activity of a synthetic glycolipid as Toll-like receptor 4 (TLR4) activator.," *J. Biol. Chem.*, vol. 286, no. 51, pp. 43782–92, Dec. 2011.
- [60] J. Ye et al., "TLR8 signaling enhances tumor immunity by preventing tumor-induced T-cell senescence," *EMBO Mol. Med.*, vol. 6, no. 10, pp. 1294–1311, Oct. 2014.
- [61] B. Lin, B. Dutta, and I. D. C. Fraser, "Systematic Investigation of Multi-TLR Sensing Identifies Regulators of Sustained Gene Activation in Macrophages," *Cell Syst.*, vol. 5, no. 1, pp. 25–37.e3, Jul. 2017.
- [62] R. S. Ting Tan et al., "The synergy in cytokine production through MyD88-TRIF pathways is co-ordinated with ERK phosphorylation in macrophages," *Immunol. Cell Biol.*, vol. 91, no. 5, pp. 377–387, May 2013.
- [63] Y. Hu et al., "Synergy of TLR3 and 7 ligands significantly enhances function of DCs to present inactivated PRRSV antigen through TRIF/MyD88-NF- $\kappa$ B signaling pathway," *Sci. Rep.*, vol. 6, no. 1, pp. 1–15, Apr. 2016.
- [64] E. Vercammen, J. Staal, and R. Beyaert, "Sensing of viral infection and activation of innate immunity by toll-like receptor 3," *Clinical Microbiology Reviews*, vol. 21, no. 1. American Society for Microbiology Journals, pp. 13–25, 01-Jan-2008.
- [65] J. Miranda, K. Yaddanapudi, M. Hornig, and W. I. Lipkin, "Astrocytes recognize intracellular polyinosinic-polycytidylic acid via MDA-5," *FASEB J.*, vol. 23, no. 4, pp. 1064–1071, Apr. 2009.
- [66] C. Petes, N. Odoardi, and K. Gee, "The Toll for trafficking: Toll-like receptor 7 delivery to the endosome," *Frontiers in Immunology*, vol. 8, no. SEP. Frontiers Media S.A., p. 1, 04-Sep-2017.

- [67] L. Huang, H. Xu, and G. Peng, "TLR-mediated metabolic reprogramming in the tumor microenvironment: potential novel strategies for cancer immunotherapy," *Cell. Mol. Immunol.*, Mar. 2018.
- [68] E. Schutysse, S. Struyf, and J. Van Damme, "The CC chemokine CCL20 and its receptor CCR6," *Cytokine Growth Factor Rev.*, vol. 14, no. 5, pp. 409–426, Oct. 2003.
- [69] J. P. O. Hebb, A. Mosley, F. Vences Catalan, P. Ellmark, P. Norlen, and D. W. Felsner, "Intratumoral Administration of the Immunotherapeutic Combination Anti-ctla4, Anti-cd137 and Anti-ox40: Comparison to Systemic Administration, Peri-Draining Lymph Node Injection, and Cellular Vaccine in a Mouse Lymphoma Model," *Blood*, vol. 128, no. 22, pp. 4172–4172, Dec. 2016.
- [70] J. M. Kaminski, E. Shinohara, J. B. Summers, K. J. Niermann, A. Morimoto, and J. Brousal, "The controversial abscopal effect," *Cancer Treat. Rev.*, vol. 31, no. 3, pp. 159–172, 2005.
- [71] M. A. Aznar, N. Tinari, A. J. Rullán, A. R. Sánchez-Paulete, M. E. Rodriguez-Ruiz, and I. Melero, "Intratumoral Delivery of Immunotherapy-Act Locally, Think Globally,," *J. Immunol.*, vol. 198, no. 1, pp. 31–39, Jan. 2017.
- [72] M. R. Crittenden, U. Thanarajasingam, R. G. Vile, and M. J. Gough, "Intratumoral immunotherapy: Using the tumour against itself," *Immunology*, vol. 114, no. 1. Wiley-Blackwell, pp. 11–22, Jan-2005.
- [73] A. P. Castano, P. Mroz, and M. R. Hamblin, "Photodynamic therapy and anti-tumour immunity," *Nature Reviews Cancer*, vol. 6, no. 7. Nat Rev Cancer, pp. 535–545, Jul-2006.
- [74] M. C. Dieu et al., "Selective recruitment of immature and mature dendritic cells by distinct chemokines expressed in different anatomic sites,," *J. Exp. Med.*, vol. 188, no. 2, pp. 373–86, Jul. 1998.
- [75] F. Liao, R. L. Rabin, C. S. Smith, G. Sharma, T. B. Nutman, and J. M. Farber, "CC-chemokine receptor 6 is expressed on diverse memory subsets of T cells and determines responsiveness to macrophage inflammatory protein 3 alpha,," *J. Immunol.*, vol. 162, no. 1, pp. 186–94, Jan. 1999.
- [76] A. Al-Aoukaty, B. Rolstad, A. Giaid, and A. A. Maghazachi, "MIP-3alpha, MIP-3beta and fractalkine induce the locomotion and the mobilization of intracellular calcium, and activate the heterotrimeric G proteins in human natural killer cells," *Immunology*, vol. 95, no. 4, pp. 618–624, Dec. 1998.
- [77] M. Lee, C. S. Park, Y. R. Lee, S. A. Im, S. Song, and C. K. Lee, "Resiquimod, a TLR7/8 agonist, promotes differentiation of myeloid-derived suppressor cells into macrophages and dendritic cells," *Arch. Pharm. Res.*, vol. 37, no. 9, pp. 1234–1240, Apr. 2014.

- [78] S. Srivastava, M. A. Koch, M. Pepper, and D. J. Campbell, "Type I interferons directly inhibit regulatory T cells to allow optimal antiviral T cell responses during acute LCMV infection," *J. Exp. Med.*, vol. 211, no. 5, pp. 961–974, May 2014.
- [79] C. Wang et al., "The TLR7 agonist induces tumor regression both by promoting CD4+T cells proliferation and by reversing T regulatory cell-mediated suppression via dendritic cells," *Oncotarget*, vol. 6, no. 3, pp. 1779–1789, 2015.
- [80] H. Shime et al., "Toll-like receptor 3 signaling converts tumor-supporting myeloid cells to tumoricidal effectors," *Proc. Natl. Acad. Sci. U. S. A.*, vol. 109, no. 6, pp. 2066–2071, Feb. 2012.
- [81] A. Vidyarthi et al., "TLR-3 stimulation skews M2 macrophages to M1 through IFN- $\alpha\beta$  signaling and restricts tumor progression," *Front. Immunol.*, vol. 9, no. JUL, p. 1650, Jul. 2018.
- [82] M. L. Salem, C. M. Diaz-Montero, S. A. EL-Naggar, Y. Chen, O. Moussa, and D. J. Cole, "The TLR3 agonist poly(I:C) targets CD8+ T cells and augments their antigen-specific responses upon their adoptive transfer into naïve recipient mice," *Vaccine*, vol. 27, no. 4, pp. 549–557, Jan. 2009.
- [83] E. V. Acosta-Rodriguez et al., "Surface phenotype and antigenic specificity of human interleukin 17-producing T helper memory cells," *Nat. Immunol.*, vol. 8, no. 6, pp. 639–646, Jun. 2007.
- [84] S. Yamashiro, J. M. Wang, D. Yang, W. H. Gong, H. Kamohara, and T. Yoshimura, "Expression of CCR6 and CD83 by cytokine-activated human neutrophils," *Blood*, vol. 96, no. 12, pp. 3958–63, Dec. 2000.



2

# COMBINATORIAL PROSPECTS OF NANO-TARGETED CHEMOIMMUNOTHERAPY

Da Silva, C.G., Felix Rueda, Löwik C.W., Ferry Ossendorp, Luis J. Cruz  
*Biomaterials* 2016 Mar; 83:308-20.

# Abstract

---

Despite the significant increase in our knowledge on cancer initiation and progression, and the development of novel cancer treatments, overall patient survival rates have thus far only marginally improved. However, it can be expected that lasting tumor control will be attainable for an increasing number of cancer patients in the foreseeable future, which is likely to be achieved by combining cancer chemotherapy with anticancer immunotherapy. A plethora of new cancer chemotherapy reagents are expected to become accessible to the clinic in the coming years which can then be used for efficient tumor debulking and aid in antigen exposure to the immune system. Durable remission and the eradication of micrometastases are likely to be achieved with specialized monoclonal antibodies and therapeutic cancer vaccines that modulate the immune system to overcome immunosuppression and kill distant cancer cells. Moreover, the method of drug delivery to tumors, stromal and immune cells is expected to shift largely from conventional 'free' drug molecules to encapsulated in targeted nano-vehicles, therapeutics often referred to or considered part of "nanomedicine". Several biocompatible nano-vehicles, such as metal-nanoparticles, biodegradable-nanoparticles, liposomes or dendrimers are potential candidates for targeted drug delivery but may also serve additional purposes. A dexterous combination of nanomedicine, cancer immunotherapy and chemotherapeutic engineering are likely to become the basis for new hope in the form of targeted cancer therapies that could attack tumors early in their development. One can envision nano-vehicles that would selectively deliver effective doses of chemotherapeutic agents to cancer cells while leaving healthy cells untouched. Furthermore, given that after chemotherapeutic treatment there often remains a limited number of



chemo-resistant tumor cells, which go on to drive tumor progression, nano-vehicles could also be engineered to provoke an appropriate immune response to destroy these cells. Here, we discuss the potential of the combinatorial role of cancer chemotherapy, cancer immunotherapy and the prospective of nanotechnology for the targeted delivery of chemoimmunotherapeutic agents.

## 1. INTRODUCTION

Cancer chemotherapy regimens, together with surgery and radiotherapy, are currently the main means of tumor mass debulking. Unfortunately these methods of intervention are often insufficient to cure cancer patients and relapse commonly follows due to clinically undetectable micrometastases. It is tempting to speculate that a combination of cancer chemotherapy, to deplete tumor cells, combined with immunotherapy, to prevent relapses, could increase patients' outcome. In fact, some types of chemotherapies reduce the number of regulatory, immunosuppressive, T cells (Tregs) in the tumor, allowing a more immune-favorable environment to form, thereby clearing a path for an effector and memory T cell response to act in concert to destroy cancer cells.<sup>1</sup> There is evidence that the phenotype and function of the immune infiltrates in tumors markedly affect prognosis of the most common cancer types and patient's outcome may be predicted following cancer chemotherapy by the characteristics of the anti-cancer specific immune responses.<sup>2</sup> Furthermore, considering the advantages and disadvantages of existing cancer therapies, a new approach in which cancer chemotherapy and immunotherapy are rationally combined is conceivably quite more effective than either modality alone. However, drug combinations are also likely to increase treatment costs and induce systemic toxicity, an issue that will need to be carefully evaluated during pre-clinical research and clinical trials.

Although a high dose of cytotoxic chemotherapeutics is immunosuppressive, and may lead to lymphopenia, properly dosed and scheduled chemotherapy can rather facilitate, and not inhibit, an immune response against cancer cells.<sup>3</sup> In more recent years it has become apparent that a few specific chemotherapeutic drugs have an attribute, in addition to conventional killing of tumor cells, that is to induce a distinct -immunogenic- form of cell death or by directly having an activating effect on immune cells when provided at low doses.<sup>4,5</sup> Therefore, low doses of immunogenic chemotherapy may synergize with other forms of immunotherapy.

In the emerging field of nanomedicine, nano-sized tools are deployed that generally aim to improve pharmacological therapies, as well as to introduce novel modalities in disease prevention, diagnosis and treatment.<sup>6</sup> Moreover, nanomedicine technology may increase the efficacy, and rationally integrate distinct modalities into one potent anti-cancer treatment. A major segment in this field is the assisted delivery of drugs, commonly with the purpose to decrease bio-distribution of a drug, thereby reducing off-target side effects, whilst increasing drug exposure to target cells only. There is also a significant segment that makes use of inherent physicochemical properties of nanomaterials themselves to achieve desired biological or chemical effects. For instance, photodynamic and photothermal therapy, and nano-agents used for molecular imaging.

In this review, we will describe the immunological state of the tumor microenvironment to illustrate the complex challenges that researchers are confronted with, and how nanotechnology is currently being adopted to improve contemporary and upcoming therapies. Next, we will describe and summarize the immunogenic properties of some commonly used chemotherapies and discuss how current approaches harness, and highlight the future potential, of rationally combined immunotherapy and chemotherapy using nanotechnology.

## 2. NANOMEDICINE

Recent developments in the field of nanomedicine have highlighted major advantages of nano-vehicles (NVs) in anti-cancer drug delivery with the aim to reduce systemic wide chemotherapy distribution and reducing adverse effects whilst increasing treatment efficacy.<sup>7</sup> These vehicles, with sizes ranging from the nano to the micro scale, are versatile and highly adaptable. A manifold of NV types are currently in research, such as NVs that react to a magnetic field, certain pH levels or temperatures, or convert light to heat and radical oxygen species. A distinct class of NVs is used for transport and delivery of therapeutic compounds of which several types are currently being developed, such as dendrimers, metallic nanoparticles, liposomes (LPs) and nanoparticles (NPs). From these, both LPs and NPs are of particular interest, as they have been proven to be biocompatible, to efficiently transport and deliver antigens to antigen presenting cells (APCs), but also to protect the antigens from degradation and to gradually release the antigens, thereby prolonging half-life. It has been demonstrated that LPs are suitable carriers

of antigens for efficient delivery to APCs for a variety of pathogens.<sup>8</sup> Among its many advantages, LPs are absent of toxicity, low immunogenic, do not induce hypersensitivity or form granuloma at the site of administration, are simple to make and are inexpensive. LPs that are taken-up via endocytosis by APCs, such as immature dendritic cells (DCs), result in a highly concentrated amount of intracellular (cytoplasmic) antigen, which favor cross-presentation via major histocompatibility complex (MHC; HLA region in humans) class I, pivotal to mount an effector T cell response.<sup>9,10</sup>

Unlike LPs, the advantages of NPs, such as the poly(lactic-co-glycolic acid; PLGA) particles, are the excellent stability benefiting long-term storage, and the exceptional biodegradability and biocompatibility. The catabolic remnants of the PLGA particle in the body are lactic and glycolic acid, both natural and non-toxic metabolites and PLGA particles have been used for decades in various therapeutic applications in the clinic. PLGA-NPs are FDA approved and like LPs its physicochemical properties can be manipulated for controlled time- and location-specific release of drugs. Particularly the size and type of coating determine the blood circulation time with particle size being the main determining factor. Particles < 20 to 30 nm in size are eliminated by renal excretion while particles > 300 nm are removed by opsonization (surface modulation) and are scavenged by circulating phagocytes and macrophages or are filtered by the liver and spleen.<sup>11,12</sup> The NP optimum circulation time size range is 70-300 nm and may be further enhanced with a surface polyethylene glycol (PEG) coating. PEGylation of NPs is reported to extend half-life, reduce immunogenicity and not to form any additional toxic metabolites.<sup>13,14</sup> Conversely, PEGylation has also been reported to decrease bioavailability, enhance serum protein binding and elicit immune responses.<sup>15</sup> From a chemical perspective, PEGylation provides a highly flexible platform that allows the attachment of chemical residues or useful molecules to target PLGA NPs to specific cells.<sup>16</sup>

## 2.1. ACTIVE AND PASSIVE TUMOR TARGETING

In the context of anti-cancer drug delivery, NVs can target the tumor in a passive or active manner. Passive targeting is a process of accumulation of NVs in solid tumors that occur due to the enhanced permeation and retention (EPR) effect, which is caused by leaky blood vessels in tumors, originated from unregulated secretion of angiogenic factors, and decreased lymphatic drainage.<sup>17</sup> The aberrant vasculature

decreases the efficient exchange of molecules into the bloodstream thereby allowing the accumulation and retention of NVs. The retention time is long enough to facilitate the NV uptake by cancer cells via pinocytosis or to be exploited by the NVs that use the retention time for self-disintegration and the release of its contents in the tumor cell and its surroundings.<sup>18</sup> In case of absence of the EPR effect, NV extravasation into the tumor bed is unlikely and therefore access to cancer cells is challenging, although some strategies may be employed to circumvent such obstacle.<sup>19,20</sup>

Interestingly, although the EPR effect does not always exist or found to be pronounced enough in cancer patients, in some cases it is possible to induce or augment the EPR effect, e.g. increase systolic blood pressure via slow angiotensin II infusion or the administration of topical nitroglycerin that is converted to nitric oxide in the tumor microenvironment.<sup>21,22</sup>

Active or targeted delivery may enhance drug delivery by covalent coupling of ligands on the NP surface (e.g. PEG residues) that increase the affinity of NVs to specific cells and may enhance retention and specific uptake.<sup>23</sup> Notwithstanding, the EPR effect is still indispensable to expose the target cells to the targeted NVs in the first place. Examples of targeting moieties that could be used are specific ligands or monoclonal antibodies targeting receptors, integrins and selectins found overexpressed in cancer cells. These targeting moieties are best directed to specific or overexpressed receptors with endocytic capability, such as the folate receptor or the gonadotropin-releasing hormone receptor, which are often found overexpressed in tumors.<sup>24–26</sup> A graphical overview depicting the main differences between passive and active tumor targeting is given in **Figure 1**.

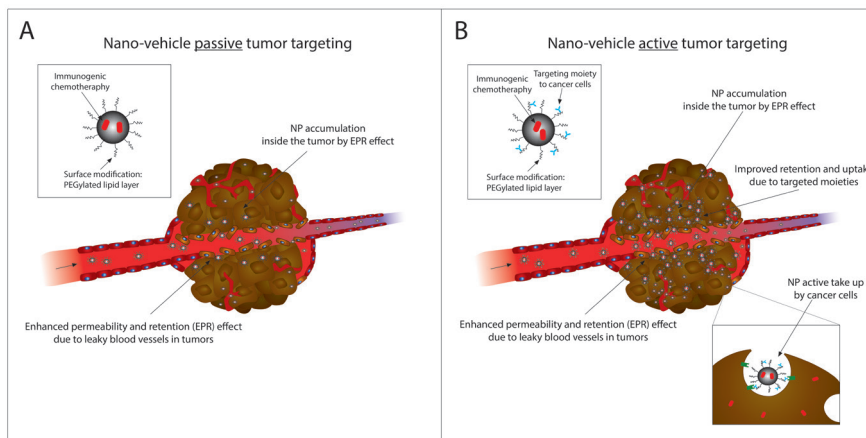


**Figure 1. An overview depicting the main differences between passive and active tumor targeting using nano-vehicles. A)** Nano-vehicles without targeting moieties accumulate in tumors exhibiting the EPR effect. **B)** Nano-vehicles with targeting moieties also accumulate in tumors exhibiting the EPR effect; however, the targeting moieties on the nano-vehicles enable more efficient retention and uptake of the nano-vehicles by cancer cells. Abbreviations: EPR: enhanced permeation and retention.

To illustrate that active targeting may indeed enhance target cell specific delivery under certain circumstances, Kirpotin et al. [27] coupled monoclonal antibodies against HER2 on LPs. Although both targeted and non-targeted LPs accumulated in the tumor equally well, the targeted LPs were found to be 6 fold more concentrated inside cancer cells while the non-targeted LPs were found mostly concentrated in the stroma and inside macrophages.

### 3. THE TUMOR IMMUNOSUPPRESSIVE MICROENVIRONMENT

Evading immune destruction by eluding immunogenicity or exhausting the extent of immunological killing is a recognized hallmark of cancer and several methods have been proposed that explain, at least in part, how some cancerous tumors can survive in an immunocompetent system.<sup>28</sup> A proposed hypothesis is that an immune response against cancer cells may actually have taken place before the tumor was clinically detectable and that the highly immunogenic cancer cell clones

were cleared while the weak immunogenic variants remained, a process known as immunoediting.<sup>29</sup> Another instance, or concurrent with immunoediting, is that the action of CD8+ cytotoxic T lymphocytes (CTLs) and natural killer cells is impaired by tumor- or tumor-stromal cells due to increased expression of negative co-stimulatory molecules, such as programmed cell death 1 receptor ligand 1 (PD-L1) or 2 (PD-L2) and the presence of high concentrations of immune inhibitory cytokines, such as the transforming growth factor beta (TGF $\beta$ ) and IL10.<sup>30-32</sup> In addition, distinct cells with immunosuppressive traits are also often found at the tumor site, such as Tregs, suppressor macrophages and M2-like type of macrophages, and myeloid-derived suppressor cells (MDSCs).<sup>33,34</sup> Tregs are known to significantly contribute to an immunosuppressed microenvironment by secreting high amounts of TGF $\beta$  and IL10 that inhibit CTLs and APCs anti-tumor function.<sup>35</sup> High expression of ectonucleotidases by Tregs also reduces the amount of extracellular ATP, secreted by dying cancer cells, thereby reducing immunogenicity and pro-inflammatory milieu.<sup>36</sup> In addition, Tregs were also found to exert immunosuppression by secreting exosome vesicles targeted to specific T helper and effector cells enriched in miRNAs with pro-apoptotic or anti-proliferative functions.<sup>37</sup>

On the other hand, suppressor macrophages in the tumor bed impede immune function through the induction of oxidative stress and secretion of immune suppressive cytokines. Oxidative stress that is induced by the secretion of reactive nitrogen and reactive oxygen intermediates, mainly disrupts the T cell receptor-CD3 complex, by interfering with the CD3  $\zeta$ -chain peptide expression, and disrupts the co-stimulatory CD3/CD28 interaction required for T cell activation and survival.<sup>38,39</sup> The complement of cytokines secreted by suppressor macrophages includes IL10, IL6 and tumor necrosis factor alpha (TNF $\alpha$ ).<sup>40</sup> Although TNF $\alpha$  is a potent pro-apoptotic cytokine, cancer cells are able to subvert TNF $\alpha$ 's effect by inducing the NF- $\kappa$ B-pathway. Based on the staging of tumorigenesis, some NF- $\kappa$ B pathway components may advocate a tumor promoter, instead of tumor suppressor, role of NF- $\kappa$ B pathway activation.<sup>41</sup> This effect is mainly achieved by subversion of apoptosis and enhancement of the production of immune suppressive cytokines, such as TGF $\beta$ , IL10, granulocyte macrophage colony-stimulating factor, granulocyte colony-stimulating factor and vascular endothelial growth factor, effectively suppressing the innate and adaptive immunity against the early stages of tumor development.

The M2-like type of macrophages, also known as alternatively activated macrophages, is another class of macrophage differentiation often found in tumors. This class of macrophages is mostly involved in mediating tissue repair with immunosuppressive traits that produce several anti-inflammatory cytokines and modulators, including IL10, TGF $\beta$ , IL1 receptor antagonist (IL1ra), IL2 $\alpha$  and arginase I.<sup>40,42</sup>

MDSCs are composed of a heterogeneous population of suppressive or immature dendritic cells, granulocytes, and early myeloid progenitors. They are able to efficiently impede an effector T cell response against cancer cells by expressing arginase I and inducible nitric oxide synthase.<sup>43</sup> As arginine is a pivotal amino acid for T cells, its deficiency induces severe dysfunctional effects including impeded cell division, T cell receptor complex and  $\zeta$ -chain peptide expression, as well as memory formation.<sup>44</sup> Additional T cell suppression is achieved through nitric oxide production by nitric oxide synthase which destabilizes IL2 mRNA and blocks the phosphorylation of Janus kinase 1 and 3, AKT, ERK, and STAT5, which are located downstream of IL2 and are regulators of T cell proliferation.<sup>45</sup> There is also accumulating evidence that MDSCs can mediate the recruitment and expansion of tumor-specific Tregs and actively contribute towards M2 type macrophage differentiation.<sup>46–48</sup>

In addition to viable cancer cells, apoptotic cancer cells also contribute to maintain an immunosuppressive microenvironment. As Sekar et al. [49] reported, priming DCs with apoptotic cancer cells prevented DCs from establishing cytotoxicity, as apoptotic cancer cells released sphingosine-1-phosphate. Sphingosine-1-phosphate induced DCs to produce IL27, which favors Treg cells thereby further contributing to tumor establishment.

Recent insights into the process on how tumors acquire an immunosuppressive environment reinforce the hypothesis that an anti-tumor effector response, such as of the CD8<sup>+</sup> T cell response, takes place but is possibly abrogated prematurely due to a negative feedback response.<sup>50</sup> Despite that the precise aetiology remains unknown, the overall effect is an impaired immune system that is incapable to effectively halt cancer progression.

## 4. CANCER IMMUNOTHERAPY

A key strategy in tumor immunology is to simultaneously disrupt the tumor immunosuppressed microenvironment, elicit a robust effector T cell response against several tumor epitopes and induce a sustainable immunological memory against a broad repertoire of cancer epitopes. In some cases, merely mounting or re(activating) a robust effector T cell response with specific immune adjuvants may provide enough momentum to overcome the tumor immunosuppressed microenvironment. Although tumor specific T cell immunity is often found in cancer patients, it is generally silenced, suppressed or tolerized and current efforts focus on (re)activating these T cells either by nonspecific or specific means.<sup>51-53</sup> Nonspecific (re)activation can be induced with check point blockers derived from humanized monoclonal antibodies such as nivolumab or ipilimumab. Nivolumab blocks the ligand activation of the PD-1 receptor on activated T cells, which is highly expressed by tumor cells. Ipilimumab binds to the cytotoxic T lymphocyte antigen 4 receptor thereby interrupting its tolerizing function. Both modalities are able to reduce the negative regulation of the immunological system in a nonspecific manner, thereby possibly inducing undesired auto-immune reactions. The non-antigen specific immune modulation of the tumor microenvironment with targeted NVs also appear to hold great potential. As reported by Kwong et al. [54] that deployed local LP-anchored anti-CD137 and IL2 that induced local and systemic antitumor immunity and cured established melanoma tumors in mice, while avoiding systemic toxicity induced by potent pro-inflammatory cytokines.

Alternatively, the inherent or adapted physicochemical properties of nanomaterials themselves may be harnessed to elicit non-antigen specific immune responses against cancers. For instance, photo-thermal tumor ablation using near infrared-absorbing nanoparticles was applied to successfully eradicate established colon tumors in mice.<sup>55</sup> Zhou et al. [56] reported the successful tumor eradication and long-term survival in mice by using an immunologically modified single-walled carbon nanotube system that killed cancer cells when the tumors were locally irradiated by a laser. This approach also induced potent anti-cancer immune responses triggered by the release of antigen and danger signals from the dying cancer cells. On the other hand, specific (re)activation also aims to break T cell clone tolerization but to specific antigens only, preferably ones that are unique or



highly expressed by cancer cells. This specific task can be achieved with several specialized immunotherapies, such as dendritic cell vaccination or therapeutic cancer vaccines (TCV).

Early TCV clinical trials where the treatment consisted of free not successful in eradicating cancer, however, current versions have been improved and a much higher rate of therapeutic success is expected in the near future. In addition to induce a robust immunological anti-tumor attack, TCV strategies must often specifically address the cancer mechanisms of immune defense and evasion. TCVs promise to be an elegant solution for tumor control and considerable advancements have been achieved in the last decade with the discovery of specific tumor antigens and tumor associated antigens. In addition, more detailed understanding of mechanisms of immunological evasion, tumor immunological recognition and destruction are contributing to better insights on how to improve TCVs. Some tumor antigens and several tumor associated antigens have been identified, which can be classified mainly into five categories: viral antigens that are associated with cancer development, mutated antigens or neo-antigens originated by chromosomal aberrations, differentiation antigens, cancer-testis or cancer germline antigens and overexpressed antigens (which can induce danger signals, but are prone to autoimmune diseases). Tumor antigens can stimulate cellular and/or humoral immune responses in cancer patients and the epitopes contained in tumor (associated) antigens are presented at the surface of cancer cells in the MHC class I molecules to cognate CD8+ T cells.<sup>57</sup> Some tumor antigens also contain epitopes for the MHC class II molecules on APCs and sometimes cancer cells, which can be recognized by cognate CD4+ T cells.<sup>58,59</sup>

The rationale behind TCVs is to onset a potent CD8+ effector CTL and a T helper type 1 (Th1) immune response against tumor antigens. The Th1 response is very effective in the activation of CTLs, memory formation and the production of associated cytokines such as IL1 $\beta$ , interferon gamma and TNF $\alpha$ . A Th1 response can be skewed by IL12 production by APCs. The induction of a T helper type 2 (Th2) immune response is less efficient because it mainly activates the humoral immunity by targeting B cells that produce non-cytolytic antibodies and IL4.<sup>60</sup> In addition to inducing a strong Th1 response, an effective TCV must also be able to induce a functional CD8+ central and effector memory subtypes in order to achieve durable and persistent tumor control.<sup>61,62</sup>

Some predicted challenges for tumor vaccines are the limited epitopes known and to properly modulate the immune system such to mount a robust enough effector response able to counteract the tumor immunosuppressed microenvironment. Furthermore, most self-derived neo-antigens generated by mutations or translocations linked to tumor development are likely poorly immunogenic and because of the use of predetermined antigens in tumor vaccines, immunoediting may take place rather than full tumor clearance. Albeit, new target epitopes are expected to be exposed after the initial tumor attack, which may allow the generation of new effector responses against these epitopes to be mounted, thereby maintaining the anti-tumor response momentum against a broader range of epitopes.

When tumors have become clinically detectable, they have, almost by definition, already mounted mechanisms to evade immune responses. This must be taken into consideration when designing an effective and durable anti-tumor immune strategy. Another foreseeable challenge is the availability of antigen specific reactive T cells. Thymic education has left only low-avidity and functionally suboptimal T cells specific for self-antigens or tumor antigens, a challenge that will be difficult to solve and is expected to play a role in cancer patients that are non-responsive to immunotherapy.

For further insight in TCVs, please refer to the thorough review of Melero et al. [63] that also include an overview of current TCV clinical trials.

NVs have also been pushed forward as ideal candidates to improve TCV by augmenting the quantity and quality of antigen-specific CTL responses against tumors. Specifically the ability for targeted and simultaneous delivery of antigen and immune stimulators render NVs an attractive method to improve TCVs.

As most antigen in the form of protein or peptides are non-immunogenic, most current formulations should include highly immunogenic adjuvants either soluble or encapsulated, such as ligands of the Toll-like receptors (TLR).<sup>5,64,65</sup> TLRs are part of a broad family of pattern-recognition receptors which recognize pathogens or damage-associated molecular patterns. Upon activation, an innate and adaptive response can be initiated. The specific aimed activation of TLRs in DCs will activate the NF- $\kappa$ B pathway, thereby inducing the production of IL12 and increase the expression of co-stimulatory receptors such as CD40. CD40 interacts with CD40L on T cells and CD80/86 that on their turn interact with CD28 or cytotoxic T lymphocyte

antigen 4 (its inhibitory counterpart) on T cells, amongst others.<sup>66-68</sup> Properly activating the TLR pathway is a potent and effective method to mature and activate DCs such to be able to reverse anergic T cell clones as found in advanced cancer patients.<sup>69,70</sup> Moreover, some TLR agonists were able to differentiate M2 type macrophages to an M1 phenotype and Tregs to (temporarily) cease the production of immune suppressive cytokines.<sup>69,71</sup> When screening for suitable TLR agonists, the target DC subtype is also relevant as several different DC subtypes have been identified that express different TLRs. Some TLRs are common to all DC subtypes while others are more specific, i.e. LC/dermal and CD141+ DCs express TLR3 but the same receptor will be less expressed in the CD1c+ DCs and monocyte-derived DC subsets whereas plasmacytoid DCs are described to express higher amounts of TLR7 and TLR9.<sup>72</sup> Some TLR agonists, such as the TLR3 ligand poly(I:C) and the TLR9 ligand CpG, are known to be able to convert the immunosuppressed tumor microenvironment from chronic to the intended acute inflammation thereby reducing the amount of Tregs present in the tumor.<sup>73</sup>

It has become evident that certain immune activating elements should be included in new strategies, although there is also reason to warrant caution. In addition to tumor hormesis for anti-cancer drugs and immunotherapy [74-76], cancer cells are commonly found to escape immune attack by altering and rewiring the activated NF- $\kappa$ B pathway to their advantage by increasing resistance against apoptosis and allowing more metastasis to occur regardless of the acute pro-inflammatory milieu.<sup>77,78</sup> Moreover, several different TLRs are in fact highly expressed in many tumors warranting that certain precaution measures should be taken not to use an unfavorable TLR agonist.<sup>79-83</sup> Alternatively, the (co)activation of nucleotide-binding oligomerization domain-like receptors could also induce an effective anti-tumor immune response.<sup>84,85</sup>

Several NVs have been described to be able to induce potent antigen-specific CTLs and anti-tumor responses. For instance, PLGA NPs have been reported to be successful transport and delivery agents for antigenic peptides to plasmacytoid DCs.<sup>86</sup> Several receptors have been described as viable targets for efficient delivery to DCs using uptake receptors such as C-type lectin DEC-205, blood DC Ag-2, CD40, CD11c, DC immunoreceptor or the FcR CD32.<sup>87-89</sup> Moreover, the concurrent delivery of TLR-ligands, e.g. R878 and unmethylated CpG oligonucleotides, were found to be potent pDC activators.<sup>90,91</sup> Moreover, a combination of antigen and

immune stimulants loaded into LPs has been shown to effectively induce antigen-specific T cell cytotoxicity and eradicate tumors.<sup>92</sup> Varypataki et al. [93] reported that the intradermal administration of cationic LPs, containing antigen and the immune adjuvant Poly (I:C), induced a 25 fold increase of the cognate CD8 T cells in mice as compared to non-encapsulated formulation. In an another study by Hansen et al. [94], cationic LPs were deployed carrying antigen and Poly (I:C) that significantly delayed tumor growth in melanoma and a lung cancer model in mice. Jérôme et al. [95] has shown that the generation of antigen-specific T cells was possible with a 1000 fold lower concentration of antigen when presented in LPs. In addition, the inclusion of the immune stimulant CpG in the LP formulation was shown to be imperative for the protection against low-immunogenic self-peptide presenting tumors in mice. A graphical overview depicting the main methods of TCV (also NV mediated) is given in **Figure 2**.

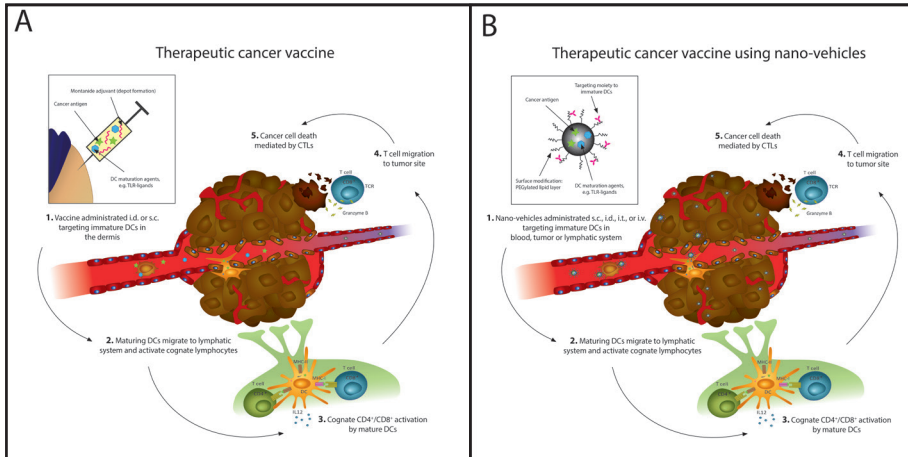


**Figure 2. An overview depicting the main steps in therapeutic cancer vaccines. A)** A cancer vaccine can be administered via a subcutaneous injection containing antigen and immunostimulants (e.g. TLR-ligands) in a depot forming solution. The resident antigen presenting cells, such as immature DCs, take-up the vaccine contents and migrate to lymphoid organs. Upon arrival at the lymphoid organs, the matured DCs present the antigenic peptides to, and activate, cognate lymphocytes. Specific cytotoxic T cells, such as CD8<sup>+</sup> T cells, migrate to the tumor area and eradicate cancer cells bearing the cognate antigen peptide. **B)** Immature dendritic cell targeted nano-vehicles containing antigen and immunostimulants (e.g. TLR-ligands) are administrated either via intravenous, intratumoral, intradermal, subcutaneous or oral (pill) route. The nano-vehicles are taken-up by immature DCs circulating in the blood, the tumor or lymphatic system after which the DCs migrate to lymphoid organs. Similarly to A, upon DC arrival at the lymphoid organs, the matured DCs present the antigenic peptides to, and activate, cognate lymphocytes. Specific cytotoxic T cells, such as CD8<sup>+</sup> T cells, migrate to the tumor area and eradicate cancer cells bearing the cognate antigen peptide. Abbreviations: CTLs: cytotoxic T lymphocytes; DCs: dendritic cells; i.d. intradermal; s.c.: subcutaneous; TLR: Toll-like receptor.

## 5. NANO-TARGETED CHEMOIMMUNOTHERAPY

It has become recently apparent that some chemotherapy types have a positive immunogenic effect on the tumor microenvironment.<sup>4,5</sup> One of these characteristics is the distinct induction of immunogenic cell death. The advantage of inducing immunogenic cell death is that the remains of the cancer cells themselves may serve as a “vaccine” and resemble the type of cell death that occurs in some other therapeutic modalities, such as photo-thermal and photodynamic therapy.<sup>96,97</sup>

Although the whole process of this unique form of cell death is not precisely understood, and is drug specific, some mechanisms have been described that involve the exposure or secretion of specific molecules. One of which is the pre-apoptotic exposure on the cell surface of calreticulin, an endoplasmic reticulum chaperone, or of heat-shock proteins, such as heat-shock protein 70 and 90, that are very potent phagocytosis signals to APCs.<sup>98,99</sup> Calreticulin is recognized by CD91 receptor on DCs while heat-shock proteins enhance cross-priming of tumor antigens to specific T cells.<sup>100–102</sup> Other strong cues leading to phagocytosis by APCs are the autophagy-dependent active secretion and extracellular accumulation of ATP as well as the nuclear non-histone high mobility group box 1 (HMGB1) proteins in the proximity of dying tumor cells.<sup>103–106</sup> ATP and HMGB1 can activate and induce maturation of DCs and stimulate the release of pro-inflammatory cytokines, such as IL1 $\beta$  and IL2.<sup>105,107</sup> Additionally to the presentation and secretion of immunogenic molecules, there are other immunogenic effects that occur in tumor cells. For example, Ramakrishnan et al. [108] recently described that paclitaxel, doxorubicin and cisplatin increased cancer cell sensitization to granzyme B, a serine protease secreted by CTLs cells, by a process that is mediated via upregulation of mannose-6-phosphate receptors on cancer cells. This process did not only take place on the cancer cells expressing the cognate antigen but also surrounding (cancer) cells that did not express the antigen. The authors hypothesized that this finding could be a possible explanation on how a limited amount of CTLs are able to mediate a potent anti-tumor effect when combined with specific types of cancer chemotherapy. In addition to the direct immunogenic effect on cancer cells, these chemotherapies can also be combined with immune adjuvants to further boost immune responses against cancer cells. For instance, Gou et al. [109] described a potent combination of oxaliplatin with IL7 that inhibited colon cancer metastasis in mice. In another

study, Bagchi [110] has shown that combining chlorambucil with obinutuzumab, an anti-CD20 antibody, substantially improved the progression-free and overall survival in patients with previously untreated chronic lymphocytic leukaemia. Despite that this type of immune modulation appears very promising, it is yet unclear whether these strategies are efficient and sufficient enough to overcome the tumor immunosuppressed microenvironment, cancer epitope T cell clone anergy or tolerization as often found in advanced cancer patients.<sup>2</sup> A graphical overview of the main immunogenic effects by (low dose) chemotherapy is given in **Figure 3**.

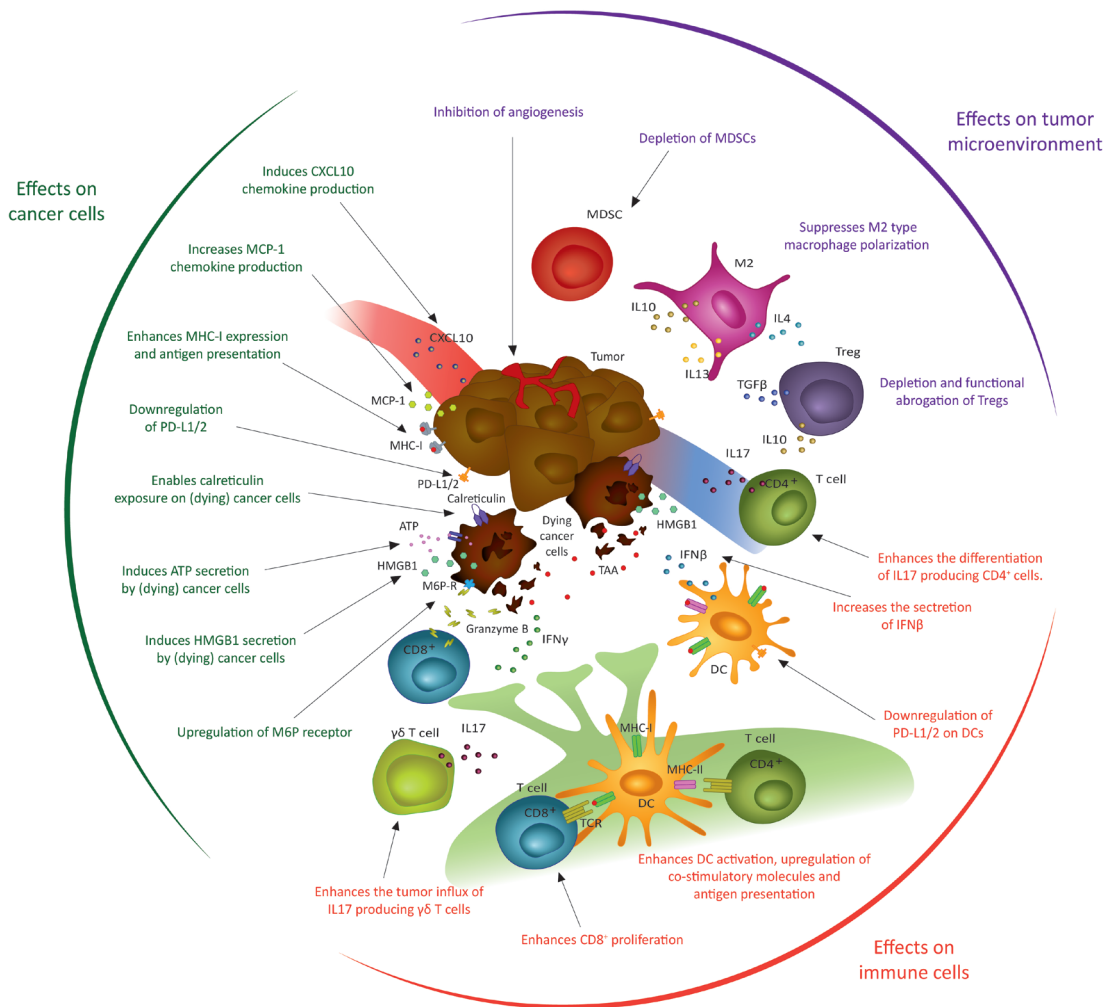


**Figure 3. Illustration of the main effects of (low dose) immunogenic chemotherapy directly on cancer cells, the tumor microenvironment and immune cells elsewhere. The individual effects of each immunogenic chemotherapy are given in Table 1.**

Abbreviations: HMGB1: nuclear non-histone high mobility group box 1; IFN $\beta$ : interferon beta; IFN $\gamma$ : interferon gamma; M6P: mannose-6-phosphate; MCP-1: macrophage chemoattractant protein-1; MDSCs: myeloid-derived suppressor cells; MHC: major histocompatibility complex; PD-L: programmed death-ligand; Tregs: regulatory T cells.



It is noteworthy to report that some immunogenic chemotherapies have been described to have ambivalent effects, exerting simultaneous positive and negative effects on the tumor. For example, 5-Fluorouracil (5-FU) can reduce the number of immune suppressive populations in the tumor. However, at the same time intracellular inflammasomes are triggered by 5-FU, in the remaining suppressive cells, which may lead to a signaling cascade to advert angiogenesis, regain tumor growth and promote metastasis.<sup>111,112</sup> Ambivalent function on anti-tumor immune responses has also been reported for bleomycin that enhances Treg cell proliferation, doxorubicin that upregulates the nuclear expression of CD274 conferring resistance against apoptosis and gemcitabine by a process similar to 5-FU. An overview with references of currently known chemotherapies that may aid the immune response to clear cancer cells is given in Table 1.

Table 1. List of chemotherapies reported to contribute to an immunological anti-tumor response. Table data was partially based on Galluzzi et al. [113] and was extended and updated.

<b>Agent</b>	<b>Mechanism</b>	<b>Refs.</b>
5-Fluorouracil	- Depletion of myeloid-derived suppressor cells.***	112,114–116
Bleomycin	- Enables calreticulin exposure on cancer cells.**/**	117
Carboplatin	- PD-L1 and PD-L2 downregulation on both human DCs and human tumor cells. - Increases macrophage chemoattractant protein-1 (MCP-1) expression by cancer cells.	118,119
Cisplatin	- PD-L2 downregulation (and PD-L1 to a lesser extent) on both human DCs and human tumor cells. - Sensitizes tumor cells to granzyme B by upregulation of the mannose-6-phosphatase receptors. - Enhances T cell proliferation by stimulating DC antigen presentation and IFN $\beta$ production. - Enhances monocyte and natural killer cell mediated cytotoxicity. - Enhances HMGB1 expression on (dying) cancer cells.** - Enhances the recruitment of macrophages and tumor-specific CD8+ T cells.*	108,118,120–125

Cyclophosphamide	<ul style="list-style-type: none"> <li>- Enhances homeostatic proliferation/activation of lymphocytes and specific tumor infiltration.</li> <li>- Enhances the differentiation of IL17 producing CD4+ cells.</li> <li>- Depletion and functional abrogation of regulatory T cells.*</li> <li>- Depletion of myeloid-derived suppressor cells.</li> <li>- Suppresses M2 type macrophage polarization and associated IL4, IL10 and IL13 production accordingly.</li> <li>- Increases MHC-I expression on tumor cells.</li> <li>- Preferential expansion of CD8<math>\alpha</math>+ DCs.</li> </ul>	126-136
Daunorubicin	<ul style="list-style-type: none"> <li>- Enhances antigen expression by tumor cells.</li> </ul>	137
Docetaxel	<ul style="list-style-type: none"> <li>- Enables calreticulin exposure on cancer cells.**</li> <li>- Depletion of myeloid-derived suppressor cells.</li> </ul>	138,139

Doxorubicin	<ul style="list-style-type: none"> <li>- Enhances antigen presentation by DCs.*</li> <li>- Enhances antigen presentation on cancer cells.</li> <li>- Sensitizes tumor cells to granzyme B by upregulation of the mannose-6-phosphatase receptors.</li> <li>- Enhances the tumor influx of IL17 producing <math>\gamma\delta</math> T cells preceding the accumulation of CTLs.</li> <li>- Enhances cancer antigen-specific, IFN<math>\gamma</math> producing CD8+ T cells in the tumor and stimulates CD8+ proliferation in the tumor draining lymph node.</li> <li>- Enables calreticulin exposure on cancer cells.**</li> <li>- Induces ATP secretion by dying cancer cells, which attracts inflammatory CD11c+CD11b+Ly6Chi cells into the tumor bed.**</li> <li>- Depletion of myeloid-derived suppressor cells.</li> <li>- Enhances DC activation (CD80 upregulation).</li> <li>- Induces a type I interferon response, including CXCL10 chemokine production.</li> <li>- PD-L1 downregulation on cancer cells.***</li> </ul>	100,108, 120,140-147
Gemcitabine	<ul style="list-style-type: none"> <li>- Increase HLA-I expression in tumor cells.</li> <li>- Enhances antigen presentation on cancer cells.</li> <li>- Depletion of myeloid-derived suppressor cells.***</li> <li>- Depletion of regulatory T cells.</li> </ul>	

Methotrexate	<ul style="list-style-type: none"> <li>- Enhances antigen presentation by DCs.*</li> <li>- Enables ATP secretion by dying cancer cells, which attracts inflammatory CD11c+CD11b+Ly6Chi cells into the tumor bed.**</li> <li>- Enhances DC activation (CD40, CD80 &amp; CD86 upregulation) and T cell proliferation.*</li> </ul>	140,143,154
Mitomycin-C	<ul style="list-style-type: none"> <li>- Enhances antigen presentation by DCs.*</li> <li>- Enhances DC activation (CD80 upregulation) and T cell proliferation.*</li> </ul>	140,154
Mitoxantrone	<ul style="list-style-type: none"> <li>- Enables calreticulin exposure on cancer cells.**</li> </ul>	100
Oxaliplatin	<ul style="list-style-type: none"> <li>- Increase HLA-I expression in tumor cells.</li> <li>- Sensitizes tumor cells to granzyme B by upregulation of the mannose-6-phosphatase receptors.</li> <li>- Enables calreticulin exposure on cancer cells.**</li> <li>- Induces a type I interferon response, including CXCL10 chemokine production.</li> </ul>	118,122,128,146

Paclitaxel	<ul style="list-style-type: none"> <li>- Enhances antigen presentation by DCs.*</li> <li>- Enhances antigen presentation on cancer cells.</li> <li>- Sensitizes tumor cells to granzyme B by upregulation of the mannose-6-phosphatase receptors.</li> <li>- Enhances DC activation (CD40, CD80 &amp; CD86 upregulation).*</li> <li>- Depletion and functional abrogation of regulatory T cells.</li> <li>- Increases macrophage chemoattractant protein-1 (MCP-1) expression by cancer cells.</li> <li>- Depletion of myeloid-derived suppressor cells.*</li> <li>- Prevents the tolerogenic state of DCs and myeloid-derived suppressor cells in the tumor microenvironment.*</li> </ul>	108,119,140,144, 154-159
Vinblastine	<ul style="list-style-type: none"> <li>- Enhances DC activation (CD40, CD80 &amp; CD86 upregulation).*</li> </ul>	154
Vincristine	<ul style="list-style-type: none"> <li>- Enhances DC activation (CD40 &amp; CD86 upregulation).*</li> <li>- Enhances antigen presentation by DCs.*</li> </ul>	140,154

\* When subjected to low (non-cytotoxic; metronomic) chemotherapy concentrations.

\*\* Immunogenic cancer cell death.

\*\*\* Ambivalent function described.

Although very promising, the combined treatment of immunotherapy with low dose immunogenic chemotherapy is not always favorable. For instance, the combination of alkylating chemotherapy and the induction of immune responses against neo-antigens, whereby the influence of Treg depletion is restricted, was found to be deleterious to responder lymphocytes.<sup>160,161</sup> However, this does not appear to be the case for self-antigens.

Moreover, most immunogenic chemotherapies appear to share the ability to deplete MDSCs from the tumor microenvironment. However, as tumor shrinkage also takes place due to cancer cells death, it is not always clear whether the reduction of MDSCs is a consequence of tumor size reduction or actually due to direct MDSCs killing by the immunogenic chemotherapy.

With the currently elucidated advantages of utilizing specific types of chemotherapy, that aid in tumor debulking and facilitate immune responses against cancer cells simultaneously, there may be additional benefit to combine these specific chemotherapies with other active immunotherapies by utilizing nanotechnology. For instance, Roy et al. [162,163] combined chemoimmunotherapy against cancer using PLGA NPs loaded with paclitaxel and the TLR4 agonist sodium salt of phthalate derivative of parent lipopolysaccharide was found more effective than any of the compounds alone. In addition, a higher number of CD4+ and CD8+ T cells, CD11c+, and CD14+ cells infiltrated the tumor and correlated to enhanced survival of mice than either standalone modalities. Another chemoimmunotherapeutic study combined doxorubicin with a carrier plasmid of unmethylated CpG oligonucleotides in an active delivery dendrimer bioconjugate, which yielded smaller tumors compared to any of the components alone.<sup>164</sup>

NVs can be modified with targeting moieties that increases cargo delivery specificity but are not only limited to be applied to standard cancer chemotherapeutic agents and TLR-agonists, they can be further adapted to modulate biological processes, including the immune system, in situ. As described by a study conducted by Calcinotto and colleagues [165], the authors conjugated TNF $\alpha$  to NGR, a tumor-homing peptide that recognizes an aminopeptidase N isoform that is selectively expressed by endothelial cells in tumor vessels. This TNF $\alpha$ -NGR conjugate combined with doxorubicin prolonged the survival of mice with B16OVA melanoma tumors and significantly increased the infiltration of CD8+ T cells into the tumor.

In a way, this is an elegant approach that directly addresses the finding of Motz et al. [166] that described that Fas-ligand expression by tumor endothelium aids in promoting tolerance in tumors by inducing apoptosis on activated effector T cells arriving at the tumor site.

Multi-step drug delivery of NPs has also recently been described by Sun et al. [167] that designed two distinct diblock copolymer NPs that fuse when in close proximity, such as in an endosome of a cell, but not while circulating in blood. This approach could enable novel applications in controlled release. For instance, one particle could carry an inactive form of a drug while the other NP acts as the activator of the same drug, thereby increasing target cell specificity whilst reducing drug adverse effects even further. Another considerable advantage of NPs is the prospect of drug delivery via the oral route. NPs can be formulated into a tablet or a pill carrying the drug. While the drug is protected from low pH, salts and enzymes from the stomach, the physicochemical parameters can be further adapted such to release the drug only at a specific pH thereby increasing the drug availability at the target site.<sup>168</sup> A study performed by Bhardwaj et al. [169] compared the efficacy of orally administrated paclitaxel loaded PLGA NPs against intravenous administrated native paclitaxel and found that the uptake via de oral route was not only feasible but improved the efficacy in chemical-induced breast cancer in rats. Similar experiments were also conducted with cisplatin loaded PLGA NPs, which yielded superior results compared to native intravenous cisplatin.<sup>170,171</sup> The prospect of cancer chemotherapy delivery as a “simple” pill, that can be taken orally, has great potential for cutting costs in the oncological health care, as patients will require less hospitalization and no intravenous administration of cancer chemotherapy, which reduces therapy burden. This method of oral administration becomes even more attractive if the application of the metronomic chemotherapy regimen, which entails the daily administration of chemotherapeutic agents at relatively low and minimally toxic doses, will become a future modality of anti-cancer therapy to delay solid tumor outgrowth.<sup>172,173</sup>

Furthermore, Morton et al. [174] described a process that used NPs for the dynamic rewiring of signaling pathways combined with cancer chemotherapy for enhanced tumor decimation. Not only did the authors combine tyrosine kinase inhibitors, such as erlotinib to rewire the apoptotic pathways, they designed their NPs in a specific



order that allowed a timed release of doxorubicin at the optimum moment when the cells were made most chemotherapy-prone.

Another aspect where NPs may be useful is in combating cancer chemotherapy resistant cancer cells. For instance, breast cancer cells are known to be initially sensitive to doxorubicin but resistance may occur when the cancer cells starts to overexpress the ABCG2 gene coding for the P-glycoprotein efflux transporter.<sup>175</sup> Doxorubicin enclosed in NPs is inherently less affected by efflux transporters compared to soluble doxorubicin while NPs coated with cyclosporin A, a P-glycoprotein inhibitor, were found to reduce the efflux of doxorubicin even further.<sup>176</sup>

Another known mechanism of doxorubicin resistance is the down-regulation of the expression of HuR, a RNA binding protein involved in the post-transcriptional regulation of a large range of mRNAs.<sup>177</sup> It would be compelling to unravel whether the sensitivity to doxorubicin resistant breast cancer cells could be restored, by using NPs that target both P-glycoprotein and HuR simultaneously. This may be possible by cyclosporine A coated NPs carrying doxorubicin and Rottlerin, a compound known to restore HuR expression.

Marrache et al. [178] recently proposed an elegant option to overcome cisplatin resistance, by adapting a PLGA NP, carrying cisplatin and guided with a triphenylphosphonium cation, aiming for cisplatin delivery not to the cell nucleus but to mitochondria. As mitochondria lack the nucleotide excision repair mechanism, the cells are not able to repair the mitochondrial DNA damage, favoring cell death. The PLGA NP was found to be 17 times more efficient against neuroblastoma cells compared to cisplatin alone.

There is also a large untapped therapeutic potential by merging cancer immunochemotherapy modalities with NP targeted delivery of shuttle vectors or RNA-guided genome editing complexes, as well as potentially beneficial combinations that include NF- $\kappa$ B pathway inhibitors, such as curcumin, to overcome chemotherapy resistance induced by tumor stromal cells in the tumor microenvironment.<sup>179</sup>

## 6. FUTURE PROSPECTS

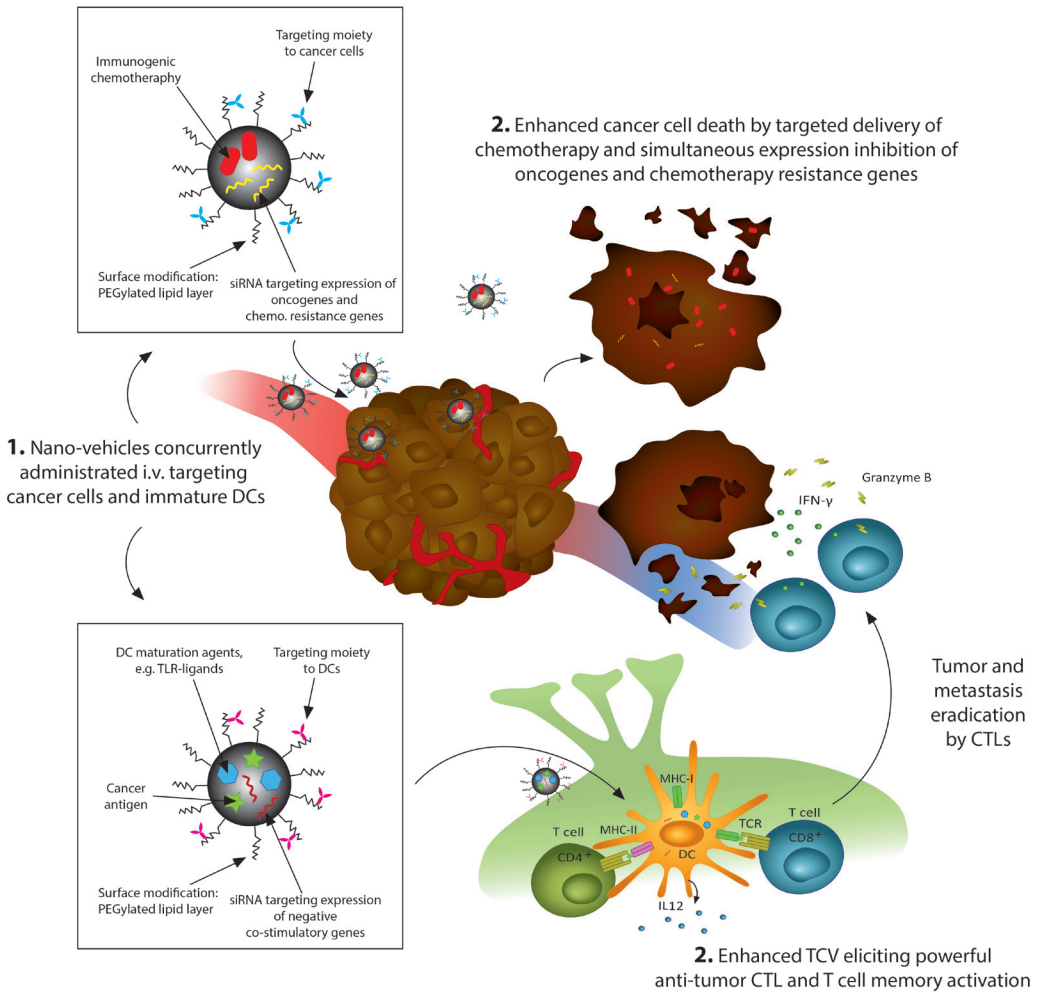
The new generation of NVs holds great promise to become the future backbone of medicine. With outstanding drug protection capabilities from the body secretion and catabolic processes, drugs previously only administrable via intravenous route may become available as NV encapsulated oral pills, potentially reducing health costs and therapy burden. Putative anticancer drugs that previously were discarded due to solubility issues may once again become potential therapeutic modalities. NVs also provide a flexible platform for novel and bold combinations, such as targeted immunogenic chemotherapy combined with local or systemic treatment with check point blockers that may yield synergistic effects and increase therapy efficacy further. Beside the possible reduction of therapy adverse effects by targeted delivery, NVs may aid in dye and contrast agent delivery to enable earlier and more accurate tumor and micrometastases detection. Moreover, NVs comprise of an untapped potential to regulate a plethora of biological processes, even in situ or organ specific, that may well reach beyond oncological therapy to cover an extent of other diseases.

To gain durable tumor control, the paradigm for cancer treatment must change from relatively nonspecific chemotherapy towards an increasingly targeted therapeutic approach. The therapy course is likely to compose targeted nano-vehicles encapsulating immunogenic cytotoxic agents combined with small molecules and immune adjuvants, aiming at vital tumor cell pathways, perturbing mechanisms of chemo resistance and immune evasion. The new generation of (nano-targeted) TCVs is coming of age and may well spark the first necessary step to halt tumor dissemination. New viable targeted modalities are impending candidates for future therapeutics in the treatment of early and advanced cancer disease.

As approximately twelve percent of human tumors are of viral aetiology, predominated by the human papillomavirus and by the hepatitis B/C virus, it would appear viable in the future to design efficient and standardized targeted TCVs against these tumors, that are likely to express unique viral antigens.<sup>180</sup>

Based on extensive immunological research over the last decades, we have learned how to harness, activate and modulate a suppressed immune potential to fight

cancer, enhancing cancer patients' survival and opening the doors for durable and efficient tumor control. Although considerable research is still required, there is a particular need to identify biomarkers that can predict which patients will benefit from chemoimmunotherapy from the patients that lack the necessary immune potential, such as cancer epitope T cell anergy or tolerization. Additionally, it is also currently unknown what the effect of chemoimmunotherapy is in effectively neutralizing the supporting tumor stroma, particularly in late stage cancer patients. A renewed outlook on NVs clinical prospective is likely to emerge as ideal delivery vehicles for gene therapy. In fact, a clinical trial is currently running that targets the mRNA of the M2 subunit of ribonucleotide reductase and another clinical trial that targets vascular endothelial growth factor and kinesin spindle protein, both using NPs as delivery agents.<sup>181,182</sup> It is tempting to speculate whether a combination of targeted NPs, one targeted to the tumor carrying chemotherapy and oncogene silencing by small interfering RNAs, and another targeting immature DCs, carrying antigen, TLR-ligands and small interfering RNAs against negative co-stimulatory mRNA molecules would yield even superior tumor clearance rates. A graphical representation of such a putative modality is given in **Figure 4**.



< **Figure 4. A putative modality for future treatment of cancer.** First, NPs targeting the overexpressed cancer cell receptors are efficiently taken-up by receptor-mediated endocytosis. The NPs contents are then released to the cytosol where the immunogenic chemotherapy promote the cancer cell death and at the same time the expression of driver oncogenes and genes mediating chemotherapy resistance are inhibited by the release of small interfering RNAs. As tumor growth is hampered, a time window is created for the immune system to mount an effective anti-tumor response and alleviate the immunosuppressive tumor microenvironment. Second, NPs targeting immature DCs are also administrated. The NPs deliver cancer antigens and immunostimulants, which activate DCs that migrate to the lymphatic system where the (matured) DCs present the antigenic peptides to, and activate, cognate lymphocytes. To improve the activation of lymphocytes further, the NPs also deliver small interfering RNAs that inhibit the expression of negative co-stimulatory receptors and cytokines. Specific cytotoxic T cells, such as CD8+ T cells, migrate to the tumor and metastasis areas and eradicate the remaining cancer cells bearing the cognate antigen peptide. Abbreviations: CTLs: cytotoxic T lymphocytes; DCs: dendritic cells; i.v.: intravenous; siRNA: small interfering RNA; TCV: therapeutic cancer vaccine; TLR: Toll-like receptor.

Finally, with the emergence of the ever more accurate RNA-guided genome editing complexes as well as improved targeted delivery agents, in situ gene repair and modulation may be within reach in the coming years as the ultimate treatment of a broad range of diseases. In addition to targeted delivery of therapeutics, targeted particulates can also be combined with highly precise nano-targeted molecular imaging compound to improve diagnostics, earlier-stage detection of disease, as well as real-time particulate tracking and visualization of therapy progression. There are a number of different probes coupled NVs reported to successfully enable molecular imaging, such as fluorocarbons, fluorescent and near-infrared dyes and <sup>19</sup>F isotopes, amongst others.<sup>183-186</sup>

## 7. CONCLUSION

Immunogenic chemotherapy, when provided at low but adequate doses, can efficiently kill cancer cells while additionally engage and stimulate the immune system. Further synergy may be achievable by rationally combining immunogenic chemotherapy with immunotherapy. Moreover, by using nanotechnology for the targeted delivery, the therapeutic effect may be augmented while side-effects are potentially reduced. As NVs have the potential of controlled release and multi-compound encapsulation, the co-delivery of immune adjuvants and small molecules, or combined with check point blockers, antibodies, and cancer vaccines, may possess an untapped potential to favorably incline the immune balance in the tumor allowing the immune system to eradicate tumors and distant metastasis.

### **Grant Support**

This work is part of the research programme 723.012.110 (Vidi), which is financed by the Netherlands Organisation for Scientific Research (NWO).

### **Acknowledgement**

Conception of idea: LJ Cruz and CG Da Silva; CG Da Silva collected initial literature, generated the graphical illustrations and drafted the first version; F. Rueda, CW Löwik and F Ossendorp revised the paper; Luis J. Cruz revised the paper and made final additions.

### **Declaration of interest**

The authors were supported by Leiden University Medical Center and the Netherlands Organisation for Scientific Research (NWO) funds. The authors have no other relevant affiliations or financial involvement with any organization or entity with a financial interest in or financial conflict with the subject matter or materials discussed in the manuscript apart from those disclosed.

## REFERENCES

1. Zitvogel, L., Galluzzi, L., Smyth, M. J. & Kroemer, G. Mechanism of action of conventional and targeted anticancer therapies: reinstating immunosurveillance. *Immunity* 39, 74–88 (2013).
2. Zitvogel, L., Kepp, O. & Kroemer, G. Immune parameters affecting the efficacy of chemotherapeutic regimens. *Nat. Rev. Clin. Oncol.* 8, 151–60 (2011).
3. Chen, G. & Emens, L. a. Chemoimmunotherapy: reengineering tumor immunity. *Cancer Immunol. Immunother.* 62, 203–16 (2013).
4. Casares, N. et al. Caspase-dependent immunogenicity of doxorubicin-induced tumor cell death. *J. Exp. Med.* 202, 1691–1701 (2005).
5. Vacchelli, E. et al. Trial Watch: Toll-like receptor agonists for cancer therapy. *Oncoimmunology* 2, e25238 (2013).
6. Duncan, R. & Gaspar, R. Nanomedicine(s) under the microscope. *Mol. Pharm.* 8, 2101–41 (2011).
7. Davis, M. E., Chen, Z. G. & Shin, D. M. Nanoparticle therapeutics: an emerging treatment modality for cancer. *Nat. Rev. Drug Discov.* 7, 771–82 (2008).
8. Henriksen-Lacey, M., Korsholm, K. S., Andersen, P., Perrie, Y. & Christensen, D. Liposomal vaccine delivery systems. *Expert Opin. Drug Deliv.* 8, 505–519 (2011).
9. Chikh, G. & Schutze-Redelmeier, M.-P. Liposomal delivery of CTL epitopes to dendritic cells. *Biosci. Rep.* 22, 339–353 (2002).
10. Whiteside, T. L. & Odoux, C. Dendritic cell biology and cancer therapy. *Cancer Immunol. Immunother.* 53, 240–8 (2004).
11. Mundargi, R. C., Babu, V. R., Rangaswamy, V., Patel, P. & Aminabhavi, T. M. Nano/micro technologies for delivering macromolecular therapeutics using poly(d,l-lactide-co-glycolide) and its derivatives. *J. Control. Release* 125, 193–209 (2008).
12. Moghimi, S. M., Hunter, A. C. & Andresen, T. L. Factors controlling nanoparticle pharmacokinetics: an integrated analysis and perspective. *Annu. Rev. Pharmacol. Toxicol.* 52, 481–503 (2012).
13. Zalipsky, S. Chemistry of polyethylene glycol conjugates with biologically. *Advanced Drug Delivery Reviews* 16, 157–182 (1995).
14. Milla, P., Dosio, F. & Cattal, L. PEGylation of proteins and liposomes: a powerful and flexible strategy to improve the drug delivery. *Curr. Drug Metab.* 13, 105–19 (2012).
15. Verhoef, J. J. F. & Anchordoquy, T. J. Questioning the Use of PEGylation for Drug Delivery. *Drug Deliv. Transl. Res.* 3, 499–503 (2013).

16. Cruz, L. J., Tacke, P. J., Fokkink, R. & Figdor, C. G. The influence of PEG chain length and targeting moiety on antibody-mediated delivery of nanoparticle vaccines to human dendritic cells. *Biomaterials* 32, 6791–803 (2011).
17. Acharya, S. & Sahoo, S. K. PLGA nanoparticles containing various anticancer agents and tumour delivery by EPR effect. *Adv. Drug Deliv. Rev.* 63, 170–83 (2011).
18. M Samarasinghe, R., K Kanwar, R. & R Kanwar, J. The role of nanomedicine in cell based therapeutics in cancer and inflammation. *Int. J. Mol. Cell. Med.* 1, 133–44 (2012).
19. Holback, H. & Yeo, Y. Intratumoral drug delivery with nanoparticulate carriers. *Pharm. Res.* 28, 1819–30 (2011).
20. Waite, C. L. & Roth, C. M. Nanoscale drug delivery systems for enhanced drug penetration into solid tumors: current progress and opportunities. *Crit. Rev. Biomed. Eng.* 40, 21–41 (2012).
21. Fang, J., Nakamura, H. & Maeda, H. The EPR effect: Unique features of tumor blood vessels for drug delivery, factors involved, and limitations and augmentation of the effect. *Adv. Drug Deliv. Rev.* 63, 136–51 (2011).
22. Kobayashi, H., Watanabe, R. & Choyke, P. L. Improving conventional enhanced permeability and retention (EPR) effects; what is the appropriate target? *Theranostics* 4, 81–9 (2013).
23. Talelli, M. et al. Intrinsically active nanobody-modified polymeric micelles for tumor-targeted combination therapy. *Biomaterials* 34, 1255–60 (2013).
24. Rothberg, K. G., Ying, Y. S., Kolhouse, J. F., Kamen, B. A. & Anderson, R. G. The glycosphospholipid-linked folate receptor internalizes folate without entering the clathrin-coated pit endocytic pathway. *J. Cell Biol.* 110, 637–649 (1990).
25. Stella, B. et al. Design of folic acid-conjugated nanoparticles for drug targeting. *J. Pharm. Sci.* 89, 1452–1464 (2000).
26. Tsutsui, K., Ubuka, T., Bentley, G. E. & Kriegsfeld, L. J. Gonadotropin-inhibitory hormone (GnIH): Discovery, progress and prospect. *General and Comparative Endocrinology* 177, 305–314 (2012).
27. Kirpotin, D. B. et al. Antibody targeting of long-circulating lipidic nanoparticles does not increase tumor localization but does increase internalization in animal models. *Cancer Res.* 66, 6732–40 (2006).
28. Hanahan, D. & Weinberg, R. A. Hallmarks of cancer: The next generation. *Cell* 144, 646–674 (2011).
29. Matsushita, H. et al. Cancer exome analysis reveals a T-cell-dependent mechanism of cancer immunoediting. *Nature* 482, 400–404 (2012).



30. Yang, L., Pang, Y. & Moses, H. L. TGF-beta and immune cells: an important regulatory axis in the tumor microenvironment and progression. *Trends Immunol.* 31, 220–7 (2010).
31. McDermott, D. F. & Atkins, M. B. PD-1 as a potential target in cancer therapy. *Cancer Med.* 2, 662–73 (2013).
32. Nishikawa, H. & Sakaguchi, S. Regulatory T cells in tumor immunity. *Int. J. Cancer* 127, 759–67 (2010).
33. Nagaraj, S. & Gabrilovich, D. I. Tumor escape mechanism governed by myeloid-derived suppressor cells. *Cancer Res.* 68, 2561–3 (2008).
34. Drake, C. G., Jaffee, E. & Pardoll, D. M. Mechanisms of immune evasion by tumors. *Adv. Immunol.* 90, 51–81 (2006).
35. O'Garra, A. & Vieira, P. Regulatory T cells and mechanisms of immune system control. *Nat. Med.* 10, 801–5 (2004).
36. Borsellino, G. et al. Expression of ectonucleotidase CD39 by Foxp3+ Treg cells: hydrolysis of extracellular ATP and immune suppression. *Blood* 110, 1225–32 (2007).
37. Okoye, I. S. et al. MicroRNA-Containing T-Regulatory-Cell-Derived Exosomes Suppress Pathogenic T Helper 1 Cells. *Immunity* 41, 89–103 (2014).
38. Otsuji, M., Kimura, Y., Aoe, T., Okamoto, Y. & Saito, T. Oxidative stress by tumor-derived macrophages suppresses the expression of CD3 zeta chain of T-cell receptor complex and antigen-specific T-cell responses. *Proc. Natl. Acad. Sci. U. S. A.* 93, 13119–24 (1996).
39. Kusmartsev, S. A., Li, Y. & Chen, S. H. Gr-1+ myeloid cells derived from tumor-bearing mice inhibit primary T cell activation induced through CD3/CD28 costimulation. *J. Immunol.* 165, 779–85 (2000).
40. Tomioka, H. et al. Characteristics of suppressor macrophages induced by mycobacterial and protozoal infections in relation to alternatively activated M2 macrophages. *Clin. Dev. Immunol.* 2012, 635451 (2012).
41. Wang, D. J., Ratnam, N. M., Byrd, J. C. & Guttridge, D. C. NF- $\kappa$ B Functions in Tumor Initiation by Suppressing the Surveillance of Both Innate and Adaptive Immune Cells. *Cell Rep.* (2014). doi:10.1016/j.celrep.2014.08.049
42. Biswas, S. K. & Mantovani, A. Macrophage plasticity and interaction with lymphocyte subsets: cancer as a paradigm. *Nat. Immunol.* 11, 889–96 (2010).
43. Serafini, P., Borrello, I. & Bronte, V. Myeloid suppressor cells in cancer: recruitment, phenotype, properties, and mechanisms of immune suppression. *Semin. Cancer Biol.* 16, 53–65 (2006).
44. Bronte, V., Serafini, P., Mazzoni, A., Segal, D. M. & Zanovello, P. L-arginine metabolism in myeloid cells controls T-lymphocyte functions. *Trends Immunol.* 24, 301–305 (2003).

45. Bronte, V. & Zanovello, P. Regulation of immune responses by L-arginine metabolism. *Nat. Rev. Immunol.* 5, 641–54 (2005).
46. Serafini, P., Mgebroff, S., Noonan, K. & Borrello, I. Myeloid-derived suppressor cells promote cross-tolerance in B-cell lymphoma by expanding regulatory T cells. *Cancer Res.* 68, 5439–49 (2008).
47. Sinha, P., Clements, V. K., Bunt, S. K., Albelda, S. M. & Ostrand-Rosenberg, S. Cross-Talk between Myeloid-Derived Suppressor Cells and Macrophages Subverts Tumor Immunity toward a Type 2 Response. *J. Immunol.* 179, 977–983 (2007).
48. Huang, B. et al. Gr-1+CD115+ immature myeloid suppressor cells mediate the development of tumor-induced T regulatory cells and T-cell anergy in tumor-bearing host. *Cancer Res.* 66, 1123–31 (2006).
49. Sekar, D., Hahn, C., Brüne, B., Roberts, E. & Weigert, A. Apoptotic tumor cells induce IL-27 release from human DCs to activate Treg cells that express CD69 and attenuate cytotoxicity. *Eur. J. Immunol.* 42, 1585–98 (2012).
50. Spranger, S. et al. Up-regulation of PD-L1, IDO, and T(regs) in the melanoma tumor microenvironment is driven by CD8(+) T cells. *Sci. Transl. Med.* 5, 200ra116 (2013).
51. Bindea, G., Mlecnik, B., Fridman, W. H., Pagès, F. & Galon, J. Natural immunity to cancer in humans. *Current Opinion in Immunology* 22, 215–222 (2010).
52. Ferrone, C. & Dranoff, G. Dual roles for immunity in gastrointestinal cancers. *J. Clin. Oncol.* 28, 4045–4051 (2010).
53. Nelson, B. H. The impact of T-cell immunity on ovarian cancer outcomes. *Immunol. Rev.* 222, 101–116 (2008).
54. Kwong, B., Gai, S. A., Elkhader, J., Wittrup, K. D. & Irvine, D. J. Localized immunotherapy via liposome-anchored Anti-CD137 + IL-2 prevents lethal toxicity and elicits local and systemic antitumor immunity. *Cancer Res.* 73, 1547–58 (2013).
55. O’Neal, D. P., Hirsch, L. R., Halas, N. J., Payne, J. D. & West, J. L. Photo-thermal tumor ablation in mice using near infrared-absorbing nanoparticles. *Cancer Lett.* 209, 171–6 (2004).
56. Zhou, F. et al. Antitumor immunologically modified carbon nanotubes for photothermal therapy. *Biomaterials* 33, 3235–42 (2012).
57. Moingeon, P. Cancer vaccines. *Vaccine* 19, 1305–1326 (2001).
58. Durrant, L. G. et al. Quantitation of MHC antigen expression on colorectal tumours and its association with tumour progression. *Br. J. Cancer* 56, 425–32 (1987).
59. Oldford, S. A., Robb, J. D., Watson, P. H. & Drover, S. HLA-DRB alleles are differentially expressed by tumor cells in breast carcinoma. *Int. J. Cancer* 112, 399–406 (2004).

60. Hannani, D. et al. Contribution of humoral immune responses to the antitumor effects mediated by anthracyclines. *Cell Death Differ.* 21, 50–8 (2014).
61. Klebanoff, C. A., Gattinoni, L. & Restifo, N. P. CD8+ T-cell memory in tumor immunology and immunotherapy. *Immunol. Rev.* 211, 214–224 (2006).
62. Perret, R. & Ronchese, F. Memory T cells in cancer immunotherapy: which CD8 T-cell population provides the best protection against tumours? *Tissue Antigens* 72, 187–194 (2008).
63. Melero, I. et al. Therapeutic vaccines for cancer: an overview of clinical trials. *Nat. Rev. Clin. Oncol.* 11, 509–24 (2014).
64. Zom, G. G. et al. Efficient induction of antitumor immunity by synthetic toll-like receptor ligand-peptide conjugates. *Cancer Immunol. Res.* 2, 756–64 (2014).
65. Zom, G. G. et al. Two in one: improving synthetic long peptide vaccines by combining antigen and adjuvant in one molecule. *Oncoimmunology* 3, e947892
66. Banchereau, J. et al. The CD40 antigen and its ligand. *Annu. Rev. Immunol.* 12, 881–922 (1994).
67. Linsley, P. S. & Ledbetter, J. A. The role of the CD28 receptor during T cell responses to antigen. *Annu. Rev. Immunol.* 11, 191–212 (1993).
68. Linsley, P. S. et al. CTLA-4 is a second receptor for the B cell activation antigen B7. *J. Exp. Med.* 174, 561–569 (1991).
69. Yang, Y., Huang, C.-T., Huang, X. & Pardoll, D. M. Persistent Toll-like receptor signals are required for reversal of regulatory T cell-mediated CD8 tolerance. *Nat. Immunol.* 5, 508–515 (2004).
70. Rouas, R. et al. Poly(I:C) used for human dendritic cell maturation preserves their ability to secondarily secrete bioactive IL-12. *Int. Immunol.* 16, 767–773 (2004).
71. Lin, Y.-S. et al. In Vitro and in Vivo Anticancer Activity of a Synthetic Glycolipid as Toll-like Receptor 4 (TLR4) Activator. *Journal of Biological Chemistry* 286, 43782–43792 (2011).
72. Radford, K. J., Tullett, K. M. & Lahoud, M. H. Dendritic cells and cancer immunotherapy. *Curr. Opin. Immunol.* 27C, 26–32 (2014).
73. Xiao, H. et al. Local Administration of TLR Ligands Rescues the Function of Tumor-Infiltrating CD8 T Cells and Enhances the Antitumor Effect of Lentivector Immunization. *J. Immunol.* 190, 5866–73 (2013).
74. Calabrese, E. J. & Blain, R. B. The hormesis database: the occurrence of hormetic dose responses in the toxicological literature. *Regul. Toxicol. Pharmacol.* 61, 73–81 (2011).

75. Pearce, O. M., Läubli, H., Bui, J. & Varki, A. Hormesis in cancer immunology: Does the quantity of an immune reactant matter? *Oncoimmunology* 3, e29312 (2014).
76. Calabrese, E. J. & Nascarella, M. A. Tumor resistance explained by hormesis. *Dose. Response.* 8, 80–2 (2010).
77. Kelly, M. G. et al. TLR-4 signaling promotes tumor growth and paclitaxel chemoresistance in ovarian cancer. *Cancer Res.* 66, 3859–3868 (2006).
78. Chen, R., Alvero, A. B., Silasi, D.-A. & Mor, G. Inflammation, cancer and chemoresistance: taking advantage of the toll-like receptor signaling pathway. *Am. J. Reprod. Immunol.* 57, 93–107 (2007).
79. Basith, S., Manavalan, B., Yoo, T. H., Kim, S. G. & Choi, S. Roles of toll-like receptors in cancer: a double-edged sword for defense and offense. *Arch. Pharm. Res.* 35, 1297–316 (2012).
80. Yan, J., Hua, F., Liu, H., Yang, H. & Hu, Z. Simultaneous TLR2 inhibition and TLR9 activation synergistically suppress tumor metastasis in mice. *Acta Pharmacologica Sinica* 33, 503–512 (2012).
81. Zanin-Zhorov, A. et al. Heat shock protein 60 enhances CD4+ CD25+ regulatory T cell function via innate TLR2 signaling. *J. Clin. Invest.* 116, 2022–2032 (2006).
82. Yang, H.-Z. et al. Blocking TLR2 activity attenuates pulmonary metastases of tumor. *PLoS One* 4, e6520 (2009).
83. Kim, S. et al. Carcinoma-produced factors activate myeloid cells through TLR2 to stimulate metastasis. *Nature* 457, 102–106 (2009).
84. Garaude, J., Kent, A., van Rooijen, N. & Blander, J. M. Simultaneous Targeting of Toll- and Nod-Like Receptors Induces Effective Tumor-Specific Immune Responses. *Science Translational Medicine* 4, 120ra16–120ra16 (2012).
85. Willems, M. M. J. H. P. et al. Design, automated synthesis and immunological evaluation of NOD2-ligand-antigen conjugates. *Beilstein J. Org. Chem.* 10, 1445–53 (2014).
86. Cruz, L. J. et al. Targeting nanoparticles to dendritic cells for immunotherapy. *Methods Enzymol.* 509, 143–63 (2012).
87. Tel, J. et al. Targeting uptake receptors on human plasmacytoid dendritic cells triggers antigen cross-presentation and robust type I IFN secretion. *J. Immunol.* 191, 5005–12 (2013).
88. Cruz, L. J. et al. Targeting nanoparticles to CD40, DEC-205 or CD11c molecules on dendritic cells for efficient CD8(+) T cell response: A comparative study. *J. Control. Release* (2014).  
doi:10.1016/j.jconrel.2014.07.040

89. Rosalia, R. A. et al. CD40-targeted dendritic cell delivery of PLGA-nanoparticle vaccines induce potent anti-tumor responses. *Biomaterials* 40, 88–97 (2015).
90. Tel, J. et al. Human plasmacytoid dendritic cells phagocytose, process, and present exogenous particulate antigen. *J. Immunol.* 184, 4276–83 (2010).
91. Tacken, P. J. et al. Targeted delivery of TLR ligands to human and mouse dendritic cells strongly enhances adjuvanticity. *Blood* 118, 6836–44 (2011).
92. Chen, W., Yan, W. & Huang, L. A simple but effective cancer vaccine consisting of an antigen and a cationic lipid. *Cancer Immunol. Immunother.* 57, 517–30 (2008).
93. Varypataki, E. M., van der Maaden, K., Bouwstra, J., Ossendorp, F. & Jiskoot, W. Cationic Liposomes Loaded with a Synthetic Long Peptide and Poly(I:C): a Defined Adjuvanted Vaccine for Induction of Antigen-Specific T Cell Cytotoxicity. *AAPS J.* (2014). doi:10.1208/s12248-014-9686-4
94. Hansen, J. et al. CAF05: cationic liposomes that incorporate synthetic cord factor and poly(I:C) induce CTL immunity and reduce tumor burden in mice. *Cancer Immunol. Immunother.* 61, 893–903 (2012).
95. Jérôme, V., Graser, A., Müller, R., Kontermann, R. E. & Konur, A. Cytotoxic T lymphocytes responding to low dose TRP2 antigen are induced against B16 melanoma by liposome-encapsulated TRP2 peptide and CpG DNA adjuvant. *J. Immunother.* 29, 294–305
96. Korbelik, M., Zhang, W. & Merchant, S. Involvement of damage-associated molecular patterns in tumor response to photodynamic therapy: surface expression of calreticulin and high-mobility group box-1 release. *Cancer Immunol. Immunother.* 60, 1431–7 (2011).
97. Kleinovink, J. W. et al. Combination of photodynamic therapy and specific immunotherapy efficiently eradicates established tumors. *Clin. Cancer Res.* (2015). doi:10.1158/1078-0432.CCR-15-0515
98. Zitvogel, L. et al. Immunogenic tumor cell death for optimal anticancer therapy: the calreticulin exposure pathway. *Clin. Cancer Res.* 16, 3100–4 (2010).
99. Srivastava, P. Roles of heat-shock proteins in innate and adaptive immunity. *Nat. Rev. Immunol.* 2, 185–94 (2002).
100. Obeid, M. et al. Calreticulin exposure dictates the immunogenicity of cancer cell death. *Nat. Med.* 13, 54–61 (2007).
101. Garg, A. D. et al. A novel pathway combining calreticulin exposure and ATP secretion in immunogenic cancer cell death. *EMBO J.* 31, 1062–79 (2012).

102. Castellino, F. et al. Receptor-mediated uptake of antigen/heat shock protein complexes results in major histocompatibility complex class I antigen presentation via two distinct processing pathways. *J. Exp. Med.* 191, 1957–64 (2000).
103. Aymeric, L. et al. Tumor cell death and ATP release prime dendritic cells and efficient anticancer immunity. *Cancer Res.* 70, 855–8 (2010).
104. Michaud, M. et al. Autophagy-dependent anticancer immune responses induced by chemotherapeutic agents in mice. *Science* 334, 1573–7 (2011).
105. Apetoh, L. et al. Toll-like receptor 4-dependent contribution of the immune system to anticancer chemotherapy and radiotherapy. *Nat. Med.* 13, 1050–9 (2007).
106. Martins, I. et al. Molecular mechanisms of ATP secretion during immunogenic cell death. *Cell Death Differ.* 21, 79–91 (2014).
107. Ghiringhelli, F. et al. Activation of the NLRP3 inflammasome in dendritic cells induces IL-1 $\beta$ -dependent adaptive immunity against tumors. *Nat. Med.* 15, 1170–8 (2009).
108. Ramakrishnan, R. et al. Chemotherapy enhances tumor cell susceptibility to CTL-mediated killing during cancer immunotherapy in mice. *J. Clin. Invest.* 120, 1111–24 (2010).
109. Gou, H.-F., Huang, J., Shi, H.-S., Chen, X.-C. & Wang, Y.-S. Chemo-immunotherapy with oxaliplatin and interleukin-7 inhibits colon cancer metastasis in mice. *PLoS One* 9, e85789 (2014).
110. Bagcchi, S. Chemoimmunotherapy improves survival in CLL. *Lancet Oncol.* 15, e56 (2014).
111. Ghiringhelli, F., Bruchard, M. & Apetoh, L. Immune effects of 5-fluorouracil: Ambivalence matters. *Oncoimmunology* 2, e23139 (2013).
112. Bruchard, M. et al. Chemotherapy-triggered cathepsin B release in myeloid-derived suppressor cells activates the Nlrp3 inflammasome and promotes tumor growth. *Nat. Med.* 19, 57–64 (2013).
113. Galluzzi, L., Senovilla, L., Zitvogel, L. & Kroemer, G. The secret ally: immunostimulation by anticancer drugs. *Nat. Rev. Drug Discov.* 11, 215–33 (2012).
114. Vincent, J. et al. 5-Fluorouracil selectively kills tumor-associated myeloid-derived suppressor cells resulting in enhanced T cell-dependent antitumor immunity. *Cancer Res.* 70, 3052–61 (2010).
115. Kanterman, J. et al. Adverse Immunoregulatory Effects of 5FU and CPT11 Chemotherapy on Myeloid-Derived Suppressor Cells and Colorectal Cancer Outcomes. *Cancer Res.* (2014). doi:10.1158/0008-5472.CAN-14-0657

116. Geary, S. M., Lemke, C. D., Lubaroff, D. M. & Salem, A. K. The combination of a low-dose chemotherapeutic agent, 5-fluorouracil, and an adenoviral tumor vaccine has a synergistic benefit on survival in a tumor model system. *PLoS One* 8, e67904 (2013).
117. Bugaut, H. et al. Bleomycin exerts ambivalent antitumor immune effect by triggering both immunogenic cell death and proliferation of regulatory T cells. *PLoS One* 8, e65181 (2013).
118. Lesterhuis, W. J. et al. Platinum-based drugs disrupt STAT6-mediated suppression of immune responses against cancer in humans and mice. *J. Clin. Invest.* 121, 3100–8 (2011).
119. Geller, M. A., Bui-Nguyen, T. M., Rogers, L. M. & Ramakrishnan, S. Chemotherapy induces macrophage chemoattractant protein-1 production in ovarian cancer. *Int. J. Gynecol. Cancer* 20, 918–25 (2010).
120. Hu, J. et al. The effects of chemotherapeutic drugs on human monocyte-derived dendritic cell differentiation and antigen presentation. *Clin. Exp. Immunol.* 172, 490–9 (2013).
121. Kang, T. H. et al. Chemotherapy acts as an adjuvant to convert the tumor microenvironment into a highly permissive state for vaccination-induced antitumor immunity. *Cancer Res.* 73, 2493–504 (2013).
122. Tesniere, A. et al. Immunogenic death of colon cancer cells treated with oxaliplatin. *Oncogene* 29, 482–91 (2010).
123. Kleinerman, E. S., Zwelling, L. A. & Muchmore, A. V. Enhancement of naturally occurring human spontaneous monocyte-mediated cytotoxicity by cis-diamminedichloroplatinum(II). *Cancer Res.* 40, 3099–102 (1980).
124. Lichtenstein, A. K. & Pende, D. Enhancement of Natural Killer Cytotoxicity by cis-Diamminedichloroplatinum (II) in Vivo and in Vitro. *Cancer Res.* 46, 639–644 (1986).
125. Chang, C.-L. et al. Dose-dense chemotherapy improves mechanisms of antitumor immune response. *Cancer Res.* 73, 119–27 (2013).
126. Bracci, L. et al. Cyclophosphamide enhances the antitumor efficacy of adoptively transferred immune cells through the induction of cytokine expression, B-cell and T-cell homeostatic proliferation, and specific tumor infiltration. *Clin. Cancer Res.* 13, 644–53 (2007).
127. Lutsiak, M. E. C. et al. Inhibition of CD4(+)25+ T regulatory cell function implicated in enhanced immune response by low-dose cyclophosphamide. *Blood* 105, 2862–8 (2005).
128. Liu, W. M., Fowler, D. W., Smith, P. & Dalglish, A. G. Pre-treatment with chemotherapy can enhance the antigenicity and immunogenicity of tumours by promoting adaptive immune responses. *Br. J. Cancer* 102, 115–23 (2010).

129. Medina-Echeverez, J. et al. Successful colon cancer eradication after chemoimmunotherapy is associated with profound phenotypic change of intratumoral myeloid cells. *J. Immunol.* 186, 807–15 (2011).
130. Ghiringhelli, F. et al. Metronomic cyclophosphamide regimen selectively depletes CD4+CD25+ regulatory T cells and restores T and NK effector functions in end stage cancer patients. *Cancer Immunol. Immunother.* 56, 641–8 (2007).
131. Taieb, J. et al. Chemoimmunotherapy of tumors: cyclophosphamide synergizes with exosome based vaccines. *J. Immunol.* 176, 2722–9 (2006).
132. Viaud, S. et al. Cyclophosphamide induces differentiation of Th17 cells in cancer patients. *Cancer Res.* 71, 661–5 (2011).
133. Schiavoni, G. et al. Cyclophosphamide synergizes with type I interferons through systemic dendritic cell reactivation and induction of immunogenic tumor apoptosis. *Cancer Res.* 71, 768–78 (2011).
134. Guerriero, J. L. et al. DNA alkylating therapy induces tumor regression through an HMGB1-mediated activation of innate immunity. *J. Immunol.* 186, 3517–26 (2011).
135. Liu, J.-Y. et al. Single administration of low dose cyclophosphamide augments the antitumor effect of dendritic cell vaccine. *Cancer Immunol. Immunother.* 56, 1597–604 (2007).
136. Ghiringhelli, F. et al. CD4+CD25+ regulatory T cells suppress tumor immunity but are sensitive to cyclophosphamide which allows immunotherapy of established tumors to be curative. *Eur. J. Immunol.* 34, 336–44 (2004).
137. Haggerty, T. J. et al. Topoisomerase inhibitors modulate expression of melanocytic antigens and enhance T cell recognition of tumor cells. *Cancer Immunol. Immunother.* 60, 133–44 (2011).
138. Hodge, J. W. et al. Chemotherapy-induced immunogenic modulation of tumor cells enhances killing by cytotoxic T lymphocytes and is distinct from immunogenic cell death. *Int. J. Cancer* 133, 624–36 (2013).
139. Kodumudi, K. N. et al. A novel chemoimmunomodulating property of docetaxel: suppression of myeloid-derived suppressor cells in tumor bearers. *Clin. Cancer Res.* 16, 4583–94 (2010).
140. Shurin, G. V, Tourkova, I. L., Kaneno, R. & Shurin, M. R. Chemotherapeutic agents in noncytotoxic concentrations increase antigen presentation by dendritic cells via an IL-12-dependent mechanism. *J. Immunol.* 183, 137–44 (2009).
141. Ma, Y. et al. Contribution of IL-17-producing gamma delta T cells to the efficacy of anticancer chemotherapy. *J. Exp. Med.* 208, 491–503 (2011).



142. Mattarollo, S. R. et al. Pivotal role of innate and adaptive immunity in anthracycline chemotherapy of established tumors. *Cancer Res.* 71, 4809–20 (2011).
143. Ma, Y. et al. Anticancer chemotherapy-induced intratumoral recruitment and differentiation of antigen-presenting cells. *Immunity* 38, 729–41 (2013).
144. Kaneno, R. et al. Chemotherapeutic agents in low noncytotoxic concentrations increase immunogenicity of human colon cancer cells. *Cell. Oncol. (Dordr.)* 34, 97–106 (2011).
145. Alizadeh, D. et al. Doxorubicin eliminates myeloid-derived suppressor cells and enhances the efficacy of adoptive T-cell transfer in breast cancer. *Cancer Res.* 74, 104–18 (2014).
146. Sistigu, A. et al. Cancer cell-autonomous contribution of type I interferon signaling to the efficacy of chemotherapy. *Nat. Med.* 20, 1301–1309 (2014).
147. Ghebeh, H. et al. Doxorubicin downregulates cell surface B7-H1 expression and upregulates its nuclear expression in breast cancer cells: role of B7-H1 as an anti-apoptotic molecule. *Breast Cancer Res.* 12, R48 (2010).
148. Nowak, A. K. et al. Induction of Tumor Cell Apoptosis In Vivo Increases Tumor Antigen Cross-Presentation, Cross-Priming Rather than Cross-Tolerizing Host Tumor-Specific CD8 T Cells. *J. Immunol.* 170, 4905–4913 (2003).
149. Mundy-Bosse, B. L. et al. Myeloid-derived suppressor cell inhibition of the IFN response in tumor-bearing mice. *Cancer Res.* 71, 5101–10 (2011).
150. Anyaegbu, C. C., Lake, R. A., Heel, K., Robinson, B. W. & Fisher, S. A. Chemotherapy enhances cross-presentation of nuclear tumor antigens. *PLoS One* 9, e107894 (2014).
151. Suzuki, E., Kapoor, V., Jassar, A. S., Kaiser, L. R. & Albelda, S. M. Gemcitabine selectively eliminates splenic Gr-1+/CD11b+ myeloid suppressor cells in tumor-bearing animals and enhances antitumor immune activity. *Clin. Cancer Res.* 11, 6713–21 (2005).
152. Mortara, L. et al. Schedule-dependent therapeutic efficacy of L19mTNF- $\alpha$  and melphalan combined with gemcitabine. *Cancer Med.* 2, 478–87 (2013).
153. Ko, H.-J. et al. A combination of chemoimmunotherapies can efficiently break self-tolerance and induce antitumor immunity in a tolerogenic murine tumor model. *Cancer Res.* 67, 7477–86 (2007).
154. Kaneno, R., Shurin, G. V., Tourkova, I. L. & Shurin, M. R. Chemomodulation of human dendritic cell function by antineoplastic agents in low noncytotoxic concentrations. *J. Transl. Med.* 7, 58 (2009).

155. Zhu, Y., Liu, N., Xiong, S. D., Zheng, Y. J. & Chu, Y. W. CD4+Foxp3+ regulatory T-cell impairment by paclitaxel is independent of toll-like receptor 4. *Scand. J. Immunol.* 73, 301–8 (2011).
156. Liechtenstein, T. et al. A highly efficient tumor-infiltrating MDSC differentiation system for discovery of anti-neoplastic targets, which circumvents the need for tumor establishment in mice. *Oncotarget* 5, 7843–7857 (2014).
157. Michels, T. et al. Paclitaxel promotes differentiation of myeloid-derived suppressor cells into dendritic cells in vitro in a TLR4-independent manner. *J. Immunotoxicol.* 9, 292–300
158. Zhong, H. et al. Origin and pharmacological modulation of tumor-associated regulatory dendritic cells. *Int. J. Cancer* 134, 2633–45 (2014).
159. Sevko, A. et al. Antitumor effect of paclitaxel is mediated by inhibition of myeloid-derived suppressor cells and chronic inflammation in the spontaneous melanoma model. *J. Immunol.* 190, 2464–71 (2013).
160. Litterman, A. J., Dudek, A. Z. & Largaespada, D. A. Alkylating chemotherapy may exert a uniquely deleterious effect upon neo-antigen-targeting anticancer vaccination. *Oncoimmunology* 2, e26294 (2013).
161. Litterman, A. J. et al. Profound impairment of adaptive immune responses by alkylating chemotherapy. *J. Immunol.* 190, 6259–68 (2013).
162. Roy, A., Singh, M. S., Upadhyay, P. & Bhaskar, S. Combined chemo-immunotherapy as a prospective strategy to combat cancer: a nanoparticle based approach. *Mol. Pharm.* 7, 1778–88 (2010).
163. Roy, A., Singh, M. S., Upadhyay, P. & Bhaskar, S. Nanoparticle mediated co-delivery of paclitaxel and a TLR-4 agonist results in tumor regression and enhanced immune response in the tumor microenvironment of a mouse model. *Int. J. Pharm.* 445, 171–80 (2013).
164. Lee, I.-H. et al. Targeted chemoimmunotherapy using drug-loaded aptamer-dendrimer bioconjugates. *J. Control. Release* 155, 435–41 (2011).
165. Calcinotto, A. et al. Targeting TNF- $\alpha$  to neoangiogenic vessels enhances lymphocyte infiltration in tumors and increases the therapeutic potential of immunotherapy. *J. Immunol.* 188, 2687–94 (2012).
166. Motz, G. T. et al. Tumor endothelium FasL establishes a selective immune barrier promoting tolerance in tumors. *Nat. Med.* 1–11 (2014). doi:10.1038/nm.3541
167. Sun, L. et al. Structural reorganization of cylindrical nanoparticles triggered by polylactide stereocomplexation. *Nat. Commun.* 5, 5746 (2014).
168. Dai, J. et al. PH-sensitive nanoparticles for improving the oral bioavailability of cyclosporine a. *Int. J. Pharm.* 280, 229–240 (2004).

169. Bhardwaj, V. et al. PLGA nanoparticles stabilized with cationic surfactant: safety studies and application in oral delivery of paclitaxel to treat chemical-induced breast cancer in rat. *Pharm. Res.* 26, 2495–2503 (2009).
170. Avgoustakis, K. et al. PLGA-mPEG nanoparticles of cisplatin: In vitro nanoparticle degradation, in vitro drug release and in vivo drug residence in blood properties. *J. Control. Release* 79, 123–135 (2002).
171. Agrahari, V., Kabra, V. & Trivedi, P. in 13th International Conference on Biomedical Engineering SE - 326 (eds. Lim, C. & Goh, J. H.) 23, 1 325–1328 (Springer Berlin Heidelberg, 2009).
172. Hanahan, D., Bergers, G. & Bergsland, E. Less is more, regularly: metronomic dosing of cytotoxic drugs can target tumor angiogenesis in mice. *J. Clin. Invest.* 105, 1045–7 (2000).
173. André, N., Carré, M. & Pasquier, E. Metronomics: towards personalized chemotherapy? *Nat. Rev. Clin. Oncol.* (2014). doi:10.1038/nrclinonc.2014.89
174. Morton, S. W. et al. A Nanoparticle-Based Combination Chemotherapy Delivery System for Enhanced Tumor Killing by Dynamic Rewiring of Signaling Pathways. *Sci. Signal.* 7, ra44–ra44 (2014).
175. Doyle, L. A. et al. A multidrug resistance transporter from human MCF-7 breast cancer cells. *Proc. Natl. Acad. Sci. U. S. A.* 95, 15665–15670 (1998).
176. Xu, L. et al. Enhanced activity of doxorubicin in drug resistant A549 tumor cells by encapsulation of P-glycoprotein inhibitor in PLGA-based nanovectors. *Oncol. Lett.* 7, 387–392 (2014).
177. Latorre, E. et al. Downregulation of HuR as a new mechanism of doxorubicin resistance in breast cancer cells. *Molecular Cancer* 11, 13 (2012).
178. Marrache, S., Pathak, R. K. & Dhar, S. Detouring of cisplatin to access mitochondrial genome for overcoming resistance. *Proc. Natl. Acad. Sci. U. S. A.* 111, 10444–9 (2014).
179. Sun, Y. et al. Treatment-induced damage to the tumor microenvironment promotes prostate cancer therapy resistance through WNT16B. *Nat. Med.* 18, 1359–68 (2012).
180. Parkin, D. M. The global health burden of infection-associated cancers in the year 2002. *Int. J. Cancer* 118, 3030–44 (2006).
181. Davis, M. E. et al. Evidence of RNAi in humans from systemically administered siRNA via targeted nanoparticles. *Nature* 464, 1067–70 (2010).
182. Taberero, J. et al. First-in-humans trial of an RNA interference therapeutic targeting VEGF and KSP in cancer patients with liver involvement. *Cancer Discov.* 3, 406–17 (2013).

183. Rahimian, S. et al. Near-infrared labeled, ovalbumin loaded polymeric nanoparticles based on a hydrophilic polyester as model vaccine: In vivo tracking and evaluation of antigen-specific CD8(+) T cell immune response. *Biomaterials* 37C, 469–477 (2014).
184. Srinivas, M. et al. Customizable, multi-functional fluorocarbon nanoparticles for quantitative in vivo imaging using <sup>19</sup>F MRI and optical imaging. *Biomaterials* 31, 7070–7 (2010).
185. Verdijk, P. et al. Sensitivity of magnetic resonance imaging of dendritic cells for in vivo tracking of cellular cancer vaccines. *Int. J. Cancer* 120, 978–84 (2007).
186. Yang, Z. et al. Long-circulating near-infrared fluorescence core-cross-linked polymeric micelles: synthesis, characterization, and dual nuclear/optical imaging. *Biomacromolecules* 8, 3422–8 (2007).



3

# THE EFFECT OF INJECTION ROUTE OF PLGA NANOPARTICLES ON THE BIODISTRIBUTION AND ICG BLOOD CLEARANCE RATE IN TUMOR BEARING MICE

Da Silva, C.G., Ossendorp, F., Cruz L.J.

*Manuscript in preparation*

# Abstract

---

Poly(lactic-co-glycolic acid; PLGA) nanoparticles are used for cargo delivery in cancer treatments. We studied the biodistribution in the vital organs and ICG blood clearance rate upon injection of PLGA nanoparticles via the intratumoral, intravenous, and subcutaneous route in tumor bearing mice. For this purpose, we developed surrogate pegylated PLGA nanoparticles loaded with the near-infrared dye indocyanine green (ICG) for nanoparticle detection in the vital organs and to determine the ICG blood clearance rate.

## INTRODUCTION

There are several routes commonly chosen for nanoparticles administration in murine disease models for the optimal therapeutic efficacy and the induction of least adverse effects [1]. It has been well established that the physicochemical properties, such as size, shape, and surface charge, are key determinants of nanoparticles biodistribution and clearance [2]. Analysis of the optimal administration route of nanoparticles in preclinical research is important since it is pivotal for clinical translation and human application. Although there are only limited studies published, the biodistribution, clearance, and tumor uptake of inorganic carbon dots and of gold nanoparticles injected via several different routes have been determined [3–5]. The biodistribution of organic pegylated PLGA nanoparticles has been determined for the intravenous and oral routes on healthy mice but relatively under-examined on mice bearing tumors [6–8]. Most cancer treatments require a high concentration of drugs in the tumor to



attain their therapeutic effect, and as low as possible elsewhere in the healthy tissue to limit adverse effects. Therefore, it is common to leverage the maximum attainable drug concentration possible in the tumor against the maximum acceptable instances and/or severity of the adverse effects, which limits the anti-cancer therapeutic effects. Cancer drugs are most administered via the intravenous (IV) or oral route which enables the (bio)distribution and accumulation of the drugs throughout all tissue, including the tumor. One strategy to improve the drug accumulation ratio in the tumor versus healthy tissue is the intratumoral (IT) administration of cancer drugs. When the drugs are loaded into PLGA nanoparticles and injected via the IT route, it is possible to attain high drug concentration and local slow release of the drugs in the tumor. In this study, we set to determine the biodistribution of ICG-loaded nanoparticles in the vital organs and tumors when administered either via the IV, IT, or subcutaneous (SC) route in tumor bearing mice. In addition, we determined the ICG blood clearance rate upon the distinct administration routes.

## MATERIALS AND METHODS

### Materials and reagents

The PLGA polymer (lactide/glycolide molar ratio of 48:52 to 52:48) was purchased from Boehringer Ingelheim (Ingelheim am Rhein, Germany). Dichloromethane (DCM; CAS 75-09-2 CH<sub>2</sub>CL<sub>2</sub> MW 84.93) and polyvinyl alcohol (PVA; CAS 9002-89-5) were purchased from Sigma-Aldrich (Zwijndrecht, The Netherlands). Chloroform (CHCL<sub>3</sub> MW 119.38 g/mol) was purchased from Merck (Darmstadt, Germany). Lipid-PEG 2000 (1,2-Distearoyl-sn-Glycero-3-Phosphoethanolamine-N-[Methoxy(Polyethylene glycol)-2000]; powder MW 2805.54) was purchased from Avanti Polar Lipids (AL, USA). ICG dye was purchased from Sigma-Aldrich.

### Synthesis of the ICG-loaded pegylated PLGA NPs

The NPs were synthesized in an oil/water emulsion, using a solvent evaporation-extraction method as per described elsewhere [9,10]. Briefly, a 1.5 mL solution of DCM was prepared that contained 50 mg of PLGA and 0.5 mg of ICG dye. Next, the solution was added dropwise to 10 mL of aqueous 2.5% (w/v) PVA and emulsified for 120 s using a sonicator (250 watts; Sonifier 250; Branson, Danbury, USA). A new beaker was prepared that contained an air-dried solution of 10 mg of Lipid-PEG 2000 dissolved in 0.1 mL of chloroform. The previous solution containing the ICG dye was transferred to the new beaker that contained the Lipid-PEG film and the whole solution was

homogenized for 60 s by sonication and stored overnight at 4 °C under continuous stirring to allow evaporation of the solvent. Using ultracentrifugation (12,800 rpm for 30 minutes) and washing with distilled water (4x) at 4 °C the NPs were collected. Finally, the NPs were ready after 3 days of lyophilization.

### **Physicochemical properties of the NPs**

The average size, polydispersity index and surface charge (zeta-potential) of the NPs were determined by dynamic light scattering. A sample of 50 µg of the NPs was dissolved in 1 mL of ultrapure MilliQ H<sub>2</sub>O and measured for size using a Zetasizer (Nano ZS, Malvern Ltd., UK). By using the same device and sample, the NPs surface charge was determined by the laser Doppler electrophoresis method.

### **Cell lines**

The murine tumor cell line TC-1 (a gift from T.C. Wu, Johns Hopkins University, Baltimore, MD, USA) was generated by retroviral transduction of lung fibroblasts of C57BL/6 origin, to express the HPV16 E6 and E7 genes and the activated human c-Ha-ras oncogene [11]. The TC-1 cell line was cultured in DMEM medium (BioWhittaker, Verviers, Belgium) supplemented with 8% heat-inactivated fetal calf serum (FCS; Greiner bio-one, Alphen a/d Rijn, The Netherlands), penicillin (50 µg/mL; Gibco, Paisley, Scotland), streptomycin (50 µg/mL; Gibco), L-glutamine (2 mM; Gibco), β-mercaptoethanol (20 µM; Sigma, Saint Louis, USA), and Geneticin (G418; 400 µg/mL). Furthermore, regular PCR analysis was performed to assure the cells were free of mycoplasma and common rodent viruses.

### **Mice strains**

C57BL/6 (H-2b haplotype) and Balb/c female mice, between 8 to 12 weeks of age, were purchased from Charles River ('s-Hertogenbosch, The Netherlands). The mice were housed at the animal facility of Leiden University Medical Center under specific pathogen free conditions. All animal experiments were approved by the Dutch Central Committee on Animal Experimentation and were strictly conducted according to the Dutch animal welfare law.

### **Biodistribution and blood analysis**

The relative signal quantification in vital organs was performed by SC syngeneic inoculation with  $1 \times 10^5$  TC-1 cells in 0.2 mL PBS in the right flank of C57BL/6 mice. When the tumors became established, at nine days after tumor inoculation, 50 µL containing

500 µg of NPs (10 mg/mL) dissolved in PBS were administered either IT, SC (left flank) or IV via caudal vein injection. Approximately 25 µL of blood was collected from the caudal vein after 5, 120, 240, and 360 minutes, and 24 hours after the injection of NPs. Upon collection of the last blood sample the mice were euthanized, and the spleen, heart, kidneys, liver, lungs and tumors removed for further ex vivo analysis. The ICG-signal emitted from the organs and the blood was detected using a Li-Cor Odyssey scanner (Li-Cor Biosciences, Lincoln, NEBR, USA) set to scan at 800 nm and analysis were conducted using the Li-Cor Odyssey v3.0.21 software.

The overview images were acquired by following the same treatment protocol as described above. However, these experiments were performed on Balb/c mice inoculated SC with  $3 \times 10^5$  CT-26 cells in 0.2 mL PBS in the right flank and the images were acquired using the IVIS Spectrum In Vivo Imaging System (PerkinElmer, Ohio, USA) and the Living Image Software version 4.7 (PerkinElmer).

## RESULTS

### Physicochemical properties and in vitro characterization of the NPs

For this study, we synthesized PLGA NPs loaded with ICG near-infrared dye in an oil/water emulsion using a solvent evaporation-extraction method and the surface functionalized with pegylation. The ICG-loaded NPs were characterized for size and surface charge (Table 1). The size of the ICG-loaded NPs was found to be 268 nm on average (Table 1, Fig. 1A) and the surface charge  $-21$  mV (Table 1, Fig. 1B). The ICG signal in the ICG-loaded NPs was positively detected with an IVIS Spectrum in vivo imaging system (Figure 1C).

**Table 1. Physicochemical characterization of PLGA NPs**

NP	Size $\pm$ SD (nm)	PDI	$\zeta$ Potentia $\pm$ SD (mV)
NP(ICG)	267.6 $\pm$ 81.0	0.412	-21.7 $\pm$ 7.7

Physicochemical characterization of ICG-loaded NPs. The NPs were characterized by dynamic light scattering and zeta potential measurements. The size and zeta potential data represent the mean value  $\pm$  SD of 10 readings.

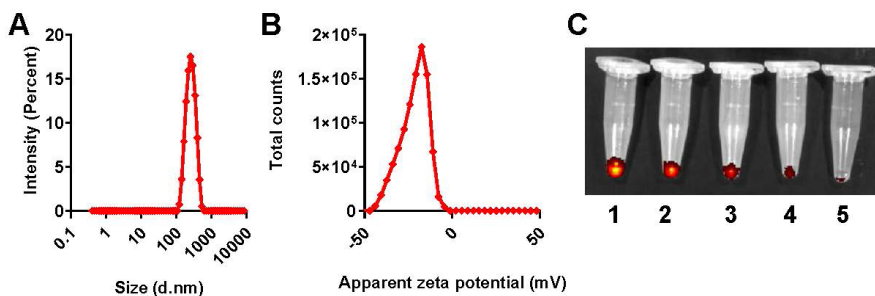


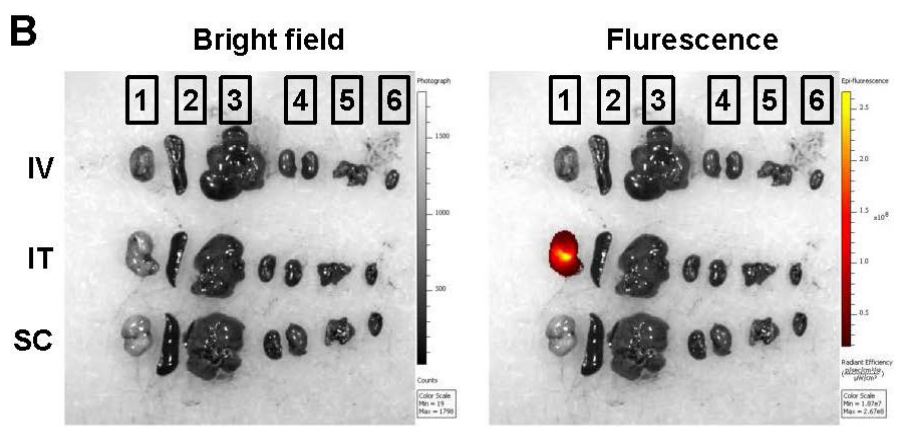
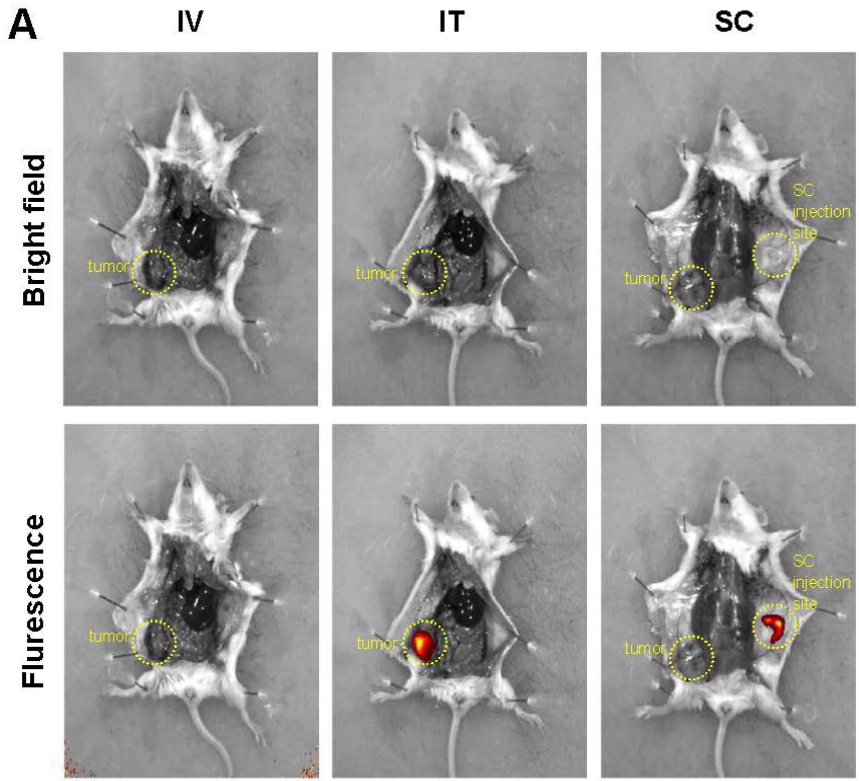
**Figure 1. The NP size and zeta potential data characterized by dynamic light scattering. The size (A) and zeta potential (B) data distributions represent the mean value  $\pm$  SD of 10 readings. (C) A picture showing positive detection of the ICG-loaded NPs in a dilution series of the NPs in PBS acquired by the IVIS Spectrum in vivo imaging system set to acquire at excitation 745 nm and emission 800 nm. The annotated numbers correspond to the nanoparticle concentration used, as follows: 1) 5 mg/mL; 2) 2.5 mg/mL; 3) 1.25 mg/mL; 4) 0.63 mg/mL; 5) 0.31 mg/mL in a total volume of 50  $\mu$ L in each Eppendorf tube.**

### **Tumor accumulation after IV, SC or IT administration of ICG-loaded NPs**

To determine whether the concentration of ICG in the tumor would differ after IV, SC or IT administration of ICG-loaded NPs, tumor-bearing mice were euthanized after 24 hours post injection and analyzed by IVIS fluorescence imaging. The sites of SC and IT injection of the ICG-loaded NPs were detectable (Figure 2A). The tumor with the highest ICG signal was the tumor treated via an IT injection (Figure 2B). However, no ICG signal in the tumor could be detected after SC or IV injection by IVIS fluorescence imaging in the CT-26 cancer model.

### **Figure 2. Anatomical and multiple organ overview of the ICG-loaded NPs biodistribution in mice bearing subcutaneous CT-26 tumors upon IV, IT, and SC injection routes.**

**A)** Representative anatomical photographs of mice with a subcutaneous tumor of mice administered with ICG-loaded NPs (50  $\mu$ L at 10 mg/mL) via IV, IT or SC injection routes acquired with the IVIS Spectrum in vivo imaging system after 24 hours. Photographs above are bright fields and photographs from below are an overlay with the ICG fluorescence signal. **B)** Representative photographs of relevant mice organs administered with ICG-loaded NPs via IV, IT or SC injection routes acquired with the IVIS Spectrum in vivo imaging system. Photograph from the left side is the bright field and the photograph from the right side is an overlay with the ICG fluorescence signal. 1: tumor; 2: spleen; 3: liver; 4: kidneys; 5: lungs; 6: heart.



### **Distinct organ accumulation and blood concentration upon distinct injection routes of ICG-loaded NPs**

To determine the ICG blood clearance rate after IV, SC or IT administration of ICG-loaded NPs, blood was collected at several intervals post-injection. The Li-Cor Odyssey scanner was used to acquire the relative quantitative signal instead of the IVIS Spectrum in vivo imaging system as it was found to be more sensitive (lower detection limit) to the ICG signal in the organs and blood. The IV route yielded the highest concentration of ICG measured 5 minutes after injection, while the SC route was observed to be slightly higher than the IT route (Figure 3A). After 120 minutes post-injection, the ICG blood concentration rapidly decreased for the IV and IT route and then remained stable for up to 24 hours. However, after 120 minutes the ICG blood concentration of the SC route was found to increase and to gradually decrease after 240 and 360 minutes; after 24 hours the SC route depicted similar concentrations of that of IV and IT routes (Figure 3A). After 24 hours, the organs of the mice were removed and the ICG concentration measured (Figure 3B). The ICG concentration of the IT route was found to be slightly elevated in the spleen, kidneys and liver, but not in the heart or lungs, and up to 800-fold higher in the tumor compared to the IV or SC route. The ICG concentration of the IV route was higher in the liver compared to SC route but not in the other organs.

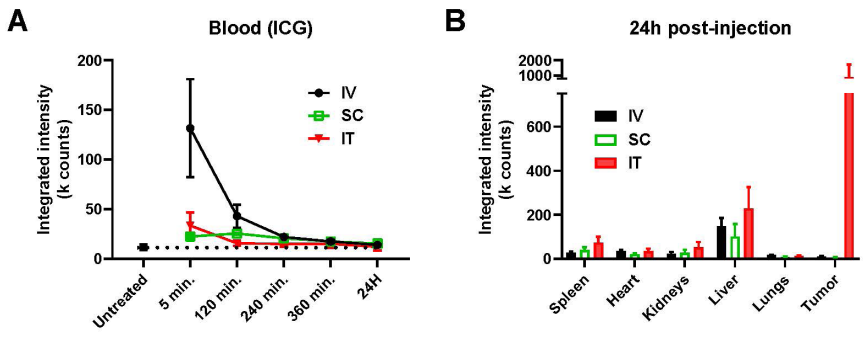


**Figure 3. Relative quantification of ICG in mice organs bearing subcutaneous TC-1 tumors and ICG blood concentration in time upon IV, SC or IT injection routes of ICG-loaded NPs. A)** ICG blood concentration measured after 5, 120, 240, and 360 minutes, or 24 hours after injection. **B)** Biodistribution of ICG-loaded NPs measured in the spleen, heart, kidneys, liver, lungs, and TC-1 tumors in mice 24 hours after injection. The relative signal quantification from the blood and vital organs was acquired by using the Li-Cor Odyssey scanner. The organ signal data was made specific by subtracting the background fluorescence from each corresponding organ from untreated mice.

### Discussion

Here we have shown that the IV, SC, or IT injection routes of pegylated PLGA nanoparticles loaded with ICG display a distinct biodistribution and blood clearance rate. There is low accumulation of the nanoparticles in the vital organs and the accumulation is higher in the liver than in the kidneys, which suggest that these types of nanoparticles are likely cleared via the hepatic route. The nanoparticle tumor accumulation was considerably higher when the nanoparticles were injected IT and very low when injected IV and SC, respectively. When the nanoparticles design is to deliver their cargo to the tumor area, and the tumor is accessible, the IT injection route would be the preferred administration route to achieve highest accumulation possible in the tumor area. Interestingly, the nanoparticle accumulation was also higher in the spleen for the IT route, which could indicate that (immune) cells from the tumor area take-up the nanoparticles (or their cargo) and migrate to the spleen. This observation also adds to the evidence reported by us and others that the IT administration of nanoparticles loaded with immune modulators or other immune stimulating cancer drugs can induce immune abscopal effects relevant for the control of metastases [9,10,12]. Nonetheless, the downside of IT administration is that the nanoparticles are

unlikely to reach metastases themselves and if the abscopal effect is absent or weak, the IV or SC route would be preferred. Alternatively, it would also be possible to treat accessible tumors IT and IV to reach the metastases. However, by combining the IT and IV administration, the rate of adverse effects is likely to increase. Moreover, the clinical practice of the administration of cancer drugs directly in the tumor of cancer patients, even in less accessible tumors such as liver cancers, is increasing due to improved methods and procedures [13]. The additional advantage of nanoparticles when injected IT, is their slow and sustained release capability, which makes them often better alternatives to non-nanoparticle drugs to exert prolonged pharmacological effects in the tumor area. The data in this report clearly shows considerably higher concentration of ICG in the tumor after 24 hours post IT injection compared to IV or SC administration, and in a previous report we have shown that nanoparticles can remain in the tumor area even after 168 hours [9]. Additionally, many cancer drugs are deleteriously toxic to vital organs such as the heart, lungs, and kidneys, which already lead to the development of Doxil®, the FDA approved pegylated nanoparticle loaded with doxorubicin [14]. The pegylated PLGA nanoparticles presented in this report also displayed favorable low biodistribution in these vital organs. Despite the pegylated layer, the nanoparticles are rapidly removed from the blood reaching very low levels after 360 minutes and below detection limit after 24 hours regardless of the injection route. This observation is in line with reports that blood circulation half-life increases from 30 minutes (without PEG coating) to 5 hours (with PEG coating) but seldomly longer for similar nanoparticles [15–17]. Although also the IV administration route, and to a lower extent the SC route, induced low but detectable signal emanating from the tumor, the signal likely came from nanoparticles that accumulated via the ‘enhanced permeability and retention’ effect [18]. However, the accumulation appears low and since the blood circulation time is relatively short, the IV injection route does not appear to be an efficient route to achieve a high accumulation in the tumor in the tested cancer models.

Although the fluorescence detection method used in this study is increasingly used in biodistribution studies, the results should be taken into consideration carefully. Namely, the ICG-detection method used here is qualitative and semi-quantitative and can only aid as an indicator of relative ICG-signal concentration. Several factors, including signal quenching, dequenching, and saturation, as well as limited tissue depth penetration, can influence the acquired signal [19]. Nonetheless, quantification by fluorescence from tissue homogenates versus planar (2D) fluorescence reflectance imaging of excised intact organs, as used in this study, was shown representative to



whole organ lysates [20]. And, besides the advantage of non-exposure to ionizing radiation, optical imaging has proven a reliable method for qualitative measurement of NPs biodistribution [21].

## REFERENCES

- [1] D. Chenthamara, S. Subramaniam, S.G. Ramakrishnan, S. Krishnaswamy, M.M. Essa, F.H. Lin, M.W. Qoronfleh, Therapeutic efficacy of nanoparticles and routes of administration, *Biomater. Res.* 23 (2019). <https://doi.org/10.1186/s40824-019-0166-x>.
- [2] H.S. Choi, W. Liu, F. Liu, K. Nasr, P. Misra, M.G. Bawendi, J. V. Frangioni, Design considerations for tumour-targeted nanoparticles, *Nat. Nanotechnol.* 5 (2010) 42–47. <https://doi.org/10.1038/nnano.2009.314>.
- [3] X. Huang, F. Zhang, L. Zhu, K.Y. Choi, N. Guo, J. Guo, K. Tackett, P. Anilkumar, G. Liu, Q. Quan, H.S. Choi, G. Niu, Y.P. Sun, S. Lee, X. Chen, Effect of injection routes on the biodistribution, clearance, and tumor uptake of carbon dots, *ACS Nano.* 7 (2013) 5684–5693. <https://doi.org/10.1021/nn401911k>.
- [4] X.D. Zhang, H.Y. Wu, D. Wu, Y.Y. Wang, J.H. Chang, Z. Bin Zhai, A.M. Meng, P.X. Liu, L.A. Zhang, F.Y. Fan, Toxicologic effects of gold nanoparticles in vivo by different administration routes, *Int. J. Nanomedicine.* 5 (2010) 771–781. <https://doi.org/10.2147/IJN.S8428>.
- [5] M. Bednarski, M. Dudek, J. Knutelska, L. Nowiński, J. Sapa, M. Zygmunt, G. Nowak, M. Luty-Błocho, M. Wojnicki, K. Fitzner, M. Tęsiorowski, The influence of the route of administration of gold nanoparticles on their tissue distribution and basic biochemical parameters: In vivo studies, *Pharmacol. Reports.* 67 (2015) 405–409. <https://doi.org/10.1016/j.pharep.2014.10.019>.
- [6] B. Semete, L. Booyesen, Y. Lemmer, L. Kalombo, L. Katata, J. Verschoor, H.S. Swai, In vivo evaluation of the biodistribution and safety of PLGA nanoparticles as drug delivery systems., *Nanomedicine.* 6 (2010) 662–71. <https://doi.org/10.1016/j.nano.2010.02.002>.
- [7] Y.P. Li, Y.Y. Pei, X.Y. Zhang, Z.H. Gu, Z.H. Zhou, W.F. Yuan, J.J. Zhou, J.H. Zhu, X.J. Gao, PEGylated PLGA nanoparticles as protein carriers: Synthesis, preparation and biodistribution in rats, *J. Control. Release.* 71 (2001) 203–211. [https://doi.org/10.1016/S0168-3659\(01\)00218-8](https://doi.org/10.1016/S0168-3659(01)00218-8).
- [8] K.S. Yadav, K. Chuttani, A.K. Mishra, K.K. Sawant, Effect of size on the biodistribution and blood clearance of etoposide-loaded PLGA nanoparticles, *PDA J. Pharm. Sci. Technol.* 65 (2011) 131–139.
- [9] C.G. Da Silva, M.G.M. Camps, T.M.W.Y. Li, L. Zerrillo, C.W. Löwik, F. Ossendorp, L.J. Cruz, Effective chemoimmunotherapy by co-delivery of doxorubicin and immune adjuvants in biodegradable nanoparticles., *Theranostics.* 9 (2019) 6485–6500. <https://doi.org/10.7150/thno.34429>.
- [10] C.G. Da Silva, M.G.M. Camps, T.M.W.Y. Li, A.B. Chan, F. Ossendorp, L.J. Cruz, Co-delivery of immunomodulators in biodegradable nanoparticles improves therapeutic efficacy of cancer vaccines, *Biomaterials.* 220 (2019) 119417. <https://doi.org/10.1016/j.biomaterials.2019.119417>.

- [11] K.Y. Lin, F.G. Guarnieri, K.F. Staveley-O'Carroll, H.I. Levitsky, J.T. August, D.M. Pardoll, T.C. Wu, Treatment of established tumors with a novel vaccine that enhances major histocompatibility class II presentation of tumor antigen., *Cancer Res.* 56 (1996) 21–6.
- [12] X.Y. Chu, W. Huang, Y.L. Wang, L.W. Meng, L.Q. Chen, M.J. Jin, L. Chen, C.H. Gao, C. Ge, Z.G. Gao, C.S. Gao, Improving antitumor outcomes for palliative intratumoral injection therapy through lecithin– chitosan nanoparticles loading paclitaxel– cholesterol complex, *Int. J. Nanomedicine.* 14 (2019) 689–705. <https://doi.org/10.2147/IJN.S188667>.
- [13] W.X. Hong, S. Haebe, A.S. Lee, C.B. Westphalen, J.A. Norton, W. Jiang, R. Levy, Intratumoral Immunotherapy for Early-stage Solid Tumors, *Clin. Cancer Res.* 26 (2020) 3091–3099. <https://doi.org/10.1158/1078-0432.CCR-19-3642>.
- [14] S. Tran, P.-J. DeGiovanni, B. Piel, P. Rai, Cancer nanomedicine: a review of recent success in drug delivery., *Clin. Transl. Med.* 6 (2017) 44. <https://doi.org/10.1186/s40169-017-0175-0>.
- [15] R. Gref, Y. Minamitake, M.T. Peracchia, V. Trubetskoy, V. Torchilin, R. Langer, Biodegradable long-circulating polymeric nanospheres, *Science* (80-. ). 263 (1994) 1600–1603. <https://doi.org/10.1126/science.8128245>.
- [16] A.L. Klibanov, K. Maruyama, V.P. Torchilin, L. Huang, Amphipathic polyethyleneglycols effectively prolong the circulation time of liposomes, *FEBS Lett.* 268 (1990) 235–237. [https://doi.org/10.1016/0014-5793\(90\)81016-H](https://doi.org/10.1016/0014-5793(90)81016-H).
- [17] J.S. Suk, Q. Xu, N. Kim, J. Hanes, L.M. Ensign, PEGylation as a strategy for improving nanoparticle–based drug and gene delivery, *Adv. Drug Deliv. Rev.* 99 (2016) 28–51. <https://doi.org/10.1016/j.addr.2015.09.012>.
- [18] J.W. Nichols, Y.H. Bae, EPR: Evidence and fallacy, *J. Control. Release.* 190 (2014) 451–464. <https://doi.org/10.1016/j.jconrel.2014.03.057>.
- [19] F. Meng, J. Wang, Q. Ping, Y. Yeo, Quantitative Assessment of Nanoparticle Biodistribution by Fluorescence Imaging, Revisited, *ACS Nano.* 12 (2018) 6458–6468. <https://doi.org/10.1021/acsnano.8b02881>.
- [20] K.O. Vasquez, C. Casavant, J.D. Peterson, Quantitative Whole Body Biodistribution of Fluorescent-Labeled Agents by Non-Invasive Tomographic Imaging, *PLoS One.* 6 (2011) e20594. <https://doi.org/10.1371/journal.pone.0020594>.
- [21] L. Arms, D.W. Smith, J. Flynn, W. Palmer, A. Martin, A. Woldu, S. Hua, Advantages and limitations of current techniques for analyzing the biodistribution of nanoparticles, *Front. Pharmacol.* 9 (2018) 802. <https://doi.org/10.3389/fphar.2018.00802>.

4

# EFFECTIVE CHEMOIMMUNOTHERAPY BY CO-DELIVERY OF DOXORUBICIN AND IMMUNE ADJUVANTS IN BIODEGRADABLE NANOPARTICLES

4

Candido G. Da Silva, Marcel G.M. Camps, Tracy M.W.Y. Li, Luana Zerrillo,  
Clemens W. Löwik, Ferry Ossendorp, Luis J. Cruz

*Theranostics* 2019; 9(22):6485-6500.

# Abstract

---

Chemoimmunotherapy is an emerging combinatorial modality for the treatment of cancers resistant to common first-line therapies, such as chemotherapy and checkpoint blockade immunotherapy. We used biodegradable nanoparticles as delivery vehicles for local, slow and sustained release of doxorubicin, two immune adjuvants and one chemokine for the treatment of resistant solid tumors.

**Methods:** Bio-compatible poly(lactic-co-glycolic acid)-PEG nanoparticles were synthesized in an oil/water emulsion, using a solvent evaporation-extraction method. The nanoparticles were loaded with a NIR-dye for theranostic purposes, doxorubicin cytostatic agent, poly (I:C) and R848 immune adjuvants and CCL20 chemokine. After physicochemical and in vitro characterization the nanoparticles therapeutic efficacy were carried-out on established, highly aggressive and treatment resistant TC-1 lung carcinoma and MC-38 colon adenocarcinoma models in vivo.

**Results:** The yielded nanoparticles average size was 180 nm and -14 mV surface charge. The combined treatment with all compounds was significantly superior than separate compounds and the compounds nanoparticle encapsulation was required for effective tumor control in vivo. The mechanistic studies confirmed strong induction of circulating cancer specific T cells upon combined treatment in blood. Analysis of the tumor microenvironment revealed a significant increase of infiltrating leukocytes upon treatment.

Conclusion: The multi-drug loaded nanoparticles mediated delivery of chemoimmunotherapy exhibited excellent therapeutic efficacy gain on two treatment resistant cancer models and is a potent candidate strategy to improve cancer therapy of solid tumors resistant to first-line therapies.

## INTRODUCTION

Triggering antitumor immunity through chemotherapy, immunotherapy, or combinations thereof is an emerging strategy to treat solid tumors [1]. Besides killing cancer cells directly, some chemotherapies can alter the tumor microenvironment and enhance immune responses [2,3]. For example, the anthracycline doxorubicin (dox) has been described to induce type I interferons (IFNs), T cell homing through induction of the chemokine CXCL10, expose calreticulin on dying cells, and other effects [2,4]. However, dox monotherapy is often insufficient to clear established solid tumors, eliciting the need for combinatorial modalities.

Immunotherapy based on immune adjuvants such as cytokines, checkpoint blocking antibodies, Toll-like receptor (TLR) agonists and other compounds, are gaining attention as a strategy to enhance anticancer immune responses [5–9]. TLR agonists trigger broad inflammatory responses, elicit rapid innate immunity, promote the activity of leukocytes, and facilitate the progression from innate to adaptive immune responses [10]. Moreover, TLRs facilitate the immune system by providing context, allow the immune system response to skew on the type that is necessary and finetune the most efficient method to eradicate the threat to the host. Numerous TLR agonists have been studied as cancer therapies (or part of combination therapies) in clinical trials. Intriguingly, several agonists have demonstrated antitumor effects, whereas others appear to promote tumor growth or metastasis [11]. In humans, activation of the endosomal TLR3, TLR7, TLR8 and TLR9 typically enhances antitumor outcomes. For example, the TLR3 agonist Poly(I:C; pIC) has been reported to have potent antitumor effects on lung and liver cancers, and the dual TLR7/8 activator Resiquimod (R848) has been reported in several clinical trials to induce tumor regression in patients with advanced leukemia and skin cancers [11,12]. Moreover, R848 has been reported to reverse effector T cell senescence [13]. Interestingly, the combination therapy of pIC and R848 appears to be synergistic *in vitro*, but this effect has not yet been demonstrated in clinical trials [14].

To date, most clinical trials on TLR agonists involved the systemic administration, which led to deleterious adverse effects, including cytokine release syndrome, which can rapidly become fatal. Thus, the anticancer efficacy of TLR agonists is limited by systemic treatment. Accordingly, TLR agonists are being actively explored within combination therapies administered intratumorally. Chemokines are specific immune adjuvants that can induce chemotaxis of immune cells to the tumor, thereby making tumors more visible to immune cells. Similarly to TLR agonists, some chemokines may exert anticancer effects, whereas others may enhance cancer progression depending on the cancer type, the tumor microenvironment phenotype, and the cancer stage [15]. One chemokine that can drive immune cells towards the tumor is the Macrophage Inflammatory Protein-3 alpha (MIP3 $\alpha$ ; CCL20) which attracts cells expressing CCR6/CD196 such as (memory) T cells, natural killer cells and immature dendritic cells (DCs), all of which can mediate tumor regressions [16–19]. Furthermore, MIP3 $\alpha$  has also been described to directly repress the proliferation of myeloid progenitors [20].

Successful therapeutic responses are commonly observed when the effective dose of a drug is maintained at the target site for a specific duration. However, drugs that are administered systemically can generate numerous off-target effects that compromises the therapy efficacy. In response, either the dose is adjusted or the treatment is stopped, both of which can be problematic for the survival of the patient. Therefore, for certain anticancer drugs, local administration may prove more effective than systemic administration [5]. However, one disadvantage of local treatment is rapid diffusion, which limits efficacy. Therefore, an attractive route of administration would be one that is local, to avoid off-target effects, but in which the drug is released slowly for a sustained period, to maximize efficacy. This approach entails the use of drug delivery vehicles such as liposomes, metallic nanoparticles (NPs) or biodegradable poly(lactic-co-glycolic acid; PLGA) polymers [21,22]. Indeed, delivery of cancer therapeutics with such vehicles is rapidly gaining recognition for its advantages. For instance, over the past several years, the FDA approved nano-vehicle formulations of previously developed chemotherapeutics: Doxil®, Abraxane®, and Onivyde® for dox, paclitaxel, and irinotecan, respectively. Interest in drug delivery vehicles is also reflected by the large number (>200) of clinical trials currently underway in which chemotherapeutics are being compared to their respective soluble and delivered forms [23–25].



Herein, we report the assembly and in vitro functional characterization and loading of PLGA NPs with dox, pIC, R848 and MIP3 $\alpha$ , and subsequent in vivo evaluation of the loaded NPs as a cancer therapy. We assessed the activity of our drug-loaded NPs in two aggressive and treatment resistant murine models of cancer: TC-1 lung carcinoma and MC-38 colon adenocarcinoma. We provide evidence of enhanced potential of chemotherapy and immunotherapy. Finally, we investigated the in vivo efficacy of the NP delivered drugs against the corresponding free drugs and analyzed the tumor microenvironment. To the best of our knowledge, this is the first published study to combine NP mediated delivery of a chemotherapeutic agent, two distinct TLR agonists and a chemokine into a single theranostic modality.

## MATERIALS AND METHODS

### Materials and reagents

PLGA polymer (lactide/glycolide molar ratio of 48:52 to 52:48) was purchased from Boehringer Ingelheim (Ingelheim am Rhein, Germany). Solvents for synthesizing the PLGA NPs including dichloromethane (DCM; CAS 75-09-2 CH<sub>2</sub>CL<sub>2</sub> MW 84.93) and polyvinyl alcohol (PVA; CAS 9002-89-5) were purchased from Sigma-Aldrich (Zwijndrecht, The Netherlands). Chloroform (CHCL<sub>3</sub> MW 119.38 g/mol) was purchased from Merck (Darmstadt, Germany). Lipid-PEG 2000 (1,2-Distearoyl-sn-Glycero-3-Phosphoethanolamine-N-[Methoxy(Polyethylene glycol)-2000]; powder MW 2805.54) was purchased from Avanti Polar Lipids (AL, USA). The near infrared (NIR) dye (IR-780 Iodide; CAS 207399-07-3) was purchased from Sigma-Aldrich; R848 from Alexis Biochemicals (Paris, France); poly(inosinic:cytidylic acid; CAS 42424-50-0 P0913) from Sigma-Aldrich; MIP3 $\alpha$  from R&D Systems (MN, USA) and doxorubicin HCL powder from Actavis (Munich, Germany).

### Synthesis of PLGA NPs

The NPs were synthesized in an oil/water emulsion, using a solvent evaporation-extraction method. Briefly, 200 mg of PLGA was dissolved in 6 mL of DCM containing 1 mg of NIR dye. Depending on the NP, the following was added: 40 mg of dox, 8 mg of pIC and/or 4 mg of R848 and/or 250  $\mu$ g of MIP3 $\alpha$ . Next, the solution containing the NP constituents was added dropwise to 40 mL of aqueous 2.5% (w/v) PVA and emulsified for 120 s using a sonicator (250 watt; Sonifier 250; Branson, Danbury, USA). Next, the previously described solution was transferred to a new vial that contained an air-dried solution of 40 mg of Lipid-PEG 2000 dissolved in

0.4 mL of chloroform and homogenized for 60 s by sonication. Following overnight evaporation of the solvent at 4 °C, the NPs were collected by ultracentrifugation (12,800 rpm for 30 minutes) at 4 °C, washed four times with distilled water, and lyophilized for 3 days. The concentration of each encapsulated constituent (dox, pIC, R848 and MIP3 $\alpha$ ) was determined by distinct methods, as described elsewhere [26]. In brief, the concentration of the TLR agonists (pIC and R848) were determined by reverse phase high-performance liquid chromatography (RP-HPLC) at room temperature using a Shimadzu system (Shimadzu Corporation, Kyoto, Japan) equipped with a RP-C18 symmetry column (250 mm x 4.6 mm). The flow rate was fixed at 1 mL/min and detection was obtained by UV detection at 254 nm. A linear gradient of 0% to 100% of acetonitrile (0.036% TFA) in water containing 0.045% TFA was used for the separation of pIC and R848. The peak of R848 was well separated from that of the pIC in the established chromatographic condition. The retention times of the pIC and R848 were approximately 19 and 26 min, respectively. The regression analysis was constructed by plotting the peak-area ratio of R848 or pIC versus concentration ( $\mu\text{g/mL}$ ). The calibration curves were linear within the range of 1  $\mu\text{g/mL}$  to 10  $\mu\text{g/mL}$  for R848 and 1  $\mu\text{g/mL}$  to 150  $\mu\text{g/mL}$  for pIC. The correlation coefficient ( $R^2$ ) was always greater than 0.99, indicating a good linearity. The concentration of pIC and R848 was calculated by interpolation into the standard curves as described previously. The concentration of MIP3 $\alpha$  was determined by RP8-HPLC at room temperature using a Shimadzu system (Shimadzu Corporation) equipped with a RP-C8 symmetry column (150 mm x 4.6 mm). The flow rate was fixed at 0.8 mL/min and detection was obtained by UV detection at 220 nm. A linear gradient of 5% to 80% of acetonitrile (0.036% TFA) in water containing 0.045% TFA was used. The concentration of the NIR dye was measured at 800 nm relative to a standard curve using an Odyssey scanning (Li-Cor) as per described previously [27]. The dox concentration was determined by SpectraMax® iD3 multi-mode microplate readers via fluorescence with an excitation peak at 488 nm and emission peak at 530 nm. The loading capacity was calculated as follows: Percentage loading capacity = [entrapped drug /NP yield weight] \* 100

### **Physicochemical properties of the NPs**

The NPs were characterized for average size, polydispersity index and surface charge (zeta-potential) by dynamic light scattering. Briefly, 50  $\mu\text{g}$  of NP sample in 1 mL of ultrapure MilliQ H<sub>2</sub>O were measured for size using a Zetasizer (Nano ZS, Malvern Ltd., UK) and a similar sample was analyzed for surface charge by laser Doppler electrophoresis on the same device.

### **Particles surface and morphology**

To visualize the structure of the NPs, transmission electron microscopy (TEM) was used. Briefly, a formvar support film attached to a copper grid (100 mesh) was coated with carbon and hydrophilized by glow-discharging for 30 s with a current of 25 mA. A droplet of 3  $\mu\text{L}$  of the NPs solution was applied to the grid and then stained for 1 min in distilled water containing 2.3% uranyl acetate. Next, the grid was air-dried and imaged in a Tecnai 12 Biotwin transmission electron microscope (FEI, The Netherlands), equipped with a LaB6 filament operated at 120 keV. The sample was imaged 3  $\mu\text{m}$  under focus with binning 2 on a 4kx4k Eagle CCD camera with a magnification of 18,500x.

Atomic force microscopy (AFM) was employed to study the surface morphology and size of NPs. Briefly, a drop of diluted and dispersed NPs suspension was placed on a clean glass surface glued to the AFM stub. The dried NPs were then visualized with AFM (JPK Nano Wizard 3) in AC mode (tapping mode), using OMCL-AC160TS silicon probes (Olympus), with nominal resonance frequency of 300 kHz and nominal spring constant of 26N/m. The images were analyzed using Gwyddion SPM Software (Czech Metrology Institute, Czech Republic). The 2D visualization was performed with JPK Data Processing Software (JPK Instruments, Germany) and the images were converted to 3D using Gwyddion v. 2.52 (open source SPM data analysis software).

### **Stability study and release kinetics of the NPs**

For the NP stability study a total of 10 mg of each described NP was carefully dissolved in 2 mL of PBS and kept at room temperature and at constant rotating velocity. At the designated time points a 50  $\mu\text{L}$  sample was taken from the supernatant and measured by dynamic light scattering as per described above. For the NP release kinetics study, 1 mL (10 mg/mL) of the NP containing all drugs was pipetted into a dialysis bag (MWCO 1000), which was immersed into a tube

containing 30 mL of PBS (pH 7.4). The tubes were placed on a shaking bed at 100 rpm and 37 °C. At the described time points, 30 mL of the release medium was collected and replenished with 30 mL of fresh PBS. The collected sample was concentrated by lyophilization in order to determine the content released for all components. The dox, NIR dye, TLR agonists R848 and pIC concentration were determined as per described above.

### **Cell lines**

The murine tumor cell line TC-1 (a kind gift from T.C. Wu, Johns Hopkins University, Baltimore, MD, USA) was generated by retroviral transduction of lung fibroblasts of C57BL/6 origin, to express the HPV16 E6 and E7 genes and the activated human c-Ha-ras oncogene [28]. The C57BL/6 MC-38 colon adenocarcinoma cell line was kindly provided by Mario Colombo. The D1 cell line is an immature splenic DC line derived from B6 mice which harbors most of the typical characteristics of that of bone marrow derived DCs [29]. The TC-1 cell line was cultured in DMEM medium (BioWhittaker, Verviers, Belgium) supplemented with 8% heat-inactivated fetal calf serum (FCS; Greiner bio-one, Alphen a/d Rijn, The Netherlands), penicillin (50 µg/mL; Gibco, Paisley, Scotland), streptomycin (50 µg/mL; Gibco), L-glutamine (2 mM; Gibco) and β-mercaptoethanol (20 µM; Sigma, Saint Louis, USA). In addition, the TC-1 cells were co-cultured with the corresponding selective agent Geneticin (G418; 400 µg/mL). The BALB/macrophage cell line RAW264.7 and the MC-38 cell line were cultured identically to the TC-1 cell line except that IMDM medium was used and no selection agent was applied. The D1 cell line was cultured as described previously [30]. All the above described cell lines were incubated at 37° C in 5% CO<sub>2</sub> and 100% humidity. Furthermore, the cell lines were confirmed to be free of mycoplasma and were regularly tested for eighteen common rodent viruses by PCR analysis.

### **Mice strains**

C57BL/6 (H-2b haplotype) mice were purchased from Envigo (Horst, The Netherlands). They were all female and ranged in age from 8 to 12 weeks. The mice were housed at the animal facility of Leiden University Medical Center under specific pathogen free conditions. All animal experiments were approved by the Dutch Central Committee on Animal Experimentation and were strictly conducted according to the Dutch animal welfare law.

### **Intracellular uptake of NPs and immunostaining**

Intracellular uptake of NPs was determined by incubating either 10 µg/mL or 20 µg/mL of NPs containing NIR dye (~ 800 nm; described above) with  $1 \times 10^4$  TC-1 or D1 cells for 1 hour, 2 hours or 4 hours. To remove unbound NPs from the cells and wells, the cells were harvested and moved to a new 96-well plate and washed several times. Then, the cells were placed in a black 96-well microplate (Greiner bio-one, Germany), fixed with 1% paraformaldehyde (PFA) and stained with To-pro 3 iodide (642/661 ~700 nm; Invitrogen; Eugene, USA) to enable cell count. Finally, the NIR dye signal in each cell line was scanned using an Odyssey scanner infrared imaging system (LI-COR). Immunostaining detected by fluorescence microscopy was determined by incubating 20 µg/mL of NPs containing NIR dye with TC-1 or D1 cells in the chambers of a glass culture slide (FALCON, NY, USA) for 48 hours. After washing, and fixating the cells with 4% PFA, the cells were stained with anti-CD44-PE (clone GL1, eBioscience) for membrane visualization, washed again with PBS and finally, mounted with VectaShield antifade mounting medium with DAPI to stain nuclei (Vector Laboratories, CA, USA). Digital images were acquired using a Leica DM6B microscope.

### **Activation and maturation of DCs**

DC activation and maturation were assessed based on upregulation of CD86 on the D1 cells and production of IL-12 in the supernatant. Briefly, a solution of pIC and an equivalent concentration of pIC encapsulated in NPs, that also contained R848 and MIP3 $\alpha$ , were separately prepared according to annotated concentrations (see corresponding figure legends). The solutions were then distributed into 96-well plates and sequentially diluted, after which  $5 \times 10^4$  D1 cells were added to each well and allowed to incubate for 48 hours at 37° C in 5% CO<sub>2</sub> and 100% humidity. The supernatant was then harvested and analyzed with an ELISA (described below). The cells were used to analyze the CD86 expression with anti-CD86-APC (clone GL1, eBioscience) on an LSR-II laser flow cytometer controlled by CELLQuest software v. 3.0 (Becton Dickinson, Franklin Lakes, USA) and analyzed with FlowJo LLC v. 10 software (Tree Star, USA). The interleukin IL-12 was detected using a standard sandwich ELISA with bottom polystyrene ELISA plates (Corning, Kennebunk, USA). Purified anti-mouse IL-12/IL-23 p40 (clone C15.6, Biolegend) and biotin-labelled anti-mouse IL-12/IL-23 p40 antibodies (clone C17.8, Biolegend) were used.

Streptavidin-horse radish peroxidase (1 µg/mL; Biolegend) and 3,3',5,5'-tetramethyl benzidine (TMB; Sigma-Aldrich) was used to generate the detection signal. Finally, the plates were read at 450 nm using a Bio-rad 680 microplate reader (Bio-rad Laboratories).

### **Cytotoxicity of empty and dox-loaded NPs**

The toxicity of empty NPs to DCs was determined by incubating DCs ( $5 \times 10^4$ ) with increasing concentrations of empty NPs for 48 hours, and then measuring cell viability. The cytotoxic compound dimethyl sulfoxide (DMSO; CAS 67-68-5; Honeywell, MI, USA) 25% (v/v) in medium was included as a positive control (100 percent cell death). To measure viability, the cells were stained with 7-AAD (Invitrogen) using standard protocols and then subjected to flow cytometry measurements on an LSR-II laser flow cytometer controlled by CELLQuest software v. 3.0 (Becton Dickinson). The cell toxicity of the dox-loaded NPs and controls was determined by using the CellTiter 96 Aqueous one solution cell proliferation assay (MTS; Promega, Madison, USA) performed per manufacturer's instructions. In brief,  $5 \times 10^3$  cells per well were distributed into a 96-wells plate and treated with indicated concentrations of compounds at 37° C in 5% CO<sub>2</sub> and 100% humidity. After 72 hours, cells were incubated with MTS solution before measuring absorbance at 490 nm using a Bio-rad 680 microplate reader (Bio-rad Laboratories).

### **Transwell chemotaxis assay**

A solution of NP(pIC+R848+MIP3α) in full medium was prepared at an equivalent MIP3α concentration of 1 µg/mL. Separately, a solution of free MIP3α at a matching concentration of 1 µg/mL, and a positive control solution of free MIP3α at 10 µg/mL, were prepared and distributed into the wells of a Transwell permeable 24-well plate (12x6.5 mm inserts; 8.0 µm PET membrane (Costar Corning, Kennebunk, USA). After 24 hours of incubation at 37 °C, to allow sufficient MIP3α to be released from the NPs, the insert was pre-warmed with warm complete culture medium and the lower chamber solution was carefully re-suspended to homogenize MIP3α into the solution. Next,  $1 \times 10^5$  RAW264.7 cells were carefully added to each upper chamber insert and allowed to migrate for 24 hours. Next, the cells were fixed with 4% PFA, washed and stained with a crystal violet solution, after which several digital pictures of each insert were acquired with a reverse microscope.

Cell migration was quantified using Image J software v. 1.5. The migration index was calculated by dividing the area (%) of migrated cells by the area (%) of migrated cells induced by the positive control.

### **Tumor challenge with NP-delivered combination therapy**

Mice were inoculated with  $1 \times 10^5$  TC-1 or  $4 \times 10^5$  MC-38 cells in 0.2 mL PBS in the right flank. When the tumors became established at day 8 after tumor inoculation, each mouse received a 30  $\mu$ L intratumoral injection of NPs dissolved in PBS and this was repeated every other day (four injections in total), unless otherwise specified. The control (untreated) group received an intratumoral injection of 30  $\mu$ L PBS every other day (four injections in total), unless otherwise specified. Each intratumoral treatment administration contained, in total: 1.5 mg/Kg (30  $\mu$ g) of dox, 1.2 mg/Kg (24  $\mu$ g) of pIC, 375  $\mu$ g/Kg (7.5  $\mu$ g) of R848, and 75  $\mu$ g/Kg (1.5  $\mu$ g) of MIP3 $\alpha$  in NP stock concentration of ca. 50 mg/mL. Concentrations were matched for the groups treated with free therapies. The limiting concentration of NPs for the experiments (see figure legends) was the MTD of dox: 6 mg/Kg (4x 1.5 mg/Kg) [31]. For the reduced dose experiment, the cumulative dose was 3 mg/Kg. For the dox and immune adjuvants combined experiments, pIC, R848 and MIP3 $\alpha$  content was matched among groups on dox or on pIC, R848 or MIP3 $\alpha$  content. Tumor dimensions were measured every other day with a standard caliper and the volume was calculated by multiplying the tumor diameters in all three dimensions. The maximal allowed tumor volume was 2,000 mm<sup>3</sup>; after this point, mice were sacrificed, which formed the basis for the Kaplan-Meier survival curves.

### **Blood analysis**

The presence of antigen-specific T cells in the blood of each mouse was determined by collecting 50  $\mu$ L of blood via a puncture of the caudal vein at day 8 and day 16 after the first treatment. After removal of red blood cells by lysis, the cells were stained with anti-CD8 $\alpha$ -PE (clone 53-6.7, eBioscience) and anti-CD3-eFluor 450 (clone 17A2, eBioscience). For mice bearing TC-1 tumors, the APC labeled HPV16 E749-57 (RAHYNIVTF) MHC class I (H-2Db) tetramer was added to the staining mix. After thorough washing, the cells were subjected to flow cytometry measurements on an LSR-II laser flow cytometer controlled by CELLQuest software v. 3.0 (Becton Dickinson) and the data analyzed with FlowJo LLC v. 10 software (Tree Star).

### **Tumor microenvironment and spleen analysis**

The tumor microenvironment and the spleens of mice were analyzed *ex vivo* by sacrificing the mice and resecting the tumors and the spleens at day 18 after tumor inoculation (after a single treatment at day 8). From the six mice per group, only four mice were selected for analysis based on their similar tumor size. The resected tumors were then mechanically broken up into small pieces of ~2-3 mm in diameter (with sterile tweezers and scissors) and incubated with Liberase TL (Roche, Mannheim, Germany) in serum-free IMDM medium for 15 minutes at 37 °C. Single cell suspensions of the tumors and the spleens were acquired by gently grinding the tumor fragments and the spleens through a 70 µm cell strainer (Falcon, NY, USA) each in separate 50 mL tubes. The red blood cells from the spleens were removed by lysis. Each tube containing the single cells was then equally divided to be stained with two distinct antibody panels. One panel contained the viability dye 7-AAD (Invitrogen) and the following antibodies against cell surface markers: anti-CD45.2-APC eFluor 780 (clone 104, eBioscience); anti-CD3-eFluor 450 (clone 17A2, eBioscience); anti-CD4-Brilliant Violet 605 (clone RM4-5, Biolegend), and anti-CD8α-APC-R700 (clone 53-6.7, BD Bioscience). The other panel contained the viability dye 7-AAD (Invitrogen) and the following antibodies against cell surface markers: anti-CD45.2-FITC (clone 104, BD Bioscience); anti-CD11b-eFluor 450 (clone M1/70, eBioscience); anti-F4/80-PE (clone BM8, eBioscience); anti-Ly6G-AlexaFluor 700 (clone 1A8, Biolegend); anti-Ly6C-Brilliant Violet 605 (clone HK1.4, Biolegend), and anti-CD11c-APC-eFluor 780 (clone N418, eBioscience). After thorough washing, the cells were subjected to flow cytometry measurements on an LSR-II laser flow cytometer controlled by CELLQuest software v. 3.0 (Becton Dickinson) and the data analyzed with FlowJo LLC v. 10 software (Tree Star). The gating strategy is depicted in Figure S1.

### **Data and statistical analysis**

Statistical analysis was performed using GraphPad Prism v. 7.0 software (GraphPad Software, La Jolla, USA). Data are represented as mean values ± SD unless stated otherwise. Tumor volumes, blood tetramer and tumor and spleen cell analysis results were compared on a fixed day between mouse groups and statistical significance was determined by using an unpaired, non-parametric, two-tailed Mann-Whitney U test. Survival curves were compared using the Gehan-Breslow-Wilcoxon test unless stated otherwise. Statistical differences were considered significant at  $p < 0.05$  and presented as: \*  $p < 0.05$ , \*\*  $p < 0.01$ , \*\*\*  $p < 0.001$ .



## RESULTS

### **Physicochemical properties and in vitro characterization of the NPs**

We loaded NPs with dox and/or different immune adjuvants and then studied their therapeutic potential (Table 1). The tumor immunity of the monotherapy NPs containing only immune adjuvants were studied separately (<https://doi.org/10.1016/j.biomaterials.2019.119417>). Due to the limited in vivo detection capability of the fluorescent anthracycline doxorubicin, we loaded a NIR dye in each batch of NPs to enable in vivo theranostic analysis and the NPs were functionalized with surface PEGylation (PEG). The NPs were first characterized to ascertain their size and surface charge (Table 1 and Figure S2). The average size was approximately 180 nm and differed depending on the cargo. The average  $\zeta$  potential was slightly negative: ca. -14 mV. The NPs were stable in PBS for at least 8 weeks (Figure S3). TEM and AFM analysis revealed that the NPs were all spherical with a smooth surface and uniform sizes (Figure 1).

**Table 1. Physicochemical characterization of the NPs**

Samples	Diameter	$\zeta$ Potential (mV)	PDI	NIR	Loading capacity (% w/w)			
					Dox	pIC	R848	MIP3 $\alpha$
NP(NIR)-PEG Denoted as NP(empty)	187.4 $\pm$ 44.7	-13.9 $\pm$ 6.2	0.064	63.6 $\pm$ 1.4	-	-	-	-
NP(NIR+dox)-PEG Denoted as NP(dox)	185.9 $\pm$ 28.2	-13.5 $\pm$ 7.5	0.127	64.9 $\pm$ 0.9	13.9 $\pm$ 1.8	-	-	-
NP (NIR+pIC+R848+MIP3 $\alpha$ )-PEG Denoted as NP (pIC+R848+MIP3 $\alpha$ )	177.3 $\pm$ 86.6	-14.3 $\pm$ 4.9	0.120	61.1 $\pm$ 7.8	-	47.7 $\pm$ 2.6	58.4 $\pm$ 3.2	63.8 $\pm$ 5.0
NP (NIR+dox+pIC+R848+MIP3 $\alpha$ )-PEG Denoted as NP (dox+pIC+R848+MIP3 $\alpha$ )	177.3 $\pm$ 86.8	-14.3 $\pm$ 4.9	0.120	62.8 $\pm$ 5.6	6.3 $\pm$ 1.1	37.9 $\pm$ 10.1	17.1 $\pm$ 3.8	63.9 $\pm$ 3.8

Physicochemical characterization of the PLGA-PEG NPs containing dox and/or different immune adjuvants. The PLGA NPs were characterized by dynamic light scattering and zeta potential measurements. PLGA NPs size and zeta potential data represent the mean value  $\pm$  SD of 10 readings of one representative batch. The loading capacity of dox and NIR dye was measured by fluorescence method. The loading capacity of pIC, R848 and MIP3 $\alpha$  was determined by RP-HPLC analysis. The loading capacity data represent the average value  $\pm$  SD of batch variation.

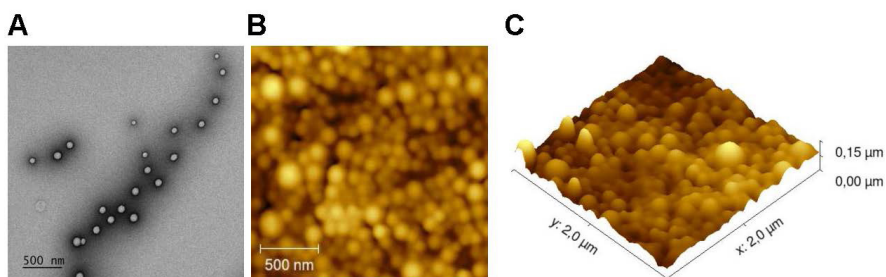


**Figure 1. NPs surface and morphology**

**A)** Representative morphology image of NP(empty) obtained by TEM.

**B)** AFM 2D image. **C)** AFM 3D image.

### Drug release kinetics

We measured the drug release kinetics of the NPs dissolved in PBS and kept at 37°C in a thermo-shaker at a constant shaking velocity. The NPs exhibited a sustained release profile with different release kinetics for each drug (Figure 2A). After 12 days, approximately 50% of pIC was released, 35% of dox, 25% of R848 and the NIR dye, respectively. MIP3 $\alpha$  release could not be determined because it was below the detection limit. The profile release of pIC was the most rapid compared to the other drugs due to its high hydrophilicity property. The other encapsulated compounds show a typical drug profile release from the PLGA (lactide/glycolide molar ratio of 50:50) standard polymer. These results suggest that the NPs release drugs in a slow, sustained manner.

### Cellular uptake of the NPs

Since dox, pIC and R848 all exert their biological effects intracellularly (unlike MIP3 $\alpha$ ), we sought to assess the uptake of drug-loaded NPs by cells. To this end, NPs containing NIR dye (at 10  $\mu\text{g}/\text{mL}$  and at 20  $\mu\text{g}/\text{mL}$ ) were incubated with TC-1 cells for 1 hour, 2 hours and 4 hours (Figure 2B). At 10  $\mu\text{g}/\text{mL}$ , the signal was detected after 2 hours and 4 hours of incubation, but not after 1 hour. At 20  $\mu\text{g}/\text{mL}$ , the signal was detected at all three time points, and it increased with increasing incubation time. To determine whether the signal was originating from inside the cells, the NPs were incubated with TC-1 cancer cells again for 2 hours at 20  $\mu\text{g}/\text{mL}$

and observed under fluorescence microscopy (Figure 2C). The NIR signal (green) from the NPs was observed within cells, indicating that the NPs had released their content into the cells. Similar results were observed when these experiments were performed with DCs instead of TC-1 cells (data not shown).

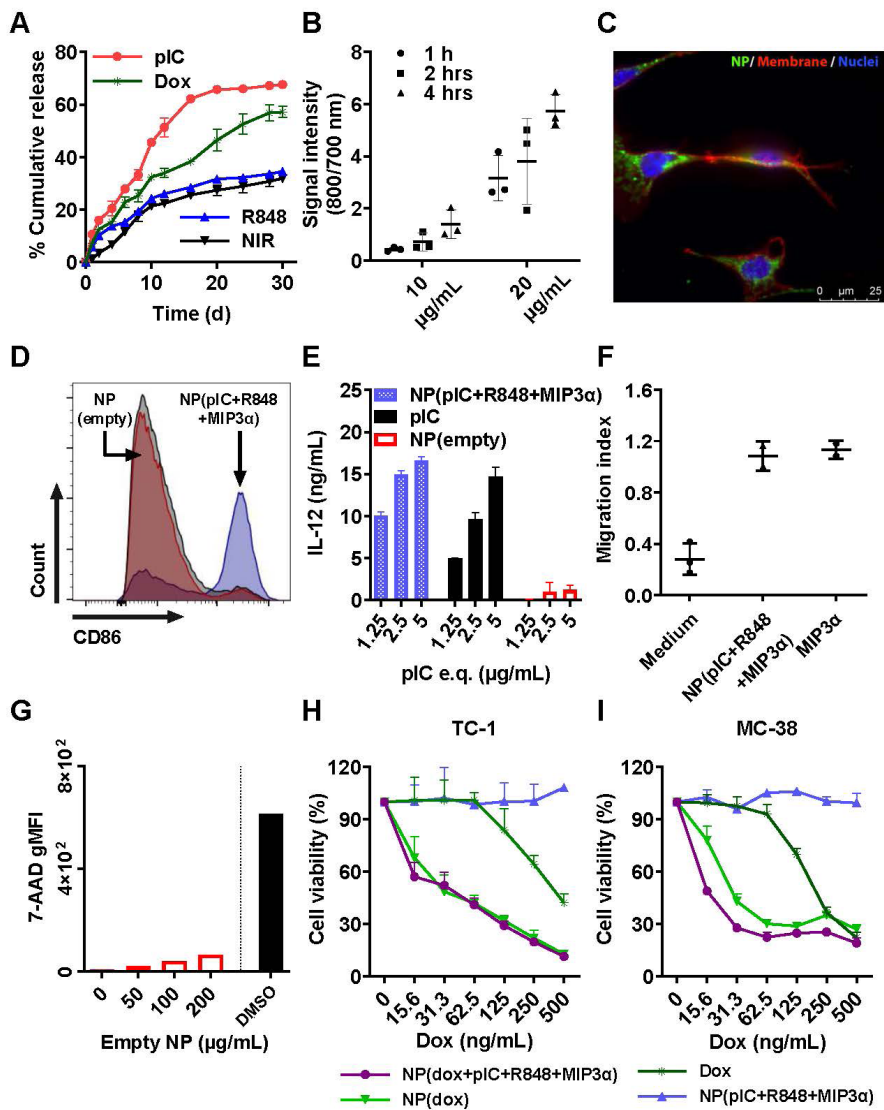
### **NPs enhance DC activation, IL-12 production, and induce chemotaxis**

The ligands pIC and R848 are agonists for the endosomal TLR3 and TLR7/8, respectively, which are predominantly located inside cells. Activation of TLR3 or TLR7/8 can be detected by measuring the expression of CD86 in D1 DCs. For this purpose, NP(pIC+R848+MIP3 $\alpha$ ) was incubated at increasing concentrations with DCs for 48 hours. The loaded NPs caused a dose-dependent increase in CD86 expression, whereas empty NPs at equivalent concentrations did not (Figure 2D). Moreover, incubation with NP(pIC+R848+MIP3 $\alpha$ ) triggered IL-12 secretion by DCs, indicating that these cells had been activated and that the TLR agonists in the NPs had remained active (Figure 2E). To determine the activity of MIP3 $\alpha$  after co-encapsulation in NPs, the chemotactic capacity of this chemokine was assessed by incubating NP(pIC+R848+MIP3 $\alpha$ ) with medium in the lower chamber of a transwell system (Figure 2F). MIP3 $\alpha$  was observed to attract approximately three times the number of cells across the membrane compared to medium only, indicating that, like the TLR agonists, MIP3 $\alpha$  also had remained active after co-encapsulation in the NPs.

### **Cytotoxicity of empty and loaded NPs**

We next sought to determine the cytotoxicity of the empty and loaded NPs (dox only, immune adjuvants only or combinations thereof). First, DCs were co-cultured in vitro with empty NPs for 48 hours at increasing NP concentrations, subsequently stained with the cell death marker 7-AAD, and finally, analyzed by flow cytometry (Figure 2G). The empty NPs did not induce any significant cytotoxicity, as measured by the low signal of 7-AAD relative to the signal of the DMSO control. Next, to ascertain the effects of loading dox into NPs on its chemotherapeutic activity, an MTS cytotoxicity assay was performed by treating TC-1, MC-38 cells and DCs with dox-loaded NPs (Figures 2H, 2I and S4A, respectively). In all cell lines, cytotoxicity was dose-dependent. For TC-1 and MC-38 the dox-loaded NPs provoked ten times the level of cell death as did the free dox. The LD50 of dox in MC-38 cells (ca.

200 ng/mL) was half of that of TC-1 cells (ca. 400 ng/mL). However, the NPs with immune adjuvants alone did not induce cell death in either cell line. In addition, we compared the effect of multi-drug encapsulation of NP(dox+pIC+R848+MIP3 $\alpha$ ) and of NP(pIC+R848+MIP3 $\alpha$ ) versus non-encapsulated (soluble) controls on cell viability (Figure S4). NP(pIC+R848+MIP3 $\alpha$ ) or the soluble controls did not affect cell viability. On the other hand, NP(dox+pIC+R848+MIP3 $\alpha$ ) was more efficient in killing cells than the soluble controls. Overall, these results indicate that empty NPs are non-cytotoxic to DCs and that NP-delivered dox shows greater cytotoxicity to two cancer cell lines than does free dox.



< **Figure 2. In vitro cumulative release kinetics, cellular uptake, DC activation, and cytotoxicity of the empty and drug-loaded NPs**

**A)** NP release kinetics of encapsulated drugs simulated at 37°C in PBS and kept in a thermo-shaker at a constant shaking velocity. n = 3 from one representative experiment. **B)** Uptake of NPs containing NIR dye (800 nm) by TC-1 cells (To-pro 3 iodide; 700 nm) over the times indicated. n = 3 from one representative experiment. **C)** Uptake of NPs by TC-1 cells after 2 hours of incubation, shown by fluorescence microscopy. Red: cell membrane; purple: cell nucleus; green: NIR dye. **D)** Activation of DCs measured by CD86 expression upon 48 hours incubation with NP(pIC+R848+MIP3 $\alpha$ ). NP(empty) and isotype controls are shown in red and grey, respectively. The cells were pooled from n = 3 from each condition, one representative out of three independent experiments. **E)** Activation of DCs measured by the secretion of IL-12p40 upon 48 hours incubation with NP(pIC+R848+MIP3 $\alpha$ ). NP(empty) and pIC controls are shown in red and black, respectively. n = 3 from one representative out of three independent experiments. **F)** Migration assessment using Boyden chamber assay. After 24 hours of pre-incubation of the lower chamber with either MIP3 $\alpha$  (in solution) or NP(pIC+R848+MIP3 $\alpha$ ), RAW264.7 cells were added to the upper chamber and allowed to migrate for 24 hours. Medium was used as a negative control. n = 3 from one representative out of two independent experiments. **G)** Cytotoxicity measurement of empty NPs on DCs incubated with increasing concentrations for 48 hours. The cytotoxic compound DMSO (black bar) was used as a positive control (100 percent of cell death). **H+I)** Cell viability assessed by MTS cell proliferation assay upon 72 hours incubation with indicated compounds on TC-1 (H) or MC-38 (I) cells. n = 3 from one representative out of four independent experiments. All data are presented as mean  $\pm$  SD.

**Intratumoral co-delivery of dox with immune adjuvants boosts lymphocyte influx in the tumor microenvironment**

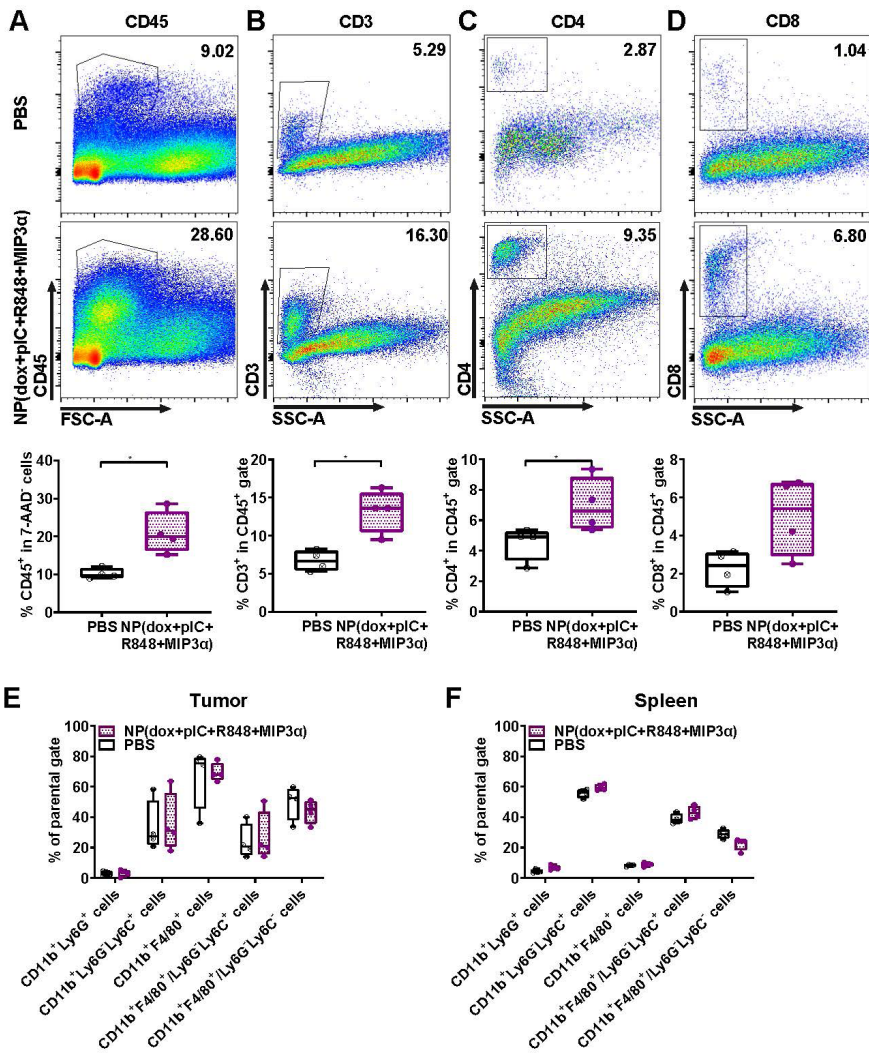
To assess alterations in the tumor and spleen upon treatment, we analyzed the lymphoid and myeloid populations of mice bearing TC-1 tumors. Mice were either treated with a single intratumoral injection of NP(dox+pIC+R848+MIP3 $\alpha$ ) or a mock injection with PBS at day 8. The tumors and spleens were resected 10 days afterwards and analyzed ex vivo. Compared to the mock treated mice, the treated mice exhibited significantly higher levels of leukocytes in the tumor, as measured by cell staining for the pan-leukocyte marker CD45 (Figure 3A). Moreover, the treated mice showed significantly higher levels of CD3+ and CD4+ T cells in the

tumor (Figures 3B & 3C). However, although they also showed higher levels of CD8+ T cells, this difference was not statistically significant (Figure 3D). In the spleen, the number of leukocytes was not found to differ significantly between the control and treated groups (data not shown). Moreover, no significant differences in the tumoral or splenic myeloid populations were observed between the two groups (Figures 3E & 3F). These results indicate that intratumoral treatment of TC-1 tumors with NP(dox+pIC+R848+MIP3 $\alpha$ ) enhances the lymphoid cell populations in the tumor but not in the spleen, and does not alter the myeloid population within the tumor microenvironment.

**Figure 3. Intratumoral co-delivery of dox with immune adjuvants boosts lymphocyte influx in the tumor microenvironment**

At day 8, mice with TC-1 tumors received a single intratumoral injection of either PBS (mock control) or NP(dox+pIC+R848+MIP3 $\alpha$ ). Ten days later, the tumors were resected and analyzed by flow cytometry: A) Representative flow cytometry plot showing CD45.2 cells in a mock (PBS) or treated tumor. The box and whiskers plot depicts n=4 from one representative out of two independent experiments (p=0.0286). B) Representative flow cytometry plot showing CD3+ cells in a mock (PBS) or treated tumor. The box and whiskers plot depicts n=4 from one representative out of two independent experiments (p=0.0286). C) Representative flow cytometry plot showing CD4+ T cells in a mock (PBS) or treated tumor. The box and whiskers plot depicts n=4 from one representative out of two independent experiments (p=0.0286). D) Representative flow cytometry plot showing CD8+ T cells in a mock (PBS) or treated tumor. The box and whiskers plot depicts n=4 from one representative out of two independent experiments (p=0.1143; n.s.). E) Different cell types within the myeloid population analyzed in the tumor is depicted upon mock treated (PBS) tumors or treated tumors. n=4 from one representative out of two independent experiments. F) Different cell types within the myeloid population analyzed in the spleen is depicted upon mock treated (PBS) tumors or treated tumors. n=4 from one representative out of two independent experiments.. Statistics were calculated using a two-tailed Mann Whitney test. Statistical differences were considered significant at p < 0.05. \* = p < 0.05; \*\* p = < 0.01; \*\*\* p < 0.001. Data plotted are presented as min to max.





**Intratumoral co-delivery of dox and immune adjuvants by NPs augments the levels of circulating CD3+, CD8+ and cancer antigen-specific CD8+ T cells**

To determine whether the combined chemoimmunotherapy approach can alter the levels of circulating lymphocytes, we collected blood at day 16 and at day 26 (8 and 16 days post-treatment) from mice with TC-1 tumors and measured the number of CD3+, CD8+ and cancer antigen-specific CD8+ T cells. We observed that on day 16, the percentage of CD3+ and CD8+ T cells was not found to be significantly different (Figure 4A & 4B, respectively). However, treatment of mice with NP(dox+pIC+R848+MIP3 $\alpha$ ) induced a significant increase in cancer antigen-specific CD8+ T cells, compared to intratumoral administration of free dox or PBS alone (Figure 4C). At day 26, the average number of CD3+ and CD8+ T cells was higher in the blood of mice treated with NP(dox+pIC+R848+MIP3 $\alpha$ ) than mice treated with dox only, but this difference was not statistically significant (Figures 4D & 4E). In contrast to day 16, at day 26 there were no differences in the levels of cancer-specific CD8+ T cells among the three groups (Figure 4F).

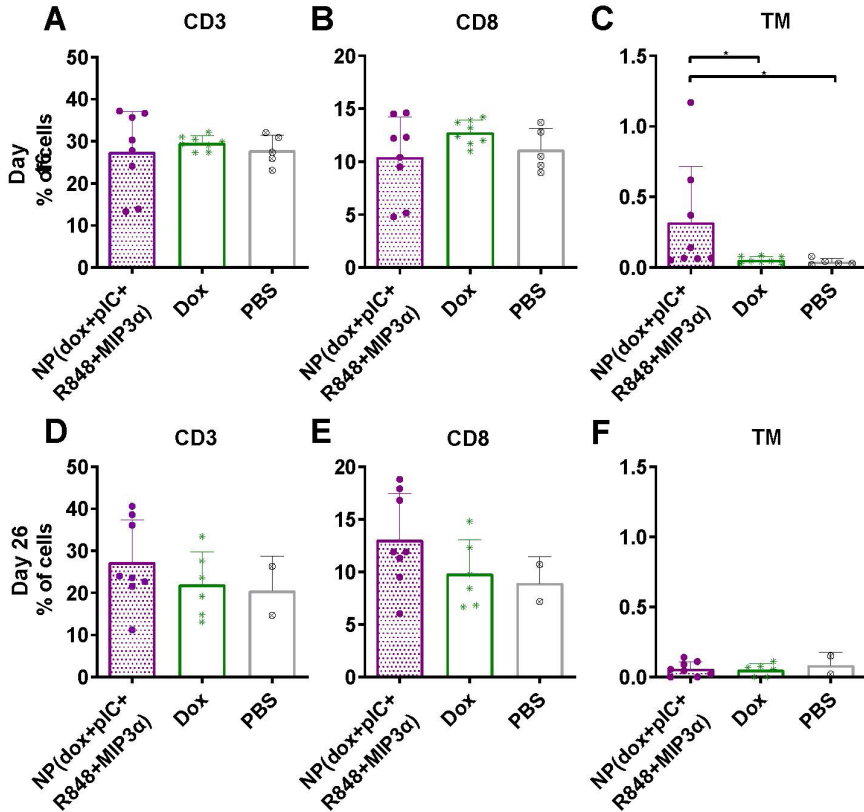


**Figure 4. Intratumoral co-delivery of dox and immune adjuvants by NPs augments the levels of circulating CD3+, CD8+ and cancer antigen-specific CD8+ T cells**

Quantification of CD3+, CD8+ and the HPV16 E7 tetramer specific T cells in blood at day 16 and at day 26 (8 and 16 days post-treatment) after treatment with intratumoral NP(dox+pIC+R848+MIP3 $\alpha$ ) as compared with free dox or PBS (mock control). A&B) The levels of CD3+ and CD8+ T cells collected from blood of mice at day 16 (8 days after treatment) are depicted. n = 8 for NP(dox+pIC+R848+MIP3 $\alpha$ ), n = 8 for Dox and n = 5 for PBS. One representative out of two independent experiments. The differences between the groups are not statistically significant. C) The levels of TM+ (cancer cell specific) CD3+CD8+ T cells collected from blood of mice at day 16 (8 days after treatment). n = 8 for NP(dox+pIC+R848+MIP3 $\alpha$ ), n = 8 for Dox and n = 5 for PBS. One representative out

of two independent experiments. NP vs. dox ( $p=0.0351$ ) and NP vs. PBS ( $p=0.0163$ ). D&E) The levels of CD3+ and CD8+ T cells collected from blood of mice at day 26 (18 days after treatment) are depicted.  $n=8$  for NP(dox+pIC+R848+MIP3a),  $n=6$  for Dox and  $n=2$  for PBS. One representative out of two independent experiments. The differences between the groups are not statistically significant. F) The levels of TM+ (cancer cell specific) CD3+CD8+ T cells collected from blood of mice at day 26 (18 days after treatment),  $n=8$  for NP(dox+pIC+R848+MIP3a),  $n=6$  for Dox and  $n=2$  for PBS. One representative out of two independent experiments. The differences between the groups are not statistically significant. Statistics were calculated using a two-tailed Mann Whitney test. Statistical differences were considered significant at  $p < 0.05$ . \* =  $p < 0.05$ ; \*\*  $p < 0.01$ ; \*\*\*  $p < 0.001$ . All data are presented as mean  $\pm$  SD. Abbreviations: TM: tetramer.

**Intratumoral co-delivery of dox and immune adjuvants by NPs provides enhanced chemoimmunotherapeutic effects in mice with established tumors**

Next, we determined the respective therapeutic contributions of dox and of the immune adjuvants (pIC, R848 and MIP3 $\alpha$ ). Treatment was initiated with one intratumoral injection at 8 days post-inoculation, followed by three additional consecutive administrations at days 10, 12 and 14 (Figure 5A). The NPs were detectable with IVIS fluorescence imaging for at least 168 hours in the tumor after last injection (Figure S5). A significant therapeutic effect was observed for all the tumors treated with NPs containing dox alone, the immune adjuvants alone or the combination therapy but not for the empty NPs (Figures 5B & 5C). The greatest statistically significant therapeutic effect was provided by the combination therapy, followed by the monotherapies; however, there was no significant therapeutic difference between either monotherapy. These results corroborate an enhanced effect between dox and the immune adjuvants when intratumorally co-delivered by NPs.

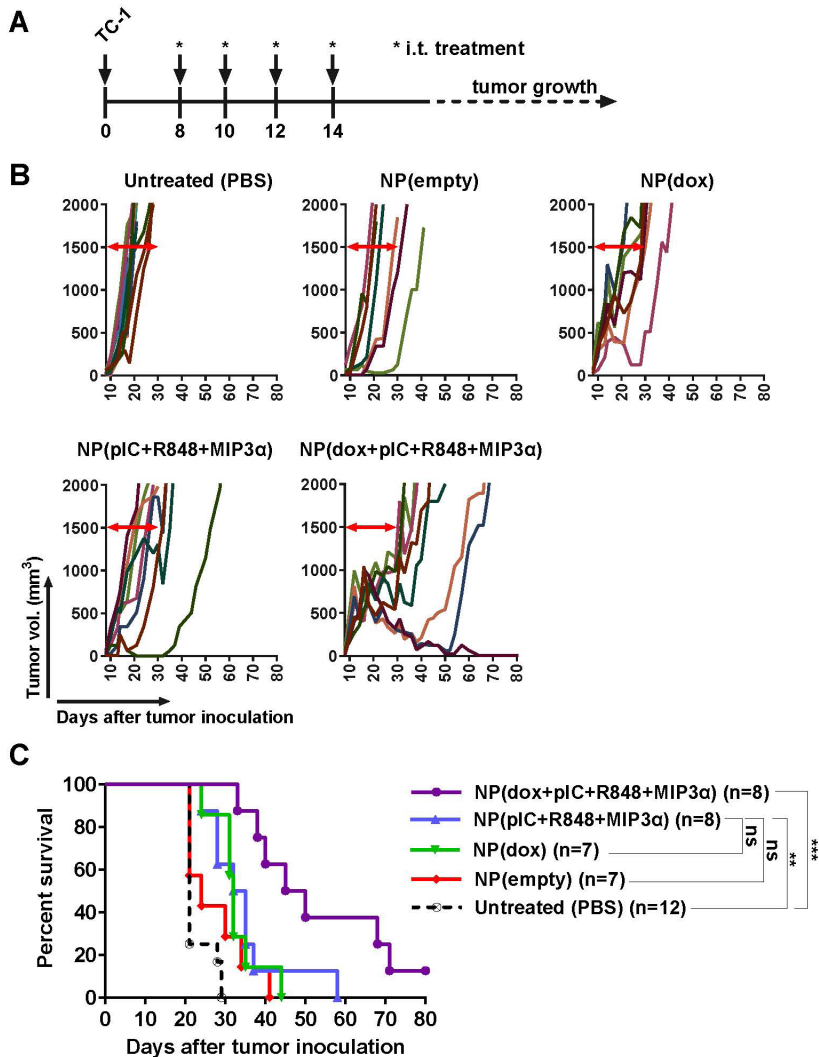


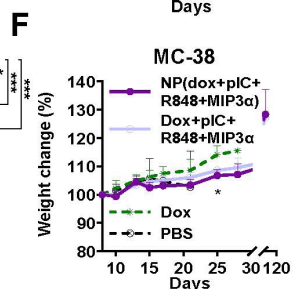
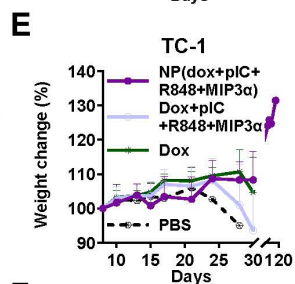
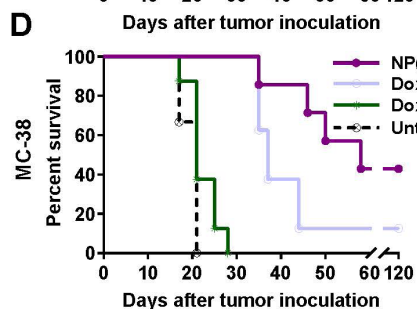
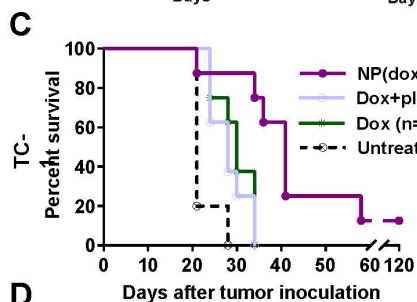
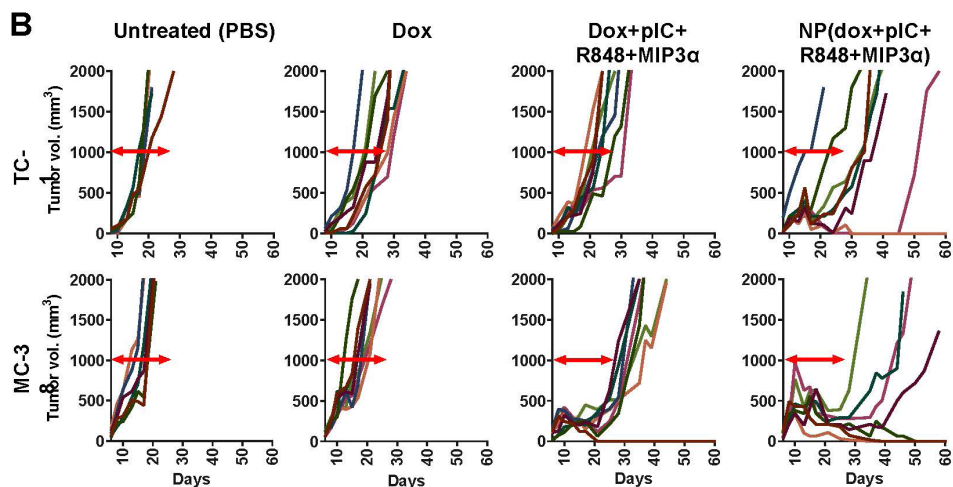
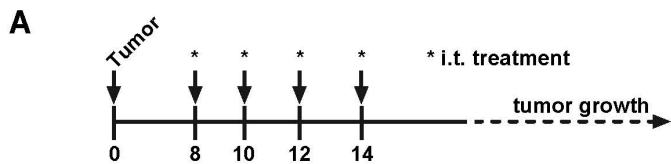
**Figure 5. Intratumoral co-delivery of dox and immune adjuvants by NPs provides enhanced chemoimmunotherapeutic effects in mice with established tumors**

**A)** Schematic diagram of the TC-1 murine model experiment (C57BL/6 mice; n=8 per group, on average), showing inoculation and treatment days. **B)** Tumor growth data from day 0 to day 80 for the PBS (control) group and four treatment groups (empty NPs, NP-delivered dox monotherapy, NP-delivered immune adjuvants and NP-delivered combination therapy). **C)** Kaplan-Meier survival plots of pooled data, depicting progression-free survival and

percent overall survival: NP(dox) vs. PBS  $p=0.0004$ ; NP(pIC+R848+MIP3 $\alpha$ ) vs. PBS  $p=0.001$ ; NP(dox+pIC+R848+MIP3 $\alpha$ ) vs. PBS  $p<0.0001$ ; NP(dox+pIC+R848+MIP3 $\alpha$ ) vs. NP(pIC+R848+MIP3 $\alpha$ )  $p=0.0082$ ; NP(dox+pIC+R848+MIP3 $\alpha$ ) vs. NP(dox)  $p=0.0024$ ; NP(empty) vs. PBS  $p=0.1082$ ; NP(empty) vs. NP(dox)  $p=0.1160$ ; NP(empty) vs. NP(pIC+R848+MIP3 $\alpha$ )  $p=0.1076$ ; NP(empty) vs. NP(dox+pIC+R848+MIP3 $\alpha$ )  $p=0.0023$ . Survival curves were compared using the Gehan-Breslow-Wilcoxon test. Statistical differences were considered significant at \*  $p < 0.05$ ; \*\*  $p < 0.01$ ; \*\*\*  $p < 0.001$ .

### **Intratumoral co-delivery of dox and immune adjuvants by NPs induces strong tumor regression and better overall survival than does of free components**

To further assess the therapeutic advantage of our NPs, we compared intratumoral treatment of free dox, the free combination therapy (dox+pIC+R848+MIP3 $\alpha$ ) and the NP-delivered combination therapy in two murine models of cancer: MC-38 and TC-1, using immunocompetent C57BL/6 mice. Treatment was initiated at day 8, followed by three additional consecutive administrations at days 10, 12 and 14 (Figure 6A). The concentrations of the free compounds were matched to the concentrations of the compounds loaded inside the NPs. The tumors in mice treated with free dox monotherapy did not regress in either model (Figure 6B). Unlike the TC-1 tumors, the MC-38 tumors did initially respond to the free combination therapy. The greatest gain in overall survival in both models was observed for the NP-delivered combination therapy (Figure 6C & 6D). Importantly, halving the total dose of NP-delivered combination therapy and increasing the time between administrations gave sustained, measurable responses in both models, but failed to completely cure any mouse (Figures S6A to S6D). In both models, the effects of all treatments on weight gain was minimal (Figure 6E & 6F). However, at day 25, the weight of MC-38 mice treated with either combination therapy (NP or free) was slightly lower than that of the mice treated with dox alone. Furthermore, all the mice whose tumors had been eradicated later rejected a tumor re-challenge, which indicates development of functional immunological memory against tumor antigens (data not shown). In conclusion, these results indicate that the NP-delivered combination therapy of dox and immune adjuvants is more effective than the corresponding free therapy at inducing long-term tumor control and even complete remission in mice with MC-38 or TC-1 tumors and does not provoke any detectable side effects.





< **Figure 6. Intratumoral co-delivery of dox and immune adjuvants by NPs induces strong tumor regression and better overall survival than does of free components**

A) Schematic diagram of the TC-1 and MC-38 murine (C57BL/6 mice) model experiments, showing inoculation and treatment days. B) Tumor-growth data from day 0 to day 60 for the PBS (control) group and three treatment groups (free dox, free combination therapy and NP-delivered combination therapy) in the TC-1 (top) and MC-38 (bottom) models. C) Kaplan-Meier survival plots depicting progression-free survival and percent overall survival for the TC-1 model upon indicated treatments.  $n = 8$  for each treatment group and  $n = 5$  for PBS. NP(dox+pIC+R848+MIP3 $\alpha$ ) vs. PBS  $p=0.0041$ ; Dox+pIC+R848+MIP3 $\alpha$  vs. PBS  $p=0.0083$ ; Dox vs. PBS  $p=0.0115$ ; NP(dox+pIC+R848+MIP3 $\alpha$ ) vs. dox  $p=0.0113$ ; NP(dox+pIC+R848+MIP3 $\alpha$ ) vs. Dox+pIC+R848+MIP3 $\alpha$   $p=0.0106$ . D) Kaplan-Meier survival plots depicting progression-free survival and percent overall survival for the MC-38 model upon indicated treatments.  $n = 8$  for NP(dox+pIC+R848+MIP3 $\alpha$ ),  $n=7$  for Dox+pIC+R848+MIP3 $\alpha$ ,  $n=8$  for Dox and  $n = 6$  for PBS. NP(dox+pIC+R848+MIP3 $\alpha$ ) vs. PBS  $p=0.0008$ ; Dox+pIC+R848+MIP3 $\alpha$  vs. PBS  $p=0.0004$ ; Dox vs. PBS  $p=0.1096$ ; NP(dox+pIC+R848+MIP3 $\alpha$ ) vs. dox  $p=0.0004$ ; NP(dox+pIC+R848+MIP3 $\alpha$ ) vs. Dox+pIC+R848+MIP3 $\alpha$   $p=0.0002$ . E) The weight change of mice with TC-1 tumors after treatments. Data are presented as mean  $\pm$  SD. F) The weight change of mice with MC-38 tumors after treatments. Data are presented as mean  $\pm$  SD. At day 25: NP(dox+pIC+R848+MIP3 $\alpha$ ) vs. dox  $p= 0.0121$ ; Dox+pIC+R848+MIP3 $\alpha$  vs. dox  $p= 0.0121$ . Survival curves were compared using the Gehan-Breslow-Wilcoxon test. Mice weight were analyzed by two-tailed Mann Whitney test. Statistical differences were considered significant at \*  $p = < 0.05$ ; \*\*  $p = < 0.01$ ; \*\*\*  $p < 0.001$ .

## DISCUSSION

Here, we report that the NP mediated delivery of dox and immune adjuvants induces complete remissions and effective long-term tumor control in both lung and colon mice tumor models. We show that the combinatorial treatment of chemotherapy with non-specific immunotherapy induces superior therapeutic responses which are attained when biomaterial nanotechnology is employed for the co-delivery. Furthermore, we show that the NP mediated chemioimmunotherapy modality augments the levels of lymphocytes and of cancer specific CD8+ T cells in the tumor and circulating in blood, leading to tumor eradications.

For this paper, we prepared PEGylated PLGA NPs with an average size of approximately 180 nm, which is within the optimal functional range (40 nm to 300 nm) reported for drug-delivery NPs [32–34]. When the NPs containing dox were co-cultured with cancer cells, more cancer cells were killed by dox inside NPs than an equal concentration of free dox. This finding could relate to a well-known drug efflux mechanism whereby transporters pump dox out of the cell [35]. Indeed, NP-delivered drugs have been reported to bypass efflux transporters, which also corroborates our results [36]. Nonetheless, the TC-1 cells were more resistant to dox treatment than the MC-38 cells, independently of the delivery method. We also analyzed the established tumors after treatment and within the cell marker panels tested, we did not find any significant changes within the myeloid populations. This could be due to tumor cells overcoming acute inflammatory cytokines triggered by the TLR agonists. However, we did observe significant increases in the numbers of lymphocytes in the tumor, but not in the spleen. Furthermore, we analyzed the blood of treated mice at two different time points and found that the combination therapy and the free dox monotherapy did not induce any reduction in the number of circulating lymphocytes. Together, these data indicate that, at the administered dose, the NP-delivered combination therapy did not reduce but rather increased the levels of lymphocytes in the tumor and did not affect the myeloid population within the parameters analyzed. However, at day 16 we found that only the combination treatment induced detectable numbers of cancer antigen-specific T cells. Similarly to radiotherapy or photo dynamic therapy, this evidences that cancer antigen-specific T cells can be generated without vaccination [37]. Furthermore, we report that co-delivery of dox and the immune adjuvants in a single NP provided significantly longer progression-free survival and overall survival in treated mice bearing MC-38 or TC-1 tumors compared to untreated mice.

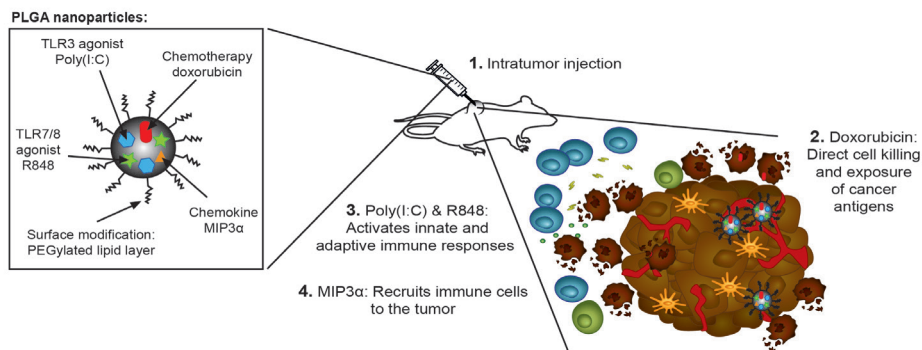


**Figure 7. Rational design of the nanoparticle-delivered chemoimmunotherapy to the tumor and tumor-draining lymph node**

Step 1) The NPs are injected in the tumors, whereby a part of the NPs are endocytosed by cancer and cancer associated cells. The NPs that were not endocytosed start to release their content in the extracellular space of which a portion also drains to the tumor-draining lymph node (and further). Due to the good NP stability, the drug release and their biological effects is sustained for a prolonged period of time. Step 2) The cytostatic doxorubicin induces (cancer) cell death and the release of cancer antigens. Step 3) The immune modulators pIC and R848 activate residing immature and suppressed immune cells in the tumor and tumor-draining lymph node. Step 4) MIP3 $\alpha$  recruits more immune cells into the tumor.

Our NP-delivered combination therapy provides a triple mechanism based on the activity of dox, the chemokine MIP3 $\alpha$ , and the TLR agonists pIC and R848 (Figure 7). Dox can induce the release of cancer antigens during cancer cell killing, but this effect alone often cannot provoke a sufficiently powerful immunological response for tumor clearance [38]. The chemokine MIP3 $\alpha$ , can amplify the intratumoral immune response by recruiting T cells to the tumor. Furthermore, given that our NP concomitantly delivers specific TLRs, their activity likely abrogates the immunosuppressive signals that tumor cells send to immature DCs that process tumor antigens. Specifically, as some of the TLR agonists that partially leak into blood stimulate dividing T cells, those remaining inside the tumor cells maintain a favorable T cell environment. Finally, while the PLGA NPs themselves are non-

cytotoxic and biocompatible, the direct activation of the inflammasome by PLGA in DCs has been reported [39,40].

Our findings are consistent with those of other groups, who have reported the benefits of NPs for delivery of chemotherapy and non-specific innate immunotherapy [41–44]. For instance, Roy et al. and Heo et al. treated murine B16 melanoma tumors with PLGA NPs containing paclitaxel and either a TLR4 or a TLR9 agonist, respectively [41,43]. The authors observed an initial delay in tumor growth and a significant influx of lymphocytes into the tumors. Moreover, Yin et al. treated B16 tumors with PLGA NPs containing dox and interferon  $\gamma$  [44]. The authors reported a delay in tumor growth, an influx of lymphocytes and NK cells into the tumors, and, in the tumor microenvironment, reduced levels of the suppressive cytokines IL-10 and TGF $\beta$ , and increased levels of IL-2 and TNF $\alpha$ .

Despite the promising results for NP-delivered combination therapies in animal models of cancer, the translation to clinical use must be judiciously guided. In the few clinical trials in which patients with solid tumors were treated TLR agonist monotherapies, the treatment caused some cancers to regress but caused others to proliferate and metastasize [45]. For example, the strategy of activating TLR3 in lung cancer tumors appears to generate contradictory effects, inducing regressions in some tumors while conferring resistance in others [45,46]. In contrast, colon cancer cells exposed to TLR3 agonists have been reported to initiate apoptosis more rapidly [45]. The usage of slow-release vehicles, such as those enabled by nanotechnology, has been advocated for clinical therapy, since humans, unlike mice, are highly susceptible to cytokine release syndrome, a common side-effect of experimental immunotherapies [47–49].

Taken together, our results underscore the potential of NP-delivered chemoimmunotherapy to induce powerful anti-cancer immunity in solid, refractory tumors. We surmise that patients who are ineligible for surgery, or non-responsive to chemotherapy or immunotherapy, may benefit from this non-specific chemoimmunotherapy modality in the future.

**Abbreviations**

AFM: Atomic Force Microscopy; Dox: doxorubicin; DCs: dendritic cells; IFNs: type I interferons; MIP3 $\alpha$ : Macrophage Inflammatory Protein-3 alpha; NIR: Near infrared; NP: nanoparticle; pIC: Poly(I:C); PLGA: poly(lactic-co-glycolic acid); TEM: Transmission Electron Microscope; TLR: Toll-like receptor; TM: tetramer.

**Acknowledgments**

This work is part of the research programme 723.012.110 (Vidi), which is financed by the Netherlands Organisation for Scientific Research (NWO). We would like to thank Fabio Baldazzi and Filippo Tamburini for assistance in the nanoparticle characterization experiments, including TEM, DLS and fluorescence microscopy. Also, we would like to thank the financial support of the LUMC fellowship grant, project grants from the EU Program H2020-MSCA-2015-RISE (644373-PRISAR) and MSCA-ITN-2015-ETN (675742-ISPIC), H2020-MSCA-2016-RISE (734684-CHARMED) and H2020-MSCA-RISE-2017-CANCER (777682).

**Competing Interests**

The authors have declared that no competing interest exists.

## REFERENCES

1. Gotwals P, Cameron S, Cipolletta D, Cremasco V, Crystal A, Hewes B, et al. Prospects for combining targeted and conventional cancer therapy with immunotherapy. *Nat Rev Cancer*. 2017; 17: 286–301.
2. Da Silva CG, Rueda F, Löwik CW, Ossendorp F, Cruz LJ. Combinatorial prospects of nano-targeted chemoimmunotherapy. *Biomaterials*. 2016; 83: 308–320.
3. Albini A, Sporn MB. The tumour microenvironment as a target for chemoprevention. *Nat Rev Cancer*. 2007; 7: 139.
4. Sistigu A, Yamazaki T, Vacchelli E, Chaba K, Enot DP, Adam J, et al. Cancer cell-autonomous contribution of type I interferon signaling to the efficacy of chemotherapy. *Nat Med*. 2014; 20: 1301–1309.
5. Fransen M, Ossendorp F, Arens R, Melief CJ. Local immunomodulation for cancer therapy: Providing treatment where needed. *Oncoimmunology*. 2013; 2: e26493.
6. Koster BD, van den Hout MFCM, Sluijter BJR, Molenkamp BG, Vuylsteke RJCLM, Baars A, et al. Local Adjuvant Treatment with Low-Dose CpG-B Offers Durable Protection against Disease Recurrence in Clinical Stage I–II Melanoma: Data from Two Randomized Phase II Trials. *Clin Cancer Res*. 2017; 23: 5679–5686.
7. Amos SM, Pegram HJ, Westwood JA, John LB, Devaud C, Clarke CJ, et al. Adoptive immunotherapy combined with intratumoral TLR agonist delivery eradicates established melanoma in mice. *Cancer Immunol Immunother*. 2011; 60: 671–683.
8. Jackaman C, Lew AM, Zhan Y, Allan JE, Koloska B, Graham PT, et al. Deliberately provoking local inflammation drives tumors to become their own protective vaccine site. *Int Immunol*. 2008; 20: 1467–1479.
9. Rahman AH, Taylor DK, Turka LA. The contribution of direct TLR signaling to T cell responses. *Immunol Res*. 2009; 45: 25–36.
10. Pasare C, Medzhitov R. Toll-like receptors: linking innate and adaptive immunity. *Microbes Infect*. 2004; 6: 1382–1387.
11. Shi M, Chen X, Ye K, Yao Y, Li Y. Application potential of toll-like receptors in cancer immunotherapy: Systematic review. *Medicine (Baltimore)*. 2016; 95: e3951.
12. Chi H, Li C, Zhao FS, Zhang L, Ng TB, Jin G, et al. Anti-tumor Activity of Toll-Like Receptor 7 Agonists. *Front Pharmacol*. 2017; 8: 304.
13. Ye J, Ma C, Hsueh EC, Dou J, Mo W, Liu S, et al. TLR8 signaling enhances tumor immunity by preventing tumor-induced T-cell senescence. *EMBO Mol Med*. 2014; 6: 1294–311.

14. Ting Tan RS, Lin B, Liu Q, Tucker-Kellogg L, Ho B, Leung BP, et al. The synergy in cytokine production through MyD88-TRIF pathways is co-ordinated with ERK phosphorylation in macrophages. *Immunol Cell Biol.* 2013; 91: 377–387.
15. Roussos ET, Condeelis JS, Patsialou A. Chemotaxis in cancer. *Nat Rev Cancer.* 2011; 11: 573–87.
16. Dieu MC, Vanbervliet B, Vicari A, Bridon JM, Oldham E, Ait-Yahia S, et al. Selective recruitment of immature and mature dendritic cells by distinct chemokines expressed in different anatomic sites. *J Exp Med.* 1998; 188: 373–86.
17. Al-Aoukaty A, Rolstad B, Giaid A, Maghazachi AA. MIP-3alpha, MIP-3beta and fractalkine induce the locomotion and the mobilization of intracellular calcium, and activate the heterotrimeric G proteins in human natural killer cells. *Immunology.* 1998; 95: 618–624.
18. Liao F, Rabin RL, Smith CS, Sharma G, Nutman TB, Farber JM. CC-chemokine receptor 6 is expressed on diverse memory subsets of T cells and determines responsiveness to macrophage inflammatory protein 3 alpha. *J Immunol.* 1999; 162: 186–94.
19. Acosta-Rodriguez EV, Rivino L, Geginat J, Jarrossay D, Gattorno M, Lanzavecchia A, et al. Surface phenotype and antigenic specificity of human interleukin 17-producing T helper memory cells. *Nat Immunol.* 2007; 8: 639–646.
20. Schutyser E, Struyf S, Van Damme J. The CC chemokine CCL20 and its receptor CCR6. *Cytokine Growth Factor Rev.* 2003; 14: 409–426.
21. Makadia HK, Siegel SJ. Poly Lactic-co-Glycolic Acid (PLGA) as Biodegradable Controlled Drug Delivery Carrier. *Polymers (Basel).* 2011; 3: 1377–1397.
22. LaVan DA, McGuire T, Langer R. Small-scale systems for in vivo drug delivery. *Nat Biotechnol.* 2003; 21: 1184–1191.
23. Schütz CA, Juillerat-Jeanneret L, Mueller H, Lynch I, Riediker M. Therapeutic nanoparticles in clinics and under clinical evaluation. 2013; 8: 449–467.
24. van der Meel R, Vehmeijer LJC, Kok RJ, Storm G, van Gaal EVB. Ligand-targeted particulate nanomedicines undergoing clinical evaluation: current status. *Adv Drug Deliv Rev.* 2013; 65: 1284–98.
25. Bobo D, Robinson KJ, Islam J, Thurecht KJ, Corrie SR. Nanoparticle-Based Medicines: A Review of FDA-Approved Materials and Clinical Trials to Date. *Pharm Res.* 2016; 33: 2373–2387.
26. Tel J, Lambeck AJA, Cruz LJ, Tacken PJ, de Vries IJM, Figdor CG. Human Plasmacytoid Dendritic Cells Phagocytose, Process, and Present Exogenous Particulate Antigen. *J Immunol.* 2010; 184: 4276–4283.

27. Cruz LJ, Stammes MA, Que I, van Beek ER, Knol-Blankevoort VT, Snoeks TJA, et al. Effect of PLGA NP size on efficiency to target traumatic brain injury. *J Control Release*. 2016; 223: 31–41.
28. Lin KY, Guarnieri FG, Staveley-O'Carroll KF, Levitsky HI, August JT, Pardoll DM, et al. Treatment of established tumors with a novel vaccine that enhances major histocompatibility class II presentation of tumor antigen. *Cancer Res*. 1996; 56: 21–6.
29. Ossendorp F, Fu N, Camps M, Granucci F, Gobin SJP, van den Elsen PJ, et al. Differential Expression Regulation of the and Subunits of the PA28 Proteasome Activator in Mature Dendritic Cells. *J Immunol*. 2005; 174: 7815–7822.
30. Zom GG, Khan S, Britten CM, Sommandas V, Camps MGM, Loof NM, et al. Efficient Induction of Antitumor Immunity by Synthetic Toll-like Receptor Ligand-Peptide Conjugates. *Cancer Immunol Res*. 2014; 2: 756–764.
31. Aston WJ, Hope DE, Nowak AK, Robinson BW, Lake RA, Lesterhuis WJ. A systematic investigation of the maximum tolerated dose of cytotoxic chemotherapy with and without supportive care in mice. *BMC Cancer*. 2017; 17: 684.
32. Mundargi RC, Babu VR, Rangaswamy V, Patel P, Aminabhavi TM. Nano/micro technologies for delivering macromolecular therapeutics using poly(d,l-lactide-co-glycolide) and its derivatives. *J Control Release*. 2008; 125: 193–209.
33. Moghimi SM, Hunter AC, Andresen TL. Factors Controlling Nanoparticle Pharmacokinetics: An Integrated Analysis and Perspective. *Annu Rev Pharmacol Toxicol*. 2012; 52: 481–503.
34. Bhattacharjee S. DLS and zeta potential – What they are and what they are not? *J Control Release*. 2016; 235: 337–351.
35. Shen F, Chu S, Bence AK, Bailey B, Xue X, Erickson PA, et al. Quantitation of Doxorubicin Uptake, Efflux, and Modulation of Multidrug Resistance (MDR) in MDR Human Cancer Cells. *J Pharmacol Exp Ther*. 2007; 324: 95–102.
36. Da Silva CG, Peters GJ, Ossendorp F, Cruz LJ. The potential of multi-compound nanoparticles to bypass drug resistance in cancer. *Cancer Chemother Pharmacol*. 2017; 80: 881–894.
37. Kleinovink JW, van Driel PB, Snoeks TJ, Prokopi N, Fransen MF, Cruz LJ, et al. Combination of Photodynamic Therapy and Specific Immunotherapy Efficiently Eradicates Established Tumors. *Clin Cancer Res*. 2016; 22: 1459–1468.
38. Zitvogel L, Apetoh L, Ghiringhelli F, Kroemer G. Immunological aspects of cancer chemotherapy. *Nat Rev Immunol*. 2008; 8: 59–73.



39. Sharp FA, Ruane D, Claass B, Creagh E, Harris J, Malyala P, et al. Uptake of particulate vaccine adjuvants by dendritic cells activates the NALP3 inflammasome. *Proc Natl Acad Sci U S A*. 2009; 106: 870–5.
40. Wolfram J, Zhu M, Yang Y, Shen J, Gentile E, Paolino D, et al. Safety of Nanoparticles in Medicine. *Curr Drug Targets*. 2015; 16: 1671–81.
41. Roy A, Singh MS, Upadhyay P, Bhaskar S. Nanoparticle mediated co-delivery of paclitaxel and a TLR-4 agonist results in tumor regression and enhanced immune response in the tumor microenvironment of a mouse model. *Int J Pharm*. 2013; 445: 171–180.
42. Lee I-H, An S, Yu MK, Kwon H-K, Im S-H, Jon S. Targeted chemoimmunotherapy using drug-loaded aptamer–dendrimer bioconjugates. *J Control Release*. 2011; 155: 435–441.
43. Heo MB, Kim S-Y, Yun WS, Lim YT. Sequential delivery of an anticancer drug and combined immunomodulatory nanoparticles for efficient chemoimmunotherapy. *Int J Nanomedicine*. 2015; 10: 5981–92.
44. Yin Y, Hu Q, Xu C, Qiao Q, Qin X, Song Q, et al. Co-delivery of Doxorubicin and Interferon- $\gamma$  by Thermosensitive Nanoparticles for Cancer Immunochemotherapy. *Mol Pharm*. 2018; acs.molpharmaceut.8b00564.
45. Kaczanowska S, Joseph AM, Davila E. TLR agonists: our best frenemy in cancer immunotherapy. *J Leukoc Biol*. 2013; 93: 847–63.
46. Estornes Y, Toscano F, Virard F, Jacquemin G, Pierrot A, Vanbervliet B, et al. dsRNA induces apoptosis through an atypical death complex associating TLR3 to caspase-8. *Cell Death Differ*. 2012; 19: 1482–1494.
47. Talmadge JE, Adams J, Phillips H, Collins M, Lenz B, Schneider M, et al. Immunomodulatory effects in mice of polyinosinic-polycytidylic acid complexed with poly-L-lysine and carboxymethylcellulose. *Cancer Res*. 1985; 45: 1058–65.
48. Levine AS, Levy HB. Phase I-II trials of poly IC stabilized with poly-L-lysine. *Cancer Treat Rep*. 1978; 62: 1907–12.
49. Shimabukuro-Vornhagen A, Gödel P, Subklewe M, Stemmler HJ, Schlößer HA, Schlaak M, et al. Cytokine release syndrome. *J Immunother Cancer*. 2018; 6: 56.

## **Effective chemoimmunotherapy by co-delivery of doxorubicin and immune adjuvants in biodegradable nanoparticles**

Candido G. Da Silva, Marcel G.M. Camps, Tracy M.W.Y. Li, Luana Zerrillo, Clemens W. Löwik, Ferry Ossendorp, Luis J. Cruz

Theranostics 2019; 9(22):6485-6500.

### **Supplementary Figures**

Figure S1. Flow cytometry gating strategy

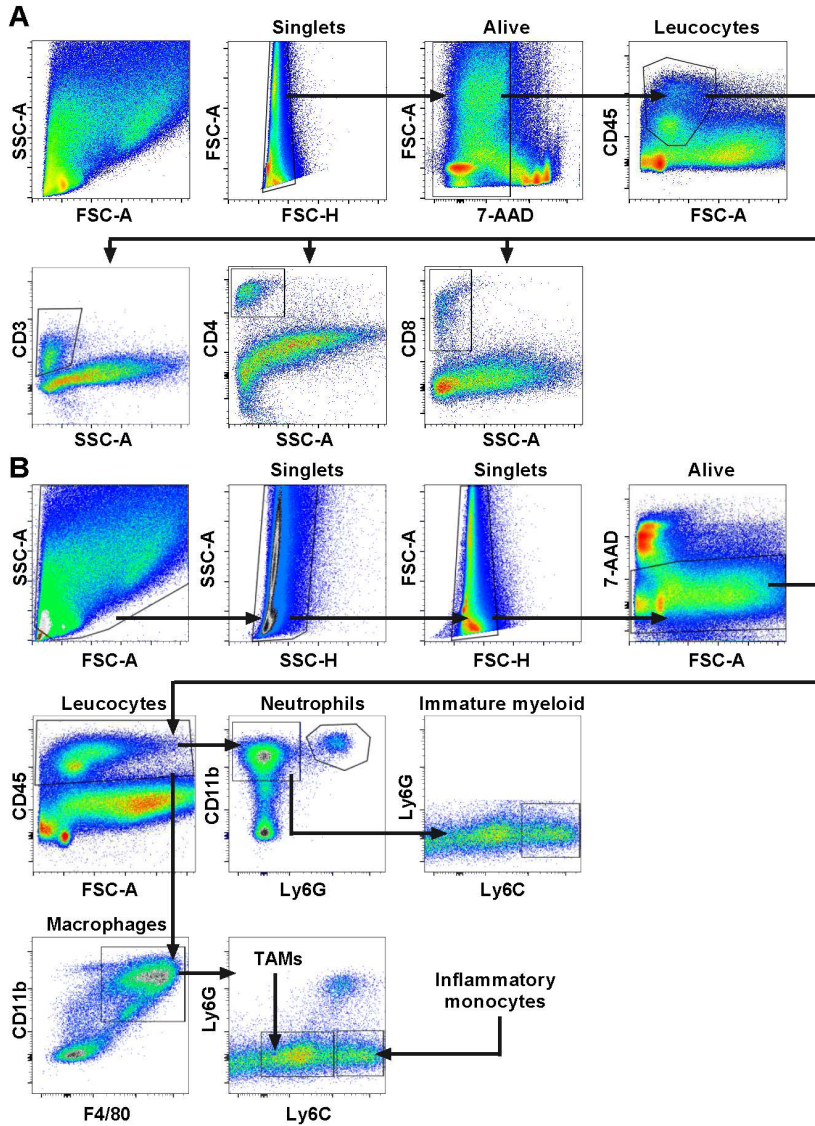
Figure S2. The size and zeta potential data characterized by dynamic light scattering

Figure S3. Stability study of PLGA NPs

Figure S4. Cytotoxicity of the drug-loaded NPs vs. solvent controls

Figure S5. IVIS imaging of TC-1 tumors after treatment

Figure S6. Halving the dose of NP-delivered combination therapy does not alter its anti-tumor efficacy but does lead to lower overall survival



**Figure S1. Flow cytometry gating strategy**

A) Flow cytometry gating strategy for the lymphoid populations.

B) Flow cytometry gating strategy for the myeloid populations.

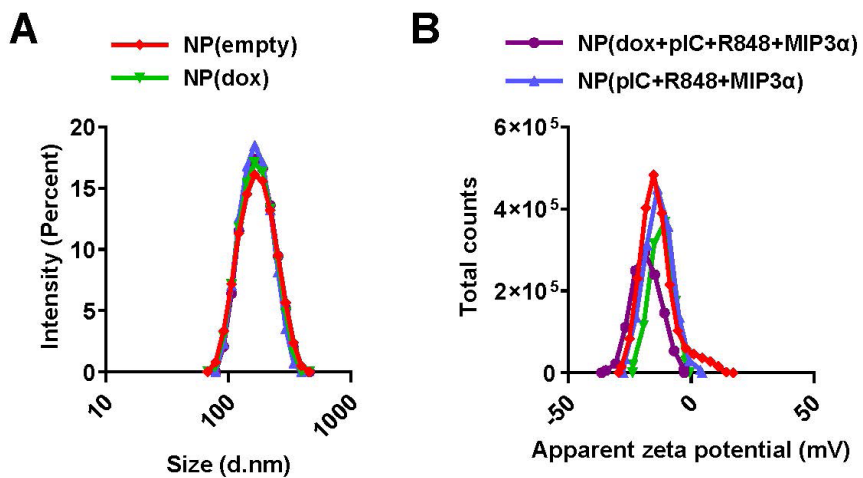


**Figure S2. The size and zeta potential data characterized by dynamic light scattering**

The size (A) and zeta potential (B) data distributions represent the mean value  $\pm$  SD of 10 readings.

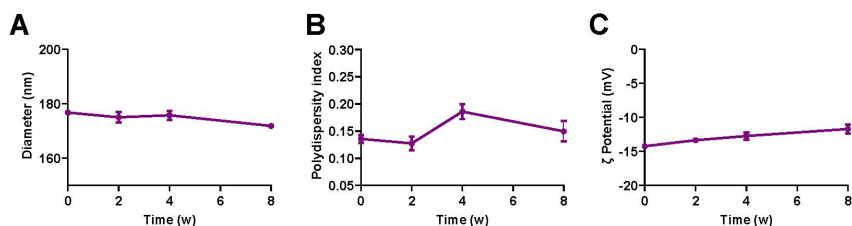


**Figure S3. Stability study of PLGA NPs**

NPs were incubated in PBS at room temperature and at constant rotation movement. Samples were taken at described time points and characterized by dynamic light scattering and zeta potential measurements. A) NP size stability study. B) NP polydispersity index (PDI) stability study. C) NP  $\zeta$  potential stability study.  $n = 3$  from one representative experiment from a representative NP batch. Data are presented as mean  $\pm$  SEM.

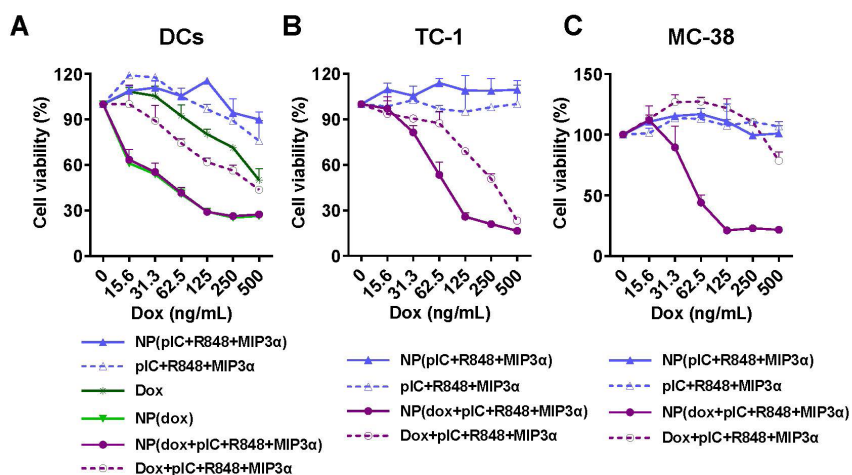


**Figure S4. Cytotoxicity of the drug-loaded NPs vs. solvent controls**

Cell viability assessed by MTS cell proliferation assay upon 72 hours incubation with indicated compounds on DCs (A), TC-1 (B) or MC-38 (C) cells.  $n = 3$  from one representative out of two independent experiments. All data are presented as mean  $\pm$  SD.

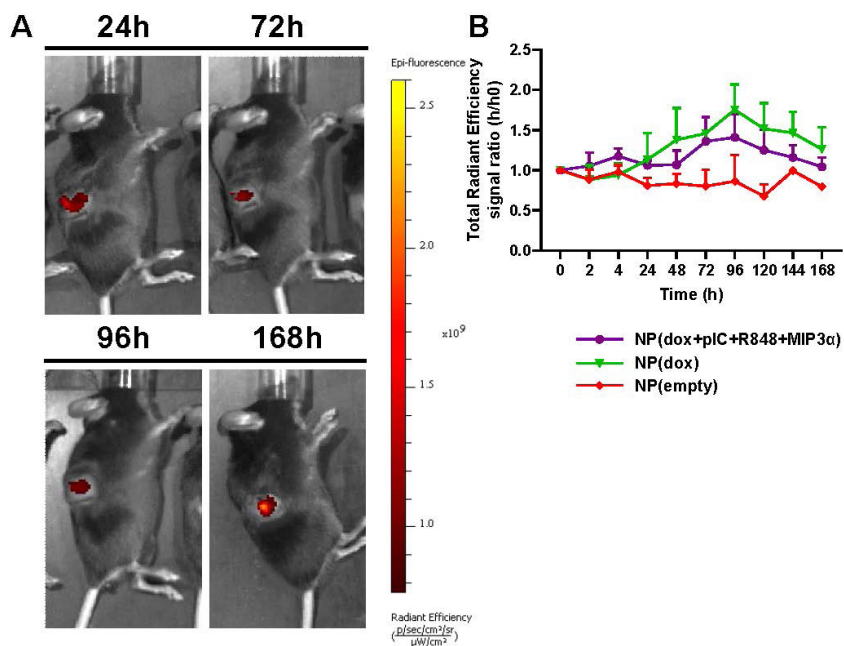


**Figure S5. IVIS imaging of TC-1 tumors after treatment**

**A)** Representative IVIS image of a mice with a TC-1 tumor in the flank followed from 24 to 168 hours after last injection with NP(dox+pIC+R848+MIP3a). **B)** Graph shows the quantification of the total radiant efficiency ( $[\text{p/s}]/[\mu\text{W}/\text{cm}^2]$ ) signal ratio (h/h0) in tumors injected with indicated NPs over time.  $n = 5$  from one representative experiment. Data are presented as mean  $\pm$  SEM.

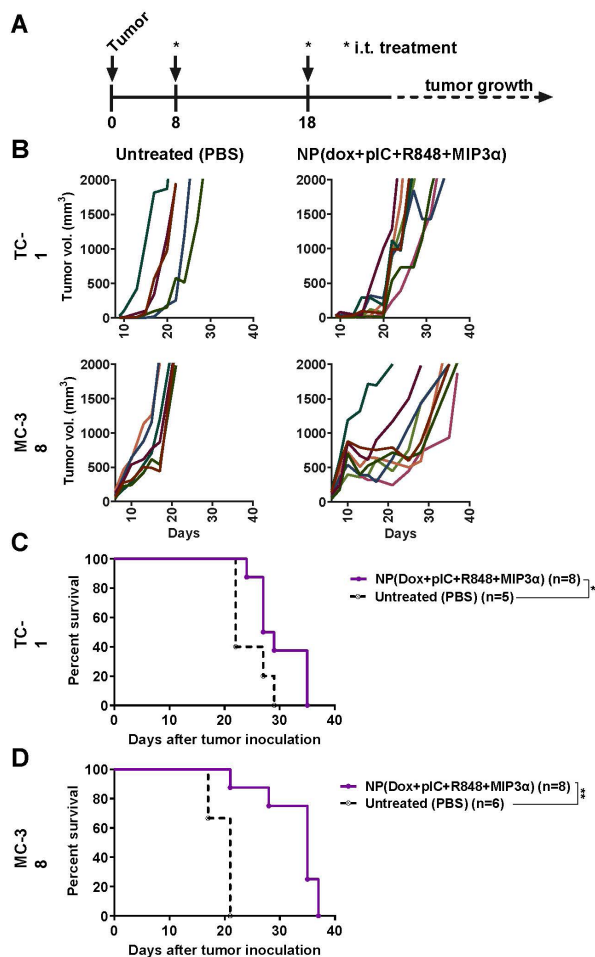


**Figure S6. Halving the dose of NP-delivered combination therapy does not alter its anti-tumor efficacy but does lead to lower overall survival**

A) Schematic diagram of the TC-1 and MC-38 murine (C57BL/6 mice) model experiments, showing inoculation and treatment days (n=8 mice per group, on average). B) Tumor growth data from day 0 to day 40 for the PBS (control) group and NP-delivered combination therapy group in the TC-1 (top) and MC-38 and (bottom) models. C) Kaplan-Meier survival plots depicting the length of progression-free survival and the overall survival (as %) for the TC-1 model: NP(dox+pIC+R848+MIP3α) vs. PBS p=0.038. D) Kaplan-Meier survival plots depicting the length of progression-free survival and the overall survival (as %) for the MC-38 model: NP(dox+pIC+R848+MIP3α) vs. PBS p=0.0014. Survival curves were compared using the Gehan-Breslow-Wilcoxon test. Statistical differences were considered significant at \* p < 0.05; \*\* p < 0.01; \*\*\* p < 0.001.

5



# CO-DELIVERY OF IMMUNOMODULATORS IN BIODEGRADABLE NANOPARTICLES IMPROVES THERAPEUTIC EFFICACY OF CANCER VACCINES

5

Da Silva, C.G., Camps, M.G.M., Li, T.M.W.Y., Chan, A.B., Ossendorp, F., Cruz L.J.  
*Biomaterials*. 2019 Nov; 220:119417.

# Abstract

---

To improve the efficacy of cancer vaccines we aimed to modulate the suppressive tumor microenvironment. In this study, the potential of intratumoral immune modulation with poly(I:C), Resiquimod (R848) and CCL20 (MIP3 $\alpha$ ) was explored. Biodegradable polymeric nanoparticles were used as delivery vehicles for slow and sustained release of these drugs in the tumor area and were combined with specific immunotherapy based on therapeutic peptide vaccination in two aggressive murine carcinoma and lymphoma tumor models. Whereas nanoparticle delivery of poly(I:C) or R848 improved therapeutic efficacy, the combination with MIP3 $\alpha$  remarkably potentiated the cancer vaccine antitumor effects. The long-term survival increased to 75-100 percent and the progression free survival nearly doubled on mice with established large carcinoma tumors. The potent adjuvant effects were associated with lymphoid and myeloid population alterations in the tumor and tumor-draining lymph node. In addition to a significant influx of macrophages into the tumor, the phenotype of the suppressor tumor-associated macrophages shifted towards an acute inflammatory phenotype in the tumor-draining lymph node. Overall, these data show that therapeutic cancer vaccines can be potentiated by the combined nanoparticle mediated co-delivery of poly(I:C), R848 and MIP3 $\alpha$ , which indicates that a more favorable milieu for cancer fighting immune cells is created for T cells induced by therapeutic cancer vaccines.

Keywords: immunotherapy, nanoparticles, therapeutic cancer vaccine, immune modulation, immune adjuvants, multi-drug nanoparticle.

## 1. INTRODUCTION

Recent breakthroughs and acquired understanding of immune mechanisms are compelling vaccines beyond the prophylactic prevention of cancer into the therapeutic class to treat fully established and advanced cancer [1]. The therapeutic potential was also recently acknowledged by the U.S. Food and Drug Administration (FDA) and European Medicines Agency (EMA) approval of Sipuleucel-T (trade name Provenge), a therapeutic cancer vaccine and a first alternative to chemotherapy for the treatment of metastatic prostate cancer [2]. Moreover, several others cancer vaccines are currently in late stage clinical trials and have demonstrated minimal toxicity in all clinical trials that have been reported to date [3]. Although the target antigens are tumor-associated antigens, that are also expressed in normal tissues, autoimmunity has rarely been reported with the exception of vitiligo induced by some melanoma vaccines [4]. Despite that therapeutic vaccines are showing promise, objective clinical responses in established cancers still remain low. Further refinement of therapeutic vaccines, or the combination treatment with other modalities, could therefore improve responses. For instance, the combination of cancer vaccines with immune checkpoint inhibitors has potential but is also currently being challenged with drawbacks, such as discontinuation due to non-responsiveness, toxicity and acquired resistance to immune check point inhibitors, warranting alternative (immune)therapies that can also address negative immune regulation and immune evasion of tumors [5,6]. Several underlying mechanisms of immune evasion have been implicated thus far, including the installment of an immune suppressed tumor microenvironment characterized by chronic inflammatory and suppressive mediators such as TGF $\beta$ , IDO, and IL10 [1]. These factors are produced non-exclusively by cancer cells, regulatory T cells (Tregs), suppressor macrophages and myeloid-derived suppressor cells (MDSCs), and can directly inhibit T cell proliferation and induce T cell senescence or apoptosis [7,8]. There is mounting evidence that immunotherapy with immune adjuvants that activate specific pattern recognition receptors (PRRs), such as Toll-Like Receptors (TLRs), may potentially reduce negative regulation [9]. Agonists that activate specific TLRs can skew the chronic inflamed tumor microenvironment towards an acute inflamed state which is a milieu more favorable for cancer fighting cells [10]. Besides to induce broad acute inflammatory responses, there are also indications that the activity of leukocytes is enhanced and the progression from innate to

adaptive immune responses is elicited [11]. The efficacy of TLR agonists as a monotherapy or adjuvant therapy in cancer has been studied in human clinical trials and ambivalent results have been reported [12,13]. Generally, the activation of the endosomal viral sensing PRRs TLR3, TLR7, TLR8 and TLR9 were reported to induce more tumor regressions in human patients than bacterial sensing PRRs but only imiquimod (i.e. TLR7 agonist) is currently FDA approved for topical application [14]. Upon systemic treatment, the TLR3 agonist Poly (I:C; pIC) has been described to be able to reprogram the tumor microenvironment towards an acute inflammatory state in liver and lung tumors while the TLR7/8 agonist Resiquimod (R848) has been described to block and reverse tumor mediated T cell senescence in advanced leukemia and skin cancers [12,15–17]. While inducing acute inflammation in the tumor microenvironment is an important factor mediating anti-tumor responses, chemokines can be useful mediators capable to attract specific (immune) cells. For instance, Macrophage Inflammatory Protein-3 alpha (MIP3 $\alpha$ ; CCL20) attracts cells expressing CCR6/CD196 often involved in mediating tumor regressions such as found on immature dendritic cells (DCs), (memory) T cells, natural killer (NK) cells and granulocytes [18–22]. Moreover, MIP3 $\alpha$  has also been described to directly repress the proliferation of myeloid progenitors [23].

Although TLR agonists are powerful immune stimulators, they can induce unwanted cytokine release syndrome which is a major factor limiting the usage of TLR agonists for the treatment of cancer [12]. In other words, a major challenge is restricting rapid systemic distribution and maintain high local confinement of these immune adjuvants to the tumor area to keep unwanted immune side effects at bay. To this end, targeted drug delivery using bio-compatible nanoparticles (NPs) can be used to minimize these side effects and enhance their efficacy due to their slow and sustained release of drugs capabilities [24]. In addition, the potential applications and advantages of NPs over 'free' compounds are recognized features vastly reviewed and currently being studied in many clinical trials [25]. The usage of drug delivery vehicles such as silica NPs, metallic NPs, liposomes, or biodegradable poly(lactic-co-glycolic acid; PLGA) polymers are prime candidates for upcoming platforms for local drug delivery [26,27].

Herein, we report the assembly and in vitro functional characterization and loading of PLGA NPs with pIC, R848 and MIP3 $\alpha$ , each individually or in combinations, and subsequent in vivo evaluation of each loaded NPs as an adjuvant modality to

improve the efficacy of two distinct synthetic long peptide based therapeutic cancer vaccines. We assessed the activity of our drug-loaded NPs in two aggressive murine models of cancer that are, to some extent, responsive to therapeutic vaccination: TC-1 lung carcinoma and RMA T cell lymphoma. We provide evidence that the two therapeutic cancer vaccines efficacy can be improved by the intratumoral administration of immune adjuvants co-delivered by NPs. In addition, we show that the combined co-delivery of pIC, R848 and MIP3 $\alpha$  is superior to any of these immune adjuvants separately. Mechanistically, we report that the NPs impacted lymphoid and myeloid populations in the tumor and in the tumor-draining lymph node. To the best of our knowledge, this is the first study to combine NP mediated delivery of two distinct TLR agonists and a chemokine into a single modality which improves the efficacy of cancer vaccines.

## 2. MATERIALS AND METHODS

### 2.1. Materials and reagents

PLGA polymer (lactide/glycolide molar ratio of 48:52 to 52:48) was purchased from Boehringer Ingelheim (Ingelheim am Rhein, Germany). The near infrared (NIR) dye (IR-780 Iodide; CAS 207399-07-3), poly(inosinic:cytidylic acid; CAS 42424-50-0 P0913), polyvinyl alcohol (PVA; CAS 9002-89-5) and dichloromethane (DCM; CAS 75-09-2 CH<sub>2</sub>CL<sub>2</sub> MW 84.93) were purchased from Sigma-Aldrich (Zwijndrecht, The Netherlands). Chloroform (CHCL<sub>3</sub> MW 119.38 g/mol) was purchased from Merck (Darmstadt, Germany). Lipid-PEG 2000 (1,2-Distearoyl-sn-Glycero-3-Phosphoethanolamine-N-[Methoxy(Polyethylene glycol)-2000]; powder MW 2805.54) was purchased from Avanti Polar Lipids (AL, USA). R848 from Alexis Biochemicals (Paris, France) and MIP3 $\alpha$  (CCL20) from R&D Systems (MN, USA).

### 2.2. Preparation of PLGA NPs

The PLGA NPs were synthesized in an oil/water emulsion, using a solvent evaporation-extraction method as described previously [28–31]. Briefly, 200 mg of PLGA powder was dissolved in 3 mL of DCM containing 1 mg of NIR dye. Depending on the NP, the following was added: 8 mg of pIC, and/or 4 mg of R848 and/or 250  $\mu$ g of MIP3 $\alpha$ . The prepared solution was then added dropwise to 40 mL of aqueous 2.5% (w/v) PVA and emulsified for 120 s using a sonicator (250 watt; Sonifier 250; Branson, Danbury, USA). Next, the emulsion was gently poured to a beaker previously prepared containing an air-dried film of 20 mg of Lipid-

PEG 2000 dissolved in 0.2 mL of chloroform, homogenized for 60 s by sonication after which the solvents were evaporated overnight at 4 °C on a magnetic stirrer. Following NP collection by ultracentrifugation and lyophilization, the concentration of the NPs constituents was determined by reverse phase high-performance liquid chromatography (RP-HPLC), as described elsewhere [32].

### **2.3. Physicochemical properties of the NPs**

The NPs were characterized for average size, polydispersity index and surface charge (zeta-potential) by dynamic light scattering. Briefly, 50 µg of NP sample in 1 mL of ultrapure MilliQ H<sub>2</sub>O were measured for size using a Zetasizer (Nano ZS, Malvern Ltd., UK) and a similar sample was analyzed for surface charge by laser Doppler electrophoresis on the same device.

### **2.4. Mice strains**

C57BL/6 (H-2b haplotype) and 8 to 12 weeks of age female mice were purchased from Envigo (Horst, The Netherlands). The mice were housed at the animal facility of Leiden University Medical Center under specific pathogen free conditions. All animal experiments were approved by the Dutch Central Committee on Animal Experimentation and were strictly conducted according to the Dutch animal welfare law.

### **2.5. Cell lines**

The murine tumor cell line TC-1 (a kind gift from T.C. Wu, Johns Hopkins University, Baltimore, MD, USA) was generated by retroviral transduction of lung fibroblasts of C57BL/6 origin, to express the HPV16 E6 and E7 genes and the activated human c-Ha-ras oncogene [33]. RMA is a Rauscher virus-induced T lymphoma line of C57BL/6 (H-2b) origin [34]. The D1 cell line is an immature splenic DC line with characteristics of that of bone marrow derived DCs [35]. The TC-1 and D1 cell lines were cultured as described previously [36]. The RMA cell line was cultured in IMDM medium (Lonza, Verviers, Belgium) containing 8% heat-inactivated fetal calf serum (FCS; Greiner bio-one, Alphen a/d Rijn, The Netherlands), penicillin (50 µg/mL; Gibco, Paisley, Scotland), streptomycin (50 µg/mL; Gibco), L-glutamine (2 mM; Gibco) and β-mercaptoethanol (20 µM; Sigma, Saint Louis, USA). The expression of RMA MHC class I H-2Kb/Db was verified before in-vivo experiments (Supplemental Figure S1). All the above described cell lines were incubated at 37° C in 5% CO<sub>2</sub> and 100% humidity and routinely screened for Mycoplasma and rodent viruses.

## 2.6. Intracellular uptake of NPs and immunostaining

The intracellular uptake of NPs was determined by incubating either 10 µg/mL or 20 µg/mL of NPs containing NIR dye (~ 800 nm) with  $1 \times 10^4$  D1 cells for 1 hour, 2 hours or 4 hours. After thorough washing to remove unbound NPs the cells were fixed and stained with To-pro 3 iodide (642/661 ~700 nm; Invitrogen; Eugene, USA) to enable cell count. Finally, the NIR dye signal was scanned using an Odyssey scanner infrared imaging system (LI-COR). Immunostaining detected by fluorescence microscopy was determined by incubating 20 µg/mL of NPs containing NIR dye with D1 cells in the chambers of a glass culture slide (FALCON, NY, USA) for 48 hours. After washing and fixation, the cells were stained with anti-I-A/I-E-FITC (clone 2G9, BD Bioscience) for membrane visualization, washed again with PBS and mounted with VectaShield antifade mounting medium with DAPI to stain nuclei (Vector Laboratories, CA, USA). Digital images were acquired using a Leica DM6B microscope.

## 2.7. Activation and maturation of DCs

The upregulation of CD40, CD80 and CD86 on D1 cells and the production of IL-12 in the supernatant were used as indicators of DC activation and maturation upon co-culture with NPs. Briefly,  $5 \times 10^4$  D1 cells were co-cultured with NPs for 48 hours at 37° C in 5% CO<sub>2</sub> and 100% humidity. The NP concentrations were matched upon pIC, R848 or PLGA concentration where applicable. The CD86 expression was analyzed with anti-CD86-APC (clone GL1, eBioscience) on an LSR-II laser flow cytometer controlled by CELLQuest software v. 3.0 (Becton Dickinson, Franklin Lakes, USA) and analyzed with FlowJo LLC v. 10 software (Tree Star, USA). The interleukin IL12 was detected using a standard sandwich ELISA with purified anti-mouse IL12/IL23 p40 (clone C15.6, Biolegend) and biotin-labelled anti-mouse IL12/IL23p40 antibodies (clone C17.8, Biolegend). The plates were read at 450 nm using a Bio-rad 680 microplate reader (Bio-rad Laboratories).

## 2.8. Blood analysis

The presence of antigen-specific T cells in the blood of TC-1 bearing mice was determined by collecting 50 µL of blood through the caudal vein at day 16. After removal of red blood cells by lysis, the cells were stained with anti-CD8α-PE (clone 53-6.7, eBioscience), anti-CD3-eFluor 450 (clone 17A2, eBioscience) and the APC labeled HPV16 E749-57 (RAHYNIVTF) MHC class I (H-2Db) tetramer.

Finally, the cells were subjected to flow cytometry measurements on an LSR-II laser flow cytometer controlled by CELLQuest software v. 3.0 (Becton Dickinson) and the data analyzed with FlowJo LLC v. 10 software (Tree Star).

## **2.9. Tumor treatments and vaccinations**

Mice were inoculated with  $1 \times 10^5$  TC-1 or  $1 \times 10^3$  RMA cells in 0.2 mL PBS in the right flank. The TC-1 tumor bearing mice were vaccinated once in the contralateral left flank at day 8 (when the tumors were established and palpable). The TC-1 vaccine consisted of an emulsion of human papillomavirus type 16 E7 43-70 synthetic long peptide (500  $\mu$ M/mouse; sequence GQAEPDRAHYNIVTFCCCKCDSTLRLCV that includes both a CD4 (underlined) and a CD8 epitope (double underlined) [37]) together with adjuvant TLR9 agonist CpG (Invivogen, San Diego, USA; 5 nmol/mouse) in 50% (v/v) of Adjuvant Incomplete Freund (IFA; Becton, Dickinson and Company, MD, USA) and sterile PBS administrated in a 100  $\mu$ L depot subcutaneously. The RMA tumor bearing mice were vaccinated once at day 10 (when the tumors were established and palpable). The RMA vaccine consisted of a mixture of Rauscher mouse leukemia virus (MuLV) synthetic long peptides coding for the Gag-encoded CD8 epitope (50 nM/mouse; sequence CCLCLTVFL) and the Env-encoded CD4 epitope (20 nM/mouse; sequence EPLTSLTPRCNTAWNRLKL) together with adjuvant TLR9 agonist CpG (Invivogen; 5 nmol/mouse) and sterile PBS injected in a 30  $\mu$ L depot intradermally in the base of the tail. The intratumoral injections of the NPs (30  $\mu$ L) on the specified mice, were administrated on the same day as the vaccination day (day 8 for TC-1 and day 10 for RMA) and then once more 10 days after. The NPs were dissolved in sterile PBS and the concentration matched between the groups on pIC concentration, otherwise on R848 or on MIP3 $\alpha$ . The concentration of the empty NP was matched on the average PLGA weight of all the groups tested. The reference NP used was the NP containing all three immune adjuvants, the concentration per administration was: pIC 2.5 mg/Kg (50  $\mu$ g), R848 720  $\mu$ g/Kg (14.4  $\mu$ g), and MIP3 $\alpha$  155  $\mu$ g/Kg (3.1  $\mu$ g). The surviving mice were re-challenged with a second tumor inoculation of cancer cells on the back at day 120 to determine the development of immunological memory against cancer epitopes. Tumor dimensions were measured every other day with a standard caliper and the volume was calculated by multiplying the tumor diameters in all three dimensions. The maximal allowed tumor volume was 2,000 mm<sup>3</sup>; after this point, mice were sacrificed, which formed the basis for the Kaplan-Meier survival curves.



## 2.10. Tumor and lymph node analysis

The tumor and the tumor-draining lymph nodes were analyzed *ex vivo* by sacrificing the mice and resecting the organs at day 18 (mice were treated as per described above). The resected tumors were mechanically broken up into small pieces using sterile scissors and forceps and then incubated with Liberase TL (Roche, Mannheim, Germany) in serum-free IMDM medium for 15 minutes at 37 °C. Single cell suspensions were acquired from the tumors and lymph nodes by gently grinding the tumor fragments through a 70 µm cell strainer (Falcon, NY, USA). Cells were then equally divided to be stained with two distinct antibody panels. The lymphoid markers panel contained the viability dye 7-AAD (Invitrogen) and the following antibodies against cell surface markers: anti-CD45.2-APC eFluor 780 (clone 104, eBioscience); anti-CD3-eFluor 450 (clone 17A2, eBioscience); anti-CD4-Brilliant Violet 605 (clone RM4-5, Biologend); anti-CD8α-APC-R700 (clone 53-6.7, BD Bioscience); anti-CD25-APC (clone PC61.5, eBioscience); anti-CD49b-PE (clone DX5, BD Bioscience) and anti-CD44-FITC (clone IM7, eBioscience). The myeloid markers panel contained the viability dye 7-AAD (Invitrogen) and the following antibodies against cell surface markers: anti-CD45.2-FITC (clone 104, BD Bioscience); anti-CD11b-eFluor 450 (clone M1/70, eBioscience); anti-F4/80-PE (clone BM8, eBioscience); anti-Ly6G-AlexaFluor 700 (clone 1A8, Biologend); anti-Ly6C-Brilliant Violet 605 (clone HK1.4, Biologend), and anti-CD11c-APC-eFluor 780 (clone N418, eBioscience). The expression of the cell markers was analyzed on an LSR-II laser flow cytometer controlled by CELLQuest software v. 3.0 (Becton Dickinson) and the data analyzed with FlowJo LLC v. 10 software (Tree Star).

## 2.11. RMA MHC class I H-2Kb/Db expression

The MHC class I H-2Kb/Db expression was determined by staining  $1 \times 10^5$  RMA and  $1 \times 10^5$  CT-26 (negative control, Balb/c genetic background) cells with anti-H-2Db-biotin (clone 28-14-8, BD Bioscience) and on a separate well with anti-H-2Kb (obtained via isolation of serum IgG). The Streptavidin-APC conjugate (BD Bioscience) and anti-IgG-Alexa647 (A21237, Life Technologies) secondary antibody were used for signal detection. Finally, after washing, the cells analyzed on an LSR-II laser flow cytometer controlled by CELLQuest software v. 3.0 (Becton Dickinson) and the data analyzed with FlowJo LLC v. 10 software (Tree Star).

## **2.12. Data and statistical analysis**

Statistical analysis was performed using GraphPad Prism v. 7.0 software (GraphPad Software, La Jolla, USA). Data are represented as mean values  $\pm$  SD unless stated otherwise. Blood, tumor and lymph nodes cell analysis results were compared on a fixed day between mouse groups and statistical significance was determined by using an unpaired, non-parametric, two-tailed Mann-Whitney U test. Survival curves were compared using the Log-rank (Mantel-Cox) test unless stated otherwise. Statistical differences were considered significant at  $p < 0.05$  and presented as: \*  $p < 0.05$ , \*\*  $p < 0.01$ , \*\*\*  $p < 0.001$ .

## **3. RESULTS**

### **3.1. Preparation, physicochemical properties and in vitro evaluation of NPs**

Here, we prepared a distinct PLGA NP formulation using a solvent evaporation-extraction method using the biodegradable polymer PLGA. For the current study, we loaded the NPs with the immune adjuvants pIC, R848 and the chemokine MIP3 $\alpha$ , either separately or in combinations (Table 1). Each batch, including the empty (control) NPs, were functionalized with surface PEGylation (PEG) and contained a NIR dye. The PLGA NPs were characterized to ascertain their size and surface charge. The size of NPs was found to range between 140 and 270 nm (Table 1, Figure S2A), depending on the encapsulated content, and the surface charge was negative ranging from -18 to -29 mV (Table 1, Figure S2B).

**Table 1. Physicochemical characterization of PLGA NPs**

Samples	Diameter	$\zeta$ Potential (mV)	PDI	Loading capacity (% w/w)			
				NIR	pIC	R848	MIP3 $\alpha$
NP(NIR)-PEG Annotated as: NP(empty)	196.5 $\pm$ 41.8	-25.2 $\pm$ 11.4	0.463	64.1	-	-	-
NP(NIR+MIP3 $\alpha$ )-PEG Annotated as: NP(MIP3 $\alpha$ )	141.4 $\pm$ 30.6	-22.5 $\pm$ 7.7	0.04	61.6	-	-	64.9
NP(NIR+R848)-PEG Annotated as: NP(R848)	149.4 $\pm$ 32.1	-18.1 $\pm$ 5.8	0.066	62.7	-	56.3	-
NP(NIR+pIC)-PEG Annotated as: NP(pIC)	149.7 $\pm$ 29.2	-211 $\pm$ 7.3	0.032	57.8	44.6	-	-
NP(NIR+pIC+R848)-PEG Annotated as: NP(pIC+R848)	157.7 $\pm$ 37.7	-26.0 $\pm$ 7.5	0.08	63.9	47.0	56.4	-
NP(NIR+pIC+R848+MIP3 $\alpha$ )-PEG Annotated as: NP(pIC+R848+MIP3 $\alpha$ )	268.5 $\pm$ 48.2	-29.4 $\pm$ 5.1	0.457	59.3 $\pm$ 7.3	43.1 $\pm$ 9.5	48.0 $\pm$ 21.0	62.4 $\pm$ 4.9

Physicochemical characterization of the PLGA-PEG NPs containing different immune adjuvants. The PLGA NPs were characterized by dynamic light scattering and zeta potential measurements. PLGA NPs size and zeta potential data represent the mean value  $\pm$  SD of 10 readings of one representative batch. The loading capacity of the NIR dye was measured by fluorescence method. The loading capacity of pIC, R848 and MIP3 $\alpha$  was determined by RP-HPLC analysis. The loading capacity data represent the average value  $\pm$  SD of batch variation where applicable.

### **3.1.1. Cellular uptake of NPs**

Efficient uptake of the NPs by cells is required for the delivery of the immune adjuvants to their intracellular targets. We incubated DCs with NPs containing NIR dye (at 10 µg/mL and at 20 µg/mL of NPs respectively) for 1, 2 and 4 hours and quantified the relative uptake (Figure 1A). For both concentrations, the uptake increased over time. To corroborate that the signal emanated from inside the cells, DCs were incubated with NPs and analyzed by fluorescence microscopy (Figure 1B). Indeed, the NIR dye signal (green) from the NPs was found to originate within the cells, indicating that these NPs were successfully taken up by DCs.

### **3.1.2. NPs enhance DC activation and IL-12 production**

The activation of the endosomal TLR3 and TLR7/8 enhances the expression of CD40, CD80 and CD86 on DCs and stimulates the production of IL-12. Therefore, we measured these parameters to determine whether pIC and R848 remained active after loading in NPs. To this end, all the distinct NP batches were independently incubated with DCs. The NP(pIC), NP(R848), NP(pIC+R848) and NP(pIC+R848+MIP3α), but not NP(empty) or NP(MIP3α), were found to efficiently enhance the expression of CD40, CD80 and CD86 (Figure 1C) and induce the production of IL-12 (Figure 1D). These results indicate that pIC and R848 remained active after loading in NPs.

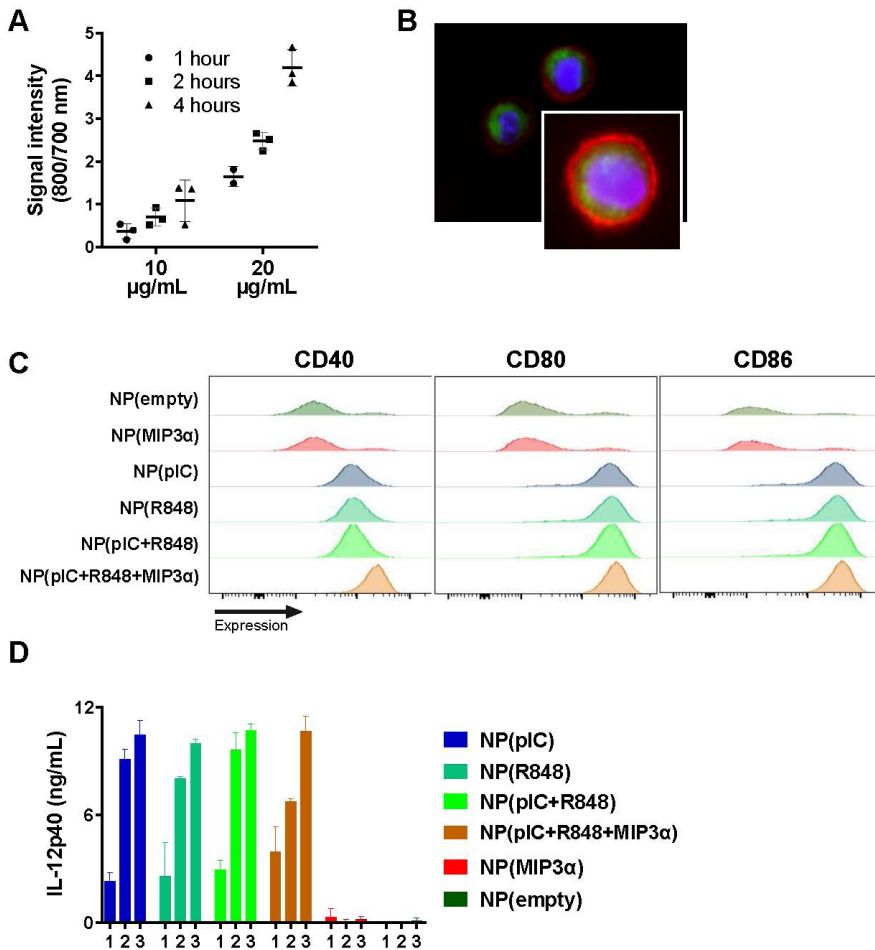


**Figure 1. In vitro DC cellular uptake and activation by PLGA NPs loaded with different immune stimulatory compounds**

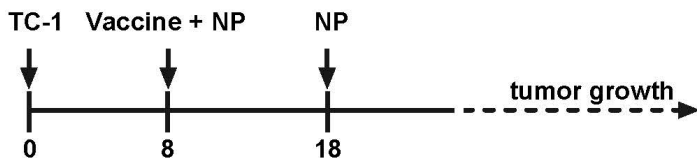
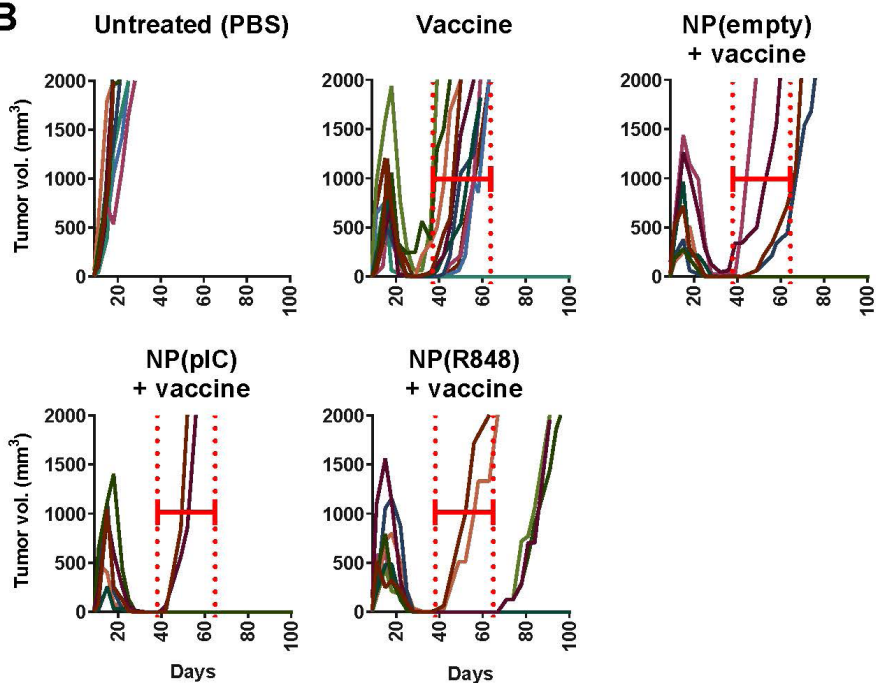
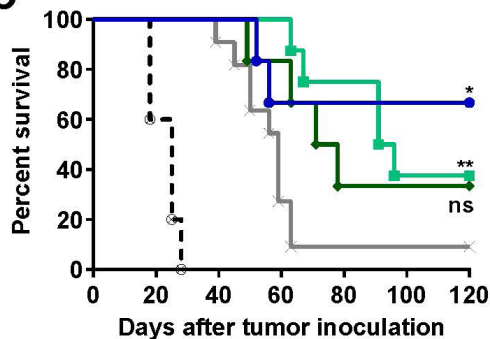
**A)** Uptake of NPs containing NIR dye (800 nm) by DCs (To-pro 3 iodide; 700 nm) over the times indicated. n = 3 from one representative experiment. **B)** Uptake of NPs by DCs after 2 hours of incubation, shown by fluorescence microscopy. Red: cell membrane; purple: cell nucleus; green: NIR dye. **C)** Activation of DCs measured by CD40, CD80 and CD86

expression upon 48 hours incubation with NP(empty), NP(MIP3 $\alpha$ ), NP(pIC), NP(R848), NP(pIC+R848) and NP(pIC+R848+MIP3 $\alpha$ ). The cells were pooled from n = 3 from each condition, one representative out of three independent experiments. D) Activation of DCs measured by the secretion of IL-12p40 upon 48 hours incubation with NP(empty), NP(MIP3 $\alpha$ ), NP(pIC), NP(R848), NP(pIC+R848) and NP(pIC+R848+MIP3 $\alpha$ ). n = 3 from one representative out of three independent experiments. Concentrations 1: 1.3  $\mu$ g/mL; 2: 2.5  $\mu$ g/mL; 3: 5  $\mu$ g/mL.

### **3.2. Co-delivery of immune adjuvants pIC and R848 by NPs improves the survival of vaccinated mice**

TC-1 tumor bearing mice were vaccinated subcutaneously in the contralateral flank at day 8 post tumor inoculation with a therapeutic synthetic long peptide vaccine containing both CD4 and CD8 epitopes against the HPV E7 protein that is expressed by TC-1 cells. At the same time, the tumors were treated with an intratumoral injection with NPs at day 8 and at day 18 (Figure 2A). All the vaccinated mice displayed strong tumor mass regressions that started approximately at day 16 and most tumors became undetectable at day 30 (Figure 2B). However, mice that were only vaccinated experienced tumor relapses rapidly approximately 8-10 days after. The survival of mice improved significantly when vaccination treatment was combined with intratumoral injections of NP(pIC) or with NP(R848), respectively (Figure 2C). The survival of mice vaccinated and treated with intratumoral injections of NP(empty) improved but not significantly. To determine whether the surviving mice developed functional memory T cells against cancer epitopes, we re-challenged the mice again with TC-1 cancer cells. We observed that all the mice were able to clear the new tumor without additional treatments (Figure S3A). We also analyzed the blood of tumor bearing mice after vaccination and intratumoral administration of NPs at day 16 and determined the percentages of circulating CD3+, CD8+ and cancer antigen-specific CD8+ T cells.

We observed that the percentage of CD3+ nor CD8+ T cells was affected by the intratumoral NP treatments with the exception of mice treated with NP(R848) that displayed a small, but significant, decrease of CD8+ T cells in blood compared to vaccinated only mice (Figure S4A). All the vaccinated mice shown detectable cancer specific T cells in blood. However, mice that also were treated with intratumoral injections with NP(pIC) displayed higher percentages of cancer antigen-specific CD8+ T cells, but this difference was not statistically significant. Furthermore, all the mice whose tumors had been eradicated, also rejected a tumor re-challenge at day 100, which indicates development of functional immunological memory against tumor antigens and blood analysis at day 110 revealed the presence of high levels of cancer specific T cells in blood (Figure S3B). These results indicate that either NP(pIC) or NP(R848) independently improved the survival of vaccinated mice significantly.

**A****B****C**

—●— NP(pIC)+vaccine (n=6)   
 —■— NP(empty)+vaccine (n=6)   
 - - - ● - - - PBS (n=10)  
—■— NP(R848)+vaccine (n=8)   
 - - - × - - - Vaccine (n=11)

**D**

Comparison	P value
PBS vs. v	<0.0001 ***
PBS vs. NP(empty)+v	0.0002 ***
PBS vs. NP(R848)+v	<0.0001 ***
PBS vs. NP(pIC)+v	0.0002 ***
V vs. NP(empty)+v	0.0693 ns
V vs. NP(R848)+v	0.0055 **
V vs. NP(pIC)+v	0.0482 *
NP(R848)+v vs. NP(empty)+v	0.5288 ns
NP(R848)+v vs. NP(pIC)+v	0.5234 ns
NP(pIC)+v vs. NP(empty)+v	0.3845 ns



< **Figure 2. Co-delivery of immune adjuvants pIC and R848 by NPs improves the survival of vaccinated mice**

**A)** Schematic diagram of the TC-1 murine model experiment (C57BL/6 mice; n=8 per group, on average), showing inoculation and treatment days. TC-1 tumor bearing mice were vaccinated subcutaneously in the contralateral flank at day 8 post tumor inoculation with a therapeutic synthetic long peptide vaccine containing both CD4 and CD8 epitopes against the HPV E7 protein that is expressed by TC-1 cells. At the same time, the tumors were treated with an intratumoral injection with NPs at day 8 and at day 18. **B)** Tumor growth data from day 0 to day 100 for the PBS (control) group and five treatment groups (vaccine only, vaccine plus empty NPs, vaccine plus R848 and vaccine plus pIC). **C)** Kaplan-Meier survival plots (PBS, vaccine only and NP(pIC+R848) groups data were pooled from two separate experiments), depicting progression-free survival and percent overall survival of vaccinated mice and also treated with NP(empty), NP(pIC) or NP(R848). **D)** Summary showing the P values for the pairwise comparisons of survival curves. Survival curves were compared using the log-rank test. Statistical differences were considered significant at \*  $p < 0.05$ ; \*\*  $p < 0.01$ ; \*\*\*  $p < 0.001$ . Abbreviations: ns: not (statistically) significant; V: Vaccine.

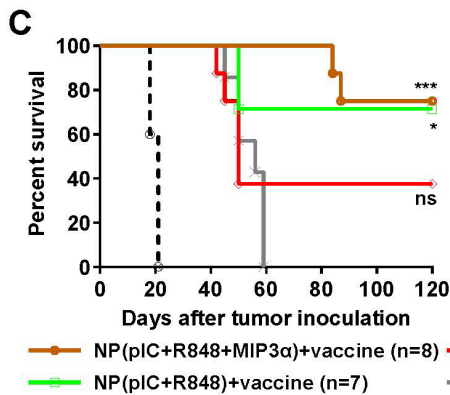
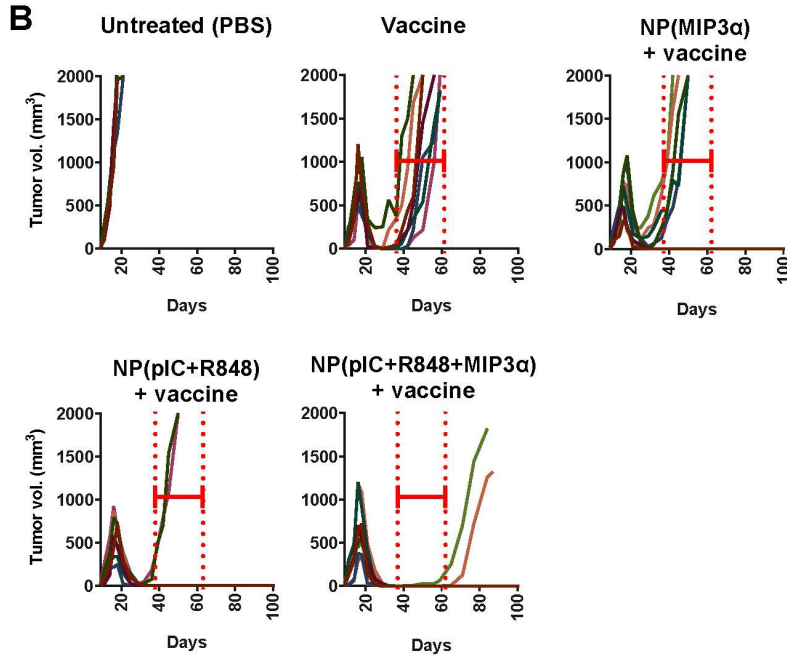
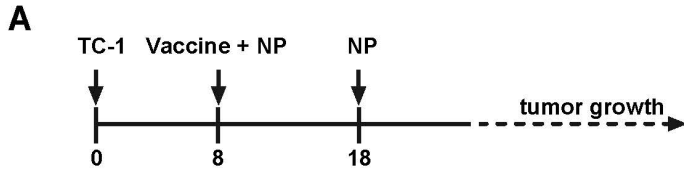
**3.3. Co-delivery of MIP3 $\alpha$ , in addition to immune adjuvants pIC and R848, improves survival and nearly doubles progression-free survival**

Next, we determined whether the survival of vaccinated mice could be further improved by the combination of pIC and R848 and/or chemokine MIP3 $\alpha$ . To this end, TC-1 tumor bearing mice were vaccinated at day 8 post tumor inoculation as described previously and treated with an intratumoral injection of NPs at day 8 and at day 18 (Figure 3A). We observed that the survival of mice vaccinated and treated with intratumoral injections of NP(MIP3 $\alpha$ ) improved but not significantly (Figure 3B & 3C). On the other hand, the survival of mice vaccinated and treated with intratumoral injections of NP(pIC+R848) or NP(pIC+R848+MIP3 $\alpha$ ) was enhanced significantly. Moreover, the progression-free survival time was found to nearly double compared to either modality (Figure 3B, depicted in the red-dotted lines). To determine whether the surviving mice developed functional memory T cells against cancer epitopes, we re-challenged the mice again with TC-1 cancer cells. We observed that all the mice were able to clear the new tumor without additional treatments (Figure S3A). We also analyzed the blood of tumor bearing mice after vaccination and intratumoral administration of NPs at day 16 and determined the percentages of circulating CD3+, CD8+ and cancer antigen-specific CD8+ T cells. We observed that the percentage of CD3+ nor CD8+ T cells was affected

by the intratumoral NP treatments (Figure S4B). All the vaccinated mice shown detectable cancer specific T cells in blood. However, mice that also were treated with intratumoral injections with NP(pIC+R848) or NP(pIC+R848+MIP3 $\alpha$ ) displayed higher percentages of cancer antigen-specific CD8+ T cells, but this difference was not statistically significant (Figure S4B). Furthermore, all the mice whose tumors had been eradicated, also rejected a tumor re-challenge at day 100, which indicates development of functional immunological memory against tumor antigens and blood analysis at day 110 revealed the presence of high levels of cancer specific T cells in blood (Figure S3C). These results indicate that the chemokine NP(MIP3 $\alpha$ ) by itself could not improve the survival of vaccinated mice significantly. However, the combination of the immune adjuvants pIC and R848 improved the overall survival significantly, while the combination of pIC, R848 and MIP3 $\alpha$  not only improved the survival of vaccinated mice up to 75%, it nearly doubled the mice progression-free survival time.

**Figure 3. Co-delivery of MIP3 $\alpha$ , in addition to immune adjuvants pIC and R848, improves survival and nearly doubles progression-free survival** >

A) Schematic diagram of the TC-1 murine model experiment (C57BL/6 mice; n=8 per group, on average), showing inoculation and treatment days. TC-1 tumor bearing mice were vaccinated subcutaneously in the contralateral flank at day 8 post tumor inoculation with a therapeutic synthetic long peptide vaccine containing both CD4 and CD8 epitopes against the HPV E7 protein that is expressed by TC-1 cells. At the same time, the tumors were treated with an intratumoral injection with NPs at day 8 and at day 18. B) Tumor growth data from day 0 to day 100 for the PBS (control) group and four treatment groups (vaccine only, vaccine plus MIP3 $\alpha$ , vaccine plus pIC and R848 combined, and vaccine plus pIC, R848 and MIP3 $\alpha$  combined). The red-dotted lines depict the different progression-free survival times. C) Kaplan-Meier survival plots depicting progression-free survival and percent overall survival of vaccinated mice and also treated with NP(MIP3 $\alpha$ ) or NP(pIC+R848+MIP3 $\alpha$ ). D) Summary showing the P values for the pairwise comparisons of survival curves. Survival curves were compared using the log-rank test. Statistical differences were considered significant at \* p = < 0.05; \*\* p = < 0.01; \*\*\* p < 0.001. Abbreviations: ns: not (statistically) significant; V: Vaccine

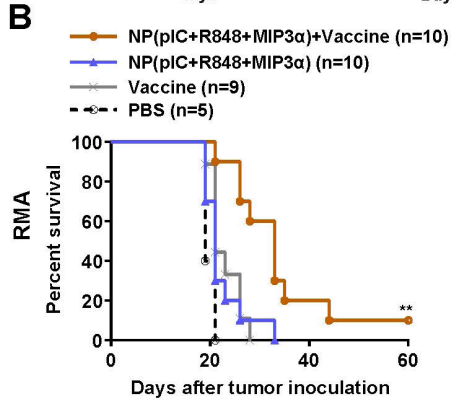
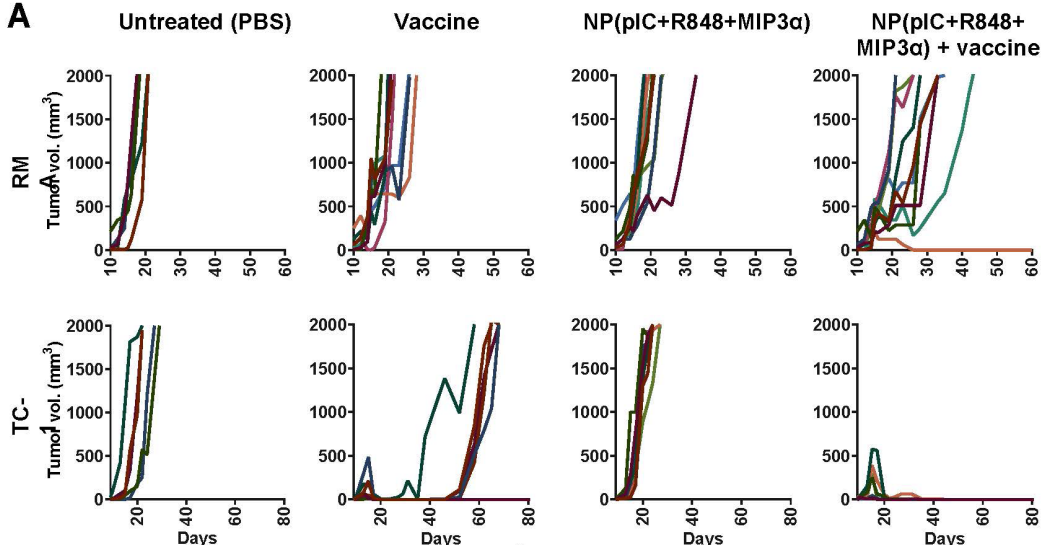


**D**

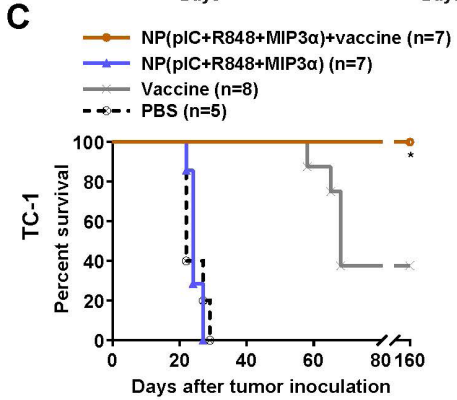
Comparison	P value
PBS vs. v	0.0007 ***
PBS vs. NP(MIP3α)+v	0.0003 ***
PBS vs. NP(pIC+R848)+v	0.0007 ***
PBS vs. NP(pIC+R848+MIP3α)+v	0.0003 ***
V vs. NP(MIP3α)+v	0.5167 ns
V vs. NP(pIC+R848)+v	0.0195 *
V vs. NP(pIC+R848+MIP3α)+v	0.0001 ***
NP(pIC+R848)+v vs. NP(MIP3α)+v	0.1499 ns
NP(pIC+R848)+v vs. NP(pIC+R848+MIP3α)+v	0.7845 ns
NP(pIC+R848+MIP3α)+v vs. NP(MIP3α)+v	0.0786 ns

**Figure 4. Effective therapeutic efficacy improvement, upon NP co-treatment, persists in distinct therapeutic cancer vaccines** >

The efficacy of the monotherapy of NP(pIC+R848+MIP3 $\alpha$ ) as well as combined with two distinct therapeutic cancer vaccines was determined. The RMA tumor bearing mice were vaccinated intradermally in the tail base at day 10 post tumor inoculation with a therapeutic synthetic long peptide vaccine containing both CD4 and CD8 epitopes against two viral proteins that is expressed by RMA cells. At the same time, the tumors were treated with an intratumoral injection with NPs at day 10 and at day 20. The TC-1 tumor bearing mice were vaccinated subcutaneously in the contralateral flank at day 8 post tumor inoculation with a therapeutic synthetic long peptide vaccine containing both CD4 and CD8 epitopes against the HPV E7 protein that is expressed by TC-1 cells. At the same time, the tumors were treated with an intratumoral injection with NPs at day 8 and at day 18. A) Tumor-growth data from day 0 to day 60 or day 80 for the PBS (control) group and three treatment groups (vaccine only, NP(pIC+R848+MIP3 $\alpha$ ) only, and vaccine plus NP(pIC+R848+MIP3 $\alpha$ ) combined) in the RMA (top) and TC-1 (bottom) models. B) Kaplan-Meier survival plots depicting progression-free survival and percent overall survival for the RMA model. C) Kaplan-Meier survival plots depicting progression-free survival and percent overall survival for the TC-1 model. Survival curves were compared using the log-rank test. Statistical differences were considered significant at \*  $p < 0.05$ ; \*\*  $p < 0.01$ ; \*\*\*  $p < 0.001$ . Abbreviations: ns: not (statistically) significant; V: Vaccine.



Comparison	P value
PBS vs. v	0.0259 *
PBS vs. NP(plC+R848+MIP3α)	0.1354 ns
PBS vs. NP(plC+R848+MIP3α)+v	0.0002 ***
V vs. NP(plC+R848+MIP3α)	0.7201 ns
V vs. NP(plC+R848+MIP3α)+v	0.0012 **
NP(plC+R848+MIP3α) vs.	0.0017 **
NP(plC+R848+MIP3α)+v	



Comparison	P value
PBS vs. v	0.0001 ***
PBS vs. NP(plC+R848+MIP3α)	0.8874 ns
PBS vs. NP(plC+R848+MIP3α)+v	0.0003 ***
V vs. NP(plC+R848+MIP3α)	<0.0001 ***
V vs. NP(plC+R848+MIP3α)+v	<b>0.0147 *</b>
NP(plC+R848+MIP3α) vs.	0.0002 ***
NP(plC+R848+MIP3α)+v	

### **3.4. Effective therapeutic efficacy improvement, upon NP co-treatment, persists in distinct therapeutic cancer vaccines**

Next, we expanded our approach to another cancer model with a different etiology. Thus, we applied our NP formulation in combination with another therapeutic cancer vaccine modality aimed to induce adaptive immune responses against epitopes of the aggressive RMA T lymphoma model. The RMA bearing mice were treated with a therapeutic cancer vaccine administered intradermally in the tail base, at day 10, and consisted of a mixture of synthetic long peptides containing both CD4 and CD8 epitopes against two viral proteins that is expressed by RMA cells. The TC-1 bearing mice were vaccinated as per described previously. In addition, we also determined the efficacy of NP(pIC+R848+MIP3 $\alpha$ ) as a monotherapy (i.e. without vaccine co-treatment), in both TC-1 and the RMA models. To this end, TC-1 and RMA tumor bearing mice were treated twice with intratumoral injections and we observed that NP(pIC+R848+MIP3 $\alpha$ ), as a monotherapy, did not improve the survival of mice in neither TC-1 or RMA model (Figure 4A). However, the combination of the therapeutic cancer vaccine and the intratumoral administration of NP(pIC+R848+MIP3 $\alpha$ ) in both TC-1 and RMA successfully enhanced the mice survival significantly (Figure 4B and 4C). These results indicate that the intratumoral administration of NP(pIC+R848+MIP3 $\alpha$ ) improved the efficacy of two distinct therapeutic cancer vaccines in two aggressive cancer models.

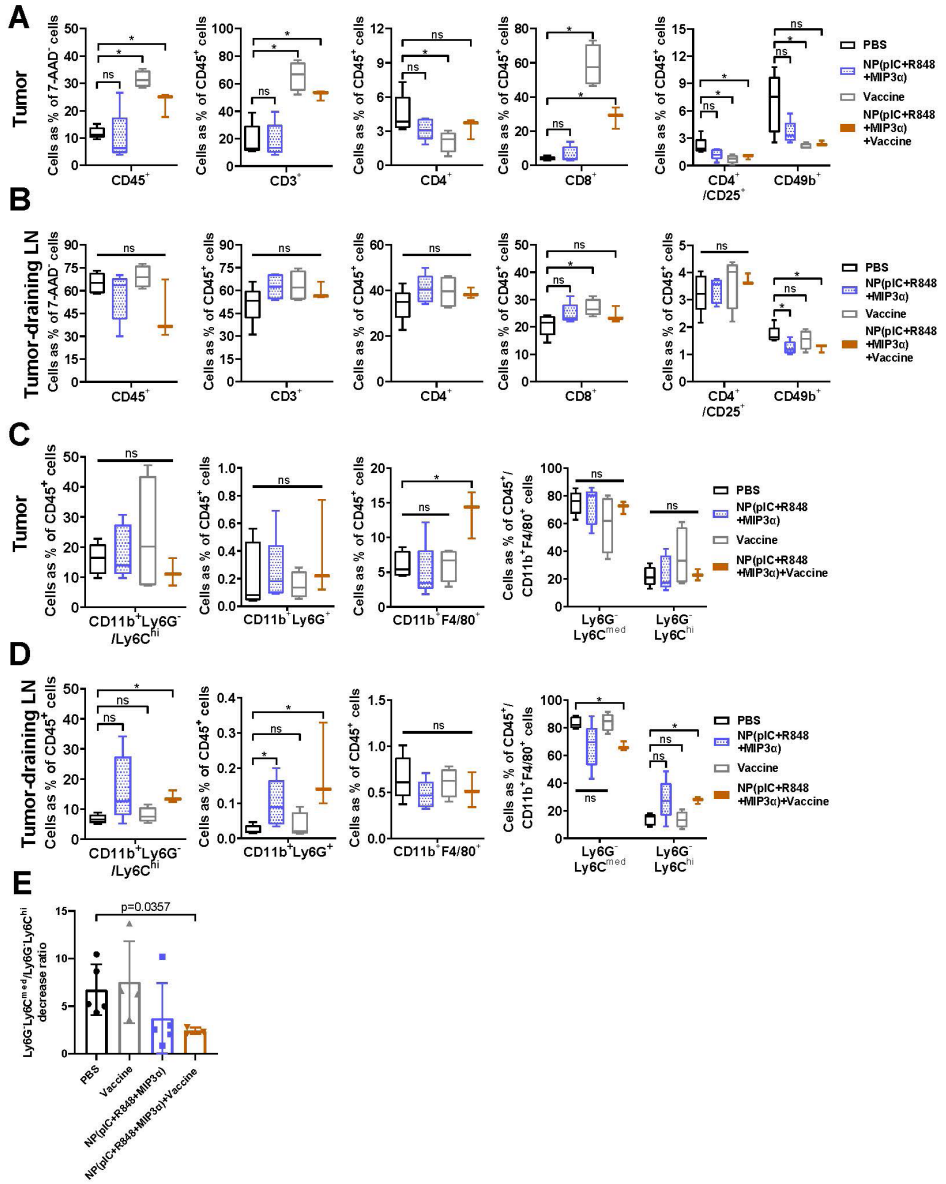
### **3.5. Local NP treatment immune modulates the tumor microenvironment and the tumor-draining lymph node**

Next, we determined the cell population alterations in the tumor and in the tumor-draining lymph node. For this purpose, we analyzed the lymphoid and myeloid populations within these organs of mice bearing TC-1 tumors. Mice were treated as described previously and the organs were resected and analyzed *ex vivo* at day 18. Cancer antigen-specific CD8<sup>+</sup> T cells were detectable in the analyzed organs of vaccinated mice and the levels were not found to increase upon combined treatment (Figure S5A-B). As a monotherapy, NP(pIC+R848+MIP3 $\alpha$ ) increased the levels of CD8<sup>+</sup> T cells and reduced the levels of CD4<sup>+</sup>, CD4<sup>+</sup>CD25<sup>+</sup> Tregs and of CD49b<sup>+</sup> NK cells in the tumor, but this difference was not statistically significant (Figure 5A). In the tumors of mice that were vaccinated or vaccinated and treated with NP(pIC+R848+MIP3 $\alpha$ ) the levels of CD45<sup>+</sup>, CD3<sup>+</sup> and of CD8<sup>+</sup> cells significantly increased and the levels of CD4<sup>+</sup>, CD4<sup>+</sup>CD25<sup>+</sup> and of CD49b<sup>+</sup> significantly

decreased (Figure 5A). In the tumor-draining lymph node, NP(pIC+R848+MIP3 $\alpha$ ) monotherapy as well as the combined treatment increased the levels of CD3+, CD4+ and of CD8+ cells, but this difference was not statistically significant (Figure 5B). On the other hand, the levels of CD49b+ decreased significantly.

Within the myeloid populations in the tumor, the combined treatment significantly increased the levels of CD11b+F4/80+ macrophages, reduced the levels of CD11b+F4/80+/Ly6G-Ly6Cmed tumor associated macrophages and increased the levels of CD11b+F4/80+/Ly6G-Ly6Chi inflammatory monocytes, but these differences were not statistically significant (Figure 5C). In the tumor-draining lymph node, NP(pIC+R848+MIP3 $\alpha$ ) monotherapy increased the levels of CD11b+Ly6G+ neutrophils significantly, and increased the levels CD11b+F4/80+/Ly6G-Ly6Chi inflammatory monocytes and decreased the levels of CD11b+F4/80+/Ly6G-Ly6Cmed tumor associated macrophages, but these differences were not statistically significant (Figure 5D). Similarly, the combination of vaccination and NP(pIC+R848+MIP3 $\alpha$ ) treatment increased the levels of CD11b+Ly6G-/Ly6Chi immature myeloid cells, CD11b+Ly6G+ neutrophils and of CD11b+F4/80+/Ly6G-Ly6Chi inflammatory monocytes significantly, and decreased the levels of CD11b+F4/80+/Ly6G-Ly6Cmed tumor-associated macrophages significantly in the tumor-draining lymph node (Figure 5D & S6). Moreover, the combination treatment of the vaccine and NP(pIC+R848+MIP3 $\alpha$ ) reduced the ratio of Ly6G-Ly6Cmed tumor-associated macrophages to Ly6G-Ly6Chi inflammatory monocytes significantly (Figure 5E).

These results combined indicate that the intratumoral administration of NP(pIC+R848+MIP3 $\alpha$ ) impacted both lymphoid and myeloid populations in the tumor and in the tumor-draining lymph. The most evident adjuvant effects of NP(pIC+R848+MIP3 $\alpha$ ) when combined with vaccination were a significant influx of macrophages into the tumor and a shift from suppressor tumor-associated macrophages towards an acute inflammatory phenotype in the tumor-draining lymph node. Overall, this indicates that the adaptive immune responses (lymphocytes) are potentiated while the innate immune responses acquire an activated state.





< **Figure 5. Local NP treatment immune modulates the tumor microenvironment and the tumor-draining lymph node**

At day 8, four groups of mice (n=5 on average) with TC-1 tumors were treated as follows: 1) received an intratumoral injection of PBS (control); 2) received an intratumoral injection of NP(pIC+R848+MIP3 $\alpha$ ); 3) were vaccinated; or 4) were vaccinated and treated with an intratumoral injection of NP(pIC+R848+MIP3 $\alpha$ ). Ten days later, the intratumoral injections were repeated. At day 18, the tumors were resected and analyzed by flow cytometry: A) Lymphoid population analyzed within the tumor: CD45+ vaccine vs. PBS, p=0.0159; CD45+ vaccine plus NP(pIC+R848+MIP3 $\alpha$ ) vs. PBS, p=0.0357; CD3+ vaccine vs. PBS, p=0.0159; CD3+ vaccine plus NP(pIC+R848+MIP3 $\alpha$ ) vs. PBS, p=0.0357; CD4+ vaccine vs. PBS, p=0.0159; CD8+ vaccine vs. PBS, p=0.0159; CD8+ vaccine plus NP(pIC+R848+MIP3 $\alpha$ ) vs. PBS, p=0.0357; CD4+CD25+ vaccine vs. PBS, p=0.159; CD4+CD25+ vaccine plus NP(pIC+R848+MIP3 $\alpha$ ), p=0.0357; CD49b+ vaccine vs. PBS, p=0.0238. B) Lymphoid population analyzed within the tumor-draining lymph node: CD8+ vaccine vs. PBS, p=0.0317; CD49b+ NP(pIC+R848+MIP3 $\alpha$ ) vs. PBS, p=0.0397; CD49b+ vaccine plus NP(pIC+R848+MIP3 $\alpha$ ) vs. PBS, p=0.0357. C) Myeloid population analyzed within the tumor: CD11b+F4/80+ vaccine plus NP(pIC+R848+MIP3 $\alpha$ ) vs. PBS, p=0.0357. D) Myeloid population analyzed within the tumor-draining lymph node: CD11b+Ly6G-/Ly6Chi vaccine plus NP(pIC+R848+MIP3 $\alpha$ ) vs. PBS, p=0.0357; CD11b+Ly6G+ NP(pIC+R848+MIP3 $\alpha$ ) vs. PBS, p=0.0159; CD11b+Ly6G+ vaccine plus NP(pIC+R848+MIP3 $\alpha$ ) vs. PBS, p=0.0357; CD11b+F4/80+/Ly6G-Ly6Cmed vaccine plus NP(pIC+R848+MIP3 $\alpha$ ) vs. PBS, p=0.0357; CD11b+F4/80+/Ly6G-Ly6Chi vaccine plus NP(pIC+R848+MIP3 $\alpha$ ) vs. PBS, p=0.0357. E) Ly6G-Ly6Cmed/Ly6G-Ly6Chi (in the CD11b+F4/80+ gate) calculated decrease ratio in the tumor-draining lymph node upon described treatments: PBS vs. vaccine, p=0.9048; PBS vs. NP(pIC+R848+MIP3 $\alpha$ ), p=0.0952; PBS vs. vaccine plus NP(pIC+R848+MIP3 $\alpha$ ), p=0.0357. Statistics were calculated using a two-tailed Mann Whitney test. Statistical differences were considered significant at p < 0.05. \* = p < 0.05; \*\* p = < 0.01; \*\*\* p < 0.001. Tregs defined as CD4+CD25+ within the 7-AAD-/CD45+ gate; NK cells defined as CD49b+ within the 7-AAD-/CD45+ gate; Immature myeloid cell population, defined as CD11b+Ly6G-/Ly6C+ cells within the 7-AAD-/CD45+ gate; Neutrophils defined as CD11b+Ly6G+ cells within the 7-AAD-/CD45+ gate; Macrophages defined as CD11b+F4/80+ cells within the 7-AAD-/CD45+ gate; Tumor-associated macrophages defined as Ly6G-Ly6Cmed cells within the CD11b+F4/80+ and the 7-AAD-/CD45+ gate; Inflammatory monocytes defined as Ly6G-Ly6Chi cells within the CD11b+F4/80+ and the 7-AAD-/CD45+ gate. Abbreviations: ns: not (statistically) significant.

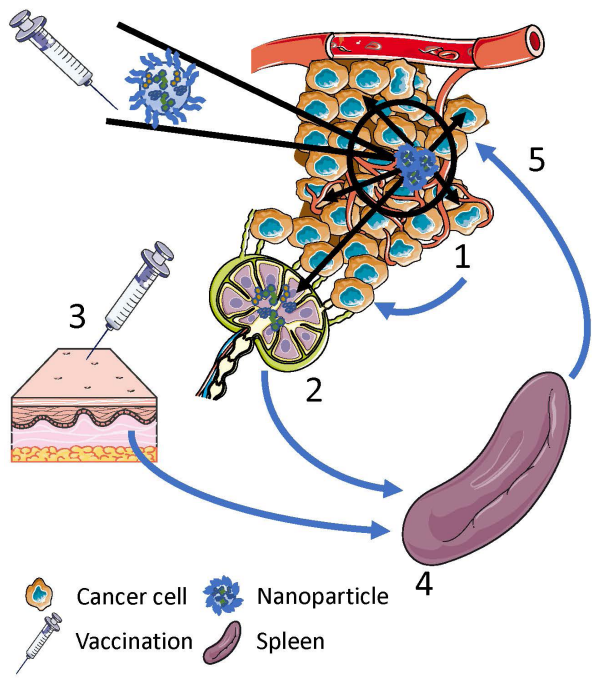
## 4. DISCUSSION

We have rationally developed a practical strategy to improve cancer vaccines by the NP mediated delivery of two TLR agonists and a chemokine to the tumor and tumor-draining lymph node. It takes advantage of the robust induction of cancer fighting T cells by the cancer vaccines while ameliorating the local negative immune regulation. Mechanistically, the combined treatment induced high influx of macrophages into the tumor and induced a shift from suppressor tumor-associated macrophages towards an acute inflammatory phenotype in the tumor-draining lymph node.

Based on our findings, we hypothesize that only a portion of the injected NPs into TC-1 tumors are actually endocytosed by cancer cells, T-regs, MDSC, macrophages and other cells. The NPs that are not endocytosed continue the slow release pIC, R848 and MIP3 $\alpha$  into the tumor area or drain to the tumor-draining lymph node where they continue to amplify acute innate and adaptive immune responses (Figure 6).

### **Figure 6. Rational design to improve the efficacy of therapeutic cancer vaccines by the co-delivery of immune adjuvants to the tumor and tumor-draining lymph node** >

**Step 1)** The NPs are injected in the tumors, whereby pIC and R848 skew the tumor microenvironment and tumor-draining lymph node from a suppressive and chronic inflamed towards an acute inflamed milieu. A portion of the injected NPs are partially endocytosed by cancer cells, T-regs, MDSC, macrophages and other cells, activating immune responses. The NPs that were not endocytosed continue the slow release of pIC, R848 and MIP3 $\alpha$  into the tumor area further maintaining an immune activated state. **Step 2)** Another portion of the NPs that were not endocytosed by cells in the tumor, as well as some of the previously released pIC, R848 and MIP3 $\alpha$ , partially drain to the tumor-draining lymph node. The pIC and R848 activate residing immature and suppressed immune cells and MIP3 $\alpha$  attracts immune cells. **Step 3)** Unaffected by the local negative regulation and robustly activated T cells against cancer antigens are induced by the therapeutic cancer vaccine. **Step 4)** Adaptive and innate immune cells proliferate and are stimulated in the spleen and lymph nodes. **Step 5)** The remaining MIP3 $\alpha$  in the tumor and tumor-draining lymph node actively recruits more cancer fighting immune cells to the tumor bed and mediate tumor mass regression. This figure was composed using Servier Medical Art templates, which are licensed under a Creative Commons Attribution 3.0 Unported License; <https://smart.servier.com>.



After screening the potential of pIC, R848 and MIP3 $\alpha$  in NPs as a monotherapy, we identified the combination to be the most potent form in the TC-1 cancer model and later in the RMA cancer model. Interestingly, a possible intrinsic therapeutic effect was observed by the vehicle control NP(empty) and vaccination. While the PLGA NPs themselves are non-cytotoxic and biocompatible, the direct activation of the inflammasome by PLGA and subsequent secretion of interleukin-1 $\beta$  by DCs has been reported which may explain the observed effect [38,39].

In the TC-1 cancer model, we show that well established and large tumors up to 1200 mm<sup>3</sup> were successfully eradicated with the combined treatment and that the mice survival was improved from 0-40 percent to 75-100 percent. Furthermore, we show that the intratumoral administration of NP(pIC+R848+MIP3 $\alpha$ ) profoundly impacted lymphoid and myeloid populations in the tumor and tumor-draining lymph node. Moreover, intratumoral administration of NP(pIC+R848+MIP3 $\alpha$ ) after vaccination induced considerable increases in circulating cancer antigen-specific CD8+ T cells, compared to vaccinated only mice, leading to more tumor eradications. Despite that the survival results in the RMA model are relatively less impressive compared to the TC-1 model, the gain in progression-free survival after combined treatment is yet remarkable considering the much higher proliferation rate of the RMA cells compared to TC-1 cells, as 1x10<sup>5</sup> TC-1 cells are injected into mice compared to only 1x10<sup>3</sup> RMA cells to achieve similar tumor sizes at day 8-10. We prepared PEGylated PLGA NPs with an average size ranging from 140 to 270 nm, which is within the optimal functional range (40 nm to 300 nm) reported for durable half-life and sustained drug release [40–42]. We injected the NPs intratumoral to reduce, but not eliminate, systemic distribution and maintain high local confinement of these immune adjuvants to the tumor area despite that intravenous injection would also concentrate NPs in the tumor, but likely less efficiently whilst possibly inducing more side-effects.

The chemokine MIP3 $\alpha$  by itself did not significantly improve the cancer vaccine efficacy but when combined with pIC and R848 the progression-free survival was nearly doubled. In addition to the observed influx of macrophages to the tumor, this could be an indication of a functional effect other than the induction of chemotaxis. MIP3 $\alpha$  is commonly produced by several tumor types and is often described as ambivalent, having both anti and pro cancer effects, exhibiting pleiotropic immune responses [43]. Despite its controversial role, it is not surprising that arriving immune

cells, attracted by MIP3 $\alpha$  to the highly suppressed tumor microenvironment, may become also suppressive and dysfunctional. However, if the arriving immune cells encounter a less immune suppressed microenvironment, as artificially induced by TLR agonists for example (as proposed here), it is conceivable that then MIP3 $\alpha$  plays an anti-cancer role. Indeed, a similar observation was made by Fushimi et al. that demonstrated that the intratumoral injection of adenovirus-mediated gene transfer of MIP3 $\alpha$  suppressed tumor growth, but only on cancer models that are highly immunogenic, and this process was mediated by DCs and lymphocytes [44]. Furthermore, we sought to broaden our understanding on possible mechanisms by which the efficacy of the combined treatment is enhanced by focusing on several types of immune cells and the differences in lymphoid and myeloid cell populations upon treatment compared to mock treated tumors. Upon monotherapy with NP(pIC+R848+MIP3 $\alpha$ ) (i.e. without vaccine), more CD8 T cells and less CD4+CD25+ regulatory T cells and CD49b+ NK cells were found in the tumor area which is consistent with previous observations [45]. The myeloid population in the tumor microenvironment appeared to be less prone to immune modulation with monotherapy of NP(pIC+R848+MIP3 $\alpha$ ) in TC-1 tumors. This could be due to tumor cells overcoming acute inflammatory cytokines triggered by the TLR agonists, or the NPs and/or most of the TLR agonists do not remain in the tumor and drain to the tumor-draining lymph node. However, the monotherapy with NP(pIC+R848+MIP3 $\alpha$ ) did affect the myeloid population in the tumor-draining lymph node as more neutrophils were observed and within the macrophage population a shift in phenotype from suppressor tumor-associated macrophages towards inflammatory monocyte phenotype was observed. Furthermore, it is possible that this observed effect was due to the direct effect of TLR agonists drained from the tumor or due to a secondary effect caused by other signals draining from the tumor area. Nonetheless, our results are in line with the finds of Muraoka et al. that described that tumor immune resistance is highly mediated by suppressor tumor-associated macrophages and the activation of these cells rendered tumors sensitive to adaptive immune responses [46].

The changes observed upon combined treatment of vaccination with NP(pIC+R848+MIP3 $\alpha$ ) that were not observed in the vaccinated only mice resembled the effects observed upon NP(pIC+R848+MIP3 $\alpha$ ) monotherapy with the addition of an almost three-fold increase of macrophages in the tumor. This may be an indication that besides T cells, enough numbers of properly activated macrophages are necessary to avoid tumor recurrences as observed by the significantly higher percentages of complete remissions and very late relapses compared to vaccinated only mice.

Most pre-clinical studies to date have focused on the delivery of TLR agonists together with antigens to boost vaccines potency by enhancing DC priming and maturation [13]. Either the antigens and TLR agonists are in soluble form, separate or conjugated, or even in a nanovesicle, but most commonly not intended to be delivered directly to the tumor [47]. In our own experiments, we administered the cancer vaccines combined with the TLR9 agonist CpG, either intradermally or subcutaneously, but in an anatomical location separate to the tumor, to induce robust antigen specific T cells. However, the mere vaccination with antigen and CpG did not result in high percentages of durable tumor clearances. On the other hand, the systemic administration and adjuvant effect of pIC combined with peptide vaccination was studied by Mohamed et al. [48]. Although our data is in line with the authors observations, such as an increase of antigen-specific CD8 T cells, the mice were not challenged with a tumor and therefore it is unclear whether systemic administration of pIC could possibly lead to more tumor clearances. Intratumoral mono immunotherapy with PRR agonists, including TLR agonists, are reported successful modalities to reduce the immunosuppressive activity in the tumor microenvironment, revert resistance to immune checkpoint inhibitors (including PD-1) and enhancing tumor eradications in several mice tumor models [49,50].

Although therapeutic cancer vaccines succeed in inducing robust cancer fighting T cells leading to temporary tumor shrinkage, our data indicates that (local) immune modulation is necessary for durable tumor eradications likely due to the functional abrogation of immune suppressor cells (T-regs, MDSCs, TAMs), boosting T cells function (inhibit senescence) and actively implicate the innate immune system in a coordinated effort to fully clear all cancer cells (Figure 7).

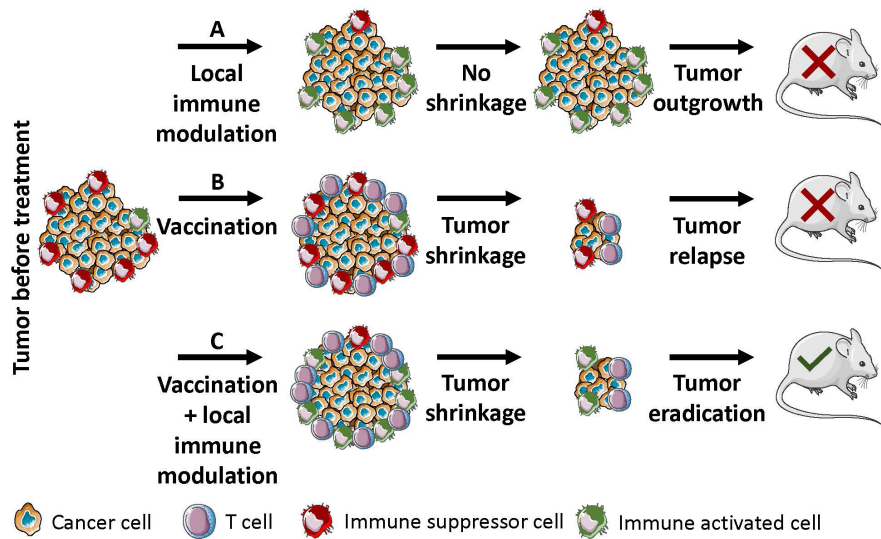


**Figure 7. Hypothetical therapeutic cancer vaccine improved efficacy proposed putative mechanism**

**A)** Local immune modulation induces immune phenotype shift from suppressor (red cells) to activated type (green cells) but this has little effect in tumors without T cells. **B)** Vaccination only induces the influx of T cells (purple cells) into the tumor. However, the strong immune suppressed environment (red cells) is not alleviated and full tumor clearance is not achieved leading to tumor relapses. **C)** Vaccination and local immune modulation therapy combined induces the influx of T cells (purple cells) into the tumor. Concurrently, the local immune modulation therapy induces a shift from suppressor (red cells) to activate (green cells) immune phenotype which together with the T cells achieves full tumor clearances. This figure was composed using Servier Medical Art templates, which are licensed under a Creative Commons Attribution 3.0 Unported License; <https://smart.servier.com>.

As we have shown, our results indicate that the NP mediated co-delivery of immune modulators alters the lymphoid and myeloid cell levels and phenotype contributing to the amelioration of negative regulation. Consequently, the efficacy of cancer vaccines to eradicate tumors is enhanced.

### **Grant Support**

This work is part of the research programme 723.012.110 (Vidi), which is financed by the Netherlands Organisation for Scientific Research (NWO). Also, we would like to thank the financial support of the LUMC fellowship grant, project grants from the EU Program H2020-MSCA-2015-RISE (644373- PRISAR) and MSCA-ITN-2015-ETN (675742-ISPIC), H2020-MSCA-2016-RISE (734684-CHARMED) and H2020-MSCA-RISE-2017-CANCER (777682).

### **Declaration of interest**

The authors were supported with funding from Leiden University Medical Center and the Netherlands Organization for Scientific Research (NWO). The authors have no other relevant affiliations or financial involvement with any organization or entity with a financial interest in, or financial conflict with, the subject matter or materials discussed in the manuscript, apart from those already disclosed.

### **Author contributions**

L.J. Cruz and F. Ossendorp designed and supervised the study. C.G. Da Silva wrote the manuscript and performed the experiments. L.J. Cruz and C.G. Da Silva assembled the nanoparticles. M.G.M. Camps supported the animal studies. T.M.W.Y. Li performed the cell immunofluorescence, NP uptake assay and supported the preparation of the tumor samples for tumor microenvironment analysis. A.B. Chan revised the paper.

### **Data availability**

The authors declare that all the data related with this study are available within the paper or can be obtained from the authors on request.



## REFERENCES

- [1] S.H. van der Burg, R. Arens, F. Ossendorp, T. van Hall, C.J.M. Melief, Vaccines for established cancer: overcoming the challenges posed by immune evasion, *Nat. Rev. Cancer*. 16 (2016) 219–233. doi:10.1038/nrc.2016.16.
- [2] M.A. Cheever, C.S. Higano, PROVENGE (Sipuleucel-T) in Prostate Cancer: The First FDA-Approved Therapeutic Cancer Vaccine, *Clin. Cancer Res.* 17 (2011) 3520–3526. doi:10.1158/1078-0432.CCR-10-3126.
- [3] H. Maeng, M. Terabe, J.A. Berzofsky, Cancer vaccines: translation from mice to human clinical trials, *Curr. Opin. Immunol.* 51 (2018) 111–122. doi:10.1016/J.COI.2018.03.001.
- [4] R.M. Luiten, E.W.M. Kueter, W. Mooi, M.P.W. Gallee, E.M. Rankin, W.R. Gerritsen, S.M. Clift, W.J. Nooijen, P. Weder, W.F. van de Kastelee, J. Sein, P.C.M. van den Berk, O.E. Nieweg, A.M. Berns, H. Spits, G.C. de Gast, Immunogenicity, including vitiligo, and feasibility of vaccination with autologous GM-CSF-transduced tumor cells in metastatic melanoma patients., *J. Clin. Oncol.* 23 (2005) 8978–91. doi:10.1200/JCO.2005.01.6816.
- [5] Z. Ye, Q. Qian, H. Jin, Q. Qian, Cancer vaccine: learning lessons from immune checkpoint inhibitors., *J. Cancer*. 9 (2018) 263–268. doi:10.7150/jca.20059.
- [6] R.W. Jenkins, D.A. Barbie, K.T. Flaherty, Mechanisms of resistance to immune checkpoint inhibitors, *Br. J. Cancer*. 118 (2018) 9–16. doi:10.1038/bjc.2017.434.
- [7] S. Kouidhi, A.B. Elgaaied, S. Chouaib, Impact of Metabolism in on T-Cell Differentiation and Function and Cross Talk with Tumor Microenvironment, *Front. Immunol.* 8 (2017) 270. doi:10.3389/fimmu.2017.00270.
- [8] J. Ye, X. Huang, E.C. Hsueh, Q. Zhang, C. Ma, Y. Zhang, M.A. Varvares, D.F. Hoft, G. Peng, Human regulatory T cells induce T-lymphocyte senescence, *Blood*. 120 (2012) 2021–2031. doi:10.1182/blood-2012-03-416040.
- [9] C. Devaud, L.B. John, J.A. Westwood, P.K. Darcy, M.H. Kershaw, Immune modulation of the tumor microenvironment for enhancing cancer immunotherapy., *Oncoimmunology*. 2 (2013) e25961. doi:10.4161/onci.25961.
- [10] A. Marabelle, H. Kohrt, C. Caux, R. Levy, Intratumoral immunization: a new paradigm for cancer therapy., *Clin. Cancer Res.* 20 (2014) 1747–56. doi:10.1158/1078-0432.CCR-13-2116.

- [11] C. Pasare, R. Medzhitov, Toll-Like Receptors: Linking Innate and Adaptive Immunity, in: *Mech. Lymph. Act. Immune Regul.* X, Springer US, Boston, MA, 2005: pp. 11–18. doi:10.1007/0-387-24180-9\_2.
- [12] M. Shi, X. Chen, K. Ye, Y. Yao, Y. Li, Application potential of toll-like receptors in cancer immunotherapy: Systematic review., *Medicine (Baltimore)*. 95 (2016) e3951. doi:10.1097/MD.0000000000003951.
- [13] B. Temizoz, E. Kuroda, K.J. Ishii, Vaccine adjuvants as potential cancer immunotherapeutics, *Int. Immunol.* 28 (2016) 329–338. doi:10.1093/intimm/dxw015.
- [14] J.K. Dowling, A. Mansell, Toll-like receptors: the swiss army knife of immunity and vaccine development., *Clin. Transl. Immunol.* 5 (2016) e85. doi:10.1038/cti.2016.22.
- [15] Y. Yang, C.-T. Huang, X. Huang, D.M. Pardoll, Persistent Toll-like receptor signals are required for reversal of regulatory T cell-mediated CD8 tolerance, *Nat. Immunol.* 5 (2004) 508–515. doi:10.1038/ni1059.
- [16] L. Huang, H. Xu, G. Peng, TLR-mediated metabolic reprogramming in the tumor microenvironment: potential novel strategies for cancer immunotherapy, *Cell. Mol. Immunol.* (2018). doi:10.1038/cmi.2018.4.
- [17] H. Chi, C. Li, F.S. Zhao, L. Zhang, T.B. Ng, G. Jin, O. Sha, Anti-tumor Activity of Toll-Like Receptor 7 Agonists., *Front. Pharmacol.* 8 (2017) 304. doi:10.3389/fphar.2017.00304.
- [18] M.C. Dieu, B. Vanbervliet, A. Vicari, J.M. Bridon, E. Oldham, S. Ait-Yahia, F. Brière, A. Zlotnik, S. Lebecque, C. Caux, Selective recruitment of immature and mature dendritic cells by distinct chemokines expressed in different anatomic sites., *J. Exp. Med.* 188 (1998) 373–86. doi:10.1084/JEM.188.2.373.
- [19] A. Al-Aoukaty, B. Rolstad, A. Giaid, A.A. Maghazachi, MIP-3alpha, MIP-3beta and fractalkine induce the locomotion and the mobilization of intracellular calcium, and activate the heterotrimeric G proteins in human natural killer cells, *Immunology*. 95 (1998) 618–624. doi:10.1046/j.1365-2567.1998.00603.x.
- [20] F. Liao, R.L. Rabin, C.S. Smith, G. Sharma, T.B. Nutman, J.M. Farber, CC-chemokine receptor 6 is expressed on diverse memory subsets of T cells and determines responsiveness to macrophage inflammatory protein 3 alpha., *J. Immunol.* 162 (1999) 186–94.

- [21] E.V. Acosta-Rodriguez, L. Rivino, J. Geginat, D. Jarrossay, M. Gattorno, A. Lanzavecchia, F. Sallusto, G. Napolitani, Surface phenotype and antigenic specificity of human interleukin 17-producing T helper memory cells, *Nat. Immunol.* 8 (2007) 639–646. doi:10.1038/ni1467.
- [22] S. Yamashiro, J.M. Wang, D. Yang, W.H. Gong, H. Kamohara, T. Yoshimura, Expression of CCR6 and CD83 by cytokine-activated human neutrophils., *Blood.* 96 (2000) 3958–63.
- [23] E. Schutyser, S. Struyf, J. Van Damme, The CC chemokine CCL20 and its receptor CCR6, *Cytokine Growth Factor Rev.* 14 (2003) 409–426. doi:10.1016/S1359-6101(03)00049-2.
- [24] B. Kwong, H. Liu, D.J. Irvine, Induction of potent anti-tumor responses while eliminating systemic side effects via liposome-anchored combinatorial immunotherapy, (2011). doi:10.1016/j.biomaterials.2011.03.067.
- [25] C.G. Da Silva, G.J. Peters, F. Ossendorp, L.J. Cruz, The potential of multi-compound nanoparticles to bypass drug resistance in cancer, *Cancer Chemother. Pharmacol.* 80 (2017) 881–894. doi:10.1007/s00280-017-3427-1.
- [26] H.K. Makadia, S.J. Siegel, Poly Lactic-co-Glycolic Acid (PLGA) as Biodegradable Controlled Drug Delivery Carrier., *Polymers (Basel).* 3 (2011) 1377–1397. doi:10.3390/polym3031377.
- [27] D.A. LaVan, T. McGuire, R. Langer, Small-scale systems for in vivo drug delivery, *Nat. Biotechnol.* 21 (2003) 1184–1191. doi:10.1038/nbt876.
- [28] L.J. Cruz, P.J. Tacken, C. Eich, F. Rueda, R. Torensma, C.G. Figdor, Controlled release of antigen and Toll-like receptor ligands from PLGA nanoparticles enhances immunogenicity, *Nanomedicine.* 12 (2017) 491–510. doi:10.2217/nnm-2016-0295.
- [29] L.J. Cruz, P.J. Tacken, F. Rueda, J.C. Domingo, F. Albericio, C.G. Figdor, Targeting Nanoparticles to Dendritic Cells for Immunotherapy, in: *Methods Enzymol.*, 2012: pp. 143–163. doi:10.1016/B978-0-12-391858-1.00008-3.
- [30] L.J. Cruz, P.J. Tacken, F. Bonetto, S.I. Buschow, H.J. Croes, M. Wijers, I.J. de Vries, C.G. Figdor, Multimodal Imaging of Nanovaccine Carriers Targeted to Human Dendritic Cells, *Mol. Pharm.* 8 (2011) 520–531. doi:10.1021/mp100356k.
- [31] L.J. Cruz, P.J. Tacken, R. Fokkink, B. Joosten, M.C. Stuart, F. Albericio, R. Torensma, C.G. Figdor, Targeted PLGA nano- but not microparticles specifically deliver antigen to human dendritic cells via DC-SIGN in vitro, *J. Control. Release.* 144 (2010) 118–126. doi:10.1016/j.jconrel.2010.02.013.

- [32] J. Tel, A.J.A. Lambeck, L.J. Cruz, P.J. Tacken, I.J.M. de Vries, C.G. Figdor, Human Plasmacytoid Dendritic Cells Phagocytose, Process, and Present Exogenous Particulate Antigen, *J. Immunol.* 184 (2010) 4276–4283. doi:10.4049/jimmunol.0903286.
- [33] K.Y. Lin, F.G. Guarnieri, K.F. Staveley-O'Carroll, H.I. Levitsky, J.T. August, D.M. Pardoll, T.C. Wu, Treatment of established tumors with a novel vaccine that enhances major histocompatibility class II presentation of tumor antigen., *Cancer Res.* 56 (1996) 21–6.
- [34] H.G. Ljunggren, K. Kärre, Host resistance directed selectively against H-2-deficient lymphoma variants. Analysis of the mechanism, *J. Exp. Med.* 162 (1985) 1745–1759. doi:10.1084/jem.162.6.1745.
- [35] F. Ossendorp, N. Fu, M. Camps, F. Granucci, S.J.P. Gobin, P.J. van den Elsen, D. Schuurhuis, G.J. Adema, G.B. Lipford, T. Chiba, A. Sijts, P.-M. Kloetzel, P. Ricciardi-Castagnoli, C.J.M. Melief, Differential Expression Regulation of the and Subunits of the PA28 Proteasome Activator in Mature Dendritic Cells, *J. Immunol.* 174 (2005) 7815–7822 doi:10.4049/jimmunol.174.12.7815.
- [36] G.G. Zom, S. Khan, C.M. Britten, V. Sommandas, M.G.M. Camps, N.M. Loof, C.F. Budden, N.J. Meeuwenoord, D. V. Filippov, G.A. van der Marel, H.S. Overkleeft, C.J.M. Melief, F. Ossendorp, Efficient Induction of Antitumor Immunity by Synthetic Toll-like Receptor Ligand-Peptide Conjugates, *Cancer Immunol. Res.* 2 (2014) 756–764. doi:10.1158/2326-6066.CIR-13-0223.
- [37] S. Zwaveling, S.C. Ferreira Mota, J. Nouta, M. Johnson, G.B. Lipford, R. Offringa, S.H. van der Burg, C.J.M. Melief, Established human papillomavirus type 16-expressing tumors are effectively eradicated following vaccination with long peptides., *J. Immunol.* 169 (2002) 350–8.
- [38] F.A. Sharp, D. Ruane, B. Claass, E. Creagh, J. Harris, P. Malyala, M. Singh, D.T. O'Hagan, V. Pétrilli, J. Tschopp, L.A.J. O'Neill, E.C. Lavelle, Uptake of particulate vaccine adjuvants by dendritic cells activates the NALP3 inflammasome., *Proc. Natl. Acad. Sci. U. S. A.* 106 (2009) 870–5. doi:10.1073/pnas.0804897106.
- [39] J. Wolfram, M. Zhu, Y. Yang, J. Shen, E. Gentile, D. Paolino, M. Fresta, G. Nie, C. Chen, H. Shen, M. Ferrari, Y. Zhao, Safety of Nanoparticles in Medicine., *Curr. Drug Targets.* 16 (2015) 1671–81. doi:10.2174/138945015666140804124808
- [40] R.C. Mundargi, V.R. Babu, V. Rangaswamy, P. Patel, T.M. Aminabhavi, Nano/micro technologies for delivering macromolecular therapeutics using poly(D,L-lactide-co-glycolide) and its derivatives, *J. Control. Release.* 125 (2008) 193–209. doi:10.1016/J.JCONREL.2007.09.013.

- [41] S.M. Moghimi, A.C. Hunter, T.L. Andresen, Factors Controlling Nanoparticle Pharmacokinetics: An Integrated Analysis and Perspective, *Annu. Rev. Pharmacol. Toxicol.* 52 (2012) 481–503. doi:10.1146/annurev-pharmtox-010611-134623.
- [42] S. Bhattacharjee, DLS and zeta potential – What they are and what they are not?, *J. Control. Release.* 235 (2016) 337–351. doi:10.1016/j.jconrel.2016.06.017.
- [43] R. Ranasinghe, R. Eri, Modulation of the CCR6-CCL20 Axis: A Potential Therapeutic Target in Inflammation and Cancer, *Medicina (B. Aires)*. 54 (2018). doi:10.3390/MEDICINA54050088.
- [44] T. Fushimi, A. Kojima, M.A. Moore, R.G. Crystal, Macrophage inflammatory protein 3 $\alpha$  transgene attracts dendritic cells to established murine tumors and suppresses tumor growth., *J. Clin. Invest.* 105 (2000) 1383–93. doi:10.1172/JCI7548.
- [45] R.-F. Wang, Y. Miyahara, H.Y. Wang, Toll-like receptors and immune regulation: implications for cancer therapy, *Oncogene.* 27 (2008) 181–189. doi:10.1038/sj.onc.1210906.
- [46] D. Muraoka, N. Seo, T. Hayashi, Y. Tahara, K. Fujii, I. Tawara, Y. Miyahara, K. Okamori, H. Yagita, S. Imoto, R. Yamaguchi, M. Komura, S. Miyano, M. Goto, S. Sawada, A. Asai, H. Ikeda, K. Akiyoshi, N. Harada, H. Shiku, Antigen delivery targeted to tumor-associated macrophages overcomes tumor immune resistance, *J. Clin. Invest.* 129 (2019) 1278–1294. doi:10.1172/JCI97642.
- [47] G.G. Zom, S. Khan, C.M. Britten, V. Sommandas, M.G.M. Camps, N.M. Loof, C.F. Budden, N.J. Meeuwenoord, D. V. Filippov, G.A. van der Marel, H.S. Overkleeft, C.J.M. Melief, F. Ossendorp, Efficient Induction of Antitumor Immunity by Synthetic Toll-like Receptor Ligand-Peptide Conjugates, *Cancer Immunol. Res.* 2 (2014) 756–764. doi:10.1158/2326-6066.CIR-13-0223.
- [48] M.L. Salem, S.A. EL-Naggar, A. Kadima, W.E. Gillanders, D.J. Cole, The adjuvant effects of the toll-like receptor 3 ligand polyinosinic-cytidylic acid poly (I:C) on antigen-specific CD8 $^+$  T cell responses are partially dependent on NK cells with the induction of a beneficial cytokine milieu, *Vaccine.* 24 (2006) 5119–5132. doi:10.1016/J.VACCINE.2006.04.010.
- [49] R. Zhang, M.M. Billingsley, M.J. Mitchell, Biomaterials for vaccine-based cancer immunotherapy, *J. Control. Release.* 292 (2018) 256–276. doi:10.1016/J.JCONREL.2018.10.008.
- [50] S. Wang, J. Campos, M. Gallotta, M. Gong, C. Crain, E. Naik, R.L. Coffman, C. Guiducci, Intratumoral injection of a CpG oligonucleotide reverts resistance to PD-1 blockade by expanding multifunctional CD8 $^+$  T cells., *Proc. Natl. Acad. Sci. U. S. A.* 113 (2016) E7240–E7249. doi:10.1073/pnas.1608555113.

# CO-DELIVERY OF IMMUNOMODULATORS IN BIODEGRADABLE NANOPARTICLES IMPROVES THERAPEUTIC EFFICACY OF CANCER VACCINES

Da Silva, C.G., Camps, M.G.M., Li, T.M.W.Y., Chan, A.B., Ossendorp, F., Cruz L.J.

Biomaterials. 2019 Nov; 220:119417.

## Supplementary Figures

### **Figure S1.**

RMA MHC class I H-2Kb/Db expression

### **Figure S2.**

The size and zeta potential data characterized by dynamic light scattering

### **Figure S3.**

Tumor re-challenge and development of functional immunological memory against cancer epitopes

### **Figure S4.**

Co-delivery of NPs containing pIC enhances the levels of circulating cancer antigen-specific CD8+ T cells

### **Figure S5.**

Cancer antigen-specific T cells in the tumor and the tumor-draining lymph node

### **Figure S6.**

Macrophage population phenotype shift in the tumor-draining lymph node upon treatment with immunomodulators

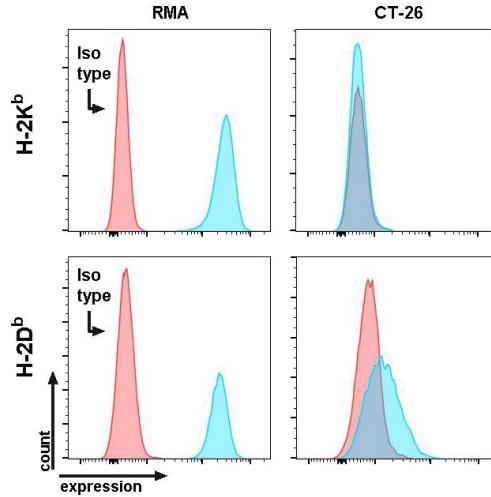


**Figure S1. RMA MHC class I H-2Kb/Db expression**

The expression of RMA MHC class I H-2Kb/Db was verified before in-vivo experiments to ascertain that the expression was not lost due to cell passages (expression in blue, red is isotype control). CT-26 was used as a negative control.

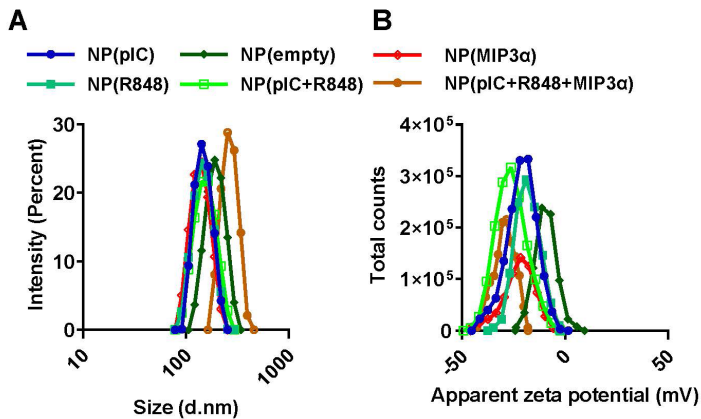


**Figure S2. The size and zeta potential data characterized by dynamic light scattering**

The size (A) and zeta potential (B) data distributions represent the mean value  $\pm$  SD of 10 readings.

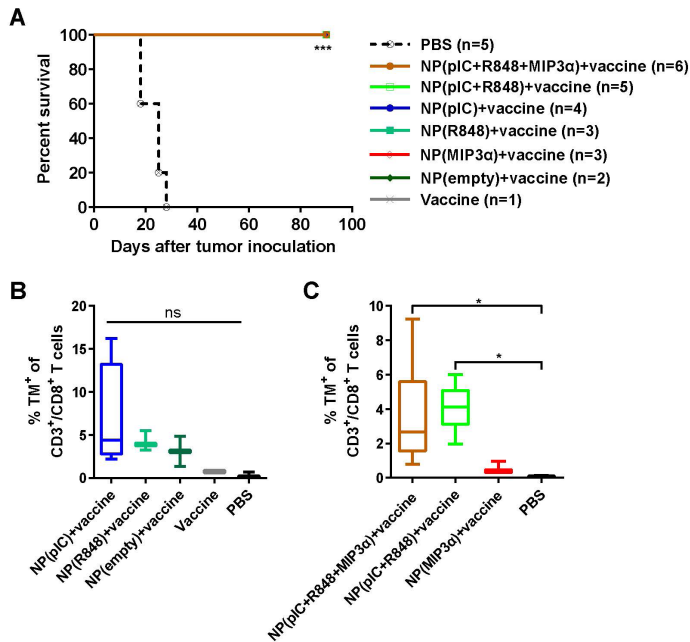


**Figure S3. Tumor re-challenge and development of functional immunological memory against cancer epitopes**

A) Kaplan-Meier survival plot depicting progression-free survival and percent overall survival of pooled data from two separate experiments for mice re-challenged with TC-1 cancer cells at day 120. Survival curves were compared using the log-rank test.

B) The levels of TM<sup>+</sup> T cells in blood of mice ten days after tumor re-challenge for mice treated with vaccination plus NP(pIC), vaccination plus NP(R848), vaccination plus NP(empty), vaccinated only and mock treated (PBS): NP(pIC)+vaccine vs. PBS  $p=0.0571$ ; NP(R848)+vaccine vs. PBS  $p=0.100$ ; NP(empty)+vaccine vs. PBS  $p=0.200$ .

C) The levels of TM<sup>+</sup> T cells in blood of mice ten days after tumor re-challenge for mice treated with vaccination plus NP(pIC+R848), vaccination plus NP(pIC+R848+MIP3 $\alpha$ ), vaccination plus NP(MIP3 $\alpha$ ) and mock treated (PBS): NP(pIC+R848+MIP3 $\alpha$ )+vaccine vs. PBS  $p=0.0238$ ; NP(pIC+R848)+vaccine vs. PBS  $p=0.0357$ ; NP(MIP3 $\alpha$ )+vaccine vs. PBS  $p=0.100$ . Statistics were calculated using a two-tailed Mann Whitney test. Statistical differences were considered significant at  $p < 0.05$ . \* =  $p < 0.05$ ; \*\*  $p < 0.01$ ; \*\*\*  $p < 0.001$ . Data plotted are presented as min to max. Abbreviations: ns: not (statistically) significant; TM: tetramer.



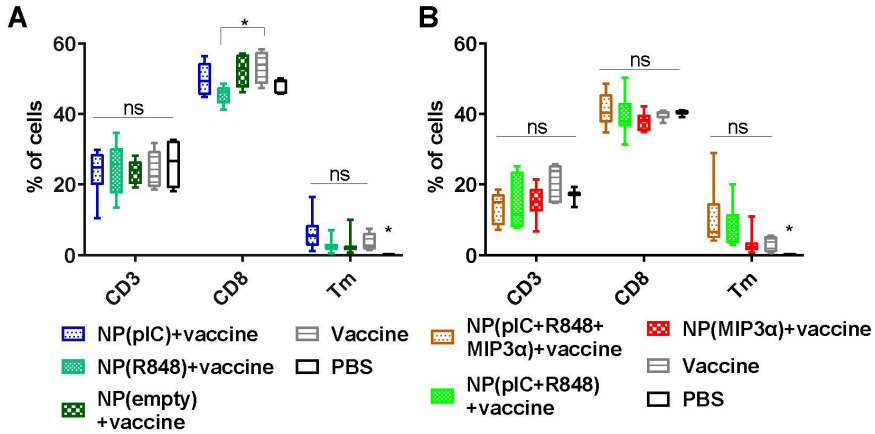


**Figure S4. Co-delivery of NPs containing pIC enhances the levels of circulating cancer antigen-specific CD8+ T cells**

Quantification of CD3+, CD8+ and the HPV16 E7 tetramer (TM) specific T cells in blood at day 16 (8 days post-treatment) after treatment with intratumoral NPs containing different immune adjuvants as compared with vaccine only or PBS (control). A) The levels of CD3+, CD8+ and TM+ T cells in control (PBS) mice and mice vaccinated as well as vaccinated and treated with NP(pIC), NP(R848) or NP(empty). B) The levels of CD3+, CD8+ and TM+ T cells in control (PBS) mice and mice vaccinated as well as vaccinated and treated with NP(MIP3 $\alpha$ ), NP(pIC+R848) or NP(pIC+R848+MIP3 $\alpha$ ). For TM levels: Vaccine vs. PBS  $p=0.0159$  and  $p=0.0357$ , respectively. Statistics were calculated using a two-tailed Mann Whitney test. Statistical differences were considered significant at \*  $p < 0.05$ ; \*\*  $p < 0.01$ ; \*\*\*  $p < 0.001$ . Abbreviations: ns: not (statistically) significant; TM: tetramer.

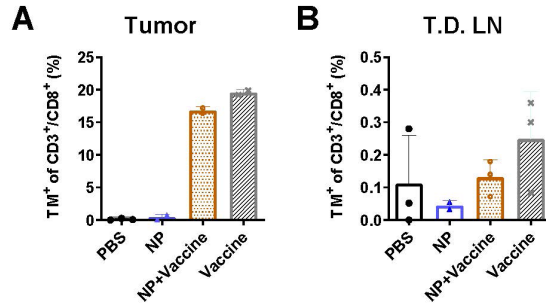


**Figure S5. Cancer antigen-specific T cells in the tumor and the tumor-draining lymph node**

Quantification of CD3<sup>+</sup>CD8<sup>+</sup>TM<sup>+</sup> specific T cells in specified organs at day 20 after mock treatment (PBS), vaccination only, intratumoral injection with NP(pIC+R848+MIP3 $\alpha$ ) only, or combined vaccination and intratumoral injection with NP(pIC+R848+MIP3 $\alpha$ ). A) The levels of CD3<sup>+</sup>CD8<sup>+</sup>TM<sup>+</sup> T cells in the tumor. B) The levels of CD3<sup>+</sup>CD8<sup>+</sup>TM<sup>+</sup> T cells in the tumor-draining lymph node. Abbreviations: NP: NP(pIC+R848+MIP3 $\alpha$ ); TM: tetramer.

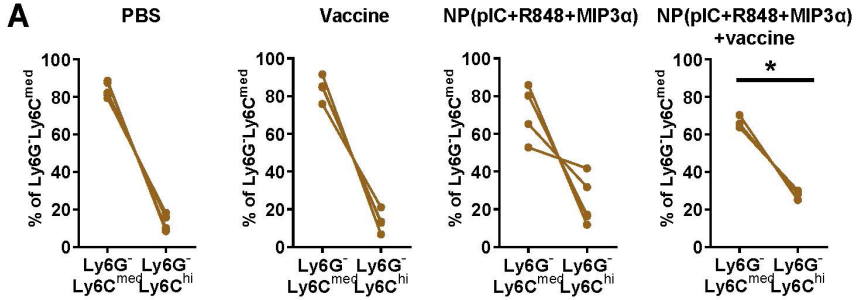


**Figure S6. Macrophage population phenotype shift in the tumor-draining lymph node upon treatment with immunomodulators**

Shown are the Ly6G-Ly6C<sup>med</sup> (suppressor tumor-associated macrophages) and the Ly6G-Ly6C<sup>hi</sup> (inflammatory monocytes) gated from CD11b+F4/80+ gate from the tumor-draining lymph node in mice treated as per described: PBS vs. vaccine,  $p=0.9048$ ; PBS vs. NP(pIC+R848+MIP3 $\alpha$ ),  $p=0.0952$ ; PBS vs. vaccine plus NP(pIC+R848+MIP3 $\alpha$ ),  $p=0.0357$ . Statistics were calculated using a two-tailed Mann Whitney test. Statistical differences were considered significant at \*  $p < 0.05$ ; \*\*  $p < 0.01$ ; \*\*\*  $p < 0.001$ .

6

# COMBINING PHOTODYNAMIC THERAPY WITH IMMUNOSTIMULATORY NANOPARTICLES ELICITS EFFECTIVE ANTI-TUMOR IMMUNE RESPONSES IN PRECLINICAL MURINE MODELS

6

Huis in 't Veld, Ruben V\*.; da Silva, Candido G.\*; Jager, Martine J.; Cruz, Luis J.;  
Ossendorp, Ferry.

\* Authors contributed equally to the study and share first authorship

*Submitted for publication*

# Abstract

---

Photodynamic therapy (PDT) has shown encouraging but limited clinical efficacy when used as a standalone treatment against solid tumors. Conversely, a limitation for immunotherapeutic efficacy is related to the immunosuppressive state observed in large, advanced tumors. In the present study, we employ a strategy in which we use a combination of PDT and immunostimulatory nanoparticles (NPs), consisting of poly(lactic-co-glycolic) acid (PLGA)-polyethylene glycol (PEG) particles loaded with the Toll-like receptor 3 (TLR3) agonist poly(I:C), the TLR7/8 agonist R848, and the lymphocyte-attracting chemokine, macrophage inflammatory protein 3 $\alpha$  (MIP3 $\alpha$ ). The combination provoked strong anti-tumor responses, including an abscopal effect, in three clinically relevant murine models of cancer: MC38 (colorectal), CT26 (colorectal) and TC-1 (human papillomavirus 16 induced). We show that the local and distal anti-tumor effects depended on the presence of CD8 $^+$  T cells. The combination elicited tumor-specific, oncoviral or neoepitope directed CD8 $^+$  T-cell immune responses against the respective tumors, providing evidence that PDT can be used as an in-situ vaccination strategy against cancer (neo)epitopes. Finally, we show that the treatment alters the tumor microenvironment in tumor-bearing mice, from cold (immunosuppressed) to hot (pro-inflammatory), based on greater neutrophil infiltration and higher levels of inflammatory myeloid and CD8 $^+$  T cells compared to untreated mice. Together, our results provide a rationale for combining PDT with immunostimulatory NPs for the treatment of solid tumors.

## INTRODUCTION

Cancer treatment currently consists of various modalities and combinations thereof, including surgical resection, radiotherapy, chemotherapy, photodynamic therapy (PDT) and immunotherapy. Interestingly, PDT can potentially serve three purposes: firstly, it can kill cancer cells directly; secondly, it can induce damage to the tumor vasculature, depending on the photosensitizer and protocols used, that lead to an impaired vascular structure or complete vascular shutdown; and thirdly, it can trigger anti-cancer immune responses.<sup>1,2</sup> Specifically, PDT functions by generating reactive oxygen species that subsequently damage cells in the tumor, its microenvironment and/or its vasculature. This type of photo-ablative damage to the tumor area can induce immunogenic cell death,<sup>3,4</sup> initiating an immune response through the exposure and/or release of damage-associated molecular patterns (DAMPs) and, in some cases, cancer (neo)antigens.<sup>3</sup> These DAMPs then activate diverse pattern-recognition receptors (PRRs) such as Receptor for Advanced Glycation End-products (RAGE), the Toll-like receptors (TLRs) TLR3/7/8/9, or Absent-in-Melanoma 2 (AIM2), among others, in dendritic cells (DCs), macrophages, epithelial and other cells. Several DAMPs have been shown to be highly important in the immune response following PDT, including high mobility group box 1 (HMBG1),<sup>5</sup> surface-exposed calreticulin (CRT),<sup>4,6,7</sup> the surface-exposed heat shock proteins HSP70 and HSP908–13, and extracellular ATP.<sup>14–16</sup> Moreover, the curative effects of PDT strongly depend on the presence of a functional adaptive immune system.<sup>15</sup> In this regard, we previously reported that depletion of CD8<sup>+</sup> T cells before treatment abrogates the survival benefits of PDT.<sup>17</sup>

Cancer immunotherapy using immunostimulatory agents administered intratumorally, systemically or otherwise, has been investigated extensively. When administered intratumorally, such agents generally function by converting the tumor microenvironment and the tumor-draining lymph nodes (dLN) from an immunosuppressed (cold) to a pro-inflammatory (hot) state.<sup>18</sup> We previously reported that intratumoral administration of the TLR3 ligand poly(I:C), the TLR7/8 ligand R848 and the chemokine MIP3 $\alpha$  is effective in murine cancer models.<sup>19,20</sup> Such TLR agonists are among the most potent of immunotherapies available and, accordingly, many of these agents are currently in clinical development.<sup>21</sup> Similarly,

Polyinosinic:polycytidylic acid (poly(I:C), an analog of double-stranded RNA (dsRNA) and a potent agonist of the dsRNA-sensor TLR3<sup>22</sup>, has been reported to inhibit the growth of certain tumors by converting them from immunologically cold to hot<sup>23–25</sup> and to indirectly facilitate adaptive anti-tumor immune responses through the induction of the innate immune system.<sup>26</sup> Additionally, poly(I:C) may also directly affect tumor cells by initiating cell death pathways via activation of caspase 8.<sup>27–30</sup> Analogously, R848, an imidazoquinolinone derivative and agonist of the single-stranded-RNA (ssRNA)-sensor TLR7/8, induces immune responses based on signaling through MyD88 and NF- $\kappa$ B.<sup>31</sup> It induces anti-tumor responses<sup>32</sup>, decreases the number of myeloid-derived suppressor cells (MDSCs) in tumors and promotes the conversion of MDSCs towards a more-mature antigen-presenting phenotype.<sup>33</sup> Moreover, R848 has been reported to promote the polarization of tumor-associated macrophages to an M1-like phenotype, contributing to inhibition of tumor growth.<sup>34</sup> Similarly, TLR8 signaling has been shown to reverse suppression and inhibit the generation of senescent tumor-specific T cells and of naïve T cells.<sup>35</sup> Interestingly, R848 was shown to increase the expression of HMGB1, indicating synergistic potential for combination with PDT.<sup>32</sup> Lastly, the chemokine MIP3 $\alpha$  (CCL20) is a strong chemoattractant for lymphocytes<sup>36</sup>, and acts by binding to the chemokine receptor CCR6.<sup>37,38</sup>

To reduce the risk of adverse systemic immune events in patients, we aim to minimize diffusion of immunostimulatory agents from the tumor area. In this context, biocompatible nanoparticles (NPs) that can release drugs in a slow and sustained fashion are ideal vehicles for intratumoral delivery of such agents<sup>39</sup>, offering clear advantages over free (nude) drugs.<sup>40</sup> Specifically, poly(lactic-co-glycolic) acid (PLGA) NPs and liposomes are both FDA-approved vehicles and already used in the clinic.<sup>41,42</sup> Recently, we have reported that in mice, PLGA-based NPs can accumulate strongly in PDT-treated tumors compared to untreated tumors after systemic administration, providing a rationale for the combination of PDT and NP-based anti-tumor therapy.<sup>43</sup> Here, we report a study in which PDT combined with intratumoral administration of PLGA NPs loaded with poly(I:C), R848 as well as MIP3 $\alpha$  was analyzed for its therapeutic efficacy compared to either modality alone, in three murine cancer models: MC38 (colon adenocarcinoma model), CT26 (colon cancer carcinoma) and TC-1 (lung epithelial tumor expressing human papillomavirus (HPV)<sup>16</sup> E6 and E7 oncoproteins). Of relevance, each of these murine models represents a human tumor that could be potentially treated



intratumorally in patients via fiber optics.<sup>44,45</sup> In all three models, the combination treatment was highly efficacious. We observed strong anti-cancer immune responses with tumor (neo)antigen specific CD8<sup>+</sup> T cells and an abscopal effect to a secondary tumor in the opposite flank. Finally, we found that our treatment modulated the immunosuppressive microenvironment into a more proinflammatory state. Together, our results indicate that a combination of PDT and intratumorally-administered PLGA NPs loaded with immunostimulatory agents elicits strong local and systemic anti-tumor immune responses in clinically relevant murine models of solid tumors.

## MATERIALS AND METHODS

### 2.1 Materials and reagents

PLGA (Resomer RG 502 H, lactide:glycolide molar ratio 48:52 to 52:48) was purchased from Boehringer Ingelheim, Germany. Solvents used for PLGA preparation were obtained from Sigma-Aldrich (The Netherlands). The lipids were purchased from Avanti Polar Lipids (USA) and included 1,2-distearoyl-sn-glycero-3-phosphoethanolamine-N-[amine (polyethylene glycol)2000] (ammonium salt) and 1,2-distearoyl-sn-glycero-3-phosphoethanolamine-N-[methoxy(polyethylene glycol)-2000] (ammonium salt) (mPEG 2000 PE). Poly (inosinic:cytidylic acid (poly(I:C)) and the near-infrared (NIR) dye IR-780 were purchased from Sigma-Aldrich (Zwijndrecht, The Netherlands), R848 was obtained from Alexis Biochemicals (Paris, France) and MIP3 $\alpha$  (CCL20) was purchased from R&D Systems (USA).

### 2.2 Preparation of PLGA-NPs

Poly-lactic-co-glycolic-acid-based NPs that encapsulate poly(I:C), R848 and MIP3 $\alpha$  were prepared using an oil/water emulsion and the solvent evaporation-extraction method.<sup>46–49</sup> In brief, 200 mg of PLGA was dissolved in 3 mL of dichloromethane (DCM), containing 8 mg of poly(I:C), 4 mg of R848 and 250  $\mu$ g of MIP3 $\alpha$  in addition to 1 mg of the NIR dye IR-780 when used for microscopy, and added drop-wise to 40 mL of aqueous 2.5 % (w/v) PVA in distilled water before emulsification for 120 sec using a sonicator (250W Sonifier 250, Branson, USA). After the DCM had been removed through air-drying, the lipid mPEG 2000 PE (20 mg) was dissolved in DCM and used to form a film layer on the bottom of a beaker. Subsequently, the emulsion was rapidly added to the beaker containing the lipids

and the solution was homogenized for 30 sec by sonification. Following overnight evaporation of the solvent at 4 °C, the PLGA NPs were collected by centrifugation at 25000 g for 10 min, washed four times with distilled water, and lyophilized. The concentration of the agents entrapped by the NPs was determined by reverse phase high-performance liquid chromatography and regression analysis, as described previously.<sup>19,50</sup>

### **2.3 Size distribution and surface charge of the NPs**

The average size and zeta-potential of PLGA NPs was determined using a Zetasizer Nano ZSP (Malvern Panalytical, Malvern, UK). In brief, 50 µg of NP was dissolved in 1 mL MilliQ H<sub>2</sub>O after which the size was determined by dynamic light scattering and the surface charge was measured by laser Doppler electrophoresis.

### **2.4 Cell lines**

The tumor cell line Murine Colon 38 (MC38) cells on C57BL/6 background and the murine colon carcinoma cell line CT26 on BALB/c background were kindly provided by Mario Colombo and used for experiments without modification. The murine tumor cell line TC-1, expressing HPV16 E6 and E7 oncoproteins and the activated human c-Ha-ras oncogene, generated by retroviral transduction of lung fibroblasts obtained from C57BL/6 mice, was a gift from T.C. Wu (John Hopkins University, Baltimore, MD).<sup>51</sup> The D1 dendritic cell (D1DCs) line, an immature splenic dendritic cell (DC) that resembles bone marrow-derived DCs<sup>52</sup>, was cultured as described previously.<sup>53</sup> All cells used were tested for mycoplasma and were MAP tested before the onset of experiments. All tumor cell lines were cultured in culture medium, consisting of Iscove's Modified Dulbecco's Medium (IMDM, Lonza, Basel, Switzerland) supplemented with 8% Fetal Calf Serum (Greiner, Kremsmünster, Austria), 2 mM glutamine (Gibco, Landsmeer, The Netherlands), 100 IU/mL penicillin/streptomycin (Gibco) and 25 µM 2-mercaptoethanol (Sigma-Aldrich) and kept in an incubator (Panasonic) at 37 °C and 5% CO<sub>2</sub>. For TC-1, the culture medium was further supplemented with 400 µg/mL of the selection antibiotic Geneticin (G418; Life Technologies).

## 2.5 Animal models

All animal experiments were performed in accordance with the Code of Practice of the Dutch Animal Ethical Commission. Female BALB/c mice (6 to 12 weeks old) were purchased from Charles River (Ecully, France) and C57BL/6J mice were purchased from ENVIGO (Horst, the Netherlands). The animals were housed in the animal facility of the LUMC under specified pathogen-free conditions.

## 2.6 Photosensitizer uptake and retention experiments

Photosensitizer uptake and retention were evaluated by seeding  $4 \times 10^4$  MC38,  $3 \times 10^4$  CT26 or  $2.5 \times 10^4$  TC-1 cells in separate wells of a 24-well plate (Corning, Glendale, USA) in culture medium and subsequent incubation overnight at 37 °C and 5 % CO<sub>2</sub>. For the uptake experiments, cells were incubated with indicated concentrations of Radachlorin® (Radapharma International, Loon op Zand, The Netherlands) for a specified time. Following incubation, the cells were washed 3 times with PBS and fixed in Phosphate Buffered Saline (PBS) containing 1% formalin (J.T. Baker) at 4 °C for 15 min. The fixative was then washed away with PBS, after which the cells were reconstituted in Fluorescence-Activated Cell Sorting (FACS) buffer (PBS with 0.5 % Bovine Serum Albumin (BSA) and 0.02 % sodium azide). The fluorescence of the photosensitizer was used to determine its uptake using flow cytometry on an LSR II (BD Biosciences, San Jose, USA). For the retention experiment, cells incubated with photosensitizer for 4 h were washed 3 times in PBS and supplied with fresh culture medium. After an indicated amount of time, the samples were washed 3 times in PBS, fixed in 1% formalin at 4 °C for 15 min before washing in PBS, reconstituting in FACS buffer and analysis by flow cytometry.

## 2.7 PDT in vitro cytotoxicity

For PDT in vitro,  $4 \times 10^4$  MC38,  $3 \times 10^4$  CT26 and  $2.5 \times 10^4$  TC-1 cells were seeded in 24-well plates (Corning) in culture medium and kept overnight at 37 °C and 5% CO<sub>2</sub>. Cells were then incubated with 2 μM Radachlorin®, unless indicated otherwise, for a specified amount of time, washed 3 times with PBS and supplied with 500 μl fresh medium. Illumination was performed at a light intensity (fluence rate) of 116 mW/cm<sup>2</sup> for a total light dose (fluence) of 20 J/cm<sup>2</sup> using a 662 nm Milon Lakhta Laser, unless indicated otherwise. The following day, the cells were collected in FACS buffer, stained with Annexin V-FITC (BD Biosciences) at 3 μL per sample and 0.5 μM 4',6-diamidino-2-phenylindole (DAPI) (Sigma-Aldrich) in

Annexin V binding buffer (0.1 M 4-(2-hydroxyethyl)-1-piperazineethanesulfonic acid (HEPES), 1.4 M NaCl, and 25 mM CaCl<sub>2</sub> in deionized water with a pH set to 7.4. sterile filtered using a 0.2 µm filter), and finally, analyzed by flow cytometry. As a positive control, cells were subjected to three freeze/thaw cycles at -20 °C before staining and analysis by flow cytometry.

### **2.8 Maturation of D1DCs after incubation with NPs**

The biological activity of the NP-encapsulated agents was evaluated by seeding  $5 \times 10^4$  D1DCs in 96-well plates (Corning) and incubating them with the NPs for 48 h in an incubator. The NP concentrations were matched to poly(I:C) at 5 µg/mL and serially diluted according to annotated concentrations to establish a dose-response curve, to enable comparison with the free ligand at 5 µg/mL. The cells were stained for the DC maturation markers CD86 and CD40 using anti-CD86-APC (clone GL1, eBioscience, Waltham, USA) and anti-CD40-PE (clone 1C10, eBioscience), respectively, and expression was measured by flow cytometry. The supernatant was collected after which IL12 was analyzed by a standard sandwich ELISA using the purified anti-mouse IL12/IL23 p40 (clone C15.6, Biolegend, San Diego, USA) and biotin-labelled anti-mouse IL12/IL23p40 antibodies (clone C17.8, Biolegend). The plates were read at 450 nm using a Bio-Rad 680 microplate reader (Bio-Rad Laboratories, Veenendaal, The Netherlands).

### **2.9 Toxicity of the NPs**

The toxicity of the NPs to MC38, CT26 and TC-1 cells was determined by seeding  $5 \times 10^4$  cells in 96-well plates (Corning) and incubating them with the NPs in a range of concentrations (6.25 µg/mL to 200 µg/mL) for 72 h. Cell viability was measured by adding 3-(4,5-dimethylthiazol-2-yl)-5-(3-carboxymethoxyphenyl)-2-(4-sulfophenyl)-2H-tetrazolium (MTS) reagent according to manufacturer instructions (Abcam, Cambridge, UK), and absorption was measured at 490 nm on a Bio-Rad iMark microplate absorbance reader after incubation.

### **2.10 Maturation of D1DCs after incubation with PDT-treated tumor cells**

The immunostimulatory effects of PDT were preliminarily ascertained in a cellular assay involving dying PDT-treated cells and D1 dendritic cells. Firstly,  $10^4$  D1DCs were seeded in 96-well plates (Corning) for 24h. The following day, tumor cells were incubated with 2 µM Radachlorin® for 4 h (as described in 2.7), and then treated with PDT at 116 mW/cm<sup>2</sup> for 20 J/cm<sup>2</sup>. These (dying) treated tumor cells were

then added to the D1DCs at a ratio of 20:1 (tumor cell/D1DC), and the cells were incubated together for a further 24 h in an incubator. The cells were then collected, stained with 0.5  $\mu\text{M}$  DAPI (Sigma-Aldrich), CD11c-APC-Cy7 (clone N418 Thermo Fisher Scientific, Waltham, USA), MHC-II-PE (H-2kb AF6-88.5, BD Biosciences) and CD86-FITC (clone GL1, eBioscience), and finally, analyzed by flow cytometry on an LSR-II (BD Biosciences). Live D1DCs were gated based on DAPI-CD11chi after size/morphology and doublet exclusion based on FSC/SCC patterns.

### **2.11 PDT and NP tumor treatments in vivo**

For PDT in vivo, C57BL/6J mice were inoculated with  $0.5 \times 10^6$  MC38 or  $1 \times 10^5$  TC-1 cells in 200  $\mu\text{L}$  PBS and BALB/c mice were inoculated with  $0.2 \times 10^6$  CT26 cells in 200  $\mu\text{L}$  PBS, on the left and/or right flanks as indicated per experiment. Once the tumors had reached an average volume of approximately 125 mm<sup>3</sup>, the mice were randomly divided into groups and treated with PDT as described previously.<sup>17,54</sup> Briefly, 20 mg/kg Radachlorin® was administered intravenously into the tail vein and allowed to distribute for 6 h. Then, the skin surrounding the tumor area was shaved before illumination under isoflurane anesthesia at a fluence rate of 116 mW/cm<sup>2</sup> over 1000 sec for a fluence of 116 J/cm<sup>2</sup>. The next day, the mice were injected intratumorally with NPs at concentrations corresponding to 2.5 mg/kg (50  $\mu\text{g}$ ) poly(I:C), at 0.7 mg/kg (14  $\mu\text{g}$ ) of R848 and 0.05 mg/kg (1  $\mu\text{g}$ ) of MIP3 $\alpha$  in a total volume of 30  $\mu\text{L}$  per treatment. These intratumoral injections were repeated every other day for a total of four treatments for the MC38 and CT26 models, and a total of two treatments for the TC-1 model. From this point onwards, the tumor growth was measured regularly until the end of the experiment.

### **2.12 Detection of blood tetramers**

The capacity of PDT and the NPs to induce antigen-specific T cells in the blood of TC-1 tumor-bearing mice were determined analyzing (25  $\mu\text{L}$ ) blood obtained from the tail vein at day 8 after PDT. Red blood cells were removed using lysis buffer after which the cells were incubated with an APC labeled, MHC class I (H-2Db) HPV16 E749-57 (RAHYNIVTF) (H-2Db) tetramer. Next, the cells were stained with anti-CD8 $\alpha$ -PE (clone 53-6.7, eBioscience), anti-CD3-eFluor 450 (clone 17A2, eBioscience) and analyzed by flow cytometry on an LSR-II (BD Biosciences). Gating of CD8<sup>+</sup> T cells was based on CD3+CD8<sup>+</sup> events after size/morphology and doublet exclusion based on FSC/SCC patterns.

### **2.13 Depletion of CD8+ cells**

Mice were treated with 1 mg/kg (20 µg) anti-CD8-depleting antibodies via subcutaneous injection (clone 2.43) in 100 µL PBS every 7 days, starting one day before treatment. Circulating CD8+ T cells were qualified by analyzing blood (50 µL) obtained from the tail vein the morning before treatment. Red blood cells were removed using lysis buffer after which the cells were stained with anti-CD8α-PE (clone 53-6.7, eBioscience), and then anti-CD3-eFluor 450 (clone 17A2, eBioscience) analyzed by flow cytometry on an LSR-II (BD Biosciences).

### **2.14 Analysis of the tumor microenvironment, draining lymph node and spleen**

Immunocompetent mice were inoculated with tumor cells in the right and left flanks, and then subcutaneously injected with CD8-depleting antibodies one day before tumors became established. When the tumors were established (~125mm<sup>3</sup>), PDT was performed on one tumor by administration of 20 mg/kg Radachlorin in the tail vein and irradiating with 662 nm light at a drug-to-light interval of 6 h at 116 mW/cm<sup>2</sup> for 116 J/cm<sup>2</sup>. The next morning, animals were intratumorally injected with the NPs at an interval of 2 days. The day following the second NP administration, the mice were sacrificed after which the tumors, tumor-draining lymph node of the treated tumor and the spleen were harvested, processed and stained for analysis by flow cytometry. Tumors were excised, and then incubated with Liberase protease mix (Sigma) for 15 min to 30 min at 37°C. Liberase-treated tumor fragments, spleens and lymph nodes were processed through a cell strainer (Corning) to obtain single-cell suspensions. The samples were washed 2 times with culture medium and then washed 2 times with FACS buffer. Samples were stained with antibody mixes (see below) for analysis by flow cytometry. All flow cytometric analyses were performed on samples provided in FACS buffer on a Cytex Aurora 5-Laser flow cytometer (Cytex, Fremont, USA). The myeloid antibody panel consisted of CD11b-eFluor450 (clone M1/70 Thermo Fisher), Ly6C-BV605 (clone HK1.4 Biolegend), F4/80-FITC (clone BM8 Biolegend), Ly6G-AF700 (clone 1A8 Biolegend), CD45.2-APC-eFluor780 (clone 104 Thermo Fisher) and 7AAD (Invitrogen) viability staining. The lymphoid antibody panel consisted of CD44-V450 (IM7 Thermo Fisher), CD3e-FITC (Clone 145-2C11 Thermo Fisher), CD4-APC (clone RM4-5 Thermo Fisher), CD8α-APC-R700 (clone 53-6.7 BD Biosciences), CD45.2-APCeFluor780 (clone 104 Thermo Fisher) and 7AAD viability staining (Invitrogen).

### 2.15 Intracellular cytokine staining

Single-cell suspensions of splenocytes obtained as in 2.14 were incubated with D1DCs that were loaded overnight with 5  $\mu$ M synthetic peptides of the MC38 neoepitopes Adpgk (peptide sequence: HLELASMTNMELMSSIVHQ) and Rpl18 (peptide sequence: KAGGKILTFDRLALESPK)<sup>55,56</sup>, in presence of 2  $\mu$ g/mL Brefeldin A for 8h at 37°C. The samples were then stained with antibody mixes for flow cytometry. Again, all cytometric analyses were performed on samples provided in FACS buffer on a Cytex Aurora 5-Laser flow cytometer. The antibody panel consisted of Granzyme B-V450 (clone NGZB Thermo Fisher), CD3-BV510 (clone 145-2C11 BD Biosciences), TNF $\alpha$ -FITC (clone MP6-XT22 Thermo Fisher), IL-2-PE (clone JES6-5H4 Thermo Fisher), IFN- $\gamma$ -PE-Cy7 (clone XMG1.2 BD Biosciences), CD8 $\alpha$ -APC-R700 (clone 53-6.7 BD Biosciences) and 7AAD viability staining (Invitrogen).

### 2.16 Statistics

Graph Pad Prism software version 8 was used for statistical analysis. Data were analyzed as indicated for individual experiments.

## RESULTS

### **PDT in vitro**

We previously studied and characterized PDT with the photosensitizer (PS) Radachlorin, reporting strong induction of anti-tumor responses and disruption of the tumor vasculature in the MC38 tumor model.<sup>43</sup> In the current study, we used flow cytometry to show that Radachlorin is internalized by MC38, CT26 and TC-1 cells over time, with uptake increasing up to 8 h post-incubation (Figure 1A). Binding of the PS, as investigated by incubation at 4 °C, induces a markedly lower fluorescent signal when compared to the uptake in all three tested cell lines over time (Figure 1A), indicating that the majority of the PS is indeed taken up by the cells. Furthermore, the PS was shown to stay inside the cells up to at least 6h post-pulse (Figure 1B). Moreover, we confirmed that Radachlorin was non-toxic to all the tested cell lines after incubation, in the absence of light (dark toxicity), at Radachlorin concentrations from 0.1  $\mu$ M to 100  $\mu$ M (Figure 1C). We investigated the effect of in vitro PDT on cell viability after 4 h of incubation at 2  $\mu$ M Radachlorin, followed by illumination with 662 nm laser light at a fluence rate of 116mW/cm<sup>2</sup> for a fluence of 20 J/cm<sup>2</sup>. Flow cytometry based on staining for the death marker DAPI and early apoptotic marker Annexin V (Figure 1D) was subsequently applied on the treated cells. The single PDT treatment induced near-complete cell death, comparable to three freeze/thaw cycles at -20 °C. Importantly, at 2 J/cm<sup>2</sup>, approximately 61 $\pm$ 4% of MC-38, 49 $\pm$ 3% of CT26 and 23 $\pm$ 6% of TC-1 cells were stained by Annexin V and/or DAPI, indicating differences in sensitivity to PDT among tumor cell lines. PDT-induced cell death diminished with decreasing fluence: at a fluence of 0.2 J/cm<sup>2</sup>, we observed levels of cell death comparable to those in the untreated tumor cells. Together, our results indicate that the photosensitizer Radachlorin is gradually internalized by MC38, CT26 and TC-1 tumor cells in vitro; that it remains in these cells for up to 6 h post-incubation; that it does not exhibit dark toxicity; and that, following PDT, it kills cells from all three tumor lines at levels similar those obtained by multiple freeze/thaw cycles.



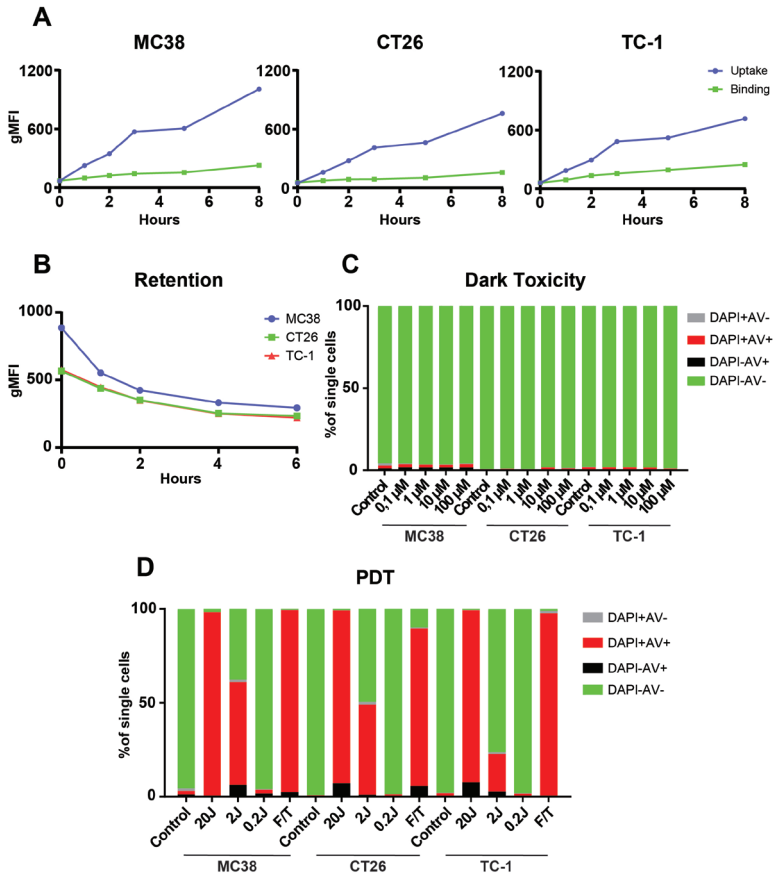


**Figure 1. Cellular uptake, binding, retention and cytotoxicity of the photosensitizer Radachlorin in three clinically relevant tumor cell lines**

**A).** Cellular uptake and binding assays with the photosensitizer Radachlorin (2  $\mu\text{M}$ ) in MC38, CT26 and TC-1 cells over time. The uptake and binding assays were performed by incubating cells with photosensitizer at 37  $^{\circ}\text{C}$  and 4  $^{\circ}\text{C}$ , respectively. Detection was performed by flow cytometry using the fluorescence of Radachlorin. **B).** Retention of Radachlorin (2  $\mu\text{M}$ ) in MC38, CT26 and TC-1 cells after a pulse of 4 h, washing and detection by flow cytometry. **C).** Dark toxicity after incubation with Radachlorin (0.1  $\mu\text{M}$  to 100  $\mu\text{M}$ ) for 4 h, followed by washing and incubation overnight. Cells were stained with DAPI and Annexin V-FITC to determine cell viability by flow cytometry. **D).** Cytotoxicity of Radachlorin (2  $\mu\text{M}$ ) treatment

followed by PDT. Cells were incubated for 4 h, after which they were washed and irradiated with 662nm light 116 mW/cm<sup>2</sup> (0.2 J/cm<sup>2</sup> to 20 J/cm<sup>2</sup>). Three freeze/thaw cycles at -20 °C were used as positive control. The next day, the cells were stained with DAPI and Annexin V-FITC to determine their viability by flow cytometry.

### **Radachlorin PDT induces immunogenic cell death**

Next, we investigated the immunological effects of PDT-induced cancer cell death on the maturation of dendritic cells (DCs). To this end, DCs were incubated for 24 h with PDT-treated cancer cells and evaluated for expression of the maturation markers CD86 and MHC-II by flow cytometry. For MC38 cells, the protocol that induced the strongest cell death also induced the greatest upregulation of both markers at levels higher than those observed for the positive control, three freeze/thaw cycles (Figure 2A). Moreover, the PDT-treated cancer cells induced upregulation of the maturation markers at levels comparable to treatment with 1 µg/mL of the TLR3 ligand poly(I:C), an immunostimulatory agent that induces strong upregulation of these markers. A similar trend was observed for CT26, although the upregulation of the markers was lower than for MC38 (Figure 2B). Finally, incubation of the DCs with TC-1 cancer cells induced a slight upregulation of the maturation markers, with levels only slightly increased compared to incubation with the positive control of three freeze/thaw cycles (Figure 2C). Taken together, these results suggest that PDT treatment of MC38 and CT26 cells, and to a much smaller extent of TC-1 cells, leads to strong upregulation of maturation markers on DCs *in vitro*.

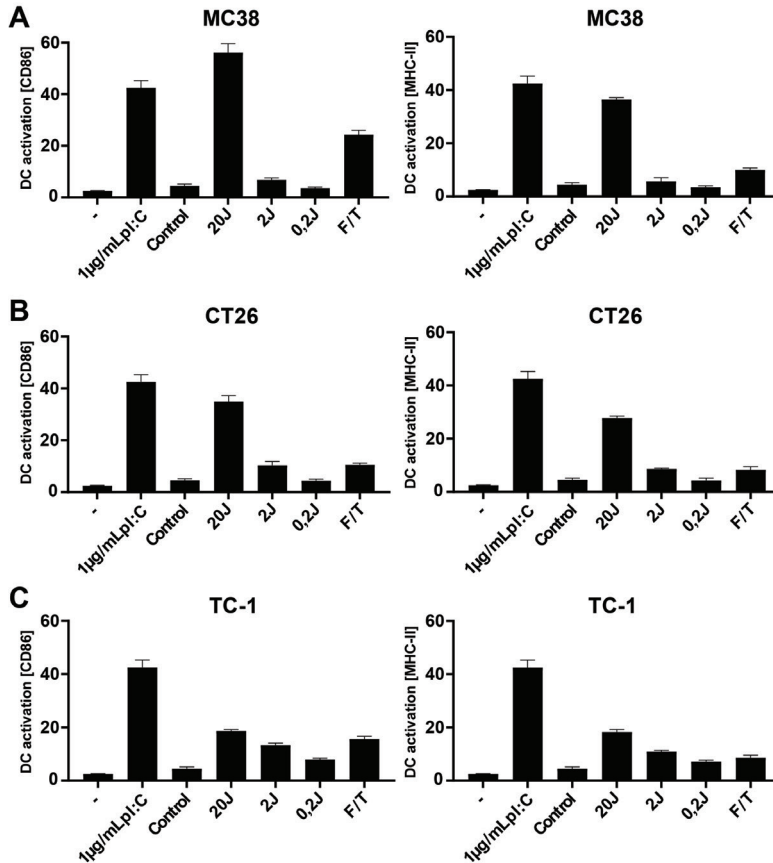


**Figure 2. Immune stimulating effects of PDT-induced cancer cell death on dendritic cells** MC38 (A), CT26 (B) or TC-1 (C) cells were treated by PDT after 4 h of incubation with Radachlorin (2 µM) at 116 mW/cm<sup>2</sup> (0.2 J/cm<sup>2</sup> to 20 J/cm<sup>2</sup>) or three freeze/thaw (F/T) cycles at -20 °C, incubated with murine DCs for 24 h immediately post-treatment. The percentage of CD86hi and MHC-IIhi cells in live DCs (CD11c+DAPI- cells) were compared to untreated DCs (-), to DCs incubated with poly(I:C) (1 µg/mL), and to DCs incubated with untreated MC38 (control). Data from three independent assays shown as a mean ± SD.

### Physicochemical characterization and biological activity of PLGA-PEG (poly(I:C), R848, MIP3 $\alpha$ ) NPs

We previously characterized the PLGA-based NPs that we used in this study for the local, slow and sustained release of poly(I:C), R848 and MIP3 $\alpha$  for size, zeta-potential, TEM morphology, stability, drug release kinetics, uptake, cytotoxicity, DC maturation and chemoattractant capacity.<sup>19</sup> Moreover, we reported in another study on the immunological effects of NP-encapsulated poly(I:C), R848 and of MIP3 $\alpha$ , either combined or separate, in MC38 and TC-1 models.<sup>20</sup> For the current study, we re-analyzed an aliquot of NPs from the pooled production batches. The NPs exhibited an average size of 249.6 nm, as evaluated by dynamic light scattering (Figure S1A and Table 1) and an average zeta-potential ( $\zeta$ ) potential of -21.4mV, as determined using a Zetasizer (Figure S1B and Table 1).

**Table 1. Physicochemical characterization of the NPs**

Sample	Diameter	$\zeta$ Potential	PDI	Loading capacity (% w/w)			
				NIR	poly(I:C)	R848	MIP3 $\alpha$
NP	249.6 $\pm$	-21.4 $\pm$	0.178	62.4 $\pm$	43.6 $\pm$ 8.6	54.2 $\pm$ 8.9	59.3 $\pm$ 7.3
(NIR+ $\alpha$ IC+R848+MIP3 $\alpha$ )-PEG	85.4	4.75		6.9			

Physicochemical characterization of the PLGA-PEG NPs containing immunostimulatory agents. The PLGA NPs were characterized by dynamic light scattering and zeta potential measurements. The size and zeta potential data represent the mean value  $\pm$  SD of 10 readings of one representative batch. The loading capacity of the NIR dye was measured by fluorescence. The loading capacity of poly(I:C), R848 and MIP3 $\alpha$  was determined by RP-HPLC analysis.

To determine whether the biological activity of the encapsulated compounds had been preserved during NP synthesis and storage, we incubated the NPs with DCs in a range of concentrations (0  $\mu$ g/mL to 5  $\mu$ g/mL poly(I:C)). The expression of the maturation markers CD40 and CD86 was evaluated after incubation with the NPs:

both maturation markers were upregulated at levels comparable to that observed for treatment with free (nude) poly(I:C) added at equimolar concentration (Figure S1C), indicating that the encapsulated compounds had retained their biological activity. Further corroborating the immunostimulatory activity of their cargo, the NPs also induced production of IL-12 at similar levels to that observed for the treatment with free poly(I:C) (Figure S1D). The toxicity of the NPs was evaluated by MTS assay, after incubation at concentrations of 0  $\mu\text{g/mL}$  to 200  $\mu\text{g/mL}$ . The NPs did not exhibit any direct cytotoxicity to MC38 (Figure S1E), CT26 (S1F) or TC-1 (Figure S1G) cells, even at the highest concentration tested. Together, these results suggest that the NPs have favorable size and charge distributions, retain the immunostimulatory activity of their cargo and are non-toxic to tumor cells.

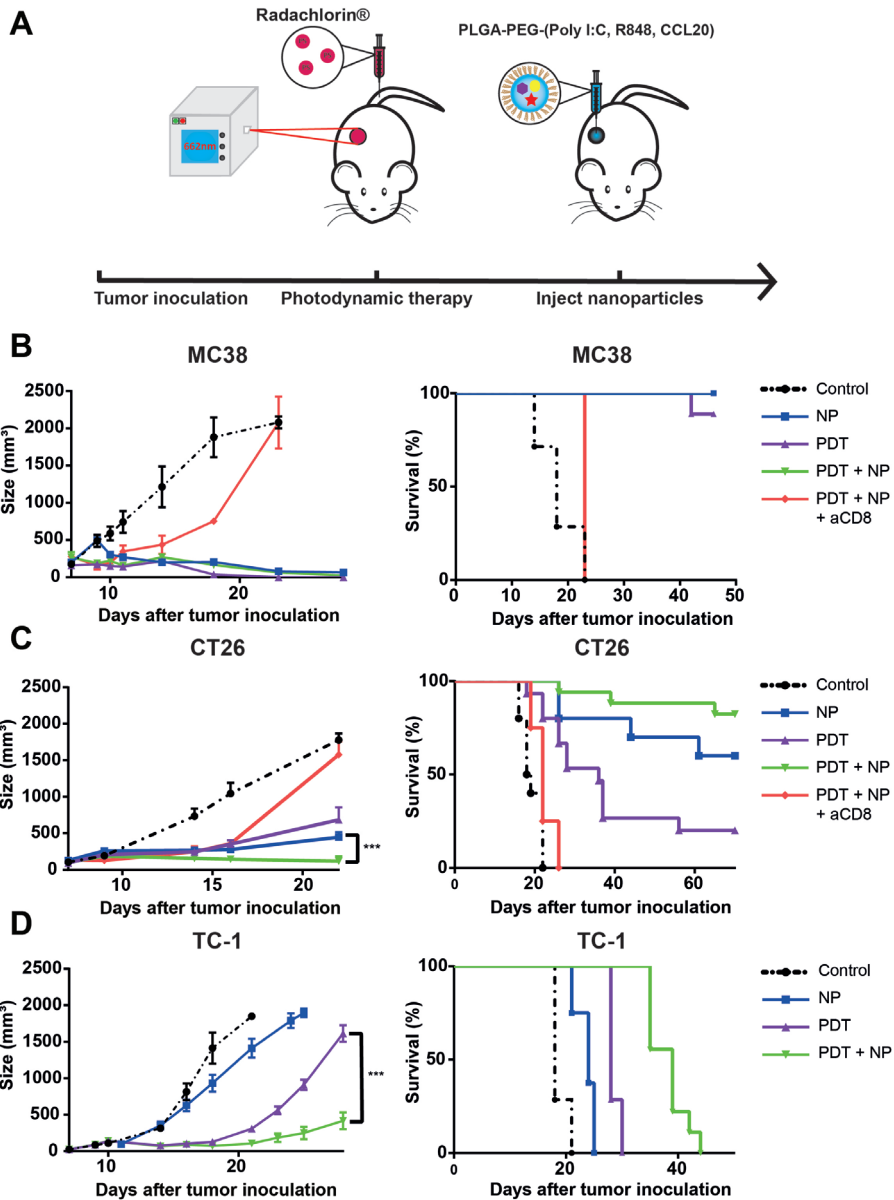
### **The combination of PDT and immunostimulatory NPs strongly inhibits tumor growth and induces anti-tumor immune responses in vivo**

Next, we assessed the tumor-debulking capacity of PDT and the immunostimulatory effects of the NPs separately and combined in mice bearing MC38, CT26 or TC-1 tumors. Thus, mice with established tumors (average volume:  $\sim 125\text{mm}^3$ ) were treated with PDT after a drug-to-light interval of 6 h with 662nm light at a fluence rate of 116  $\text{mW/cm}^2$  for a fluence of 116  $\text{J/cm}^2$  (Figure 3A). The debulking effects of this PDT treatment on the tumor mass were pronounced in all three models, although the duration of the delay in tumor growth varied. Whereas the PDT treatment eradicated all MC38 tumors (Figure 3B), approximately half of the CT26 tumors resumed growth at a slow rate after 10 days (Figure 3C), while all the TC-1 tumors resumed growth after 10 days (Figure 3D). Treatment with intratumoral injections of NPs with the three immunostimulatory agents induced strong anti-tumor responses in the MC38 and CT26 models (Figure 3B and 3C); however, it showed little effect on the TC-1 model (Figure 3D). The combination of PDT and the NPs was as effective as PDT alone and as NPs alone in the MC38 model, as both treatments alone induced near-complete cures (Figure 3B); however, the combination showed superior efficacy to either treatment alone in the CT26 model, as the tumors remained in regression 10 days after co-treatment and induced an enhanced survival rate up to 70 days post treatment (Figure 3C). Furthermore, the combination treatment significantly delayed tumor growth in the TC-1 model, initially similar to PDT alone; however, the TC-1 tumor growth developed at a much slower

rate three weeks after the co-treatment than did those treated with PDT alone (Figure 3D). In cancer immunotherapy, CD8+ T cells are often central in successful tumor clearance. Therefore, we investigated the importance of this population in our setting by administering CD8-depleting antibodies starting one day before PDT treatment, and subsequently administering them periodically for the remainder of the experiment. For mice bearing MC38 or CT26 tumors, pre-treatment depletion of their CD8+ cells (Figures S2A and S2B) led to rapid tumor growth after an initial delay in growth that had directly followed treatment. Together, the above results demonstrate that the combination of PDT and immunostimulatory NPs in tumor-bearing mice induces strong, CD8-dependent anti-tumor immune responses with near-complete survival of MC38, strongly enhanced survival of CT26 and a delay in growth of TC-1 tumors.

**Figure 3. Anti-tumor efficacy of PDT combined with immunostimulatory NPs in mice bearing MC38, CT26 or TC-1 tumors.** >

A). Description of the protocol: immunocompetent mice were inoculated with tumor cells in the right flank ( $n \geq 10$  mice per group). CD8-depleting antibodies were injected 1 day before treatment. Once the tumors had become established ( $\sim 125 \text{ mm}^3$ ), the mice were treated with PDT by administering Radachlorin (20 mg/kg) via a tail-vein injection, followed by irradiation (662 nm) at a drug/light interval of 6 h, at 116 mW/cm<sup>2</sup> for 116 J/cm<sup>2</sup>. The next morning, treatment with NPs was started with an interval of 2 days for a total of four (MC38 and CT26) or two (TC-1) i.t. administrations. B). Tumor-growth and survival curves for C57BL/6J mice bearing MC38 tumors. C). Tumor-growth and survival curves for BALB/c mice bearing CT26 tumors. D). Tumor-growth and survival curves for C57BL/6J mice bearing TC-1 tumors. Statistical analysis was done using the Students t-test, by comparing experimental groups at the indicated timepoints (\* $p < 0.05$ , \*\* $p < 0.01$  and \*\*\* $p < 0.0001$ ).



**The combination of PDT and NP elicits a CD8+ T-cell dependent abscopal effect in mice bearing bilateral MC38 or CT26 tumors**

To study the induction of an abscopal effect by the treatments in the MC38 and CT26 models, we inoculated mice with two tumors, one on each opposing flank, and then treated only one of the tumors using the same protocol as above for mice bearing a single tumor (Figure 4A). For MC38, both the separate and combination treatment induced a delay in tumor growth on the untreated tumors compared to the control (untreated) mice, with the NP treatment and the combination treatment showing the strongest effects (Figure 4B). At 14 days post-inoculation, the combination induced an enhanced tumor growth inhibition on the total tumor burden compared to either treatment alone (Figure 4B), consequently extending the survival compared to PDT alone or control (untreated), but not versus NP alone (Figure S3A). A similar tumor growth delay was observed for the CT26 model (Figure 4C). As in MC38, in CT26 the NP treatment and the combination treatment induced the greatest effect, whereby PDT and the combination treatment induced the strongest effects on the treated tumors (Figure 4C). The combination treatment induced an enhanced tumor growth inhibition on the total tumor burden, when compared to PDT or NP alone (Figure 4C); however, as in MC38, it only provided superior survival relative to the control (untreated) (Figure S3B). Importantly and consistent with our previous results from the single-tumor experiments, CD8+ T cells were essential for greater survival of the treated groups: thus, in mice bearing bilateral MC38 (Figure 4A) or CT26 (Figure 4C) tumors, the benefits of the combination treatment on survival are completely abrogated after depletion of CD8+ T cells. Together, these results show that the combination of PDT and immunostimulatory NPs provides superior systemic anti-tumor immune responses in mice bearing bilateral MC38 or CT26 tumors compared to either treatment alone.



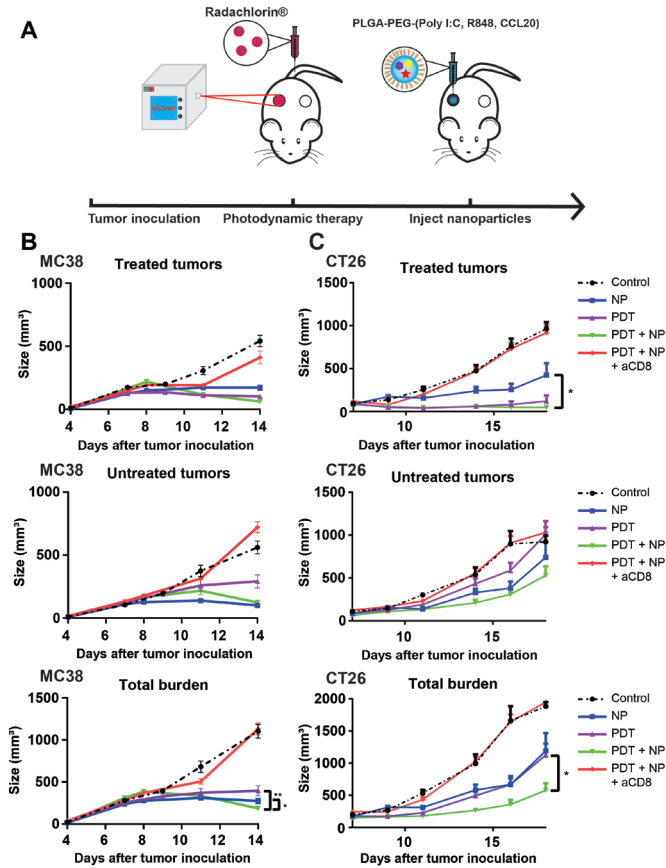


**Figure 4. The combination of PDT and NP induces an abscopal effect in mice bearing bilateral MC38 or CT26 tumors.**

A). Description of the protocol: immunocompetent mice were inoculated with tumor cells in the right and left flanks ( $n \geq 9$  mice per group), and injected with CD8-depleting antibodies 1 day before treatment. Once the tumors had become established ( $\sim 125 \text{ mm}^3$ ), the mice were treated with PDT by administering Radachlorin (20 mg/kg) via a tail-vein injection, followed by irradiation (662 nm) at a drug/light interval of 6 h, at  $116 \text{ mW/cm}^2$  for  $116 \text{ J/cm}^2$ . The next morning, the mice were treated with NPs at an interval of 2 days for a total of four administrations. B). Tumor-growth curves of the treated tumors (upper panel), untreated tumors (middle panel) and total tumor burden (lower panel) for C57BL/6J mice bearing MC38 tumors. C). Tumor-growth curves of the treated tumors (upper panel), untreated tumors (middle panel) and total tumor burden (lower panel) tumors for BALB/c mice bearing CT26 tumors. Statistical analysis was done using the Students t-test, by comparing experimental groups at the indicated timepoints (\* $p < 0.05$ , \*\* $p < 0.01$  and \*\*\* $p < 0.0001$ ).

**The combination of PDT and immunostimulatory NPs provides enhanced tumor-specific immune responses in mice bearing bilateral MC38 or TC-1 tumors**

PDT-induced tumor cell death has been suggested to promote the exposure of previously inaccessible (neo)epitopes, which could then trigger tumor-specific immune responses. Accordingly, PDT could simultaneously function both as a direct tumor-killing modality and as an in-situ vaccination strategy. We reasoned that the immunostimulatory effects of PDT might be enhanced through combination with immunostimulatory NPs, which would serve as a potent adjuvant to facilitate tumor-specific T-cell activity. To explore this hypothesis, we inoculated mice with one tumor on each flank, and then treated only one of the tumors with the combination of PDT and NP, as described above (Figure 4A). The day following the second NP administration, the mice were sacrificed and the organs were subsequently collected, and then processed for further analysis. The presence of tumor-specific T cells among splenocytes obtained from these mice was investigated by stimulation with D1 dendritic cells preloaded with the MC38 neoepitopes Adpgk or Rpl1856, and subsequent analysis of intracellular cytokine production. Interestingly, splenocytes from the mice treated with the combination exhibited greater levels of CD8+ T cells positive for IFN  $\gamma$  and TNF $\alpha$  after incubation with Adpgk- (Figure 5A) or Rpl18- (Figure 5B). These results indicate that the combination can enhance specific anti-tumor immune responses, for which the NPs appear to have a stronger effect than PDT. Furthermore, for the TC-1 model, we measured the HPV-E7-specific CD8+ T cells in blood 8 days post-treatment, and observed a considerably higher number of these cells in the animals that had been treated with the combination than in those treated with either single treatments or in the control (untreated) mice (Figure 6C). Together, these results suggest that the combination enhances MC38-neoepitope-specific CD8+ T cells in the spleen and induces high circulating levels of TC-1-specific CD8+ T cells, and that these effects are superior compared to those observed for either PDT or immunostimulatory NPs alone.

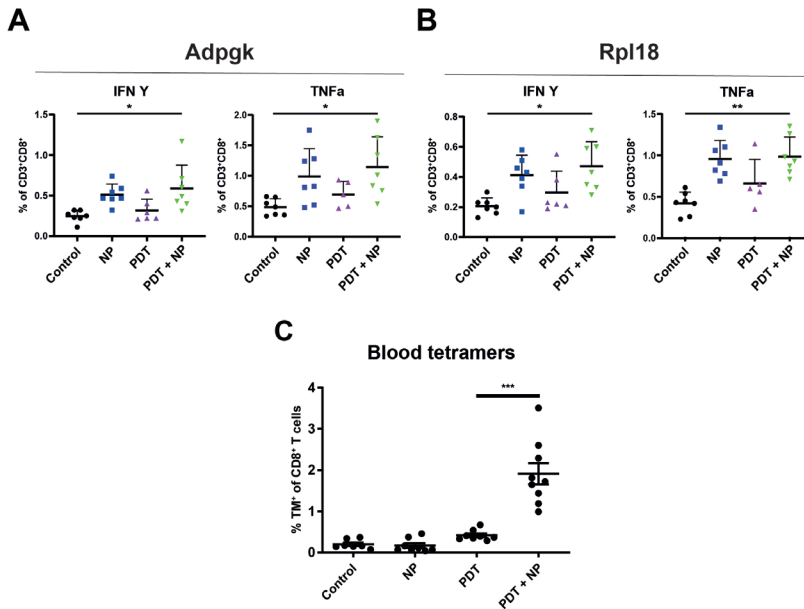


**Figure 5. The combination of PDT and immunostimulatory NPs induces enhanced tumor-specific immune responses**

Description of the protocol: immunocompetent mice were inoculated with tumor cells in the right and left flanks ( $n \geq 5$  mice per group), and then injected with CD8-depleting antibodies 1 day before treatment. Once the tumors had become established ( $\sim 125 \text{ mm}^3$ ), the mice were treated with PDT by administering Radachlorin (20 mg/kg) via a tail-vein injection, followed by irradiation (662 nm) at a drug/light interval of 6 h, at 116 mW/cm<sup>2</sup> for 116 J/cm<sup>2</sup>. The next morning, the mice were treated with NPs at an interval of 2 days for a total of two administrations. The day following the second NP administration, the mice were sacrificed, and their spleens were collected and processed for further analysis. Isolated splenocytes were incubated with D1DCs loaded with the MC38 neoepitopes Adpgk (A) or Rpl18 (B) in the presence of Brefeldin A, after which, the CD8<sup>+</sup> T cells were analyzed for production of intracellular cytokines. C). Evaluation of tumor-antigen-specific CD8<sup>+</sup> T cells in the blood of C57BL/6J mice bearing a single TC-1 tumor at day 8 post-treatment. Tumor-antigen-specific CD8<sup>+</sup> T cells were stained with APC-labeled HPV16 E749-57 (RAHYNIVTF) MHC class I (H-2Db) tetramers and then, detected by flow cytometry. Significance was determined using the Mann-Whitney U test (\* $p < 0.01$ ; \*\* $p < 0.001$ , \*\*\* $P < 0.0001$ ).

### **The combination treatment induces an inflammatory state in colon tumors in mice**

Having demonstrated that the combination of PDT and immunostimulatory NPs reduced the tumor burden of colon cancers in vivo in a CD8+ T cell-dependent manner, we further investigated the anti-tumor immune response elicited by this treatment, by analyzing diverse immune cell populations present in the tumor microenvironment and secondary lymphoid organs. To this end, we inoculated mice with two MC38 or two CT26 tumors, one on each flank, and then treated only one tumor with the combination, as described above (Figure 4A). The day following the second NP administration, the mice were sacrificed, and several of their several organs were collected and prepared for analysis by flow cytometry. In the MC38 model, all treatments induced the infiltration of neutrophils in the treated tumor (Figure 6A), as previously described for PDT.<sup>57</sup> Interestingly, NPs also induced infiltration of neutrophils in the untreated tumor (Figure S4A). The levels of mature (CD86+) and inflammatory (Ly6Chigh) myeloid cells have recently been shown to increase in treatment-responsive tumors but not in relapsed tumors that display resistance to treatment.<sup>58</sup> In line with this, we observed an increase in the levels of mature inflammatory myeloid cells and a decrease in non-inflammatory (Ly6C-) cells in the treated tumor after treatment with the combination compared to all other treatments (Figure 6A). In the untreated tumor, the levels of mature inflammatory monocytes were slightly decreased while the non-inflammatory myeloid cells were increased (Figure S4A). These data indicate the ability of the combination to increase mature inflammatory myeloid cells in the treated tumor, but not in the untreated tumor, which in turn is reflected by the responsiveness to treatment. In the dLN of MC38 tumor-bearing mice, the NP and combination treatments led to increased populations of CD11b+ and DC (Figure S4A). In the spleen, the CD11b+ population was also increased whereas the DC population was decreased after the combination treatment (Figure S4A). In both the dLN and the spleen, the number of CD4+ T cells were decreased whereas the CD8+ T cells were increased (Figure S4A). These results indicate that CD11b+ cells, including antigen-presenting cells, are increased in the dLN of treated mice, while the CD4+/CD8+ T-cell ratio is skewed to favor CD8+ T cells in the dLN and spleen, which corroborate the tumor-specific, CD8+ T-cell responses that we previously found to be essential for efficacy. We observed a similar trend in the CT26 tumor-bearing mice, in which the combination treatment increased the levels of neutrophils in the

treated tumor (Figure 6B) and, to a lesser extent, in the untreated tumor (Figure S4B). Furthermore, the combination increased the number of mature inflammatory myeloid cells and decreased the non-inflammatory cells, in both the treated and the untreated tumors. In the dLN and spleens of the CT26 tumor-bearing mice, the combination induced a strong increase in the number of CD11b+ cells and DCs (Figure S4B). In the dLN, the CD4+/CD8+ T-cell ratio was similar among all treatments (Figure S4B); however, in the spleen, the NP and combination treatments shifted this ratio to CD8+ T cells, albeit marginally (Figure S4B). Together, these data indicate that in tumor-bearing mice, the combination of PDT and immunostimulatory NPs induces inflammation in the tumor microenvironment, coinciding with greater neutrophil infiltration, and higher levels of CD11b+ cells and DCs in secondary lymphoid organs. Moreover, this combination appears to skew the CD4+/CD8+ T-cell ratio in favor of CD8+ T cells, in line with our previous observation that the efficacy of this combination is dependent on tumor-specific CD8+ T cells.

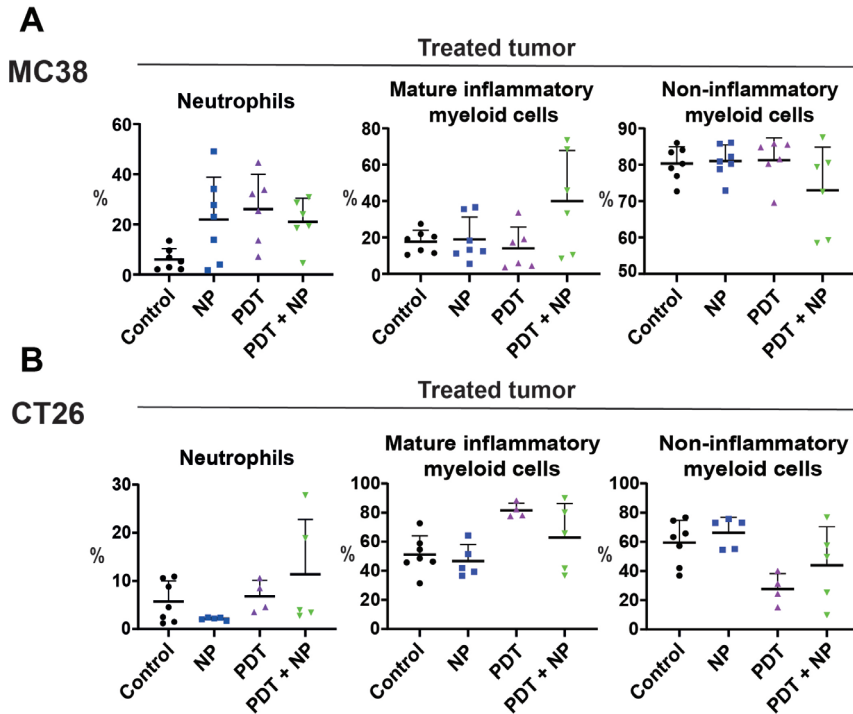


**Figure 6. The combination of PDT and immunostimulatory NPs induces an inflammatory state in the tumor microenvironment**

Immunocompetent mice were inoculated with bilateral MC38 or CT26 tumors ( $n \geq 5$  mice), in the right and left flanks ( $n \geq 5$  mice per group). Once the tumors had become established ( $\sim 125 \text{ mm}^3$ ), the mice were treated with PDT by administering Radachlorin (20 mg/kg) via a tail-vein injection, followed by irradiation (662 nm) at a drug/light interval of 6 h, at 116 mW/cm<sup>2</sup> for 116 J/cm<sup>2</sup>. The next morning, the mice were treated with the immunostimulatory NPs at an interval of 2 days for a total of two administrations. The day following the second NP administration, the mice were sacrificed, after which the tumors were collected, processed, and stained for analysis by flow cytometry. Cell populations are shown in percentages for mice bearing bilateral MC38 (A) or CT26 (B) tumors. Gating was performed in FlowJo and included only living (7AAD<sup>-</sup>) CD45.2<sup>+</sup> cells. Populations were further gated to include neutrophils (CD11b+Ly6G<sup>+</sup>), mature inflammatory myeloid cells (CD11b+CD86+Ly6Chi) and non-inflammatory myeloid cells (CD11b+Ly6Clow).

## DISCUSSION

The tumor debulking effects of photodynamic therapy are often insufficient to induce complete and lasting therapeutic efficacy. However, recent studies that exploit the ability of PDT to initiate immune responses in combination with immunotherapy show great promise.<sup>59–61</sup> In the present study, we combined PDT with immunostimulatory NPs loaded with poly(I:C), R848 and MIP3. We synthesized these biodegradable PLGA NPs, loaded them with immunostimulatory agents, and characterized them, finding favorable physicochemical properties, a lack of inherent cytotoxicity, and retention of biological activities of the encapsulated immunostimulatory agents. Consistent with literature reports on the immunostimulatory activities of PDT on myeloid cells,<sup>4,14,62–66</sup> in our studies, PDT-induced tumor cell death led to the upregulation of dendritic cell maturation markers *in vitro*.

Expanding on our *in vitro* findings, we explored our therapeutic combination in mice bearing a single tumor. All treatments fully eradicated the MC38 tumors, extended the survival of MC38-tumor-bearing mice and were highly effective in delaying the growth of CT26 tumors, with the combination being significantly more effective against CT26 than either treatment alone. TC-1 tumors were less responsive to all treatments, with the combination strongly inhibiting tumor growth compared to either treatment alone in addition to the control, but not inducing significant gains in survival. Our therapeutic combination performs well compared to similar strategies that use PDT and immunostimulatory agents. It shows an efficacy equal to or better than PDT combined with photo-thermal therapy (PTT) and TLR9-agonist CpG,<sup>65</sup> PDT combined with CpG and a hypoxia inducible factor (HIF) inhibitor,<sup>64</sup> CD276-targeted PDT combined with immune checkpoint inhibitors,<sup>67</sup> and PDT with magnetic hyperthermia and immune checkpoint inhibitors,<sup>68</sup> that all show a tumor growth inhibition at early timepoints after treatment, but do not show long term survival (up to 50 days). The differences in response to PDT-treatment *in vivo* among the tumor models is further reflected by our observation of upregulation of DC maturation markers in the PDT-treated tumor cells *in vitro*, whereby MC38 cells exhibited the greatest upregulation of maturation markers, followed by CT26, while TC-1 cells showed only a slight upregulation. These results suggest a link between the propensity of dying PDT-treated tumor cells to upregulate DC maturation markers and the anti-tumor efficacy of PDT.

In the *in vivo* experiments exploring bilateral tumors, the PDT-nanoparticle combination most effectively reduced the total tumor burden compared to either treatment alone. The efficacy of our combination is comparable to a study combining PDT with PTT,<sup>69</sup> and a study combining PDT with PTT and an indoleamine 2,3-dioxygenase inhibitor.<sup>66</sup> However, studies that combine PDT with immune checkpoint inhibitors often show improved results, mostly on the untreated (distal) tumors.<sup>59–61</sup> Importantly, in both the unilateral and the bilateral tumor models, pre-treatment depletion of CD8<sup>+</sup> cells abrogated the efficacy of the combination treatment. This observation is in line with previously published results,<sup>17</sup> and confirms the importance of CD8<sup>+</sup> cells to the benefits of this treatment. Furthermore, the ability of the treatment to induce tumor-specific immune responses was investigated by stimulating the splenocytes of treated, tumor-bearing mice *ex vivo* with the MC38 neoepitopes Adpgk and Rpl18. This revealed an expansion of these tumor-specific CD8<sup>+</sup> T cells producing the cytokines IFN- $\gamma$  and TNF- $\alpha$  in the treated mice compared to control (untreated) mice, in which the NPs played the largest role (Fig 5). Additionally, the combination induced significantly higher levels of tumor specific CD8<sup>+</sup> T cells to TC-1 tumors compared to either treatment alone. These observations corroborate literature that describes PDT as a modality that facilitates the exposure of previously inaccessible tumor epitopes to induce and/or enhance tumor-specific immune responses. This ability of PDT to function as an *in situ* vaccination modality has often been hypothesized, however, it has to our knowledge only been shown for exogenous antigens (ovalbumin),<sup>70</sup> and not for cancer neoepitopes (Rpl18 and Adpgk). Although high levels of circulating tumor-specific T cells to TC-1 (HPV16 E7) have been shown after combining PDT with specific vaccination using synthetic long peptides for TC-1,<sup>54</sup> we report strongly elevated blood levels of such T cells after combination with nonspecific immunostimulatory NPs, thereby providing proof to the *in situ* vaccination ability of PDT when it is combined with a strong adjuvant.

Finally, we evaluated the immunological composition of the tumor microenvironment after treatment of tumor-bearing mice. Our data show that the combination treatment alters the immunosuppressive tumor microenvironment into a more proinflammatory one, by increasing the presence of mature inflammatory myeloid cells and decreasing the non-inflammatory monocytes in the treated tumor. This observation is in line with other studies combining PDT and immunotherapy that also show an increased inflammatory state in the tumor after treatment.<sup>61,64–66,68,71</sup> Immune



checkpoint inhibitors have been shown to enhance the infiltration of CD8+ T cells in the untreated (distal) tumor, whereas PDT alone did not.<sup>59,60</sup> Our observations that local treatment with immune stimulating nanoparticles combined with PDT induces a potent tumor-specific CD8+ T cell response, provides a rationale for further enhancing abscopal effects by systemic treatment with immune checkpoint inhibitors. Clinical efficacy of immune checkpoint inhibitors is often hampered by the immunosuppressive state present in the tumor microenvironment,<sup>72</sup> which we may repolarize to more proinflammatory after our local nanoparticle treatment. In practice, also intravenous injection may result in accumulation of the immunostimulatory NP in untreated (distal) tumors. Therefore, a protocol that combines PDT with intravenously administered PLGA-PEG(poly(I:C), R848, MIP-3 $\alpha$ ) and immune checkpoint inhibitors could be of clinical advantage. Our future studies will explore the potential of such protocols in the treatment of primary and metastatic tumors.

Together, our results show that the combination of PDT and immunostimulatory NPs functions as an in situ vaccination strategy that induces strong, CD8+ T cell-dependent, anti-tumor immune responses and elicits abscopal effects. As the benefits of combining classical ablation and immune therapies treatments are increasingly appreciated,<sup>73-75</sup> the potential of our PDT-nanoparticle combination that we have presented in this study may contribute to more effective treatment protocols for solid tumors.

## REFERENCES

1. van Straten D, Mashayekhi V, de Bruijn HS, Oliveira S, Robinson DJ. Oncologic photodynamic therapy: Basic principles, current clinical status and future directions. *Cancers (Basel)*. 2017;9(2). doi:10.3390/cancers9020019
2. Beltrán Hernández I, Yu Y, Ossendorp F, Korbely M, Oliveira S. Preclinical and Clinical Evidence of Immune Responses Triggered in Oncologic Photodynamic Therapy: Clinical Recommendations. *J Clin Med*. 2020;9(2):333. doi:10.3390/jcm9020333
3. Nath S, Obaid G, Hasan T. The Course of Immune Stimulation by Photodynamic Therapy: Bridging Fundamentals of Photochemically Induced Immunogenic Cell Death to the Enrichment of T-Cell Repertoire. *Photochem Photobiol*. 2019;95(6):1288-1305. doi:10.1111/php.13173
4. Li W, Yang J, Luo L, et al. Targeting photodynamic and photothermal therapy to the endoplasmic reticulum enhances immunogenic cancer cell death. *Nat Commun*. 2019;10(1):3349. doi:10.1038/s41467-019-11269-8
5. Scaffidi P, Misteli T, Bianchi ME. Release of chromatin protein HMGB1 by necrotic cells triggers inflammation. *Nature*. 2002;418(6894):191-195. doi:10.1038/nature00858
6. Obeid M, Tesniere A, Ghiringhelli F, et al. Calreticulin exposure dictates the immunogenicity of cancer cell death. *Nat Med*. 2007;13(1):54-61. doi:10.1038/nm1523
7. Obeid M, Tesniere A, Panaretakis T, et al. Ecto-calreticulin in immunogenic chemotherapy. *Immunol Rev*. 2007;220(1):22-34. doi:10.1111/j.1600-065X.2007.00567.x
8. Korbely M, Sun J, Cecic I. Photodynamic Therapy – Induced Cell Surface Expression and Release of Heat Shock Proteins : Relevance for Tumor Response. *Cancer Res*. 2005;65(3):1018-1026.
9. Krysko D V, Garg AD, Kaczmarek A, Krysko O, Agostinis P, Vandenabeele P. Immunogenic cell death and DAMPs in cancer therapy. *Nat Rev Cancer*. 2012;12. doi:10.1038/nrc3380
10. Panzarini E, Inguscio V, Fimia GM, Dini L. Rose Bengal Acetate PhotoDynamic Therapy (RBAc-PDT) Induces Exposure and Release of Damage-Associated Molecular Patterns (DAMPs) in Human HeLa Cells. 2014. doi:10.1371/journal.pone.0105778
11. Vabulas RM, Wagner H, Schild H. Heat shock proteins as ligands of Toll-like receptors. *Curr Top Microbiol Immunol*. 2002;270:169-184. doi:10.1007/978-3-642-59430-4\_11

12. Jessica B. Flechtner, Kenya Prince Cohane, Sunil Mehta, Paul Slusarewicz, Alexis Kays Leonard BHB, Andjelic DLL and S. High-Affinity Interactions between Peptides and Heat Shock Protein 70 Augment CD8+ T Lymphocyte Immune Responses. *J Immunol.* 2006;(177):1017-1027. doi:10.4049/jimmunol.177.2.1017
13. Salimu J, Spary LK, Al-Taei S, et al. Cross-Presentation of the Oncofetal Tumor Antigen 5T4 from Irradiated Prostate Cancer Cells--A Key Role for Heat-Shock Protein 70 and Receptor CD91. *Cancer Immunol Res.* 2015;3(6):678-688. doi:10.1158/2326-6066.CIR-14-0079
14. Garg AD, Krysko D V, Verfaillie T, et al. A novel pathway combining calreticulin exposure and ATP secretion in immunogenic cancer cell death. *EMBO J.* 2012;31(5):1062-1079. doi:10.1038/emboj.2011.497
15. Elliott MR, Chekeni FB, Trampont PC, et al. Nucleotides released by apoptotic cells act as a find-me signal to promote phagocytic clearance. *Nature.* 2009;461(7261):282-286. doi:10.1038/nature08296
16. Ghiringhelli F, Apetoh L, Tesniere A, et al. Activation of the NLRP3 inflammasome in dendritic cells induces IL-1 $\beta$ -dependent adaptive immunity against tumors. *Nat Med.* 2009;15(10):1170-1178. doi:10.1038/nm.2028
17. Kleinovink JW, Fransen MF, Löwik CW, Ossendorp F. Photodynamic-Immune Checkpoint Therapy Eradicates Local and Distant Tumors by CD8(+) T Cells. *Cancer Immunol Res.* 2017;5(10):832-838. doi:10.1158/2326-6066.CIR-17-0055
18. Maria Theopheil Van Nuffel A, Garg AD, Leuven K, et al. Immunomodulation of the Tumor Microenvironment: Turn Foe Into Friend. *Front Immunol* | www.frontiersin.org. 2018;9:2909. doi:10.3389/fimmu.2018.02909
19. Da Silva CG, Camps MGM, Li TMWY, Zerrillo L, Löwik CW, Cruz LJ. Effective chemoimmunotherapy by co-delivery of doxorubicin and immune adjuvants in biodegradable nanoparticles. *Theranostics.* 2019;9:22. doi:10.7150/thno.34429
20. Da Silva CG, Camps MGM, Li TMWY, Chan AB, Ossendorp F, Cruz LJ. Co-delivery of immunomodulators in biodegradable nanoparticles improves therapeutic efficacy of cancer vaccines. *Biomaterials.* 2019;220. doi:10.1016/j.biomaterials.2019.119417
21. Smith M, García-Martínez E, Pitter MR, et al. Trial Watch: Toll-like receptor agonists in cancer immunotherapy. 2018. doi:10.1080/2162402X.2018.1526250
22. Cheng Y-S, Xu F. Anticancer function of polyinosinic-polycytidylic acid. *Cancer Biol Ther* 1219 *Cancer Biol Ther.* 2010;10:1219-1223. doi:10.4161/cbt.10.12.13450

23. Shime H, Matsumoto M, Seya T. Double-stranded RNA promotes CTL-independent tumor cytotoxicity mediated by CD11b+Ly6G+ intratumor myeloid cells through the TICAM-1 signaling pathway. *Cell Death Differ.* 2017;24:385-396. doi:10.1038/cdd.2016.131
24. Shime H, Matsumoto M, Oshiumi H, et al. Toll-like receptor 3 signaling converts tumor-supporting myeloid cells to tumoricidal effectors. doi:10.1073/pnas.1113099109
25. Takemura R, Takaki H, Okada S, et al. PolyI:C-Induced, TLR3/RIP3-Dependent Necroptosis Backs Up Immune Effector-Mediated Tumor Elimination In Vivo. *Cancer Immunol Res.* 2015;3(8):902-914. doi:10.1158/2326-6066.CIR-14-0219
26. Salmon H, Idoyaga J, Rahman A, et al. Expansion and activation of CD103 + dendritic cell progenitors at the tumor site enhances tumor responses to therapeutic PD-L1 and BRAF inhibition HHS Public Access. *Immunity.* 2016;44(4):924-938. doi:10.1016/j.immuni.2016.03.012
27. Friboulet L, Pioche-Durieu C, Rodriguez S, et al. Recurrent Overexpression of c-IAP2 in EBV-Associated Nasopharyngeal Carcinomas: Critical Role in Resistance to Toll-like Receptor 3-Mediated Apoptosis 1,2. 2008;10:1183. doi:10.1593/neo.08590
28. Paone A, Starace D, Galli R, et al. Toll-like receptor 3 triggers apoptosis of human prostate cancer cells through a PKC- $\alpha$ -dependent mechanism. *Carcinogenesis.* 2008;29(7):1334-1342. doi:10.1093/carcin/bgn149
29. Weber A, Kirejczyk Z, Besch R, Potthoff S, Leverkus M, Häcker G. Proapoptotic signalling through Toll-like receptor-3 involves TRIF-dependent activation of caspase-8 and is under the control of inhibitor of apoptosis proteins in melanoma cells. 2010. doi:10.1038/cdd.2009.190
30. Estornes Y, Toscano F, Virard F, et al. dsRNA induces apoptosis through an atypical death complex associating TLR3 to caspase-8. *Cell Death Differ.* 2012;19:1482-1494. doi:10.1038/cdd.2012.22
31. Zhou Z, Sun L. Immune effects of R848: Evidences that suggest an essential role of TLR7/8-induced, Myd88- and NF- $\kappa$ B-dependent signaling in the antiviral immunity of Japanese flounder (*Paralichthys olivaceus*). *Dev Comp Immunol.* 2015;49(1):113-120. doi:10.1016/j.dci.2014.11.018
32. YIN T, HE S, WANG Y. Toll-like receptor 7/8 agonist, R848, exhibits antitumoral effects in a breast cancer model. *Mol Med Rep.* 2015;12(3):3515-3520. doi:10.3892/mmr.2015.3885

33. Spinetti T, Spagnuolo L, Mottas I, et al. TLR7-based cancer immunotherapy decreases intratumoral myeloid-derived suppressor cells and blocks their immunosuppressive function. *Oncoimmunology*. 2016;5(11):e1230578. doi:10.1080/2162402X.2016.1230578
34. Rodell CB, Arlauckas SP, Cuccarese MF, et al. TLR7/8-agonist-loaded nanoparticles promote the polarization of tumour-associated macrophages to enhance cancer immunotherapy. *Nat Biomed Eng*. 2018;2:578-588. <http://www.ncbi.nlm.nih.gov/pubmed/30345161>. Accessed April 30, 2019.
35. Ye J, Ma C, Hsueh EC, et al. TLR8 signaling enhances tumor immunity by preventing tumor-induced T-cell senescence. doi:10.15252/emmm.201403918
36. Hieshima K, Imai T, Opdenakker G, et al. Molecular cloning of a novel human CC chemokine liver and activation-regulated chemokine (LARC) expressed in liver. Chemotactic activity for lymphocytes and gene localization on chromosome 2. *J Biol Chem*. 1997;272(9):5846-5853. doi:10.1074/jbc.272.9.5846
37. Mclean MH, Murray GI, Stewart KN, et al. The Inflammatory Microenvironment in Colorectal Neoplasia. doi:10.1371/journal.pone.0015366
38. Frick VO, Rubie C, Keilholz U, Ghadjar P. Chemokine/chemokine receptor pair CCL20/CCR6 in human colorectal malignancy: An overview. *World J Gastroenterol*. 2016;22(2):833-841. doi:10.3748/wjg.v22.i2.833
39. Kwong B, Liu H, Irvine DJ. Induction of potent anti-tumor responses while eliminating systemic side effects via liposome-anchored combinatorial immunotherapy. *Biomaterials*. 2011;32(22):5134-5147. doi:10.1016/j.biomaterials.2011.03.067
40. Da Silva CG, Rueda F, Löwik CW, Ossendorp F, Cruz LJ. Combinatorial prospects of nano-targeted chemoimmunotherapy. *Biomaterials*. 2016;83:308-320. doi:10.1016/J.BIOMATERIALS.2016.01.006
41. Makadia HK, Siegel SJ. Poly Lactic-co-Glycolic Acid (PLGA) as Biodegradable Controlled Drug Delivery Carrier. *Polymers (Basel)*. 2011;3(3):1377-1397. doi:10.3390/polym3031377
42. LaVan DA, McGuire T, Langer R. Small-scale systems for in vivo drug delivery. *Nat Biotechnol*. 2003;21(10):1184-1191. doi:10.1038/nbt876
43. Huis in 't Veld R V., Ritsma L, Kleinovink JW, Que I, Ossendorp F, Cruz LJ. Photodynamic cancer therapy enhances accumulation of nanoparticles in tumor-associated myeloid cells. *J Control Release*. 2020;320:19-31. doi:10.1016/j.jconrel.2019.12.052



44. Barr H, Krasner N, Boulos PB, Chatlani P, Bown SG. Photodynamic therapy for colorectal cancer: A quantitative pilot study. *Br J Surg.* 1990;77(1):93-96. doi:10.1002/bjs.1800770132
45. McCaughan JS, Hawley PC, Bethel BH, Walker J. Photodynamic therapy of endobronchial malignancies. *Cancer.* 1988;62(4):691-701. doi:10.1002/1097-0142(19880815)62:4<691::AID-CNCR2820620408>3.0.CO;2-I
46. Cruz LJ, Tacke PJ, Fokkink R, et al. Targeted PLGA nano- but not microparticles specifically deliver antigen to human dendritic cells via DC-SIGN in vitro. *J Control Release.* 2010;144(2):118-126. doi: 10.1016/j.jconrel.2010.02.013
47. Cruz LJ, Tacke PJ, Bonetto F, et al. Multimodal Imaging of Nanovaccine Carriers Targeted to Human Dendritic Cells. *Mol Pharm.* 2011;8(2): 520-531. doi:10.1021/mp100356k
48. Cruz LJ, Tacke PJ, Rueda F, Domingo JC, Albericio F, Figdor CG. Targeting Nanoparticles to Dendritic Cells for Immunotherapy. *Methods Enzymol.* 2012;509:143-163. doi:10.1016/B978-0-12-391858-1.00008-3
49. Cruz LJ, Stammes MA, Que I, et al. Effect of PLGA NP size on efficiency to target traumatic brain injury. *J Control Release.* 2016;223:31-41. doi:10.1016/J.JCONREL.2015.12.029
50. Tel J, Lambeck AJA, Cruz LJ, Tacke PJ, de Vries IJM, Figdor CG. Human Plasmacytoid Dendritic Cells Phagocytose, Process, and Present Exogenous Particulate Antigen. *J Immunol.* 2010;184(8):4276-4283. doi:10.4049/jimmunol.0903286
51. Lin K-Y, Guarnieri FG, Staveley-O'Carroll KF, et al. Treatment of Established Tumors with a Novel Vaccine That Enhances Major Histocompatibility Class II Presentation of Tumor Antigen. *Cancer Res.* 1996;56(1).
52. Ossendorp F, Fu N, Camps M, et al. Differential Expression Regulation of the  $\alpha$  and  $\beta$  Subunits of the PA28 Proteasome Activator in Mature Dendritic Cells. *J Immunol.* 2005;174(12):7815-7822. doi:10.4049/jimmunol.174.12.7815
53. Zom GG, Khan S, Britten CM, et al. Efficient induction of antitumor immunity by synthetic toll-like receptor ligand-peptide conjugates. *Cancer Immunol Res.* 2014;2(8):756-764. doi:10.1158/2326-6066.CIR-13-0223
54. Kleinovink JW, van Driel PB, Snoeks TJA, et al. Combination of photodynamic therapy and specific immunotherapy efficiently eradicates established tumors. *Clin Cancer Res.* 2015. doi:10.1158/1078-0432.CCR-15-0515

55. Yadav M, Jhunjhunwala S, Phung QT, et al. Predicting immunogenic tumour mutations by combining mass spectrometry and exome sequencing. *Nature*. 2014;515(7528):572-576. doi:10.1038/nature14001
56. Hos BJ, Camps MGM, Bulk J van den, et al. Identification of a neo-epitope dominating endogenous CD8 T cell responses to MC-38 colorectal cancer. *Oncoimmunology*. 2020;9(1). doi:10.1080/2162402X.2019.1673125
57. Cecic I, Parkins CS, Korbek M. Induction of Systemic Neutrophil Response in Mice by Photodynamic Therapy of Solid Tumors¶. *Photochem Photobiol*. 2001;74(5):712. doi:10.1562/0031-8655(2001)074<0712:iosnri>2.0.co;2
58. Beyranvand Nejad E, Labrie C, Abdulrahman Z, et al. Lack of myeloid cell infiltration as an acquired resistance strategy to immunotherapy. *J Immunother Cancer*. 2020;8(2):1326. doi:10.1136/jitc-2020-001326
59. Xu J, Xu L, Wang C, et al. Near-Infrared-Triggered Photodynamic Therapy with Multitasking Upconversion Nanoparticles in Combination with Checkpoint Blockade for Immunotherapy of Colorectal Cancer. doi:10.1021/acsnano.7b00715
60. He C, Duan X, Guo N, et al. Core-shell nanoscale coordination polymers combine chemotherapy and photodynamic therapy to potentiate checkpoint blockade cancer immunotherapy. *Nat Commun*. 2016;7(1):12499. doi:10.1038/ncomms12499
61. Zhou Y, Liu S, Hu C, Cai L, Pang M. A covalent organic framework as a nanocarrier for synergistic phototherapy and immunotherapy †. *J Mater Chem B*. 2020;8:5451. doi:10.1039/d0tb00679c
62. Ji J, Fan Z, Zhou F, et al. Improvement of DC vaccine with ALA-PDT induced immunogenic apoptotic cells for skin squamous cell carcinoma. 2015;6(19):17135-17146.
63. Jung N, Jung H, Kang M, et al. Photodynamic therapy-mediated DC immunotherapy is highly effective for the inhibition of established solid tumors. 2012;324:58-65.
64. Cai Z, Xin F, Wei Z, et al. Photodynamic Therapy Combined with Antihypoxic Signaling and CpG Adjuvant as an In Situ Tumor Vaccine Based on Metal–Organic Framework Nanoparticles to Boost Cancer Immunotherapy. *Adv Healthc Mater*. 2020;9(1):1900996. doi:10.1002/adhm.201900996
65. Chen L, Zhou L, Wang C, et al. Tumor-Targeted Drug and CpG Delivery System for Phototherapy and Docetaxel-Enhanced Immunotherapy with Polarization toward M1-Type Macrophages on Triple Negative Breast Cancers. *Adv Mater*. 2019;31(52):1904997. doi:10.1002/adma.201904997

66. Yang W, Zhang F, Deng H, et al. Smart Nanovesicle-Mediated Immunogenic Cell Death through Tumor Microenvironment Modulation for Effective Photodynamic Immunotherapy. *ACS Nano*. 2020;14(1):620-631. doi:10.1021/acsnano.9b07212
67. Bao R, Wang Y, Lai J, et al. Enhancing Anti-PD-1/PD-L1 Immune Checkpoint Inhibitory Cancer Therapy by CD276-Targeted Photodynamic Ablation of Tumor Cells and Tumor Vasculature. *Mol Pharm*. November 2018;acs.molpharmaceut.8b00997. doi:10.1021/acs.molpharmaceut.8b00997
68. Wang Z, Zhang F, Shao D, et al. Janus Nanobullets Combine Photodynamic Therapy and Magnetic Hyperthermia to Potentiate Synergetic Anti-Metastatic Immunotherapy. *Adv Sci*. 2019;6(22). doi:10.1002/advs.201901690
69. Yang J, Hou M, Sun W, et al. Sequential PDT and PTT Using Dual-Modal Single-Walled Carbon Nanohorns Synergistically Promote Systemic Immune Responses against Tumor Metastasis and Relapse. *Adv Sci*. 2020;7(16). doi:10.1002/advs.202001088
70. Yang W, Zhu G, Wang S, et al. In Situ Dendritic Cell Vaccine for Effective Cancer Immunotherapy. *ACS Nano*. 2019;13(3):3083-3094. doi:10.1021/acsnano.8b08346
71. Wu X, Yang H, Chen X, et al. Nano-herb medicine and PDT induced synergistic immunotherapy for colon cancer treatment. *Biomaterials*. 2021;269:120654. doi:10.1016/j.biomaterials.2021.120654
72. Jenkins RW, Barbie DA, Flaherty KT. Mechanisms of resistance to immune checkpoint inhibitors. *Br J Cancer*. 2018;118(1):9-16. doi:10.1038/bjc.2017.434
73. Lopez JS, Banerji U. Combine and conquer: challenges for targeted therapy combinations in early phase trials. *Nat Rev Clin Oncol*. 2017;14(1):57-66. doi:10.1038/nrclinonc.2016.96
74. Mahoney KM, Rennert PD, Freeman GJ. Combination cancer immunotherapy and new immunomodulatory targets. *Nat Rev Drug Discov*. 2015;14(8):561-584. doi:10.1038/nrd4591
75. Gotwals P, Cameron S, Cipolletta D, et al. Prospects for combining targeted and conventional cancer therapy with immunotherapy. *Nat Rev Cancer*. 2017;17(5):286-301. doi:10.1038/nrc.2017.17



# COMBINING PHOTODYNAMIC THERAPY WITH IMMUNOSTIMULATORY NANOPARTICLES ELICITS EFFECTIVE ANTI-TUMOR IMMUNE RESPONSES IN PRECLINICAL MURINE MODELS

Huis in 't Veld, Ruben V.; da Silva, Candido G.; Jager, Martine J.; Cruz, Luis J.; Ossendorp, Ferry.

## Supplementary Figures

**Figure S1.** Synthesis and characterization of PLGA-PEG(poly(I:C), R848, MIP-3 $\alpha$ )

**Figure S2.** Blood levels of CD8+ cells after treatment with CD8-depleting antibodies

**Figure S3.** Survival curves of mice bearing bilateral MC38 or CT26 tumors

**Figure S4.** Analysis of the tumor microenvironment after treatment

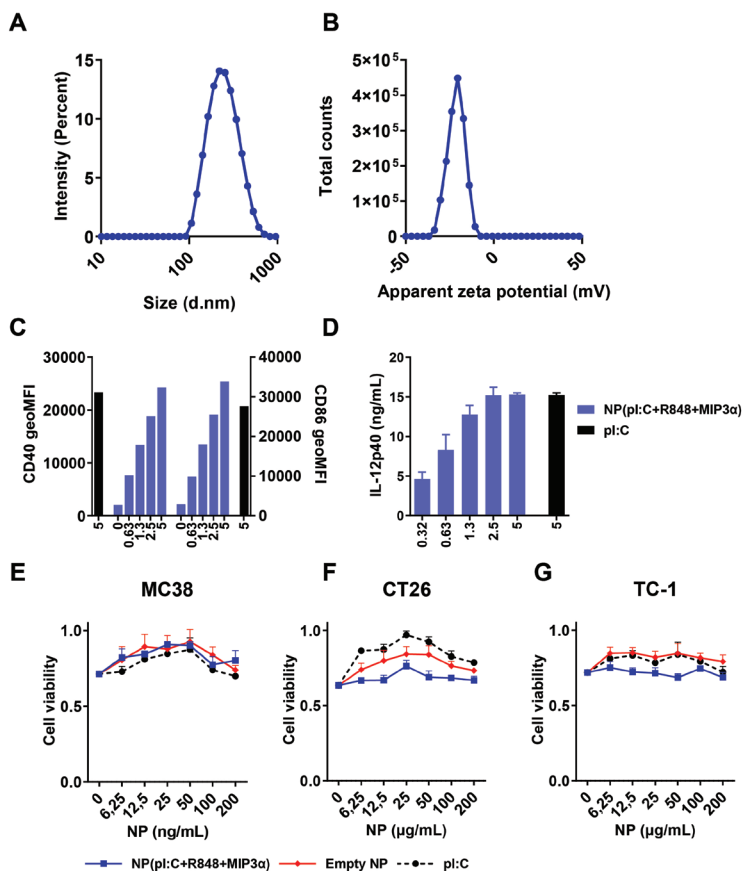


**Figure S1. Synthesis and characterization of PLGA-PEG(poly(I:C), R848, MIP-3α)**

A). Size distribution and B). distribution of the  $\zeta$ -potential of the PLGA-PEG-NPs used in this study. C). Maturation of D1DCs after 24 h of incubation with the NP added to correspond to concentrations of 0-5  $\mu\text{g/mL}$  poly(I:C) (light blue bars) compared to 5  $\mu\text{g/mL}$  pure poly(I:C) (black bars), shown as expression of CD40 (left bars) and CD86 (right bars). D). IL-12P40 expression by D1DCs after 24 h of incubation with the NP at indicated concentration (light blue bars) compared to 5  $\mu\text{g/mL}$  pure poly(I:C) (black bars). E-G). Toxicity of the NPs to MC38, CT26 and TC-1 after 72 h of incubation at indicated concentrations compared to free poly(I:C) and empty NPs incubated at equal concentrations, determined using the MTS assay.

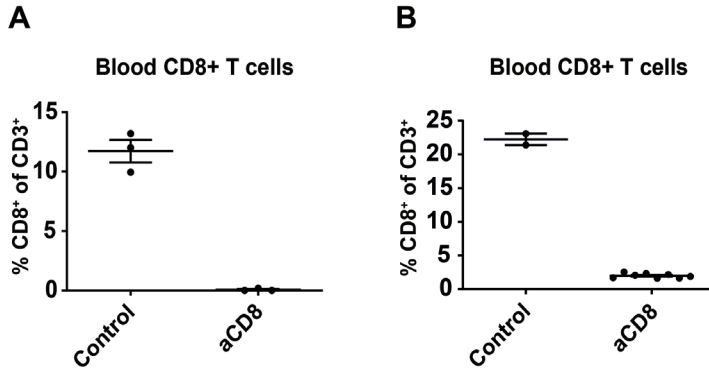
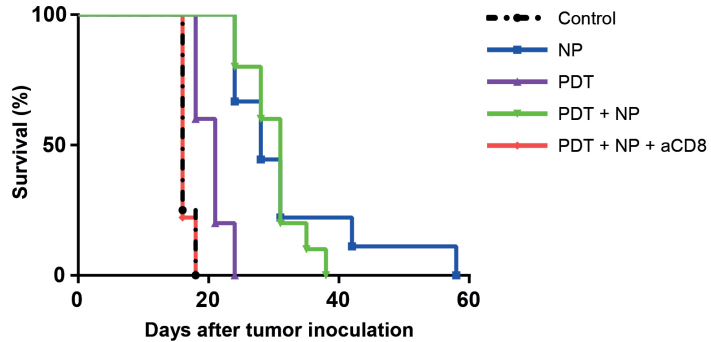


**Figure S2. Blood levels of CD8+ cells after treatment with CD8-depleting antibodies**

Levels of CD8+ cells in blood of mice bearing a single MC38 (A) or CT26 (B) tumor in control (untreated) mice and mice that received CD8-depleting antibodies (aCD8), measured 1 day after administering CD8-depleting antibodies.

## A MC38



## B CT26

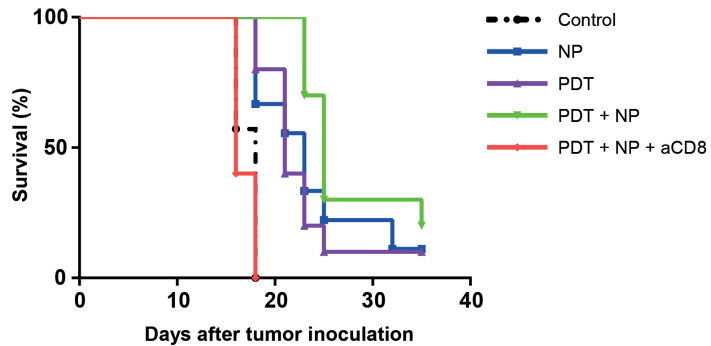
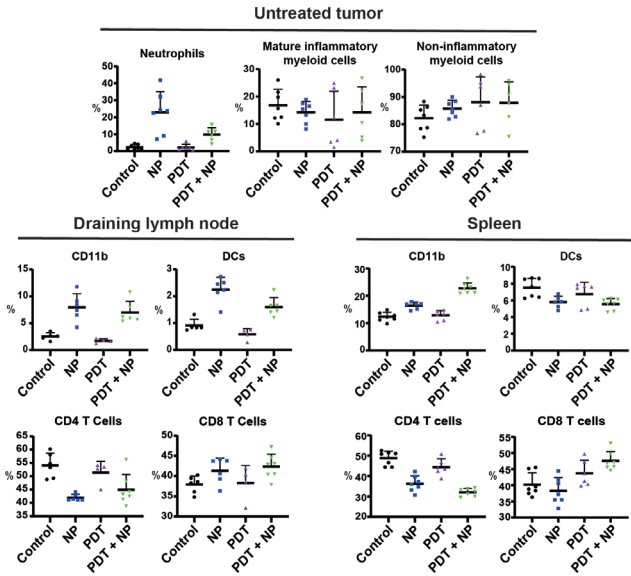


### Figure S3. Survival curves of mice bearing bilateral MC38 or CT26 tumors

Immunocompetent mice were inoculated with tumor cells in the right and left flanks and injected with CD8-depleting antibodies one day before tumors became established. When the tumors were established (~125mm<sup>3</sup>), PDT was performed on one tumor by administration of 20 mg/kg Radachlorin in the tail vein and irradiating with 662 nm light at a drug-to light interval of 6h and 116 mW/cm<sup>2</sup> for 116 J/cm<sup>2</sup>. The next morning, animals were injected with NPs at an interval of 2 days for a total of 4 administrations. Survival curves of mice bearing two A). MC38 tumors (C57BL/6J mice) and B). CT26 tumors (BALB/c mice), one on each opposite flank.

**A** MC38



**B** CT26

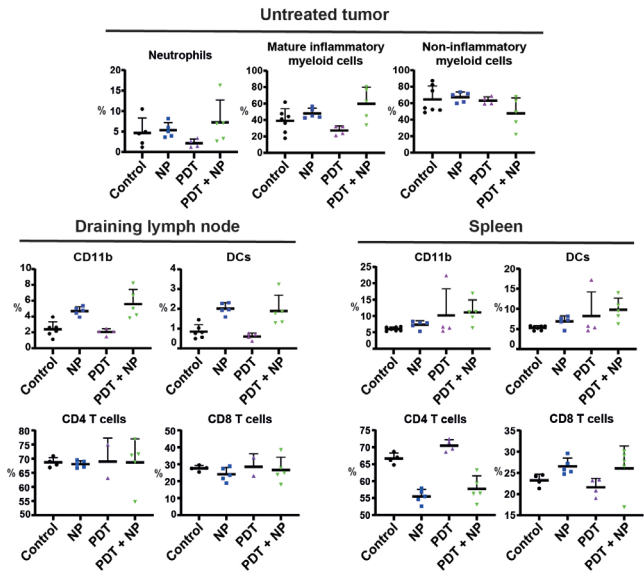


**Figure S4. Analysis of the tumor microenvironment after treatment**

Immunocompetent mice were inoculated with cancer cells in the right and left flanks ( $n \geq 5$ ). When the tumors were established ( $\sim 125 \text{ mm}^3$ ), PDT was performed on one tumor by administration of 20 mg/kg Radachlorin in the tail vein and irradiating with 662 nm light at a drug-to light interval of 6h and 116 mW/cm<sup>2</sup> for 116 J/cm<sup>2</sup>. The next morning, animals were injected with NPs at an interval of 2 days for a total of 2 administrations. The day following the second NP administration, the mice were sacrificed after which the dLN and spleen were collected, processed, and stained for analysis by flow cytometry. Populations are shown in percentages for A). MC38 and B). CT26 tumor-bearing mice. Gating was performed in FlowJo and included only living (7AAD-) CD45.2+ cells. Populations were further gated to include neutrophils (CD11b+Ly6G+), mature inflammatory myeloid cells (CD11b+CD86+Ly6Chi), non-inflammatory myeloid cells (CD11b+Ly6Clow), CD11b (total CD11b+), dendritic cells (DCs, CD11b+CD11chi), CD4 T cells (CD3+CD4+) and CD8 T cells (CD3+CD8+).



7



# THE POTENTIAL OF MULTI-COMPOUND NANOPARTICLES TO BYPASS DRUG RESISTANCE IN CANCER

Da Silva, C.G., Godefridus J. Peters, Ferry Ossendorp, Luis J. Cruz  
*Cancer Chemother Pharmacol.* 2017 Nov;80(5):881-894.

# Abstract

---

### Purpose

The therapeutic efficacy of conventional chemotherapy against several solid tumors is generally limited and this is often due to the development of resistance or poor delivery of the drugs to the tumor. Mechanisms of resistance may vary between cancer types. However, with current development of genetic analyses, imaging and novel delivery systems we may be able to characterize and bypass resistance e.g. by inhibition of the right target at the tumor site. Therefore, combined drug treatments, where one drug will revert or obstruct the development of resistance and the other will concurrently kill the cancer cell, are rational solutions. However, drug exposure of one drug will defer greatly from the other due to their physicochemical properties. In this sense, multi-compound nanoparticles are an excellent modality to equalize drug exposure, i.e. one common physicochemical profile. In this review, we will discuss novel approaches that employ nanoparticle technology that addresses specific mechanisms of resistance in cancer.

### Methods

PubMed literature was consulted and reviewed.

### Results

Nanoparticle technology is emerging as a dexterous solution that may address several forms of resistance in cancer. For instance, we discuss advances that address mechanisms of resistance with multi-compound nanoparticles which co-deliver chemotherapeutics with an anti-resistance agent.

Promising anti-resistance agents are 1) targeted in-vivo gene silencing methods aimed to disrupt key resistance gene expression or 2) protein kinase inhibitors to disrupt key resistance pathways or 3) efflux pumps inhibitors to limit drug cellular efflux.

## INTRODUCTION

Nanoparticles are emerging as ideal candidates for targeted delivery of drugs. A novel development is nanoparticles capable to encapsulate or bind multiple compounds at once and release the drugs at the target site either simultaneously or in a predetermined sequence. Nanoparticles are commonly composed of organic or inorganic materials with sizes ranging from 10 to 1000 nanometers (nm) and are generally 500 nm or smaller. Organic nanoparticles are usually composed of biodegradable polymers [1–5] or lipids [6] whereas inorganic nanoparticles are usually composed of gold, silver, titanium dioxide, iron, carbon or silicon [7–9].

Nanoparticles as drug delivery agents have several advantages compared to 'free' drugs, including reduced bio-distribution, sustained and slow release, and protect drugs against degradation thereby prolonging drug half-life. A tissue wide bio-distribution of a drug is often unwanted, as the drug will not only go to the site of interest but also go to many other tissues, inducing dose limiting side-effects. The consequence is that the critical dose is therefore not attainable and the efficacy of the drug is reduced. In contrast to 'free' drugs, nanoparticles can increase drug blood circulation time considerably by protecting the drug from rapid catabolism by detoxification enzymes and body clearance. In addition, nanoparticles can widen the drug repertoire to the clinic to include abandoned potent putative drugs. These include drugs with 1) a low therapeutic index, or 2) that are very hydrophobic and due to poor solubility were regarded as unsafe for in-vivo application, or 3) in their 'free' form that would be degraded too rapidly, or 4) that become unstable, or 5) that accumulate in organs of disinterest thereby inducing severe toxicity. Nanoparticles are also increasingly modified with targeting moieties to mitigate side-effects to increase their efficacy even further. The targeting moieties are designed to increase cell type specificity by targeting molecules such as peptides, ligands or antibodies to cell specific receptors thereby enhancing specific uptake by receptor-mediated endocytosis or increasing local retention time.

Nanoparticles have clear advantages and their adoption for medical usage is emerging, as more than 40 therapeutic nanoparticles have been approved for the application in the clinic worldwide and at least 200 more are in clinical trials [10–12]. Although nanoparticles for drug delivery have several advantages over 'free' drugs, there are also some disadvantages, which may differ greatly from type-to-type of nanoparticle [13, 14]. For instance, while nanoparticles may help to reduce tissue wide bio-distribution, it is also this feature that is limiting its access to tissues that are located beyond blood vessels and filter organs, which limits the application of nanoparticles for some pathologies. For the specific treatment of solid tumors however, a phenomenon entitled 'Enhanced Permeability and Retention' (EPR) effect, occasionally observed in human cancers, may be exploited to circumvent this obstacle [15]. The EPR effect is characterized by leaky blood vessels at the tumor site, originating from unregulated secretion of angiogenic factors, and decreased lymphatic drainage. Although the EPR effect is not always present, or found very pronounced in humans, it may be induced or augmented in some specific cases, allowing nanoparticles to extravasate and still gain access to cancer cells [16–18]. An important disadvantage of some nanoparticle types is possibly organ specific toxicity, due to their propensity to accumulate in filter organs, such as liver and kidney, or spleen and lungs, although the degree of accumulation may vary considerably from type-to-type [19]. Nanoparticle surface modifications, such as amalgamation of polyethylene glycol (PEG) polymer chains (PEGylation; PEG) or adjusting the physicochemical properties, can attenuate this accumulation and therefore reduce toxicity in these organs. However, the demand for innovation maintains the pressure to continuously design novel and dexterous formulations to overcome these disadvantages and further exalt the therapeutic potential of nanoparticles to the clinic [20, 21]. For the treatment of cancer, several genotoxic and cytotoxic drugs are being encapsulated into or bound to nanoparticles to increase their efficacy and reduce side-effects. For example, Doxil®, Abraxane® and more recently Onivyde® were approved and are clinically available nanoparticle formulations of doxorubicin, paclitaxel and irinotecan, respectively. These modalities may be superior to their 'free' counterparts, either because of their specific delivery preventing e.g. cardiotoxicity (Doxil), or activation at their target site. However, they do not specifically deal with existing or evolving mechanisms of resistance. As treatment resistance commonly arises in cancer, there is a dire need of a more 'sophisticated' class of drugs that are able to address these treatment impediments. Here onwards, this review will focus on recent

developments of (multi-compound) nanoparticle modalities that, in addition to kill cancer cells, may be employed to prevent or circumvent evolving mechanisms of resistance in cancer.

## MECHANISMS OF RESISTANCE IN CANCER

A few cancer types, such as chorionic carcinoma, seminoma and some (sub) types of lymphoma, actually respond well to cytostatic chemotherapy, commonly leading to clinical remission and cancer cures. Unfortunately, the vast majority of solid tumors will not respond as favorably. This is generally mediated by intrinsic resistance to cytotoxic drugs after an initial reduction of the tumor mass [22]. As tumors are quite heterogeneous of composition, it is not completely clear whether drug resistance is attained exclusively by clonal selection, i.e. selection of mutants resistant to the drug, a certain degree of adaptation, or both [23]. Common mechanisms of resistance include pathway rewiring to accommodate enhanced proliferation, anti-apoptosis and pro-survival signals, enhanced drug efflux and reduced influx, acquired (additional) DNA mutations, enhanced DNA repair, epithelial to mesenchymal phenotype transition, epigenetic modifications, drug inactivation and drug target alteration, amongst others [24].

For example, a common aberrantly activated and pharmaceutically targeted pathway in cancer is the Mitogen-Activated Protein Kinase (MAPK) signaling pathway. This pathway provides strong survival and proliferative signals, effectively antagonizing the induction of apoptosis triggered by many oncological drugs [25]. Several signaling pathways, including the MAPK pathway, converge in the activation of the c-Myc gene, that is frequently found overexpressed and mutated in a vast range of cancer types [26–29]. The Myc protein is a basic helix-loop-helix transcription factor controlling efficient proliferation of somatic and germ cells. Unfortunately, Myc has been defined to be lacking targetable active sites for drugs and therefore considered “undruggable” for conventional pharmaceuticals. Another protein involved in survival and conferring drug resistance in cancer is the Epidermal growth factor receptor (EGFR), often found aberrantly (over)expressed in carcinomas.

A distinct and predominant mechanism of drug resistance found in cancer cells is the overexpression of specific efflux pumps. These efflux pumps are part of the ABC superfamily of transporters and can translocate substrates (drugs) from the inside to the outside of the cell, thereby reducing intracellular drug accumulation. Currently, there are 49 human ABC transporter proteins described. From these 49 transporters, 15 are commonly associated with cancer and conferring resistance to chemotherapeutic agents. P-glycoprotein, BCRP and MRP1 are amongst the most described efflux pumps to play a key role in multidrug resistance (MDR)-mediated resistance in cancer [30].

Some of these mechanisms of resistance may be addressed by employing specifically adapted nanoparticles. The number of scientific publications of nanoparticles for single drug delivery is immense and their therapeutic potential is evident however, novel strategies are required to improve cancer therapy efficacy to deal with evolving mechanisms of resistance. To achieve this goal, the delivery of several drugs, with a diverse mode of action, may be combined in nanoparticles (see Figure 1 for an illustration). Additionally, the required level of control over the drug release time and release sequence is for this demanding task considerably higher. Notably, as the complexity of chemical assembly of such nanoparticles raises, so may the costs for GMP mass production and the costs of QA/QC [31]. In addition, the FDA/CDER approval of multi-compound nanoparticles may, in some specific cases, be more complex and slower to attain due to their polyvalent nature [31, 32].

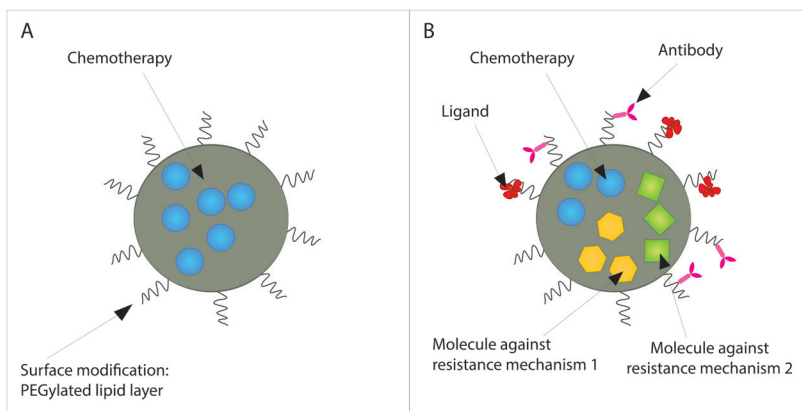


**Figure 1. Schematic representation of distinct types of nanoparticle approaches.** A, mono-chemotherapy nanoparticle approach containing one type of drug without targeting moieties; B, depiction of a multi-drug nanoparticle approach with active targeting moieties.

## TARGETING MECHANISMS OF RESISTANCE WITH PROTEIN KINASE INHIBITORS NANOPARTICLE FORMULATIONS

Several drugs are currently in the clinic or are being developed that can inhibit or repress specific mechanisms of resistance. These drugs are so-called small molecule inhibitors, anti-signaling drugs or biologicals, e.g. protein kinase inhibitors (PKIs) and monoclonal antibodies. However, the cure rate of solid tumors by these modalities alone is low and acquired resistance occurs as well [33].

In addition, chronic administration is often required leading to toxicity over time. It appears that, similar to conventional chemotherapy, PKIs that are encapsulated in nanoparticles also induce less side-effects, compared to 'free' PKI drug administration. For instance, poly(lactic-co-glycolic acid; PLGA) nanoparticles encapsulating erlotinib induced significantly less sub-acute toxicity in Wistar rats compared to 'free' administration [34]. In a similar study, Marslin et al. [35] have shown that cardiotoxicity, often a complication of prolonged administration of imatinib mesylate, could be avoided by encapsulating this drug in PLGA nanoparticles whilst increasing the efficacy compared to the 'free' drug.

Instead of monotherapy, a rational combination of PKIs with other drugs may harbor great synergetic potential. Some combinations may enhance cancer treatment efficacy by predisposing tumors to conventional chemotherapy. For example, Basu and colleagues [36] assembled nanoparticles carrying PD98059, a selective MAPK inhibitor, to predispose cancer cells dependent on this oncogenic pathway to chemotherapy. The authors combined the nanoparticles containing PD98059 with cisplatin and observed an impressive tumor growth disparity compared to either compound alone. A clear synergistic effect was observed when these compounds were combined for simultaneous delivery to melanoma cells *in vivo*. Although the concurrent administration of these two modalities was beneficial in this setting, it may differ with PKI, cancer and chemotherapy type. Lee et al. [37] have recently shown that sequential administration, but not simultaneous, may be crucial for some PKIs and conventional chemotherapy combinations. The authors showed that pre-treatment of breast cancer cells with erlotinib, a targeted EGFR inhibitor, was required to sensitize cancer cells to doxorubicin and that co-administration of both (i.e. erlotinib and doxorubicin simultaneously) was not nearly as effective. By inhibiting EGFR, the cancer cell re-acquired a working apoptosis pathway responsive to DNA damage. Furthermore, Morton et al. [38] described how liposomes could be employed to achieve such time controlled release of drugs. By loading doxorubicin into the hydrophilic core and entrapping erlotinib in the hydrophobic compartment of the membrane, erlotinib is released before doxorubicin. The sequential release effectively forces an internal rewiring of signaling pathways effected by erlotinib before DNA damage is induced by doxorubicin. This incites the cancer cell proneness towards apoptosis considerably. Figure 2 illustrates a putative modality to circumvent multiple mechanisms of resistance in cancer.



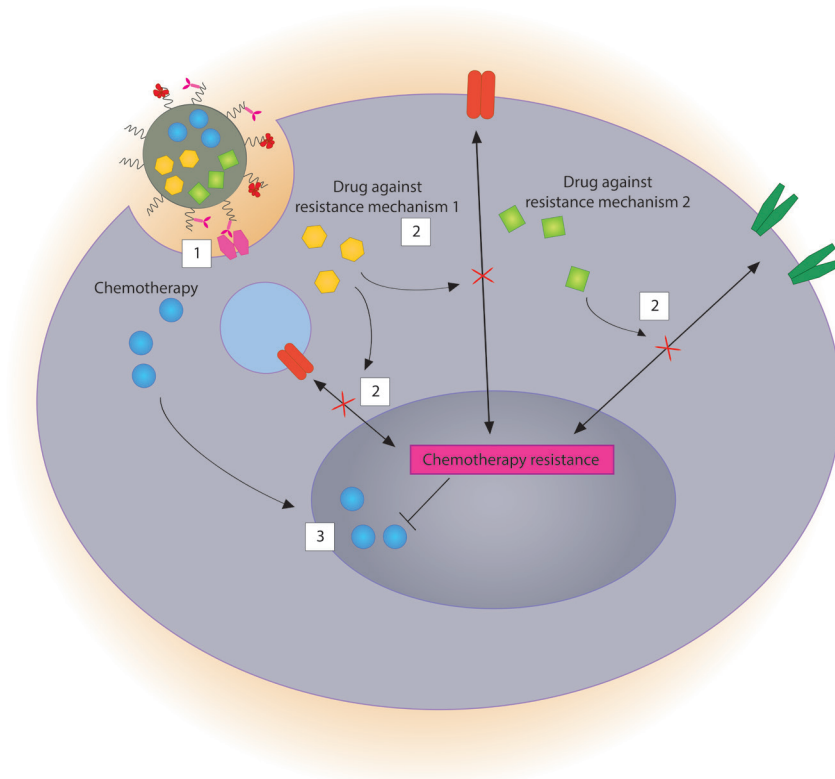


**Figure 2. Schematic representation of a putative multi-compound nanoparticle that releases multiple compounds simultaneously, or in sequence.**

1, A targeted nanoparticle triggers the receptor mediated endocytosis uptake of the nanoparticle by the target cell; 2, After intracellular processing of the nanoparticle (not depicted), selective small molecule compounds are released that inhibit mechanisms of resistance either simultaneously or in sequence, depending on the nanoparticle design. In this illustration, two distinct drugs “Drug against resistance mechanism” 1 and 2 are depicted, each suppressing a different mechanism of resistance. One of these drugs could inhibit efflux pumps, to ascertain that chemotherapy is not excreted from the cell, while the second drug could suppress an (active) anti-apoptotic pathway hindering cell death related to DNA damage. 3, Cell cycle is disrupted by conventional chemotherapy by inducing DNA damage and trigger apoptosis that can now be executed unobstructed due to the inhibited anti-apoptotic pathway and the cancer cell dies.

This elegant approach achieved a much higher rate of cancer cell killing by hampering the cancer cells resistance mechanisms against apoptosis before releasing the cell killing agent. Au et al. [39] recently showed that sequential release of drugs for cancer therapy is also possible with polymer nanoparticles, by incorporating the hydrophobic drugs wortmannin and docetaxel into an adapted formulation of PLGA-PEG nanoparticles. Wortmannin inhibits, non-exclusively, the phosphoinositide 3 kinases (PI3Ks), in essence sensitizing cancer cells to apoptosis, allowing docetaxel to successfully disrupt cell division. The PI3K and the earlier mentioned MAPK pathway are actually survival pathways preventing chemotherapeutic drugs to induce cell death; therefore inhibition of these survival pathways will activate the chemotherapeutic drug and cell death [40]. As the molecular weight of wortmannin is lower compared to docetaxel, it was released prior to docetaxel, allowing a controlled sequential release of these drugs. Also in this setting, the pathway rewiring process before interfering with cell division, was essential. Several other combined nanoparticle and protein kinase inhibitor strategies are emerging and are summarized in Table 1.

**Table 1. Nanoparticle protein kinase inhibitor delivery targeting pathways involved in therapy resistance.**

Nanoparticle type	Active targeting	PKI	Primary kinase targeted	Other compounds	Model	Refs.
Accurin polymer based	-	AZD2811	Aurora B kinase	-	Human colon cancer	[83]
Glutaraldehyde-crosslinked albumin	Anti-EGFR nanobody *	17864 (platinum-bound sunitinib analogue)	PDGF-R/ VEGFR	-	Human head and neck squamous cell carcinoma (in-vitro)	[84]
Gold	-	Erlotinib	EGFR	-	Human adenocarcinoma and non-small-cell lung cancer (in-vitro)	[85]
Gold	Anti-EGFR antibody *	Gefitinib	EGFR		Lung cancer (in-vitro)	[86]
Hexadentate-PLGA	-	PD98059	MEK	Cisplatin (not in nanoparticle)	Melanoma and lung carcinoma	[36]

Iron oxide/ magnetite	-	AM-005 + AT-9283	Aurora kinase	-	Liver cancer	[87]
Liposomal	-	WHI-131	JAK3/ EGFR	-	Human B-lineage ALL/breast cancer	[88, 89]
Liposomal	-/Anti-CD19 antibody *	SYK-P-site inhibitor C61	SYK	-	B-precursor acute lymphoblastic leukemia	[90- 92]
Liposomal	Anti-EGFR nanobody *	AG538	IGF-1R		Human head and neck squamous cell carcinoma and breast adenocarcinoma	[42]
Liposomal	Folate	Erlotinib	EGFR	Doxorubicin	Human breast and lung cancer	[38]
Liposomal (layer-by-layer)	CD44 *	Selumetinib + PX-866	MEK1/2 + PI3K	-	Human breast cancer	[93]
Oleic acid based	-	AZD6244	MAPK	Cisplatin	Human cervical/ breast/liver cancer (in-vitro)	[94]
PLGA-PEG di- block copolymer	-	Wortmannin	PI3K	Docetaxel	Human lung and prostate cancer	[39]
PLGA	-	LY294002	PI3K	-	Murine melanoma and human breast cancer	[95]
Reverse micelles	-	Erlotinib	EGFR	-	Pancreatic adenocarcinoma (in-vitro)	[96]

EGFR: Epidermal growth factor receptor; IGF-1R: Insulin-like growth factor 1 receptor; JAK3: Janus kinase 3; MEK: Mitogen-activated protein kinase kinase; PDGF-R: Platelet-derived growth factor receptor; PI3K: Phosphoinositide 3-kinase; PLGA: Poly(lactic-co-glycolic acid); SYK: Spleen tyrosine kinase; VEGFR: Vascular endothelial growth factor receptor;

\* Activate targeting with dual role: 1) NP targeting moiety and 2) direct perturbing mechanism of resistance by receptor agonism/antagonism or may trigger antibody mediated cytotoxicity.

Cancer cells rapidly develop resistance against PKIs commonly by the activation of compensatory pathways or target site mutations [41]. For instance, it has been described that inhibition of the EGFR pathway with PKIs may eventually induce the activation of the insulin-like growth factor 1 (IGF-1R) pathway, as an acquired method of resistance. To address this adaptation, Van der Meel et al. [42] developed liposomes carrying an anti-IGF-1R kinase inhibitor and coated the liposomes with antagonistic anti-EGFR nanobodies. This approach led to considerable less pro-survival and proliferation signaling in cancer cells. The majority of the studies summarized in Table 1 describe nanoparticle approaches to target oncogenic pathways, often implicated in cancer mechanisms of resistance. Most of these studies did not combine nanoparticles with 'conventional' chemotherapy. However, combining PKIs with chemotherapy may hold a considerable therapeutic benefit, as indicated by the combinatorial studies described above.

In summary, several PKIs have less favorable physicochemical properties that decrease their therapeutic potential [43] and encapsulation of PKIs into nanoparticles appears to be a viable strategy to circumvent some of these limitations. In addition, PKI associated toxicity may be reduced [34]. Nonetheless, it appears that combining nanoparticle formulated PKIs with conventional chemotherapy could be an effective strategy to hinder therapy induced resistance. It also appears evident that the order of administration is paramount for the efficacy of the treatment modality for some cancer types; sequential rather than simultaneous and PKI exposure before cytotoxic agent.

## TARGETING MECHANISMS OF RESISTANCE WITH SILENCING RNA NANOPARTICLE FORMULATIONS

Several mechanisms of resistance in cancer have been previously targeted by suppression of specific gene expression, most commonly by small interfering RNA (siRNA) or to a lesser extent small hairpin RNA (shRNA) delivery to cancer cells. An siRNA molecule is a double-stranded RNA molecule of 20-25 base-pairs whereby its sequence is complementary to a part of its target gene mRNA transcript. It is often employed to disrupt the translation of a specific gene transcript into protein by exploiting the RNA interference pathway [44].

Traditionally, gene therapy treatment with siRNA is performed by the injection of 'naked' siRNA directly into the bloodstream or packed in modified viruses [45, 46]. Specifically the targeting of 'naked' siRNA to the cells of interest

without the use of a delivery agent is generally found inefficient as it is rapidly cleared from the bloodstream due to degradation by serum nucleases and renal clearance. In contrast, adapted viruses are, in comparison, quite efficacious delivery agents for siRNA however, immune responses against the viral proteins abate the efficacy of this modality [47]. As an alternative, nanoparticles can encapsulate, protect and deliver siRNA intracellularly. Conversely, nanoparticles have limitations as well, as described in the first section of this paper, and are applicable to siRNA delivery as well, i.e. mainly the dependence of EPR effect to gain access to cancer cells in solid tumors. From an immunological perspective, immune responses against nanoparticles have been sparsely studied and may vary greatly from type and composition. For instance, nanoparticles containing 1,2-Dioleoyl-3-trimethylammonium-propane (DOTAP), mainly an ingredient for cationic liposomes, has been reported to induce potent type I and type II interferon responses [48]. However, PEGylation of nanoparticles reduces immunogenicity without the formation of any additional toxic metabolites and appears essential for successful prolonged blood circulation [20, 49]. A multifold of mono-therapeutic-nanoparticle formulations that aim to modulate driver oncogenes have also been reported but are beyond the scope of this review. Multi-compound nanoparticles targeting specifically mechanisms of resistance by targeted siRNA gene silencing in cancer are summarized in Table 2.

**Table 2. Nanoparticle small interfering RNA delivery targeting pathways involved in therapy resistance.**

Nanoparticle type	Active targeting	siRNA*	Compounds*	Model	Refs.
Glycol chitosan	-	Bcl-2	Doxorubicin	Human prostate cancer	[50]
LCP	-	c-Myc	Gemcitabine monophosphate	Human lung cancer	[51]
LCP	Anisamide to sigma receptors	VEGF	Gemcitabine monophosphat	Human lung cancer	[52]
Liposomal	-	MRP1/ BCL2	Doxorubicin	Human ovarian, breast, lung and colon cancer. (in-vitro)	[97]

Liposomal	Asparagine-glycine-arginine peptide to CD13	c-Myc	Doxorubicin	Human fibrosarcoma	[98]
Liposomal	Anisamide to sigma receptors	VEGF/c-Myc	Doxorubicin	Human ovarian cancer	[99]
Liposomal	GC4 scFv antibody	c-Myc/MDM2/VEGF	miR-34a	Murine melanoma	[100]
Liposomal	-	Mcl1	SAHA (Vorinostat)	Human cervical cancer	[101]
Liposomal	-	MRP1/BCL2	Doxorubicin	Human lung cancer	[102]
Liposomal	-	BCL2	d-(KLAKLAK) <sub>2</sub> peptide	Murine melanoma	[103]
Liposomal	Hyaluronic acid	MRP1	Doxorubicin	Human breast cancer	[104]
DSPE-PEG lipid	Folate	Survivin	Docetaxel	Human liver cancer	[105]
Micellar	-	HIF-1 $\alpha$	Doxorubicin (combined treatment; i.e. not in delivery vehicle)	Human prostate cancer	[106]
Micellar	-	Plk1	Paclitaxel	Human breast cancer	[107]
Minicell	EGFR antibody	MDR1	Doxorubicin	Uterine cancer	[108]
PDHA	-	Snail/Twist	Paclitaxel	Murine breast cancer	[109]
PEI-GO	-	Bcl-2	Doxorubicin	Human cervical cancer. In-vitro study only	[110]
PEO-PbAE/PCL	-	P-glycoprotein	Paclitaxel	Human ovarian cancer. (in-vitro)	[111]
PLGA-PEI	Biotin to biotin receptors	P-glycoprotein	Paclitaxel	Murine breast cancer	[112]

PLGA	-	DCAMKL-1	DAPT (combined treatment; i.e. not in delivery vehicle)	Human colorectal cancer	[113]
PLGA	-	REV1/REV3L	Cisplatin prodrug	Human prostate cancer	[114]
Mesoporous silica	-	Bcl-2	Doxorubicin	Human ovarian cancer. (in-vitro)	[115]
Mesoporous silica	-	P-glycoprotein	Doxorubicin	Human cervical cancer	[116]
Mesoporous silica	Hyaluronic acid + PEGA-pVEC peptide	CTGF	Doxorubicin	Human breast cancer	[117]

BCL2: B-cell lymphoma 2; CTGF: Connective tissue growth factor; DAPT: N-[N-(3,5-difluorophenacetyl)-l-alanyl]-S-phenylglycine t-butyl ester; DCAMKL-1: Doublecortin-like and CAM kinase-like 1; DSPE: Distearoyl-phosphatidylethanolamine; HIF-1 $\alpha$ : Hypoxia-inducible factor-1 $\alpha$ ; LCP: Lipid/calcium/phosphate; MDR1: Multidrug resistance 1; MRP1: multidrug resistance-associated protein 1; PEI-GO: polyethylenimine-functionalized graphene oxide; PEG: Ethylene glycol; PEO-PbAE: Poly(ethylene oxide)-modified poly(beta-amino ester); PDHA: Poly[(1,4-butanediol)-diacrylate- $\beta$ -5-hydroxyamylamine]; PEO-PCL: Poly(ethylene oxide)-modified poly(epsilon-caprolactone); PLGA: Poly(lactic-co-glycolic acid); PLGA-PEI: PLGA polyethylenimine; Plk1: polo-like kinase 1; SAHA: suberoylanilide hydroxamic acid; scFv: single chain fragment variable; VEGF: vascular endothelial growth factor;

\* compounds are encapsulate in delivery vehicles unless stated otherwise.

Similar to previously discussed PKIs nanoparticle modalities, combining specific siRNA treatment with 'conventional' chemotherapy appears to yield superior results than any of the modalities alone. For instance, Yoon et al. [50] designed two glycol chitosan based nanoparticles, one containing doxorubicin and another containing siRNA targeted to the Bcl-2 gene transcript. As Bcl-2 is involved in conferring resistance against apoptosis triggered by doxorubicin, durable in-vivo tumor growth repression was observed after repeated injections of the nanoparticles containing doxorubicin followed by the nanoparticles containing the Bcl-2 siRNA. Moreover, combinatorial targeted nanoparticle delivery approaches of chemotherapy and siRNA targeted against (driver) oncogenes are highly anticipated. One of such oncogenes is the c-Myc gene. For instance, Zhang et al. [51, 52] recently combined gemcitabine monophosphate and c-Myc siRNA in one nanoparticle to efficiently suppress both subcutaneous and orthotopic human lung cancer growth in vivo with minimum toxicity in nude mice. As the involvement of c-Myc is quite prevalent in cancer, a prudent combinatorial nanoparticle approach of chemotherapy and c-Myc siRNA may therefore hold great potential to become one single potential treatment for a wide range of cancers of diverse aetiology. The authors also combined gemcitabine monophosphate with VEGF siRNA and found increased efficacy as well. This system had an additional advantage since gemcitabine monophosphate delivery would bypass resistance due to decreased activation [53–55].

## TARGETING EFFLUX PUMP AND OTHER MECHANISMS OF MULTIDRUG RESISTANCE WITH NANOPARTICLE FORMULATIONS

Dose escalation is a common pharmacological strategy to overcome mechanisms of resistance mediated by drug efflux pumps. While an effective approach, it is commonly accompanied by deleterious adverse effects. For instance, doxorubicin effective dose is limited by severe cardiotoxicity [56]. The upregulation of efflux pumps is a common and yet distinct method of resistance against cancer therapy. The upregulation of efflux pumps, such as the P-glycoprotein but more importantly MRPs and BCRP (ABCG2) [57], reduces the intracellular accumulation of specific drugs and is known to confer resistance against many chemotherapeutic agents including anthracyclines, paclitaxel and vincristine but also several protein kinase inhibitors [58, 59]. By employing nanoparticle technology to serve as delivery agents, drug efflux is inherently reduced, as nanoparticles enter the cells mainly by endocytosis and facilitate endosomal/lysosomal escape of distinct payloads to



the cytosol before their cargo is released [60–62]. Therefore, most of nanoparticle delivered drugs are less affected by drug efflux pumps due to their location inside the cell, usually outside the reach of membrane efflux pumps [13, 63–65]. Albeit, while the drug efflux pumps are partially bypassed by encapsulating drugs in nanoparticles, the effect is not absolute, as once the drugs are released inside the cells, a portion of the drug may still become in reach of efflux pumps. In that sense, it may be prudent to actively co-inhibit efflux pumps while delivering drugs to the targets cells. For this purpose, Xu et al. [66] reported that drug efflux mediated resistance in lung cancer cells could be effectively overcome by coating nanoparticles containing doxorubicin with cyclosporin A, which is a multimodal efflux pump inhibitor of both P-glycoprotein and MRP1 (ABCC1).

Alternatively, the co-delivery of a chemosensitizer such as curcumin (diferuloylmethane), may considerably decrease drug efflux. Curcumin is a relatively non-toxic plant derived polyphenol that has been described to have anti-carcinogenic effects, mainly mediated by pathway rewiring and interfering with the cell cycle [67–70]. It is also described as a potent inhibitor of the Nuclear Factor Kappa-light-chain-enhancer of activated B cells (NF- $\kappa$ B) pathway, as well as a strong suppressor of ABC transporters, including P-glycoprotein, MRP1 and BCRP [69, 71, 72]. However, curcumin by itself has a poor uptake by the intestinal tract and a notable low bioavailability, which makes this compound an ideal candidate to be integrated in nanoparticles approaches for targeted delivery [73]. Distinct multi-compound nanoparticle approaches that addresses cancer mechanisms of resistance, including curcumin co-encapsulation, are summarized in Table 3.

**Table 3. Nanoparticle (multiple) compound delivery targeting pathways involved in therapy resistance.**

Nanoparticle type	Active targetin	Compounds*	Primary method of resistance targeted **	Model	Refs.
Amphiphilic polymer	-	Curcumin + doxorubicin	ABC pumps/NF- $\kappa$ B	Human multiple myeloma, acute leukemia, prostate and ovarian cancers	[74]
Cationic amphiphilic copolymer	-	IL12 plasmid + Paclitaxel	Immune suppression	Murine breast cancer	[118]

Chitosan based	-	Curcumin + doxorubicin	ABC pumps/NF-κB	Human breast cancer (in-vitro)	[75]
Dendrimer	Transferrin receptor-specific peptide	TRAIL + doxorubicin	FADD	Human liver cancer	[119]
Flaxseed oil emulsion	-	Curcumin + paclitaxel	ABC pumps/NF-κB	Human ovarian adenocarcinoma (in-vitro)	[120]
Gel-Liposome	Hyaluronic acid	TRAIL + doxorubicin	FADD	Human breast cancer	[121]
Graphene	-	TRAIL + doxorubicin	FADD	Human lung cancer	[122]
Lipid	-	Curcumin + doxorubicin	ABC pumps/NF-κB	Human liver cancer	[123]
Liposomal	RGDK-lipopeptide	Curcumin + doxorubicin	ABC pumps/anti-angiogenic	Murine melanoma	[124]
Liposomal	DQA	Lonidamine + epirubicin (in a separate liposomal formulation)	Mitochondrial hexokinase 2	Human lung cancer	[125]
Liposomal	-	TRAIL + doxorubicin (in separate nanoparticles)	FADD	Human lung cancer	[126]
Liposomal (plus [D]-H6L9)	-	MiR-10b + paclitaxel	RhoC	Murine breast cancer	[127]
Liposomal (plus MG)	Her-2 antibody	Verapamil + doxorubicin	P-glycoprotein	Human breast cancer	[128]
Micellar based	-	Curcumin + doxorubicin	ABC pumps/NF-κB	Murine lung cancer	[129]
Micellar based	-	Disulfiram + Doxorubicin	P-glycoprotein	Human breast cancer	[130]
PCDA based	Biotin	Curcumin + doxorubicin	P-glycoprotein	Human breast cancer	[131]

PLGA based	EGFR-peptide	Paclitaxel + lonidamine	Mitochondrial hexokinase 2	Human breast and ovarian cancer	[132, 133]
PLGA	-	Cyclosporin A + doxorubicin	P-glycoprotein	Human lung cancer	[66]
PLGA	Anti-EGFR antibody *	Rapamycin	mTOR	Human breast cancer (in-vitro)	[134]
PLGA	Folate	Nutlin-3a + curcumin	ABC pumps/NF-κB	Human retinoblastoma (in-vitro)	[135]
PLGA	-	HPI-1 + Gemcitabine (Gemcitabine not in nanoparticle)	Hedgehog/Smo	Murine medulloblastoma, human pancreatic and liver cancer	[136, 137]
PLGA	-	Curcumin + doxorubicin	ABC pumps /NF-κB	Human chronic myelogenous leukemia (in-vitro)	[138]
PLGA	Biotin	Tariquidar + paclitaxel	P-glycoprotein	Murine mammary tumor	[139]
PLGA	iRGD	Camptothecin + TRAIL plasmid	FADD	Human colon cancer	[140]
PLGA	Anisamide	Resveratrol + doxorubicin	ABC pumps /NF-κB	Human breast cancer	[141]

DQA: Dequalinium; FADD: Fas-associated protein with death domain; MG: Malachite green carbinol base; FADD: Fas-Associated protein with Death Domain; PCDA: Poly(curcumin-dithiodipropionic acid); PLGA: Poly(lactic-co-glycolic acid); RhoC: Ras homolog gene family, member C; TRAIL: Tumor necrosis factor-related apoptosis-inducing ligand;

\* Activate targeting with dual role: 1) NP targeting moiety and 2) direct perturbing mechanism of resistance by receptor agonism/antagonism or trigger antibody induced cytotoxicity.

\*\* The described inhibitor mode of action is pleiotropic and may have several targets other than described.

There are several studies of nanoparticle encapsulated drug combinations with curcumin available in the literature that shown efficient circumvention of multi-drug resistance in a variety of models. For instance, Pramanik and colleagues [74] have shown that doxorubicin-curcumin amphiphilic polymer based nanoparticles successfully overcome drug efflux mediated resistance, reduced cardiotoxicity and bone marrow suppression compared to 'free' DOX and Doxil® in several cancer models. Successful reversal of chemo sensitivity has also been described by several other groups. For example, Duan et al. [75] have reported the successful reversal of drug efflux mediated resistance in an adriamycin resistant cell line by the simultaneous delivery of doxorubicin and curcumin in poly(butyl cyanoacrylate) nanoparticles. The inclusion of curcumin and cytotoxic drugs in nanoparticle formulations appears to be a logical strategy to circumvent, in a non-exclusive manner, efflux pump mediated cancer therapy resistance and possibly other mechanisms of resistance, accompanied with low toxicity to non-cancerous tissue. It should, however, be mentioned that these experiments were all performed in preclinical models with relatively high induced P-glycoprotein expression, a condition that has not been found in patients with solid tumors, but only in some hematological malignancies.

## CONCLUSION AND OUTLOOK

Nanoparticles are evolving from general, non-targeted, mono-drug delivery devices to become sophisticated multi-drug, targeted, sequence and time controlled drug release delivery devices. Moreover, nanoparticles can be designed to deliver drugs to cancer cells in a highly efficient manner while at the same time be able to address existing mechanisms of resistance. It is even possible to disrupt complex resistance mechanisms that require a sequence specific inhibition of pathways to bypass drug resistance. This will pave the way for the design of highly efficient, multi-functional, personalized theranostic nanomedicine [76]. This can be of immense benefit, for example, when cancer whole-genome sequencing becomes of age. This will allow specifically tailored nanoparticles to be made that can target individual cancer characteristics while therapy progression is tracked in real time by following the included imaging or reporter molecules [77]. Besides rewiring of pathways in cancer cells that overcome mechanisms of resistance to cytolytic drugs, the same design principle may be applied to modulate the tumor microenvironment. For example, modulation of specific pathways that stimulate immune suppressive cells, may be

interesting candidates for targeted pathway rewiring as described by Kawakami et al. [78]. The authors provide a considerable repertoire of possible targets that are involved in maintaining an immunosuppressed environment, including STAT3, IL10 and TGF $\beta$ , or even immune modulatory antibodies [79].

As described above, several ABC efflux pumps, such as MRPs and BCRP, are upregulated in many cancer types and often found to be involved in conferring resistance against numerous oncological drugs. Several nanoparticle based strategies have been published addressing these mechanisms of resistance (Table 2 and 3). Indeed, it appears that combining cytostatic drugs with efflux pump inhibitors increases the therapy efficacy considerably.

On the other hand, there are still obstacles that need to be overcome before nanoparticles may become successful and widely available clinical modalities [14]. Out of several, two important obstacles are: 1) the dependence of the EPR effect to gain access to target cells in solid tumors; 2) designing nanoparticles that can be assembled according to GMP regulations without becoming excessively complex and expensive to produce. These issues can be solved by emerging technologies. For instance, the dependence of the EPR effect may be effectively reduced by the design of nanoparticles that stimulate specific transcytosis [80] or combined with photodynamic therapy to enhance nanoparticle accumulation specifically in tumors [81, 82].

To conclude, when curative cancer surgery fails or is not feasible, there is currently no effective curative alternative treatment for chemotherapy resistant solid tumors. Despite the obstacles that need resolving, dexterous and specifically formulated multi-compound and multi-functional nanoparticles may become a viable modality for the treatment of non-resectable and chemotherapy resistant cancer in the foreseeable future.

## ACKNOWLEDGEMENT

Conception of idea: LJ Cruz and CG Da Silva; CG Da Silva collected initial literature, generated the graphical illustrations and drafted the first version; Godefridus J Peters, Ferry Ossendorp and Luis J. Cruz revised the paper and made final additions.

## COMPLIANCE WITH ETHICAL STANDARDS

Funding: This study was funded by the research programme 723.012.110 (Vidi), which is financed by the Netherlands Organisation for Scientific Research (NWO) and by the FP7 European Union Marie Curie IAPP program, BRAINPATH, under grant number 612360 (EvB, MS, AC, CL) and funding from the H2020-Marie Skłodowska-Curie Action Research and Innovation Staff Exchange (RISE) Grant 644373-PRISAR.

**Conflict of Interest:**

The authors declare that they have no conflict of interest.

**Ethical approval:**

This article does not contain any studies with human participants or animals performed by any of the authors.

**Informed consent:**

Not applicable.

## REFERENCES

1. Da Silva CG, Rueda F, Löwik CW, et al (2016) Combinatorial prospects of nano-targeted chemoimmunotherapy. *Biomaterials* 83:308–320. doi: 10.1016/j.biomaterials.2016.01.006
2. Srinivas M, Tel J, Schreibelt G, et al (2015) PLGA-encapsulated perfluorocarbon nanoparticles for simultaneous visualization of distinct cell populations by 19F MRI. *Nanomedicine (Lond)* 10:2339–48. doi: 10.2217/NNM.15.76
3. Srinivas M, Cruz LJ, Bonetto F, et al (2010) Customizable, multi-functional fluorocarbon nanoparticles for quantitative in vivo imaging using 19F MRI and optical imaging. *Biomaterials* 31:7070–7077. doi: 10.1016/j.biomaterials.2010.05.069
4. Cruz LJ, Stammes MA, Que I, et al (2016) Effect of PLGA NP size on efficiency to target traumatic brain injury. *J Control Release* 223:31–41. doi: 10.1016/j.jconrel.2015.12.029
5. Cruz LJ, Que I, Aswendt M, et al (2016) Targeted nanoparticles for the non-invasive detection of traumatic brain injury by optical imaging and fluorine magnetic resonance imaging. *Nano Res* 9:1276–1289. doi: 10.1007/s12274-016-1023-z
6. Naseri N, Valizadeh H, Zakeri-Milani P (2015) Solid Lipid Nanoparticles and Nanostructured Lipid Carriers: Structure, Preparation and Application. *Adv Pharm Bull* 5:305–13. doi: 10.15171/apb.2015.043
7. Hosta-Rigau L, Olmedo I, Arbiol J, et al (2010) Multifunctionalized Gold Nanoparticles with Peptides Targeted to Gastrin-Releasing Peptide Receptor of a Tumor Cell Line. *Bioconjug Chem* 21:1070–1078. doi: 10.1021/bc1000164
8. Hosta L, Pla-Roca M, Arbiol J, et al (2009) Conjugation of Kahalalide F with Gold Nanoparticles to Enhance in Vitro Antitumoral Activity. *Bioconjug Chem* 20:138–146. doi: 10.1021/bc800362j
9. Kogan MJ, Olmedo I, Hosta L, et al (2007) Peptides and metallic nanoparticles for biomedical applications. *Nanomedicine* 2:287–306. doi: 10.2217/17435889.2.3.287
10. Schütz CA, Juillerat-Jeanneret L, Mueller H, et al (2013) Therapeutic nanoparticles in clinics and under clinical evaluation. *Nanomedicine (Lond)* 8:449–67. doi: 10.2217/nnm.13.8
11. van der Meel R, Vehmeijer LJC, Kok RJ, et al (2013) Ligand-targeted particulate nanomedicines undergoing clinical evaluation: current status. *Adv Drug Deliv Rev* 65:1284–98. doi: 10.1016/j.addr.2013.08.012

12. Bobo D, Robinson KJ, Islam J, et al (2016) Nanoparticle-Based Medicines: A Review of FDA-Approved Materials and Clinical Trials to Date. *Pharm Res* 33:2373–2387. doi: 10.1007/s11095-016-1958-5
13. Davis ME, Chen ZG, Shin DM (2008) Nanoparticle therapeutics: an emerging treatment modality for cancer. *Nat Rev Drug Discov* 7:771–82. doi: 10.1038/nrd2614
14. Park K (2013) Facing the truth about nanotechnology in drug delivery. *ACS Nano* 7:7442–7. doi: 10.1021/nn404501g
15. Acharya S, Sahoo SK (2011) PLGA nanoparticles containing various anticancer agents and tumour delivery by EPR effect. *Adv Drug Deliv Rev* 63:170–83. doi: 10.1016/j.addr.2010.10.008
16. Fang J, Nakamura H, Maeda H (2011) The EPR effect: Unique features of tumor blood vessels for drug delivery, factors involved, and limitations and augmentation of the effect. *Adv Drug Deliv Rev* 63:136–51. doi: 10.1016/j.addr.2010.04.009
17. Kobayashi H, Watanabe R, Choyke PL (2013) Improving conventional enhanced permeability and retention (EPR) effects; what is the appropriate target? *Theranostics* 4:81–9. doi: 10.7150/thno.7193
18. Pantziarka P, Bouche G, Meheus L, et al (2014) The Repurposing Drugs in Oncology (ReDO) Project. *Ecancermedicalsecience* 8:442. doi: 10.3332/ecancer.2014.442
19. Semete B, Booyesen L, Lemmer Y, et al (2010) In vivo evaluation of the biodistribution and safety of PLGA nanoparticles as drug delivery systems. *Nanomedicine* 6:662–71. doi: 10.1016/j.nano.2010.02.002
20. Milla P, Dosio F, Cattel L (2012) PEGylation of proteins and liposomes: a powerful and flexible strategy to improve the drug delivery. *Curr Drug Metab* 13:105–19.
21. Palombo M, Deshmukh M, Myers D, et al (2014) Pharmaceutical and toxicological properties of engineered nanomaterials for drug delivery. *Annu Rev Pharmacol Toxicol* 54:581–98. doi: 10.1146/annurev-pharmtox-010611-134615
22. Fodale V, Pierobon M, Liotta L, Petricoin E Mechanism of cell adaptation: when and how do cancer cells develop chemoresistance? *Cancer J* 17:89–95. doi: 10.1097/PPO.0b013e318212dd3d
23. Ahmed M, Li L-C (2013) Adaptation and clonal selection models of castration-resistant prostate cancer: current perspective. *Int J Urol* 20:362–71. doi: 10.1111/iju.12005
24. Housman G, Byler S, Heerboth S, et al (2014) Drug resistance in cancer: an overview. *Cancers (Basel)* 6:1769–92. doi: 10.3390/cancers6031769
25. Dhillon AS, Hagan S, Rath O, Kolch W (2007) MAP kinase signalling pathways in cancer. *Oncogene* 26:3279–3290. doi: 10.1038/sj.onc.1210421



26. Felsher DW, Bishop JM (1999) Transient excess of MYC activity can elicit genomic instability and tumorigenesis. *Proc Natl Acad Sci* 96:3940–3944. doi: 10.1073/pnas.96.7.3940
27. Arvanitis C, Felsher DW (2005) Conditionally MYC: insights from novel transgenic models. *Cancer Lett* 226:95–9. doi: 10.1016/j.canlet.2004.10.043
28. Jain M, Arvanitis C, Chu K, et al (2002) Sustained loss of a neoplastic phenotype by brief inactivation of MYC. *Science* 297:102–4. doi: 10.1126/science.1071489
29. Dang C V (2012) MYC on the path to cancer. *Cell* 149:22–35. doi: 10.1016/j.cell.2012.03.003
30. Gottesman MM, Fojo T, Bates SE (2002) MULTIDRUG RESISTANCE IN CANCER: ROLE OF ATP-DEPENDENT TRANSPORTERS. *Nat Rev Cancer* 2:48–58. doi: 10.1038/nrc706
31. Goldberg MS, Hook SS, Wang AZ, et al (2013) Biotargeted nanomedicines for cancer: six tenets before you begin. *Nanomedicine (Lond)* 8:299–308. doi: 10.2217/nnm.13.3
32. Tyner K, Sadrieh N (2011) Considerations when submitting nanotherapeutics to FDA/CDER for regulatory review. *Methods Mol Biol* 697:17–31. doi: 10.1007/978-1-60327-198-1\_3
33. Chen Y, Fu L (2011) Mechanisms of acquired resistance to tyrosine kinase inhibitors. *Acta Pharm Sin B* 1:197–207. doi: 10.1016/j.apsb.2011.10.007
34. Marslin G, Sheeba CJ, Kalaichelvan VK, et al (2009) Poly(D,L-lactic-co-glycolic acid) nanoencapsulation reduces Erlotinib-induced subacute toxicity in rat. *J Biomed Nanotechnol* 5:464–71.
35. Marslin G, Revina AM, Khandelwal VKM, et al (2015) Delivery as nanoparticles reduces imatinib mesylate-induced cardiotoxicity and improves anticancer activity. *Int J Nanomedicine* 10:3163–70. doi: 10.2147/IJN.S75962
36. Basu S, Harfouche R, Soni S, et al (2009) Nanoparticle-mediated targeting of MAPK signaling predisposes tumor to chemotherapy. *Proc Natl Acad Sci U S A* 106:7957–61. doi: 10.1073/pnas.0902857106
37. Lee MJ, Ye AS, Gardino AK, et al (2012) Sequential application of anticancer drugs enhances cell death by rewiring apoptotic signaling networks. *Cell* 149:780–94. doi: 10.1016/j.cell.2012.03.031
38. Morton SW, Lee MJ, Deng ZJ, et al (2014) A nanoparticle-based combination chemotherapy delivery system for enhanced tumor killing by dynamic rewiring of signaling pathways. *Sci Signal* 7:ra44. doi: 10.1126/scisignal.2005261
39. Au KM, Min Y, Tian X, et al (2015) Improving Cancer Chemoradiotherapy Treatment by Dual Controlled Release of Wortmannin and Docetaxel in Polymeric Nanoparticles. *ACS Nano*. doi: 10.1021/acsnano.5b02913

40. Avan A, Narayan R, Giovannetti E, Peters GJ (2016) Role of Akt signaling in resistance to DNA-targeted therapy. *World J Clin Oncol* 7:352. doi: 10.5306/wjco.v7.i5.352
41. Wheeler DL, Dunn EF, Harari PM (2010) Understanding resistance to EGFR inhibitors-impact on future treatment strategies. *Nat Rev Clin Oncol* 7:493–507. doi: 10.1038/nrclinonc.2010.97
42. van der Meel R, Oliveira S, Altintas I, et al (2013) Inhibition of tumor growth by targeted anti-EGFR/IGF-1R nanobullets depends on efficient blocking of cell survival pathways. *Mol Pharm* 10:3717–27. doi: 10.1021/mp400212v
43. Da Silva CG, Honeywell RJ, Dekker H, Peters GJ (2015) Physicochemical properties of novel protein kinase inhibitors in relation to their substrate specificity for drug transporters. *Expert Opin Drug Metab Toxicol* 11:703–17. doi: 10.1517/17425255.2015.1006626
44. Wilson RC, Doudna JA (2013) Molecular mechanisms of RNA interference. *Annu Rev Biophys* 42:217–39. doi: 10.1146/annurev-biophys-083012-130404
45. Yin H, Kanasty RL, Eltoukhy AA, et al (2014) Non-viral vectors for gene-based therapy. *Nat Rev Genet* 15:541–555. doi: 10.1038/nrg3763
46. Kay MA (2011) State-of-the-art gene-based therapies: the road ahead. *Nat Rev Genet* 12:316–28. doi: 10.1038/nrg2971
47. Kiang A, Hartman ZC, Everett RS, et al (2006) Multiple innate inflammatory responses induced after systemic adenovirus vector delivery depend on a functional complement system. *Mol Ther* 14:588–98. doi: 10.1016/j.ymthe.2006.03.024
48. Ma Z, Li J, He F, et al (2005) Cationic lipids enhance siRNA-mediated interferon response in mice. *Biochem Biophys Res Commun* 330:755–9. doi: 10.1016/j.bbrc.2005.03.041
49. Zalipsky S (1995) Chemistry of polyethylene glycol conjugates with biologically active molecules. *Adv Drug Deliv Rev* 16:157–182. doi: 10.1016/0169-409X(95)00023-Z
50. Yoon HY, Son S, Lee SJ, et al (2014) Glycol chitosan nanoparticles as specialized cancer therapeutic vehicles: sequential delivery of doxorubicin and Bcl-2 siRNA. *Sci Rep* 4:6878. doi: 10.1038/srep06878
51. Zhang Y, Peng L, Mumper RJ, Huang L (2013) Combinational delivery of c-myc siRNA and nucleoside analogs in a single, synthetic nanocarrier for targeted cancer therapy. *Biomaterials* 34:8459–68. doi: 10.1016/j.biomaterials.2013.07.050
52. Zhang Y, Schwerbrock NM, Rogers AB, et al (2013) Codelivery of VEGF siRNA and gemcitabine monophosphate in a single nanoparticle formulation for effective treatment of NSCLC. *Mol Ther* 21:1559–69. doi: 10.1038/mt.2013.120

53. Adema AD, Bijnsdorp I V, Sandvold ML, et al (2009) Innovations and opportunities to improve conventional (deoxy)nucleoside and fluoropyrimidine analogs in cancer. *Curr Med Chem* 16:4632–43.
54. Peters GJ (2014) Novel Developments in the Use of Antimetabolites. *Nucleosides, Nucleotides and Nucleic Acids* 33:358–374. doi: 10.1080/15257770.2014.894197
55. Hooijberg JH, de Vries NA, Kaspers GJL, et al (2006) Multidrug resistance proteins and folate supplementation: therapeutic implications for antifolates and other classes of drugs in cancer treatment. *Cancer Chemother Pharmacol* 58:1–12. doi: 10.1007/s00280-005-0141-1
56. Swain SM, Whaley FS, Ewer MS (2003) Congestive heart failure in patients treated with doxorubicin: a retrospective analysis of three trials. *Cancer* 97:2869–79. doi: 10.1002/cncr.11407
57. Gottesman MM, Pastan IH (2015) The Role of Multidrug Resistance Efflux Pumps in Cancer: Revisiting a JNCI Publication Exploring Expression of the MDR1 (P-glycoprotein) Gene. *J Natl Cancer Inst* 107:djv222. doi: 10.1093/jnci/djv222
58. Nobili S, Landini I, Mazzei T, Mini E (2012) Overcoming tumor multidrug resistance using drugs able to evade P-glycoprotein or to exploit its expression. *Med Res Rev* 32:1220–62. doi: 10.1002/med.20239
59. Lemos C, Jansen G, Peters GJ (2008) Drug transporters: recent advances concerning BCRP and tyrosine kinase inhibitors. *Br J Cancer* 98:857–862. doi: 10.1038/sj.bjc.6604213
60. Cruz LJ, Tacke PJ, Bonetto F, et al (2011) Multimodal Imaging of Nanovaccine Carriers Targeted to Human Dendritic Cells. *Mol Pharm* 8:520–531. doi: 10.1021/mp100356k
61. Cruz LJ, Tacke PJ, Zeelenberg IS, et al (2014) Tracking Targeted Bimodal Nanovaccines: Immune Responses and Routing in Cells, Tissue, and Whole Organism. *Mol Pharm* 11:4299–4313. doi: 10.1021/mp400717r
62. Cruz LJ, Tacke PJ, Eich C, et al (2017) Controlled release of antigen and Toll-like receptor ligands from PLGA nanoparticles enhances immunogenicity. *Nanomedicine* 12:491–510. doi: 10.2217/nnm-2016-0295
63. Dong X, Mattingly CA, Tseng MT, et al (2009) Doxorubicin and paclitaxel-loaded lipid-based nanoparticles overcome multidrug resistance by inhibiting P-glycoprotein and depleting ATP. *Cancer Res* 69:3918–26. doi: 10.1158/0008-5472.CAN-08-2747
64. Liang X-J, Meng H, Wang Y, et al (2010) Metallofullerene nanoparticles circumvent tumor resistance to cisplatin by reactivating endocytosis. *Proc Natl Acad Sci U S A* 107:7449–54. doi: 10.1073/pnas.0909707107

65. Zeng X, Morgenstern R, Nyström AM (2014) Nanoparticle-directed sub-cellular localization of doxorubicin and the sensitization breast cancer cells by circumventing GST-mediated drug resistance. *Biomaterials* 35:1227–39. doi: 10.1016/j.biomaterials.2013.10.042
66. Xu L, Li H, Wang Y, et al (2014) Enhanced activity of doxorubicin in drug resistant A549 tumor cells by encapsulation of P-glycoprotein inhibitor in PLGA-based nanovectors. *Oncol Lett* 7:387–392. doi: 10.3892/ol.2013.1711
67. Sa G, Das T (2008) Anti cancer effects of curcumin: cycle of life and death. *Cell Div* 3:14. doi: 10.1186/1747-1028-3-14
68. Choi BH, Kim CG, Lim Y, et al (2008) Curcumin down-regulates the multidrug-resistance *mdr1b* gene by inhibiting the PI3K/Akt/NF kappa B pathway. *Cancer Lett* 259:111–8. doi: 10.1016/j.canlet.2007.10.003
69. Chearwae W, Wu C-P, Chu H-Y, et al (2006) Curcuminoids purified from turmeric powder modulate the function of human multidrug resistance protein 1 (ABCC1). *Cancer Chemother Pharmacol* 57:376–88. doi: 10.1007/s00280-005-0052-1
70. Chearwae W, Anuchapreeda S, Nandigama K, et al (2004) Biochemical mechanism of modulation of human P-glycoprotein (ABCB1) by curcumin I, II, and III purified from Turmeric powder. *Biochem Pharmacol* 68:2043–52. doi: 10.1016/j.bcp.2004.07.009
71. Aggarwal BB, Shishodia S, Takada Y, et al (2005) Curcumin suppresses the paclitaxel-induced nuclear factor-kappaB pathway in breast cancer cells and inhibits lung metastasis of human breast cancer in nude mice. *Clin Cancer Res* 11:7490–8. doi: 10.1158/1078-0432.CCR-05-1192
72. Limtrakul P, Chearwae W, Shukla S, et al (2007) Modulation of function of three ABC drug transporters, P-glycoprotein (ABCB1), mitoxantrone resistance protein (ABCG2) and multidrug resistance protein 1 (ABCC1) by tetrahydrocurcumin, a major metabolite of curcumin. *Mol Cell Biochem* 296:85–95. doi: 10.1007/s11010-006-9302-8
73. Sharma RA, McLelland HR, Hill KA, et al (2001) Pharmacodynamic and pharmacokinetic study of oral Curcuma extract in patients with colorectal cancer. *Clin Cancer Res* 7:1894–900.
74. Pramanik D, Campbell NR, Das S, et al (2012) A composite polymer nanoparticle overcomes multidrug resistance and ameliorates doxorubicin-associated cardiomyopathy. *Oncotarget* 3:640–50.
75. Duan J, Mansour HM, Zhang Y, et al (2012) Reversion of multidrug resistance by co-encapsulation of doxorubicin and curcumin in chitosan/poly(butyl cyanoacrylate) nanoparticles. *Int J Pharm* 426:193–201. doi: 10.1016/j.ijpharm.2012.01.020
76. Pene F, Courtine E, Cariou A, Mira J-P (2009) Toward theragnostics. *Crit Care Med* 37:S50-8. doi: 10.1097/CCM.0b013e3181921349

77. Bao G, Mitragotri S, Tong S (2013) Multifunctional nanoparticles for drug delivery and molecular imaging. *Annu Rev Biomed Eng* 15:253–82. doi: 10.1146/annurev-bioeng-071812-152409
78. Kawakami Y, Yaguchi T, Sumimoto H, et al (2013) Cancer-induced immunosuppressive cascades and their reversal by molecular-targeted therapy. *Ann N Y Acad Sci* 1284:80–6. doi: 10.1111/nyas.12094
79. Rahimian S, Fransen MF, Kleinovink JW, et al (2015) Polymeric microparticles for sustained and local delivery of antiCD40 and antiCTLA-4 in immunotherapy of cancer. *Biomaterials* 61:33–40. doi: 10.1016/j.biomaterials.2015.04.043
80. Lu W, Xiong C, Zhang R, et al (2012) Receptor-mediated transcytosis: a mechanism for active extravascular transport of nanoparticles in solid tumors. *J Control Release* 161:959–66. doi: 10.1016/j.jconrel.2012.05.014
81. Gao W, Wang Z, Lv L, et al (2016) Photodynamic Therapy Induced Enhancement of Tumor Vasculature Permeability Using an Upconversion Nanoconstruct for Improved Intratumoral Nanoparticle Delivery in Deep Tissues. *Theranostics* 6:1131–44. doi: 10.7150/thno.15262
82. Zhen Z, Tang W, Chuang Y-J, et al (2014) Tumor Vasculature Targeted Photodynamic Therapy for Enhanced Delivery of Nanoparticles. *ACS Nano* 8:6004–6013. doi: 10.1021/nn501134q
83. Ashton S, Song YH, Nolan J, et al (2016) Aurora kinase inhibitor nanoparticles target tumors with favorable therapeutic index in vivo. *Sci. Transl. Med.* 8:
84. Altintas I, Heukers R, van der Meel R, et al (2013) Nanobody-albumin nanoparticles (NANAPs) for the delivery of a multikinase inhibitor 17864 to EGFR overexpressing tumor cells. *J Control Release* 165:110–8. doi: 10.1016/j.jconrel.2012.11.007
85. Lam ATN, Yoon J, Ganbold E-O, et al (2014) Adsorption and desorption of tyrosine kinase inhibitor erlotinib on gold nanoparticles. *J Colloid Interface Sci* 425:96–101. doi: 10.1016/j.jcis.2014.03.032
86. Lam ATN, Yoon J, Ganbold E-O, et al (2014) Colloidal gold nanoparticle conjugates of gefitinib. *Colloids Surf B Biointerfaces* 123:61–7. doi: 10.1016/j.colsurfb.2014.08.021
87. Zhang X, Xie L, Zheng M, et al (2015) Aurora kinase inhibitors attached to iron oxide nanoparticles enhances inhibition of the growth of liver cancer cells. *J Nanoparticle Res* 17:247. doi: 10.1007/s11051-014-2708-4
88. Uckun FM, Dibirdik I, Qazi S, Yiv S (2010) Therapeutic nanoparticle constructs of a JAK3 tyrosine kinase inhibitor against human B-lineage ALL cells. *Arzneimittelforschung* 60:210–7. doi: 10.1055/s-0031-1296275

89. Dibirdik I, Yiv S, Qazi S, M. Uckun F (2010) In vivo Anti-Cancer Activity of a Liposomal Nanoparticle Construct of Multifunctional Tyrosine Kinase Inhibitor 4-(4'-Hydroxyphenyl)-Amino-6,7-Dimethoxyquinazoline. *J Nanomed Nanotechnol*. doi: 10.4172/2157-7439.1000101
90. Uckun FM, Myers DE, Cheng J, Qazi S (2015) Liposomal Nanoparticles of a Spleen Tyrosine Kinase P-Site Inhibitor Amplify the Potency of Low Dose Total Body Irradiation Against Aggressive B-Precursor Leukemia and Yield Superior Survival Outcomes in Mice. *EBioMedicine* 2:554–562. doi: 10.1016/j.ebiom.2015.04.005
91. Myers DE, Yiv S, Qazi S, et al (2014) CD19-antigen specific nanoscale liposomal formulation of a SYK P-site inhibitor causes apoptotic destruction of human B-precursor leukemia cells. *Integr Biol (Camb)* 6:766–80. doi: 10.1039/c4ib00095a
92. Uckun FM, Qazi S, Cely I, et al (2013) Nanoscale liposomal formulation of a SYK P-site inhibitor against B-precursor leukemia. *Blood* 121:4348–54. doi: 10.1182/blood-2012-11-470633
93. Dreaden EC, Kong YW, Morton SW, et al (2015) Tumor-Targeted Synergistic Blockade of MAPK and PI3K from a Layer-by-Layer Nanoparticle. *Clin Cancer Res* 1078-0432.CCR-15-0013-. doi: 10.1158/1078-0432.CCR-15-0013
94. Palvai S, More P, Mapara N, et al (2016) Self-Assembled Oleic Acid Nanoparticle Mediated Inhibition of Mitogen-Activated Protein Kinase Signaling in Combination with DNA Damage in Cancer Cells. *ChemNanoMat* 2:201–211. doi: 10.1002/cnma.201500195
95. Harfouche R, Basu S, Soni S, et al (2009) Nanoparticle-mediated targeting of phosphatidylinositol-3-kinase signaling inhibits angiogenesis. *Angiogenesis* 12:325–338. doi: 10.1007/s10456-009-9154-4
96. Vrignaud S, Hureauux J, Wack S, et al (2012) Design, optimization and in vitro evaluation of reverse micelle-loaded lipid nanocarriers containing erlotinib hydrochloride. *Int J Pharm* 436:194–200. doi: 10.1016/j.ijpharm.2012.06.026
97. Saad M, Garbuzenko OB, Minko T (2008) Co-delivery of siRNA and an anticancer drug for treatment of multidrug-resistant cancer. *Nanomedicine (Lond)* 3:761–76. doi: 10.2217/17435889.3.6.761
98. Chen Y, Wu JJ, Huang L (2010) Nanoparticles targeted with NGR motif deliver c-myc siRNA and doxorubicin for anticancer therapy. *Mol Ther* 18:828–34. doi: 10.1038/mt.2009.291
99. Chen Y, Bathula SR, Li J, Huang L (2010) Multifunctional nanoparticles delivering small interfering RNA and doxorubicin overcome drug resistance in cancer. *J Biol Chem* 285:22639–50. doi: 10.1074/jbc.M110.125906
100. Chen Y, Zhu X, Zhang X, et al (2010) Nanoparticles modified with tumor-targeting scFv deliver siRNA and miRNA for cancer therapy. *Mol Ther* 18:1650–6. doi: 10.1038/mt.2010.136

101. Shim G, Han S-E, Yu Y-H, et al (2011) Trilysinoyl oleylamide-based cationic liposomes for systemic co-delivery of siRNA and an anticancer drug. *J Control Release* 155:60–66. doi: 10.1016/j.jconrel.2010.10.017
102. Garbuzenko OB, Saad M, Pozharov VP, et al (2010) Inhibition of lung tumor growth by complex pulmonary delivery of drugs with oligonucleotides as suppressors of cellular resistance. *Proc Natl Acad Sci U S A* 107:10737–42. doi: 10.1073/pnas.1004604107
103. Ko YT, Falcao C, Torchilin VP (2009) Cationic Liposomes Loaded with Proapoptotic Peptide d -(KLAKLAK) 2 and Bcl-2 Antisense Oligodeoxynucleotide G3139 for Enhanced Anticancer Therapy. *Mol Pharm* 6:971–977. doi: 10.1021/mp900006h
104. Deng ZJ, Morton SW, Ben-Akiva E, et al (2013) Layer-by-Layer Nanoparticles for Systemic Codelivery of an Anticancer Drug and siRNA for Potential Triple-Negative Breast Cancer Treatment. *ACS Nano* 7:9571–9584. doi: 10.1021/nn4047925
105. Xu Z, Zhang Z, Chen Y, et al (2010) The characteristics and performance of a multifunctional nanoassembly system for the co-delivery of docetaxel and iSur-pDNA in a mouse hepatocellular carcinoma model. *Biomaterials* 31:916–22. doi: 10.1016/j.biomaterials.2009.09.103
106. Liu X-Q, Xiong M-H, Shu X-T, et al (2012) Therapeutic delivery of siRNA silencing HIF-1 alpha with micellar nanoparticles inhibits hypoxic tumor growth. *Mol Pharm* 9:2863–74. doi: 10.1021/mp300193f
107. Sun T-M, Du J-Z, Yao Y-D, et al (2011) Simultaneous delivery of siRNA and paclitaxel via a “two-in-one” micelleplex promotes synergistic tumor suppression. *ACS Nano* 5:1483–94. doi: 10.1021/nn103349h
108. MacDiarmid JA, Amaro-Mugridge NB, Madrid-Weiss J, et al (2009) Sequential treatment of drug-resistant tumors with targeted micelles containing siRNA or a cytotoxic drug. *Nat Biotechnol* 27:643–651. doi: 10.1038/nbt.1547
109. Tang S, Yin Q, Su J, et al (2015) Inhibition of metastasis and growth of breast cancer by pH-sensitive poly ( $\beta$ -amino ester) nanoparticles co-delivering two siRNA and paclitaxel. *Biomaterials* 48:1–15. doi: 10.1016/j.biomaterials.2015.01.049
110. Zhang L, Lu Z, Zhao Q, et al (2011) Enhanced chemotherapy efficacy by sequential delivery of siRNA and anticancer drugs using PEI-grafted graphene oxide. *Small* 7:460–4. doi: 10.1002/sml.201001522
111. Yadav S, van Vlerken LE, Little SR, Amiji MM (2009) Evaluations of combination MDR-1 gene silencing and paclitaxel administration in biodegradable polymeric nanoparticle formulations to overcome multidrug resistance in cancer cells. *Cancer Chemother Pharmacol* 63:711–22. doi: 10.1007/s00280-008-0790-y

112. Patil YB, Swaminathan SK, Sadhukha T, et al (2010) The use of nanoparticle-mediated targeted gene silencing and drug delivery to overcome tumor drug resistance. *Biomaterials* 31:358–65. doi: 10.1016/j.biomaterials.2009.09.048
113. Sureban SM, May R, Mondalek FG, et al (2011) Nanoparticle-based delivery of siDCAMKL-1 increases microRNA-144 and inhibits colorectal cancer tumor growth via a Notch-1 dependent mechanism. *J Nanobiotechnology* 9:40. doi: 10.1186/1477-3155-9-40
114. Xu X, Xie K, Zhang X-Q, et al (2013) Enhancing tumor cell response to chemotherapy through nanoparticle-mediated codelivery of siRNA and cisplatin prodrug. *Proc Natl Acad Sci U S A* 110:18638–43. doi: 10.1073/pnas.1303958110
115. Chen AM, Zhang M, Wei D, et al (2009) Co-delivery of doxorubicin and Bcl-2 siRNA by mesoporous silica nanoparticles enhances the efficacy of chemotherapy in multidrug-resistant cancer cells. *Small* 5:2673–7. doi: 10.1002/smll.200900621
116. Meng H, Liong M, Xia T, et al (2010) Engineered design of mesoporous silica nanoparticles to deliver doxorubicin and P-glycoprotein siRNA to overcome drug resistance in a cancer cell line. *ACS Nano* 4:4539–50. doi: 10.1021/nn100690m
117. Ding J, Liang T, Zhou Y, et al (2017) Hyaluronidase-triggered anticancer drug and siRNA delivery from cascaded targeting nanoparticles for drug-resistant breast cancer therapy. *Nano Res* 10:690–703. doi: 10.1007/s12274-016-1328-y
118. Wang Y, Gao S, Ye W-H, et al (2006) Co-delivery of drugs and DNA from cationic core-shell nanoparticles self-assembled from a biodegradable copolymer. *Nat Mater* Publ online 24 Sept 2006; | doi:10.1038/nmat1737 5:791. doi: 10.1038/nmat1737
119. Han L, Huang R, Li J, et al (2011) Plasmid pORF-hTRAIL and doxorubicin co-delivery targeting to tumor using peptide-conjugated polyamidoamine dendrimer. *Biomaterials* 32:1242–1252. doi: 10.1016/j.biomaterials.2010.09.070
120. Ganta S, Amiji M (2009) Coadministration of Paclitaxel and curcumin in nanoemulsion formulations to overcome multidrug resistance in tumor cells. *Mol Pharm* 6:928–39. doi: 10.1021/mp800240j
121. Jiang T, Mo R, Bellotti A, et al (2014) Gel-Liposome-Mediated Co-Delivery of Anticancer Membrane-Associated Proteins and Small-Molecule Drugs for Enhanced Therapeutic Efficacy. *Adv Funct Mater* 24:2295–2304. doi: 10.1002/adfm.201303222
122. Jiang T, Sun W, Zhu Q, et al (2015) Furin-Mediated Sequential Delivery of Anticancer Cytokine and Small-Molecule Drug Shuttled by Graphene. *Adv Mater* 27:1021–1028. doi: 10.1002/adma.201404498



123. Zhao X, Chen Q, Liu W, et al (2015) Codelivery of doxorubicin and curcumin with lipid nanoparticles results in improved efficacy of chemotherapy in liver cancer. *Int J Nanomedicine* 10:257–70. doi: 10.2147/IJN.S73322
124. Barui S, Saha S, Mondal G, et al (2014) Simultaneous delivery of doxorubicin and curcumin encapsulated in liposomes of pegylated RGDK-lipopeptide to tumor vasculature. *Biomaterials* 35:1643–56. doi: 10.1016/j.biomaterials.2013.10.074
125. Li N, Zhang C-X, Wang X-X, et al (2013) Development of targeting lonidamine liposomes that circumvent drug-resistant cancer by acting on mitochondrial signaling pathways. *Biomaterials* 34:3366–80. doi: 10.1016/j.biomaterials.2013.01.055
126. Guo L, Fan L, Ren J, et al (2011) A novel combination of TRAIL and doxorubicin enhances antitumor effect based on passive tumor-targeting of liposomes. *Nanotechnology* 22:265105. doi: 10.1088/0957-4484/22/26/265105
127. Zhang Q, Ran R, Zhang L, et al (2015) Simultaneous delivery of therapeutic antagonists with paclitaxel for the management of metastatic tumors by a pH-responsive anti-microbial peptide-mediated liposomal delivery system. *J Control Release* 197:208–18. doi: 10.1016/j.jconrel.2014.11.010
128. Liu Y, Li L-L, Qi G-B, et al (2014) Dynamic disordering of liposomal cocktails and the spatio-temporal favorable release of cargoes to circumvent drug resistance. *Biomaterials* 35:3406–15. doi: 10.1016/j.biomaterials.2013.12.089
129. Wang B-L, Shen Y, Zhang Q, et al (2013) Codelivery of curcumin and doxorubicin by MPEG-PCL results in improved efficacy of systemically administered chemotherapy in mice with lung cancer. *Int J Nanomedicine* 8:3521–31. doi: 10.2147/IJN.S45250
130. Duan X, Xiao J, Yin Q, et al (2013) Smart pH-Sensitive and Temporal-Controlled Polymeric Micelles for Effective Combination Therapy of Doxorubicin and Disulfiram. *ACS Nano* 7:5858–5869. doi: 10.1021/nn4010796
131. Guo S, Lv L, Shen Y, et al (2016) A nanoparticulate pre-chemosensitizer for efficacious chemotherapy of multidrug resistant breast cancer. *Sci Rep* 6:21459. doi: 10.1038/srep21459
132. Milane L, Duan Z, Amiji M (2011) Development of EGFR-targeted polymer blend nanocarriers for combination paclitaxel/Ionidamine delivery to treat multi-drug resistance in human breast and ovarian tumor cells. *Mol Pharm* 8:185–203. doi: 10.1021/mp1002653
133. Milane L, Duan Z, Amiji M (2011) Therapeutic efficacy and safety of paclitaxel/Ionidamine loaded EGFR-targeted nanoparticles for the treatment of multi-drug resistant cancer. *PLoS One* 6:e24075. doi: 10.1371/journal.pone.0024075

134. Acharya S, Dilnawaz F, Sahoo SK (2009) Targeted epidermal growth factor receptor nanoparticle bioconjugates for breast cancer therapy. *Biomaterials* 30:5737–50. doi: 10.1016/j.biomaterials.2009.07.008
135. Das M, Sahoo SK (2012) Folate decorated dual drug loaded nanoparticle: role of curcumin in enhancing therapeutic potential of nutlin-3a by reversing multidrug resistance. *PLoS One* 7:e32920. doi: 10.1371/journal.pone.0032920
136. Chenna V, Hu C, Pramanik D, et al (2012) A polymeric nanoparticle encapsulated small-molecule inhibitor of Hedgehog signaling (NanoHHI) bypasses secondary mutational resistance to Smoothed antagonists. *Mol Cancer Ther* 11:165–73. doi: 10.1158/1535-7163.MCT-11-0341
137. Xu Y, Chenna V, Hu C, et al (2012) Polymeric nanoparticle-encapsulated hedgehog pathway inhibitor HPI-1 (NanoHHI) inhibits systemic metastases in an orthotopic model of human hepatocellular carcinoma. *Clin Cancer Res* 18:1291–302. doi: 10.1158/1078-0432.CCR-11-0950
138. Misra R, Sahoo SK (2011) Coformulation of Doxorubicin and Curcumin in Poly(d,l-lactide-co-glycolide) Nanoparticles Suppresses the Development of Multidrug Resistance in K562 Cells.
139. Patil Y, Sadhukha T, Ma L, Panyam J (2009) Nanoparticle-mediated simultaneous and targeted delivery of paclitaxel and tariquidar overcomes tumor drug resistance. *J Control Release* 136:21–29. doi: 10.1016/j.jconrel.2009.01.021
140. Ediriwickrema A, Zhou J, Deng Y, Saltzman WM (2014) Multi-layered nanoparticles for combination gene and drug delivery to tumors. *Biomaterials* 35:9343–54. doi: 10.1016/j.biomaterials.2014.07.043
141. Zhao Y, Huan M, Liu M, et al (2016) Doxorubicin and resveratrol co-delivery nanoparticle to overcome doxorubicin resistance. *Sci Rep* 6:35267. doi: 10.1038/srep35267



8

# GENERAL DISCUSSION

# General discussion

---

Immunotherapy is a rapidly growing class of cancer therapies that attempts to harness the power of the immune system to eradicate cancer cells. Despite great progress in recent years, a significant proportion of cancer patients remain unresponsive to (any) treatment and are in a dire need for new or improved therapies. The integration of nanotechnology in medicine has been remarkable in the last years, specifically concerning the improvement of the therapeutic index of existing drugs. Namely, nanotechnology can resolve specific problems faced by existing drugs, such as drug efflux mediated drug resistance, but also by enabling local slow and controlled drug release, as well as to enable the uptake of insoluble drugs by tumor cells. The integration of nanotechnology and immunotherapy, and specifically immunomodulatory drugs, brings the best of these two disciplines together to establish a new level of therapeutic benefit to eradicate cancer.

In this thesis, a novel combination of immunomodulatory drugs was tested that consisted of poly (I:C), resiquimod (also known as R848), and CCL20 (also known as MIP3 $\alpha$ ) for the treatment of cancer. The rationally combined drugs aim was to modulate the tumor microenvironment by reducing the immunosuppressive state, thereby introducing a less favorable milieu for cancer cells to survive immune attack. The combination of poly (I:C), an agonist of the endosomal Toll-Like Receptor (TLR)3, with R848, an agonist of the endosomal TLR7/8, was chosen based on the work of Tan et al. that described that the combination of poly (I:C) and R848, from several other combinations of TLR-agonists, induced the highest synergy in cytokine production in macrophages [1]. This was also later observed in human DCs and CD4 T cells [2–4] of which the mechanism was further studied

by Kreutz et al [5]. The effects on the immune system of poly (I:C) and R848 separately are quite distinct and it may therefore be a powerful combination that enhances different aspects of immune responses. Another advantage of utilizing agonists that target endosomal (viral sensing) TLRs, and not cell surface (bacterial sensing) TLRs (e.g. TLR2/4), is of relevance for human translational potential. Since humans are up to hundred fold more lethally sensitive to systemic introduction of endotoxins of bacterial origin (e.g. LPS) compared to rodents such as mice and rats, it may declassify the usage of TLR2/4 agonists for direct cancer treatment [6]. Moreover, an increasing number of studies are revealing that the activation of surface TLR2/4, but much less so of endosomal TLR3/7/8/9, in tumors can have unwarranted pro-tumor effects [7]. On the other hand, humans can tolerate, up to a degree, the systemic introduction of TLR-agonists for the activation of endosomal TLRs (i.e. TLR3/7/8/9) without acute morbidity [8]. In part this is due to poor uptake of these TLR-agonists in somatic tissue since their respective receptors are located intracellularly but this also indicates that it is difficult to achieve an effective dose in the tumor. Alternatively, these endosomal TLR-agonists could be injected at high doses in the tumor directly to force a higher uptake but a swift diffusion of these drugs from the tumor microenvironment into the blood would greatly reduce the efficacy and likely induce unwarranted systemic side-effects [9]. In addition to Poly (I:C) and R848, MIP3 $\alpha$  was added to the drug combination to enhance the recruitment of dendritic cells and lymphocytes to the tumor area [10–12]. The use of MIP3 $\alpha$  in cancer treatment has been tested before and was found to be controversial. Although MIP3 $\alpha$  can initiate the recruitment of these cells, the sole treatment of tumors with MIP3 $\alpha$  (without any other treatment or drugs) in cancer patients has led to pleiotropic outcomes [13]. However, this reported phenomenon could indicate that the mere recruitment of immune cells to the tumor is insufficient because to the negative effects of the immune suppressed tumor microenvironment on these cells, and that aspect remained unaddressed. Indeed, Fushimi et al. has shown that MIP3 $\alpha$  can induce anti-cancer effects directly but this observation was dependent on the tumor immune (suppressed) state and of the cancer model (i.e. more immunogenic, more responsive) [14]. In this sense, the combination of MIP3 $\alpha$  with Poly (I:C) and/or R848 to ameliorate the suppressed environment, is rationally justifiable and we hypothesized less pleiotropic outcomes and instead more additive or synergism in therapeutic outcomes.

As described above, the poor uptake of Poly (I:C) and R848 by tumor cells and the swift diffusion of these drugs from the tumor microenvironment could hamper therapy responses. Specifically to address these issues, nanotechnology in the

form of nanoparticles can provide solutions by enhancing the uptake of Poly (I:C) and R848 by tumor cells, via pinocytosis, while simultaneously enhancing the slow and controlled release both intra and extracellularly [15, 16]. Both properties can be utilized when the nanoparticles are administered directly in the tumor. There, a significant portion of the intact nanoparticles is taken-up by cells, where they first start to slowly release their cargo in early and late endosomes activating TLR3 and 7/8, and then in lysosomes after which the remaining cargo is released in the cytoplasm [16]. The MIP3 $\alpha$  that was also released intracellularly, would be lost in the lysosomes. However, the fraction of nanoparticles that was not taken-up by any cells also start to slowly release their cargo in the extracellular space, which includes the building of a gradient concentration of MIP3 $\alpha$ .

In **chapter 3**, it was determined whether the PLGA nanoparticle backbone technology could indeed reduce drug diffusion from the tumor area when injected directly in the tumor, subcutaneously elsewhere, or intravenously. In addition, the biodistribution into vital organs and blood concentration of a drug surrogate (i.e. ICG) was studied to determine the drug release kinetics. Here it is shown that the intratumoral injection of the nanoparticles is the most effective administration method to achieve the highest concentration of nanoparticles in the tumor. Generally, the method of intratumoral administration of cancer drugs is rapidly increasing for several tumor types, including less accessible tumors in the thorax and abdominal area [17, 18]. The same trend is also applicable for the administration of nanomedicine. For instance, Hensify® received recent approval by the EMA as a nanoparticle formulation for the combinatorial treatment of sarcoma to be administered by intratumoral injection [19]. Although the treatment is performed locally and the nanoparticles are unlikely to reach the metastases themselves, systemic protection for metastases control can be attainable via the abscopal effect, by which locally activated tumor-specific immune cells will migrate and eradicate distant lesions.[20]. Hence, the intratumoral administration method was chosen to establish a proof of principle for the nanoparticle technology developed specifically for the work presented in this thesis.

In **chapter 4**, the efficacy of the nanoparticle mediated therapy with poly (I:C), R848, and MIP3 $\alpha$  was tested in vivo on the TC-1 cancer model. The TC-1 model, compared to MC-38 or CT-26, is considerably less responsive to conventional (immune)therapies, including chemotherapy, except for specific immunotherapy in the form of a therapeutic cancer vaccine. Hence, the TC-1 model is one of the most relevant cancer models for human cancer patients, because it very difficult to treat



and cure, similar to human cancers, and as such by achieving TC-1 cures, it would increase the translation relevance to human cancers. When TC-1 tumor-bearing mice were treated with the nanoparticle mediated treatment with poly (I:C), R848, and MIP3 $\alpha$ , they were found to be irresponsive. This could indicate that, despite the presence of highly immunogenic antigens in TC-1 cells, no effective immunity (i.e. cognate T cells) is present that can be enhanced by the nanoparticle treatment. To overcome this problem, doxorubicin was added to the drug combination to induce TC-1 cancer cell death and to release antigens to which immune cells could target. This resulted in a nanoparticle mediated chemoimmunotherapy modality consisted of poly (I:C), R848, MIP3 $\alpha$ , and of doxorubicin. The co-loading of doxorubicin not only did improve the overall survival (cures) but also improved the progression-free survival time, which was nearly doubled. Moreover, it was established that the nanoparticle mediated delivery of these drugs for the therapeutic efficacy is pivotal, as established by the observation that TC-1 tumor-bearing mice treated with equal concentrations of the drugs injected intratumorally (but not loaded in nanoparticles) induced no cures and the gain of the progression-free survival time was not nearly as significant. The MC-38 model was found to be much more responsive to the chemoimmunotherapy modality than TC-1, but also in this model the nanoparticle mediated delivery was found pivotal to achieve higher percentages of cures. These results warranted a more in-depth literature study of the current development stages of chemoimmunotherapy and most specifically when the treatment is mediated by nanotechnology. The results of the literature study and the discussion thereof is presented in **chapter 2**.

In **chapter 5**, the individual therapeutic potential of poly (I:C), R848, and MIP3 $\alpha$  was studied. Since the TC-1 model is responsive to a therapeutic cancer vaccine, but generally little to no cures are attained long-term with only vaccination, it provided an ideal basis to establish possible improvements with other therapeutic combinations. When mice bearing TC-1 tumors were vaccinated and the tumors treated with nanoparticles containing either one or more combination of drugs, it was observed that both poly (I:C) and R848, but not MIP3 $\alpha$ , separately increased the percentages of overall survival. However, the triple combination of poly (I:C), R848, and of MIP3 $\alpha$  induced significantly better overall survival outcomes and the progression-free survival time was nearly doubled. The same combination of drugs was also tested on the RMA cancer model. Although a significant therapy response was attained, the RMA model was found to be much less responsive than the TC-1 model. This observation underlines the potential of the modality to improve distinct therapeutic cancer vaccines, but the actual enhancing potential of the modality

is dependent on the model and on the initial potency of the therapeutic cancer vaccine itself. Nonetheless, this study established a proof of principle that the immune modulation of tumors with the nanoparticle delivery of poly (I:C), R848, and MIP3 $\alpha$  can improve response of therapeutic cancer vaccines.

In **chapter 6**, the nanoparticle modality was combined with photodynamic therapy and tested on the TC-1, MC-38, and CT-26 cancer models. The co-treatment induced high overall survival percentages on both MC-38 and CT-26 models. Also, the nanoparticle treatment alone without photodynamic therapy enhanced the overall survival percentages of MC-38 and of CT-26. However, the co-treatment with photodynamic therapy did not improve the overall survival percentages on the TC-1 model, however, the progression-free survival time was observed to increase significantly. Kleinovink et al. has reported that the local treatment of tumors with photodynamic therapy affects the growth of distant tumors, a process that is likely mediated by the abscopal effect via CD8 cytotoxic effector T cells [21]. In chapter 6, this effect was reproduced and further enhanced with the co-treatment of the nanoparticle modality. This effect that was most pronounced in the CT-26 cancer model. This suggests that the combination of photodynamic therapy with immunomodulatory nanoparticles are an ideal combination for the treatment of tumors and of metastases.

## FUTURE PERSPECTIVES

To date, fifty-one nanomedicine formulations of existing drugs are FDA/EMA approved and are used to treat cancer in humans, and many more are in clinical trials or pending approval [22, 23]. In general, nanomedicine formulations tend to face additional problems during research & development phases and the production under GMP conditions before attaining clinical approval compared to 'regular' drug development [24–26]. For instance, common variations between production batches during smaller scale production and pre-clinical phase, issues during large-scale manufacturing, and overall cost-effectiveness compared to 'regular' drugs are additional obstacles faced during the development of nanoparticle formulations [27]. Despite these caveats, the advantages of nanoparticle formulations can outweigh the disadvantages, but only in specific cases. One case is Doxil®, a nanomedicine formulation of doxorubicin [28]. In this example, Doxil® resolves cardiotoxicity by reducing biodistribution (i.e. to the heart; as it is a major limiting adverse effect of doxorubicin), which Doxil® reduces significantly without loss of therapeutic efficacy. Although the production costs are higher

and technically more difficult to produce than doxorubicin, Doxil® is a common chemotherapy administered to cancer patients for the treatment of several cancer types. However, in many other cases the nano formulation products were discontinued in early clinical phases due to a discrepancy between preclinical and clinical outcomes. The safe delivery of drugs to cancer cells, while sparing healthy cells, is commonly claimed but this effect is often later not observed in cancer patients [29, 30]. Since many applications of nanomedicine are currently designed as therapeutics for the treatment of cancer via systemic administration (i.e. intravenous administration) and did show significant improvement and therapeutic effect in preclinical (murine) models, they also often fail to show improvement in clinical trials. Arguably, one of the several reasons for this failure is related to the enhanced permeability and retention (EPR) effect. Many publications regarding nanomedicine formulations of oncological drugs lean greatly on the premises of the EPR effect to explain the observed therapeutic effects observed in mice. However, the existence of EPR effect in human cancers is of a strong debate and even if it exists, whether the EPR effect may be pronounced enough and as such, whether EPR-dependent nanomedicine formulations present any value for large scale application for the treatment of human cancers if they are truly dependent on the EPR effect for the therapeutic efficacy. Another reason for nanomedicine discontinuation is the considerable pathological and physiological variations between cancer patients compared to the uniformity of tumor specific preclinical (murine) models, albeit this is also applicable for non-nanomedicine formulations. However, this suggests that the putative absence of the EPR effect is not the only reason for the unsuccessful application of nanomedicine drugs in clinical trials. A potential solution for this problem may be the intratumoral administration of the nanomedicine, which would be less dependent on the EPR effect, and is in fact already becoming a more common method of administration indeed. Another potential solution that would not depend on the EPR effect to access cancer cells directly is the active extravasation of nanoparticles into tumors, but progression in this area is slow [31]. On the other hand, the application of nanomedicine to improve immunotherapeutics, that largely target immune cells rather than cancer cells, would also not depend on the EPR effect. As such, the outlook on the future of nanomedicine is still looking promising and likely to improve the therapeutic index of many drugs in the future but researchers should consider the known disadvantages of nanomedicine application during the nanomedicine design phase to reduce early clinical trial failures.

Nonetheless, new proof of principle research exploring bright new ideas in the field of nanomedicine research are still accomplished and are pushing the field forward. Another aspect to be considered are the varying therapy responses between the different cancer models to the same therapy. For instance, it would be interesting to determine which populations of immune cells are pivotal for tumor regressions after treatment in these distinct models. This could be studied in the TC-1 model by combining the therapeutic cancer vaccine with the immune modulation nanoparticles and then perform cell type clonal deletions of NK cells, macrophages, etc. The contribution of both adaptive and of the innate immune system could be further established by depleting CD8 T cells while applying therapeutic pressure with immune modulatory nanoparticles (targeting innate immune cells) in the tumor. The dose-response of the immunomodulatory nanoparticles was not determined in this work, but it is probably a relevant aspect for therapeutic efficacy. For instance, it has been described that the dose concentration of STING-agonist in the tumor determine the type of immune response, and it is currently not know whether this is similar for TLR-agonists [32]. Moreover, the effectiveness of the immunomodulatory nanoparticles combined with different immune checkpoint inhibitors, such as those targeted against PD-1, CTLA-4, LAG-3, or other small molecules, was not studied here and the combination is likely be of great therapeutic benefit.

Another important fact to be considered is that successes of pre-clinical mice studies are not always reproducible in clinical studies in humans. Should in the future the immunomodulatory nanoparticles presented in this thesis be considered for a future clinical trial, then the combination of with other ablative modalities would be suggested because of the induction of abscopal effects as indicated with chemotherapy (chapter 4) or photodynamic therapy (chapter 6). Similarly, the potential to improve the efficacy of therapeutic cancer vaccines with the immunomodulatory nanoparticles could also be further studied for cancer patients eligible for such specific immunotherapy.

Besides the challenges of production under GMP conditions of the immunomodulatory nanoparticles, neither poly (I:C), resiquimod, or CCL20 are currently FDA/EMA approved for the direct therapy of cancer. Only resiquimod is approved for topical application in the treatment of cutaneous T cell lymphoma. Also, the patents of these immune adjuvants have expired decades ago and unfortunately, drugs that are not protected by non-expired patents are often

considered economically non-viable, specially to larger pharmaceutical companies. However, there are subsidies and procedures available within the European Union and the EMA to conduct clinical trials and the economic exploitation of (orphan) drugs. Alternately, novel and perhaps more powerful immune adjuvants currently in development should consider the usage of nanomedicine technology as well as the intratumoral administration for possible improved therapeutic outcomes.

## CONCLUSIONS

The work presented in this thesis forms the basis of a proof of principle treatment for the immunomodulation of tumors upon the intratumoral administration of poly (I:C), R848, and MIP3 $\alpha$  in mice. The nanoparticle mediated delivery of these drugs was repeatedly shown to be pivotal for enhanced therapeutic outcomes. A discrepancy of responses to this treatment was observed between different cancer models, since the modality independently of ablative co-modalities was quite effective to treat the colon cancer models MC-38 and CT-26, but not the TC-1 or RMA models. When combined with ablative co-modalities, the immunomodulatory nanoparticles have shown remarkable good adjuvant potential when combined with chemotherapy and photodynamic therapy, but also with therapeutic cancer vaccines in the TC-1 and RMA models. This underlines the therapeutic benefit of the combinational treatment of these modalities with immunomodulatory nanoparticles due to their enhancing potential of the abscopal effect to control distant metastases. Furthermore, it was established that the combination of poly (I:C) and R848 is of therapeutic benefit and that the addition of MIP3 $\alpha$  increases the therapeutic potential further. Mechanistically, a phenotype shift of tumor-associated macrophages towards inflammatory monocytes within tumors and tumor-draining lymph nodes was recurrently observed, which underlines the importance of the collaboration between the adaptive and innate immunity to achieve durable anti-cancer responses. Collectively, the immunomodulatory nanoparticles have great potential to mediate the local controlled delivery of synergistic drug combinations and can be further tailor-made as an ideal adjuvant therapy for exiting treatment modalities of several different cancer types.

## REFERENCES

- [1] Ting Tan, R. S.; Lin, B.; et al. The Synergy in Cytokine Production through MyD88-TRIF Pathways Is Co-Ordinated with ERK Phosphorylation in Macrophages. *Immunol. Cell Biol.* 2013; 91: 377–387.
- [2] Pearson, F. E.; Chang, K.; et al. Activation of Human CD141 + and CD1c + Dendritic Cells in Vivo with Combined TLR3 and TLR7/8 Ligation. *Immunol. Cell Biol.* 2018; 96: 390–400.
- [3] Surendran, N.; Simmons, A.; et al. TLR Agonist Combinations That Stimulate Th Type I Polarizing Responses from Human Neonates. *Innate Immun.* 2018; 24: 240–251.
- [4] Madera, R. F.; Wang, J. P.; et al. The Combination of Early and Rapid Type I IFN, IL-1 $\alpha$ , and IL-1 $\beta$  Production Are Essential Mediators of RNA-Like Adjuvant Driven CD4+ Th1 Responses. *PLoS One* 2011; 6: e29412.
- [5] Kreutz, M.; Bakdash, G.; et al. Type I IFN-Mediated Synergistic Activation of Mouse and Human DC Subsets by TLR Agonists. *Eur. J. Immunol.* 2015; 45: 2798–2809.
- [6] Munford, R. S. Murine Responses to Endotoxin: Another Dirty Little Secret? *J. Infect. Dis.* 2010; 201: 175–177.
- [7] Kaczanowska, S.; Joseph, A. M.; et al. TLR Agonists: Our Best Frenemy in Cancer Immunotherapy. *J. Leukoc. Biol.* 2013; 93: 847–863.
- [8] Shi, M.; Chen, X.; et al. Application Potential of Toll-like Receptors in Cancer Immunotherapy: Systematic Review. *Medicine (Baltimore)*. 2016; 95: e3951.
- [9] Engel, A. L.; Holt, G. E.; et al. The Pharmacokinetics of Toll-like Receptor Agonists and the Impact on the Immune System. *Expert Review of Clinical Pharmacology*, 2011, 4, 275–289.
- [10] Dieu, M. C.; Vanbervliet, B.; et al. Selective Recruitment of Immature and Mature Dendritic Cells by Distinct Chemokines Expressed in Different Anatomic Sites. *J. Exp. Med.* 1998; 188: 373–386.
- [11] Liao, F.; Rabin, R. L.; et al. CC-Chemokine Receptor 6 Is Expressed on Diverse Memory Subsets of T Cells and Determines Responsiveness to Macrophage Inflammatory Protein 3 Alpha. *J. Immunol.* 1999; 162: 186–194.
- [12] Al-Aoukaty, A.; Rolstad, B.; et al. MIP-3alpha, MIP-3beta and Fractalkine Induce the Locomotion and the Mobilization of Intracellular Calcium, and Activate the Heterotrimeric G Proteins in Human Natural Killer Cells. *Immunology* 1998; 95: 618–624.
- [13] Ranasinghe, R.; Eri, R. Modulation of the CCR6-CCL20 Axis: A Potential Therapeutic Target in Inflammation and Cancer. *Medicina (B. Aires)*. 2018; 54: .

- [14] Fushimi, T.; Kojima, A.; et al. Macrophage Inflammatory Protein 3alpha Transgene Attracts Dendritic Cells to Established Murine Tumors and Suppresses Tumor Growth. *J. Clin. Invest.* 2000; 105: 1383–1393.
- [15] Hines, D. J.; Kaplan, D. L. Poly(Lactic-Co-Glycolic) Acid-Controlled-Release Systems: Experimental and Modeling Insights. *Crit. Rev. Ther. Drug Carrier Syst.* 2013; 30: 257–276.
- [16] Cartiera, M. S.; Johnson, K. M.; et al. The Uptake and Intracellular Fate of PLGA Nanoparticles in Epithelial Cells. *Biomaterials* 2009; 30: 2790–2798.
- [17] Hamid, O.; Ismail, R.; et al. Intratumoral Immunotherapy—Update 2019. *Oncologist* 2020; 25: .
- [18] Hong, W. X.; Haebe, S.; et al. Intratumoral Immunotherapy for Early-Stage Solid Tumors. *Clinical cancer research : an official journal of the American Association for Cancer Research*, 2020, 26, 3091–3099.
- [19] Bonvalot, S.; Rutkowski, P. L.; et al. NBTXR3, a First-in-Class Radioenhancer Hafnium Oxide Nanoparticle, plus Radiotherapy versus Radiotherapy Alone in Patients with Locally Advanced Soft-Tissue Sarcoma (Act.In.Sarc): A Multicentre, Phase 2–3, Randomised, Controlled Trial. *Lancet Oncol.* 2019; 20: 1148–1159.
- [20] Kaminski, J. M.; Shinohara, E.; et al. The Controversial Abscopal Effect. *Cancer Treat. Rev.* 2005; 31: 159–172.
- [21] Kleinovink, J. W.; Fransen, M. F.; et al. Photodynamic-Immune Checkpoint Therapy Eradicates Local and Distant Tumors by CD8 + T Cells. *Cancer Immunol. Res.* 2017; 5: 832–838.
- [22] Bobo, D.; Robinson, K. J.; et al. Nanoparticle-Based Medicines: A Review of FDA-Approved Materials and Clinical Trials to Date. *Pharm. Res.* 2016; 33: 2373–2387.
- [23] Anselmo, A. C.; Mitragotri, S. Nanoparticles in the Clinic: An Update. *Bioeng. Transl. Med.* 2019; 4: .
- [24] Shi, J.; Kantoff, P. W.; et al. Cancer Nanomedicine: Progress, Challenges and Opportunities. *Nature Reviews Cancer*, 2017, 17, 20–37.
- [25] Heiligtag, F. J.; Niederberger, M. The Fascinating World of Nanoparticle Research. *Materials Today*, 2013, 16, 262–271.
- [26] Santiago, I. Nanoscale Active Matter Matters: Challenges and Opportunities for Self-Propelled Nanomotors. *Nano Today* 2018; 19: 11–15.
- [27] Hua, S.; de Matos, M. B. C.; et al. Current Trends and Challenges in the Clinical Translation of Nanoparticulate Nanomedicines: Pathways for Translational Development and Commercialization. *Frontiers in Pharmacology*, 2018, 9, 790.
- [28] Gyöngyösi, M.; Lukovic, D.; et al. Liposomal Doxorubicin Attenuates Cardiotoxicity via Induction of Interferon-Related DNA Damage Resistance. *Cardiovasc. Res.* 2020; 116: 970–982.

- [29] Pasut, G. Grand Challenges in Nano-Based Drug Delivery. *Front. Med. Technol.* 2019; 1: 1.
- [30] Wilhelm, S.; Tavares, A. J.; et al. Analysis of Nanoparticle Delivery to Tumours. *Nature Reviews Materials*, 2016, 1, 1–12.
- [31] Moghimi, S. M.; Simberg, D. Nanoparticle Transport Pathways into Tumors. *J. Nanoparticle Res.* 2018; 20: .
- [32] Sivick, K. E.; Desbien, A. L.; et al. Magnitude of Therapeutic STING Activation Determines CD8+ T Cell-Mediated Anti-Tumor Immunity. *Cell Rep.* 2018; 25: 3074-3085.e5







# Appendices

Nederlandse samenvatting

Dankwoord

Curriculum Vitae

List of publications

## **Nederlandse samenvatting**

In dit proefschrift zijn de effecten van een nieuwe vorm van immunotherapie onderzocht en hoe deze ingezet kan worden tegen verschillende typen kankers. De onderzochte immunotherapie is gebaseerd op het injecteren van nanopartikels geladen met verschillende immunologisch actieve moleculen (immunomodulerende nanopartikels) die het afweersysteem kunnen moduleren om kankercellen efficiënter te laten vernietigen. De effectiviteit van deze immunomodulerende nanopartikels zijn bestudeerd op verschillende muizenmodellen en onderzocht als alleenstaande behandeling of in combinatie met andere bekende therapieën, zoals chemotherapie, vaccinatie, of fotodynamische therapie.

In **hoofdstuk 2** wordt een overzicht gegeven van de bestaande literatuur over de combinatie van chemo- en immunotherapie met behulp van nanopartikels. Tevens wordt de mate van immunogeniciteit van de verschillende type chemotherapieën en het belang van het type celdood dat daarmee wordt geïnduceerd voor het afweersysteem bediscussieerd.

In **hoofdstuk 3** wordt bestudeerd wat het effect is van drie verschillende vormen van toediening van nanopartikels, namelijk via de intratumorale, elders subcutane, of intraveneuze toediening. Specifiek wordt hierbij gekeken naar de bio-distributie en de bloedzuiveringssnelheid van nanopartikels die geladen zijn met een fluorescerende stof. Om dit te bepalen is gebruik gemaakt van in vivo beeldvorming en ex vivo orgaan analyses.

In **hoofdstuk 4** is een aangepaste vorm van de immunomodulerende nanopartikels toegepast. Hierbij worden de nanopartikels ook geladen met doxorubicine, een bekend chemotherapeuticum. Op basis van de bevindingen beschreven in hoofdstuk 2, is doxorubicine gekozen wegens de brede toepassing in de kliniek en de goede fysicochemische eigenschappen dat zich goed leent om beladen te worden in nanopartikels. In dit hoofdstuk wordt bepaald of agressieve en therapie resistente kankermodellen vatbaar zijn deze chemoimmunotherapeutische nanopartikels.

In **hoofdstuk 5** is bestudeerd of therapeutische vaccins voor de behandeling van kanker verbeterd zouden kunnen worden met de co-behandeling van immunomodulerende nanopartikels. Hierbij zijn muizenmodellen gebruikt die gedeeltelijk gevoelig zijn voor de behandeling met therapeutische vaccins. Tevens zijn de tumoren, drainerende lymfklieren, en de milten ex vivo geanalyseerd na de verschillende behandelingen waarbij de reacties van de verschillende immuuncellen zijn geanalyseerd.

In **hoofdstuk 6** is de combinatietherapie van fotodynamische therapie met de immunomodulerende nanopartikels onderzocht. Fotodynamische therapie is een opkomende en veelbelovende behandeling van kanker met als voordeel dat deze niet mutageen is en de tumor lokaal behandeld kan worden. Daarbij wordt alleen de tumor die een lichtgevoelig stofje heeft opgenomen bestraald met een laser die niet-ioniserende licht uitzendt van een specifiek spectrum. In dit hoofdstuk wordt ook gekeken naar het vermogen van de behandeling, zelfstandig of gecombineerd, om distale tumoren (als model voor metastasen) te behandelen. Hierbij worden tevens de primaire en secundaire tumoren, drainerende lymfklieren, en immuun organen ex vivo geanalyseerd. Tenslotte is vastgesteld dat de contributie van CD8 cytotoxische T cellen noodzakelijk is voor het anti-tumor effect van deze behandelingen.

In **hoofdstuk 7** wordt een overzicht gegeven van de bestaande kennis over de combinatie van nanopartikels die geladen zijn met verschillende drugs tegelijk voor de behandeling van therapie-resistente tumoren. Mogelijke strategieën en mechanismen voor efficiëntere nanopartikel modaliteiten gericht tegen moeilijk te behandelen tumoren worden bediscussieerd.

## **Dankwoord**

Het tot stand brengen van dit proefschrift verenigt een bijzondere periode van wetenschappelijk onderzoek vol uitdagingen en persoonlijke wederwaardigheid. Aan alle personen die tijdens deze periode betrokken zijn geweest wil ik graag mijn dank tonen.

Luis, I would like to thank you for the opportunity to fulfill the honorable task to answer the research questions forthcoming of your formulated hypotheses. Your insight in nanomedicine is admirable and it was my privilege to have learned the intricacies of his field from you.

Ferry, graag wil ik je bedanken voor de fijne begeleiding. Het was voor mij een eer om de kleinste details van de werking van de (tumor) immunologie van je te hebben mogen leren. Daarnaast was je betrokkenheid en toewijding tot het project subliem.

Clemens, je openheid en gastvrijheid heeft ervoor gezorgd dat ik snel welkom voelde. De wetenschappelijke gespreken die wij hebben gehad heb ik als inspirerend ervaren.

Mijn beminde paranimfen Ruben en Koen. Wat een rijkdom aan mooie momenten hebben wij samen beleefd dat zich tot een vriendschap heeft gesmeed. Ruben, ik wil je graag bedanken voor de sparsessies (letterlijk, tijdens de kickboksen lessen) maar ook over de sparsessies over de wetenschappelijke resultaten. Koen, ik wil je graag bedanken voor je steun, deze heeft impact gehad. Ik koester de gekkigheid en de avonturen die wij hebben gedeeld.

Marcel, van jou heb ik de fijne praktische kneepjes van het vak geleerd en altijd kon ik bij jou terecht voor vragen of voor hulp, maar ook 'gewoon' voor een gezellig praatje of het delen van een goede grap.

Ook voor de steun en inbreng van vele andere mensen wil ik oprecht hartelijk bedanken. In het bijzonder Luana, Marieke, Chih Kit, Timo, Eric, Yuedan, Mehrman, Olena, Zili, Anton, Yang, YiYi, Dong, Pablo, Carla, Jomarien, Yaima, Raimundo, Luis, Sabine, Somayeh, Christina, Alice, YuanYuan, Sana, Ana Luiza, Taís, Katarzyna,

Alireza, Gaston, Tracy, Filippo, Fabio, Alan, Katja, Ramon, Tetje, Suzanne, Anke, Gijs, Jan Willem, Rodney, Eleni, Elham, Wendy, Elena, Nataschja, Brett, Koen, Jeroen, Guillaume, Marieke, Hreinn, Heng Sheng, Esmé, Iris, Tsolere, Thorbald en Sjoerd.

Lieve Hilde, wat zijn wij toch een goede match. Wat bof ik met je steun om dit proefschrift tot stand te laten komen. Wat een enorme liefde hebben wij voor elkaar en voor onze kinderen. Ik kan niet wachten op de vele leuke avonturen die wij nog samen in de toekomst gaan beleven.

Voorschoten, 23 maart 2021.

## **Curriculum Vitae**

Cândido Geraldo da Silva was born on the 28th of July 1981 in Delft, the Netherlands. During his early childhood Candido emigrated with his parents and sibling to Portugal where he finished his early education. Candido later returned to the Netherlands and attained a bachelor's degree in Molecular Biology at the University of Applied Sciences Leiden combined with an extracurricular minor in beta education and an extracurricular capita selecta of the Leiden University Medical Centre bachelors' degree in the Biomedical Sciences. Candido concluded his undergraduate thesis based on an internship at the Ophthalmology department under the supervision of Dr. Mieke Versluis and Dr. Pieter van der Velden on the molecular mechanisms in uveal melanoma and targeted therapies.

In 2013 Candido graduated with a Master of Science degree in Oncology at the VU University of Amsterdam with two compulsory internships. The first internship was performed at the Pathology department from the VU University Medical Center Amsterdam under the supervision of Dr. Saskia Wilting and Prof. Dr. Renske Steenbergen on target gene identification of oncogenic microRNAs in cervical cancer. The second internship was performed at the Immunology department from the Leiden University Medical Center under the supervision of Dr. Gijs Zom and Prof. Dr. Ferry Ossendorp on peptide based anti-tumor vaccination strategies. The internship report was evaluated by Prof. Dr. Tanja de Gruijl. Under the supervision of Prof. Dr. Frits Peters, Candido concluded and published his master thesis on the role of influx transporters in the uptake of protein kinase inhibitors.

In 2014 Candido started his PhD project described in this thesis at both the Radiology and Immunology departments from the Leiden University Medical Center under the supervision of Prof. Assist. Dr. Luis Cruz and Prof. Dr. Ferry Ossendorp. Next to his PhD project, Candido enrolled to the doctoral specialization and certification in SMBWO Immunology of the Dutch Society for Immunology (NVVI) institute to acquire the credentials to become a certified immunologist. During his PhD project, Candido presented his acquired scientific results on several occasions to international scientific audiences through congresses in the Netherlands, Portugal, United Kingdom, and in Cuba, and published several scientific and review articles in the field renowned peer-reviewed scientific journals.



During his PhD project, Candido had several relevant side activities, including a two year role as a member of the board of Leids Promovendi Overleg and one year as a voluntary researcher at the think tank organization SMO Promovendi that led to the co-authorship and publication of a book aimed for policy makers as a guide for the implementation of innovation in healthcare titled 'Riding the techwave in an era of change - The healthcare guide to the future'.

Currently, Candido is working as a post-doc researcher at Prof. Assist. Dr. Luis Cruz's lab Translational Nanobiomaterials and Imaging Group at the Radiology department from the Leiden University Medical Center on several projects based on the interface of immunology, oncology and nanotechnology.

## List of publications

1. Luana Zerrillo, Karthick Babu Sai Sankar Guptar, Fons A.W.M. Lefeber, Candido G. Da Silva, Federica Galli, Alan Chan, Andor Veltien, Weiqiang Dou, Roberta Censi, Piera Di Martino, Mangala Srinivas, Luis Cruz (2021). "Novel Fluorinated Poly (Lactic-Co-Glycolic acid) (PLGA) and Polyethylene Glycol (PEG) Nanoparticles for Monitoring and Imaging in Osteoarthritis". *Pharmaceutics*. 2021 Feb 7;13(2):235. doi: 10.3390/pharmaceutics13020235.
2. Zili Gu, Candido G. Da Silva, Koen Van der Maaden, Ferry Ossendorp, Luis J. Cruz (2020). "Liposome-based drug delivery systems in cancer immunotherapy". *Pharmaceutics*. 2020 Nov 4;12(11):1054. doi: 10.3390/pharmaceutics12111054.
3. CG Da Silva, MGM Camps, TMWY Li, L Zerrillo, CW Löwik, F Ossendorp, Luis J Cruz (2019). "Effective chemoimmunotherapy by co-delivery of doxorubicin and immune adjuvants in biodegradable nanoparticles". *Theranostics* 9 (22), 6485
4. CG Da Silva, MGM Camps, T Li, AB Chan, F Ossendorp, LJ Cruz (2019). "Co-delivery of immunomodulators in biodegradable nanoparticles improves therapeutic efficacy of cancer vaccines". *Biomaterials* 220, 119417
5. Jannes ten Berge, Joost Blok, Constantino Garcia Maldonado, Esther Heckendorf, Stephanie Holst-Bernal, Malou Noten, Candido da Silva, Klodiana-Daphne Tona, Daphne Truijens, Eleonoor Verlinden (2018). "Riding the techwave in an era of change". *Stichting Maatschappij en Onderneming (SMO)* ISBN 978-90-6962-270-5
6. CK Chung, CG Da Silva, D Kralisch, A Chan, F Ossendorp, LJ Cruz (2018). "Combinatory therapy adopting nanoparticle-based cancer vaccination with immune checkpoint blockade for treatment of post-surgical tumor recurrences". *Journal of controlled release* 285, 56-66
7. CG Da Silva, Godefridus J Peters, Ferry Ossendorp, Luis J Cruz (2017). "The potential of multi-compound nanoparticles to bypass drug resistance in cancer". *Cancer chemotherapy and pharmacology* 80 (5), 881-894

8. R Huis In't Veld, C G Da Silva, E L Kaijzel, A B Chan, L J Cruz (2017). "The Potential of nano-vehicle mediated therapy in vasculitis and multiple sclerosis". *Current pharmaceutical design* 23 (13), 1985-1992
9. CG Da Silva, Felix Rueda, CW Löwik, Ferry Ossendorp, Luis J Cruz (2016). "Combinatorial prospects of nano-targeted chemoimmunotherapy". *Biomaterials* 83, 308-320
10. Candido G Da Silva, Richard J Honeywell, Henk Dekker, Godefridus J Peters (2015). "Physicochemical properties of novel protein kinase inhibitors in relation to their substrate specificity for drug transporters". *Expert opinion on drug metabolism & toxicology* 11 (5), 703-717
11. PA Van Der Velden, M De Lange, CG Da Silva, M Versluis, GPM Luyten, MJ Jager (2011). "C-Met signaling and preclinical analysis of Crizotinib in uveal melanoma". *Acta Ophthalmologica* 89